Land use changes and salinization: Impacts on lake phosphorus cycling and water quality

by

Jovana Radosavljevic

A thesis

presented to the University of Waterloo

in fulfillment of the thesis requirement for the degree of

Doctor of Philosophy

in

Earth Sciences (Water)

Waterloo, Ontario, Canada, 2023

Examining Committee Membership

The following served on the Examining Committee for this thesis. The decision of the Examining Committee is by majority vote.

External Examiner	Dr. Claire Oswald Assistant Professor
Supervisor	Dr. Philippe Van Cappellen Professor, Canada Excellence Research Chair
Internal Member(s)	Dr. Nandita Basu Professor, Canada Research Chair
	Dr. Fereidoun Rezanezhad Research Associate Professor
Internal-external Member	Dr. Bruce MacVicar Associate Professor
External Member	Dr. Bahram Gharabaghi Professor

Author’s declaration

This thesis consists of material all of which I authored or co-authored: see Statement of Contributions included in the thesis. This is a true copy of the thesis, including any required final revisions, as accepted by my examiners. I understand that my thesis may be made electronically available to the public.

Statement of contributions

This thesis consists of co-authored papers. I was primarily responsible of the study design and its execution. The following summarizes the contributions of the co-authors of each chapter.

Chapter 2

I and SS designed the research questions, and together with Kate Thomas (KT) coordinated the lab analyses. Johan Wiklund (JW) dated the core and provided inputs on data interpretation. Methodology was developed by myself, Stephanie Slowinski (SS) and Philippe Van Cappellen (PCV), and I, SS and PVC interpret the data, with inputs from Chris T. Parsons (CTP), KT and Rolland Hall (RH). I, SS, and PVC wrote the paper with inputs from CTP. All co-authors provided feedback on data interpretation.

Chapter 3

I developed research questions, data curation and data analysis. Methodology was developed by me and SS with inputs from PVC, CTP and Mahyar Shafii (MS). I and SS interpret the data with guidance of PVC and inputs from CTP. I wrote the paper with input from PVC. All other authors provided feedback on data interpretation.

Chapter 4

I developed the research questions and methodology, with inputs from SS, Fereidoun Rezanezhad (FR) and PVC. I wrote the paper with input from PVC. All co-authors provided feedback on data interpretation.

Chapter 5

I collected, synthesized, and analyzed the data, and together with PVC designed the research. I wrote the chapter with the input from SS and Nandita B. Basu (NB). All other authors provided feedback on data interpretation.

Abstract

Over the past few decades, there has been a rapid global increase in urbanization accompanied by the conversion of natural or agricultural land into more impervious land cover. This ongoing acceleration of global urbanization has raised significant concerns regarding the deterioration of water quality in urban lakes, such as worsening eutrophication symptoms. Eutrophication of inland waters, primarily driven by phosphorus (P) enrichment caused by human activities, is characterized by increased primary production that, in the most extreme cases, results in harmful algal blooms. Additionally, anthropogenic salinization has emerged as another stressor affecting the health of urban freshwater ecosystems. Although the ecological ramifications of both P enrichment and salinization on freshwater ecosystems are recognized, their combined impacts on water quality have hitherto been considered separately.

The work presented in this thesis is based on an extensive acquisition and analysis of data for a lake currently located along the edge of the Greater Toronto metropolitan area: Lake Wilcox. Before the most recent phase of rapid urban development, the lake's watershed underwent the conversion of its original forested land cover to agricultural use. Based on the data, I investigated the following questions: (1) How did the successive historical changes in land use/land cover (LULC) impact the water quality and P cycling in the lake?; (2) How has the rapid expansion of imperviousness during urban growth impacted the lake's eutrophication symptoms, in particular, the oxygenation of the deeper water and the remobilization of P from the bottom sediments?; (3) How effective have agricultural and urban stormwater best management practices been in mitigating the external input of P to Lake Wilcox?; (4) Of the road salt applied in the watershed during winter, how much reaches the lake and how much is retained in the watershed?; and (5) What is the rate of salinization of Lake Wilcox and management intervention could help the lake recover from excessive use of the road salt?

To address these research questions for Lake Wilcox, I combined sediment core analyses, statistical data time series tests, and mass balance modeling. I further evaluated the transferability of the findings for Lake Wilcox to other lakes in North America. In this final research activity, I tested the key hypothesis that emerged from my

work on Lake Wilcox, namely that the changes in a freshwater lake's mixing regime caused by salinization exacerbates eutrophication symptoms, even in cases where the external P inputs to the lake are reduced.

In chapter 2, a dated sediment core, recent water quality data, and historical records were used to reconstruct changes in P loading to and cycling in Lake Wilcox associated with changes in land use/land cover (LULC) since the 1920s. The lake's originally forested watershed was cleared for farming and, starting in the 1950s underwent agricultural intensification. Since the 1980's, urbanization rapidly increased the watershed's impervious land cover, now accounting for about 60% of the total surface area. The results illustrate the absolute and relative changes in P external and internal loading resulting from the LULC changes and the implementation of various agricultural and urban stormwater management practices. By analyzing the sediment core data, I reconstructed the historical P loading patterns, as well as the response of the lake's P dynamics to the evolving human activities in the watershed. The results of this chapter highlight the large differences in the impact of agricultural versus urban land use on the lake's P budget and cycling, and on other aspects of the lake's biogeochemistry.

Chapter 3 focuses on the most recent phase of rapid urbanization of Lake Wilcox' watershed. Of particular interest is to understand why Lake Wilcox remains in an apparent eutrophic state even though external P inputs to the lake have been declining since the 1980s. I analyzed 22 years of water chemistry, land use, and climate data (1996–2018) using principal component analysis (PCA) and multiple linear regression (MLR) to identify the contributions of climate and urbanization to the observed changes in water chemistry. The results show that the progressive salinization of the lake impacts the lake mixing regime by strengthening thermal stratification during summer. A major consequence is a worsening oxygen depletion of the hypolimnion that increases internal P recycling in the lake. My research therefore establishes a novel link between salinization and eutrophication symptoms.

Building on the significant increase in salinity presented in the earlier chapters, Chapter 4 delves into a deeper investigation of the road salt management practices in the watershed of Lake Wilcox. I delineate the changes in geochemical water type in the period

2000-2020 while using mass balance calculations for dissolved chloride and sodium to reconstruct the yearly salt loading to the lake and the amounts of salt ions that are retained within the watershed. Results showed that further increase in salinity may eventually inhibit the fall overturn of the lake. They also point to the large salt legacies accumulating in the watershed, likely in soil and groundwater compartments. The fate of these legacies will require further research to determine the long-term risks they pose to water resources and receiving aquatic ecosystems.

In chapter 5, I use water chemistry data for several other urban lakes in Ontario, Wisconsin, and Minnesota to analyze how lake salinization intersects with water temperature and lake morphometry to modify lake stratification. The goal is to determine to what extent salinization in these lakes can cause eutrophication-like symptoms such as those seen in Lake Wilcox. Trend analyses of chemical and physical variables are carried out for all the lakes, and the Brunt-Väisälä frequency is used as a measure of the summer stratification intensity. The results consistently indicate that salinity is becoming an increasingly stronger regulator of water density than temperature in urban freshwater lakes experiencing cold winters.

Overall, my research demonstrates that rising salinity can have a significant impact on water column stratification of freshwater lakes. This, in turn, can reduce the oxygenation of the hypolimnion and enhance internal P loading from the sediments. These findings thus highlight that the management of salt inputs to urban lakes, including de-icing salt applications in cold and cold-temperate regions, should be taken into consideration to control lake eutrophication symptoms.

Acknowledgements

I am grateful to my supervisor, Philippe Van Cappellen, for providing me with a remarkable opportunity to be a part of a dynamic and innovative research group. I am truly appreciative of your continuous guidance, limitless support, and patience. Collaborating with you has been an immensely inspiring and enriching journey and it made my Ph.D. experience fulfilling with boundless joy, excitement, and a plethora of exciting opportunities.

To Fereidoun Rezanezhad, thank you for your unwavering support and positive feedback throughout this PhD. Your energy helped me through some challenging moments, and you made this project better.

To my thesis committee, Nandita, Bruce and Bahram, thank you for your guidance and support, your criticism and your encouragement.

To my friends and colleagues in Ecohydrology Research Group, you are an outstanding community of scientists and researchers. You have all helped me grow as a researcher. I am grateful to Steph for being such a great colleague and friend. Thank you, Zahra, for being a great friend and encouraging me and my work and being here in all possible ways and bringing me the hot chocolate. Thank you, Bowen and Haoyu, for all the non-productive but unique and priceless hours that we spent together. Thank you Bhaleka and Anita, for helping with all those “small” things.

To Milos, for always being here and supporting me in all ways. To my mother for limitless encouragement; to my father and aunt; to my brother for always annoying me. To my friend, Marina, for listening to my nonsense and trying to understand me. To Nadja, for all speeches and voice messages in the early morning.

Table of Contents

List of figures

List of tables

Chapter 1
Introduction

1.1. Effects of urbanization on freshwater ecosystems

Over the past few decades, there has been a global rapid increase in urbanization leading to the conversion of natural or agricultural land into more impervious land cover (Stammler et al., 2017). Urbanization is an ongoing phenomenon, both globally and in Canada. As of 2007, about half of the world's population lived in urban areas, and this number is expected to exceed 65% by 2050 (Leeson, 2018; McGrane, 2016; Montgomery et al., 2007). In Ontario, Canada, the population has more than doubled since the 1960s, with the highest population density in the southern part of the province (Van Staden, 2022). Generally, urbanization has negative effects on biodiversity, water quality and air quality.

Numerous urban centers are located in proximity to water bodies which provide important ecosystem services such as drinking water, food, regional climate regulation, biodiversity habitat, and recreational activities. However, urban development alters the natural functions of ecosystems, including the physical and chemical attributes of rivers, streams, lakes, ponds, and wetlands (Allan, 2004; Heino et al., 2017), with significant impact on hydrology (Lindh, 1972; Walsh et al., 2005).

Urban development involves the replacement of natural land cover with impervious surfaces, resulting in reduced infiltration of rain and snow through the soil (Brabec et al., 2002; Walsh et al., 2005). Instead, precipitation generates runoff, which flows at much higher volumes and velocities compared to natural environments (Brown, 1988; Walsh et al., 2005). This has the greatest impact on hydrology, increasing runoff, and decreasing infiltration and evapotranspiration (see Figure 1.1).

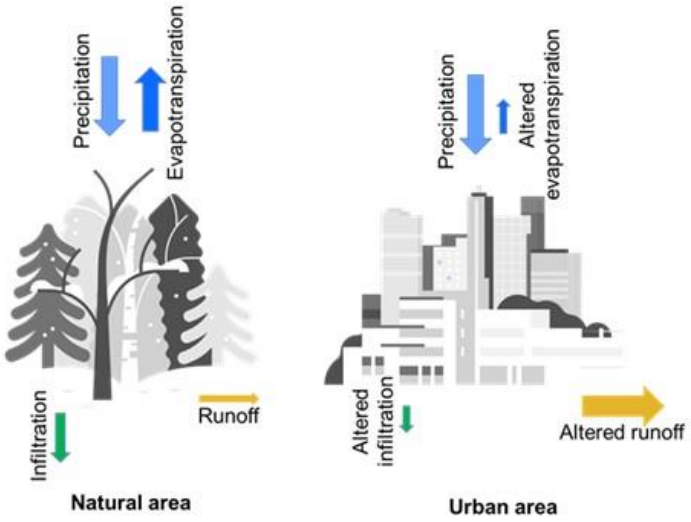

Figure 1.1. Impact of urbanization on hydrology cycle. Note, the change in the size of arrows in natural vs. urban areas represents the change in fluxes.

In addition, urban runoff can carry pollutants such as sediments, nutrients, heavy metals, and microbes that can significantly impair the water quality of receiving waters, such as rivers and lakes (Ferreira et al., 2016, 2018). The elevated water temperature of runoff is another challenge for water quality in urban areas, especially in colder climates like Canada, as it can affect ecosystem communities (McGrane, 2015; Walsh et al., 2005; Miller, 2017).

To mitigate peak runoff and maintain the water quality of receiving water bodies, authorities frequently employ stormwater management (SWM) infrastructures like ponds or low-impact development (LID) systems (Oertli & Parris, 2019).

1.2. Importance of phosphorus (P) in freshwater ecosystems and potential solutions for urban P control

Anthropogenic activities significantly alter global biogeochemical cycles, including the cycling of phosphorus (P) (Bennett et al., 2001). Urban areas, in particular, are hotspots for P transformations (Kaushal et al., 2005), which can result in the deposition and transport of P with stormwater during rainfall events (Carpenter et al., 2015, 2018) to receiving waters, which can further cause a significant deterioration in water quality (Song et al., 2015, 2017; Zhou et al., 2023). Freshwater ecosystems are often limited by the availability of nutrients, with P being a primary (or co-limiting) nutrient. Therefore, excessive input of P can lead to eutrophication, where the overgrowth of algae and other aquatic plants can cause severe ecological problems (Bouraï et al., 2020; Carey et al., 2012, 2013; Carpenter, 2005; Carpenter et al., 1998; Jenny et al., 2016).

Phosphorus (P) has diverse sources and transport pathways in the environment. Global primary P flows and inputs are linked to synthetic fertilizers' production and application, with a significant portion lost in agriculture (Campbell et al., 2020; Cordell et al. 2009). Despite this, studies on urban areas are essential as they often represent the final sinks for P, and substantial amounts can potentially accumulate in urban areas, eventually becoming sources to receiving water bodies (Kalmykova et al., 2012). While urban runoff accounts for a small proportion of total phosphorus (TP) inputs on a global scale, urban P sources can be significant contributors within the area or water body (Burns et al., 2012; Macintosh et al., 2018). Stormwater is a significant source of P to water bodies, which

enters storm drains and flows into stormwater ponds before eventually discharging into connected surface waters (Yang and Lusk, 2018).

Controlling P transport from urban areas to receiving waters requires a comprehensive understanding of both the sources and temporal changes in P concentrations and loadings, as well as the composition of P species along the transport pathways at the watershed-water interface. The composition of stormwater, and overall water quality in urbanized areas, is dependent on the various P sources (Figure 1.2), including (1) natural sources such as erosion and atmospheric deposition, (2) anthropogenic sources such as synthetic fertilizers, pet waste, automobile exhaust, detergents, leaking sanitary sewers, street solids, effluents from wastewater treatment plants (WWTP), and landfills, as well as (3) biogenic sources like leaf litter and grass clippings (Bratt et al., 2017; Hobbie et al., 2017; Indris et al., 2020; Kalmaykova et al., 2012). Compared to other land use systems such as agriculture, where part of the P can be removed by plants and livestock, the removal of P from urban watersheds is limited. As a result, relatively low P inputs can translate into relatively high runoff P concentrations or high P loads during intense precipitation events (Kalmaykova et al., 2012). Furthermore, P can accumulate in urban watersheds during dry climate conditions, leading to the potential for increased P concentrations and loads during subsequent storm events (Yang et al., 2021).

The transport of P in urban areas can occur directly through impervious surfaces, which can convey runoff containing P directly to receiving water bodies, or indirectly through stormwater management (SWM) systems (Figure 1.3). Stormwater as a significant source of P can enter SWM systems such as retention ponds (RPs) or low-impact development facilities (LIDs), including bioretention cells, before eventually draining into water bodies (Yang and Lusk, 2018; Yang et al., 2021). SWM infrastructures such as RPs and LIDs are widely used to retain runoff and enhance the sedimentation of mobilized particles to reduce pollutant loading in urban runoff (Chiandet & Xenopoulos, 2016). However, these SWM infrastructures can also have an impact on the urban P dynamics by either reducing P loadings in the retained runoff (Goh et al., 2019; Kratky et al., 2017, 2021; Zahmatkesh et al., 2015) or by accumulating P loading and modifying P speciation (Frost et al., 2019; Marvin et al., 2020; Song et al., 2017; Zhou et al., 2023).

SOURCES OF *P* IN URBAN AREAS:

a – atmospheric deposition
b – pet waste
c – construction sites
d – automobile exhaust and non-exhaust
e – inadequately functioning septic systems + detergents from house hold waste
f, g – decomposition of soils and plant materials (e.g. leaf litter)
h – lawn fertilizing
i – grass clipping
j – waste water treatment plants (effluents)
k – landfills
l – street solids
m, n, o – miscellaneous sources (e.g. cemetery, gas stations, husbandry)

***P* TRANSORT PATHWAYS:**

1 – Impervious surface as pathway for urban runoff to stormwater (SW) pipes or receiving water bodies
2 – Runoff which enters in SW systems discharge either directly into receiving water or to SW management systems such as ponds or bioretention cells (from where it is redirected to receiving waters)
3 – Leaching or infiltration of P to soil/groundwater, where it can be connected to receiving waters

Figure 1.2. Potential P sources in urban areas.

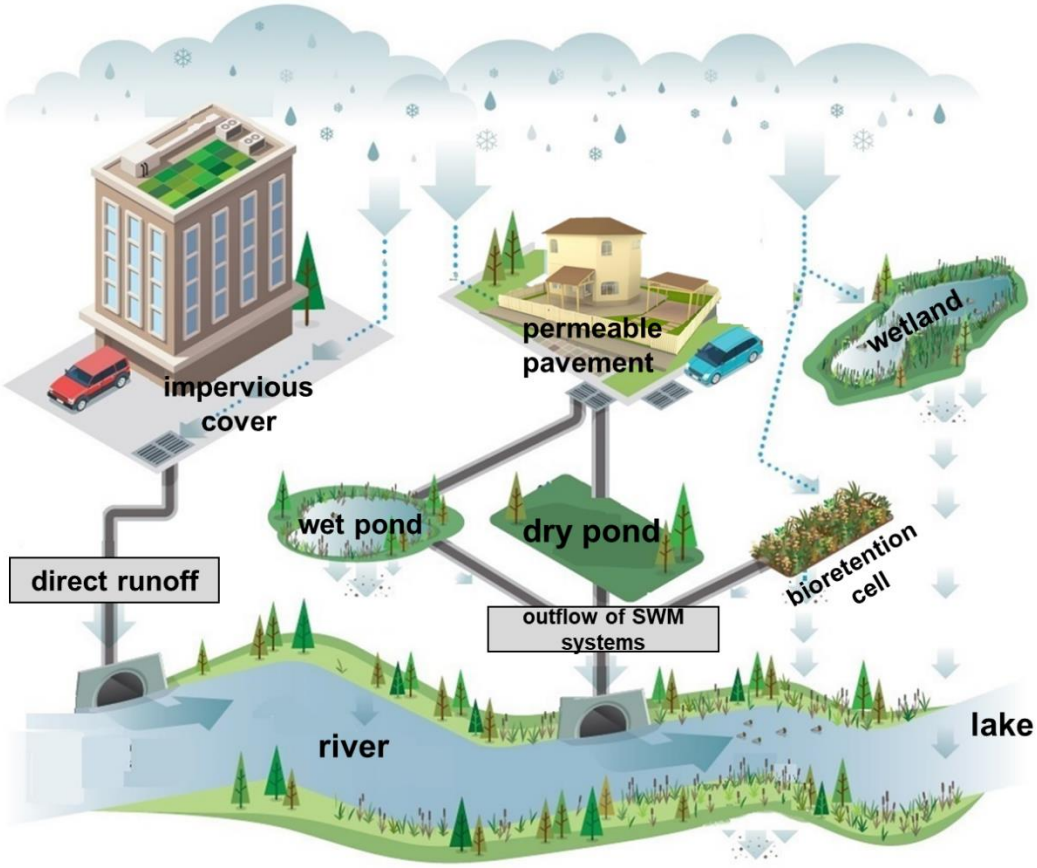

Figure 1.3. Transport pathways of P in urban areas with examples of stormwater management facilities.

1.3. P delivery to and cycling in lakes

Lakes play a critical role in regulating and sustaining global biogeochemical cycles of elements, P included. The concurrent influence of changes in water chemistry and nutrient inputs to lake systems due to changes in land cover (Lin et al., 2021; Pham et al., 2019) can result in the algae's reproduction, potentially triggering anoxic conditions, modifying fish populations, diminishing biodiversity, and disrupting plankton communities, thereby exacerbating the occurrence of harmful algal blooms (Jeppesen et al., 2014). P is the limiting nutrient for freshwater lakes (Correll, 1999; Correll et al., 1999; Maavara et al., 2015). P occurs in a number of different species and its cycling in the landscape and in lakes is complex, owing to its active participation in various biological and biogeochemical cycles (Schindler et al., 1993). Upon entering the lake ecosystem, P often undergoes efficient retention via uptake and assimilation by plants, followed by deposition in the sedimentary layers in an organic form. Lakes also accumulate allochthonous and autochthonous organic matter and inorganic solids that settle from the water column, further influencing the fate of P in these systems (Ingall & Van Cappellen, 1990; Ruttenberg, 2003).

Sediments are critical components of the phosphorus cycle in lakes and serve as both sinks and sources of this element (Markelov et al., 2019). The accumulation of phosphorus in lake sediments can occur in various forms, including dissolved and solid species, as well as organic and inorganic compounds (Parsons et al., 2017). Nevertheless, most of the phosphorus in sediments is stored in the solid phase. The process of internal phosphorus loading, which involves the mobilization of phosphorus from sediments into the water column, plays a fundamental role in determining the availability of this element (Boström et al., 1988; Carlton & Wetzel, 1988). P released from the sediments is bioavailable, usually in dissolved form, and often refers to the P species either as soluble reactive phosphorus (SRP) or dissolved inorganic P (DIP). The diagram of different P species that could be found in water is shown in Figure 1.4. The release of phosphorus from sediments is regulated by multiple mechanisms, including oscillating redox conditions, mineralization, microbial processes, and temperature (Boström et al., 1988; Penn et al., 2000), but also it depends on the pH and alkalinity. Notably, redox conditions play a significant role in controlling the retention of phosphorus within

sediments (Markelov et al., 2019). Periodic oxygen depletion (hypoxia or anoxia) related to lake thermal stratification leads to relatively high phosphorus internal loading rates (Carey et al., 2022).

As it has been described, the P cycle in lakes is a complex process impacted by a myriad of factors (Markelov et al., 2019). Alterations in land cover within the watershed of a lake can have significant impacts on P loading to and cycling within the lake (Bunting et al., 2016), with potential consequences for the entire lake ecosystem (Yang et al., 2020). Changes in land use, such as agricultural intensification, urbanization, and deforestation, can impact the loading of nutrients, including phosphorus (Chowdhury & Chakraborty, 2016), into the lake, often resulting in a change in water chemistry and potentially impacting the lake's mixing regime (Ladwig et al., 2021). Moreover, land use changes can also modify hydrological regimes (Wong et al., 2012), leading to alterations in the delivery of soil erosion (Czemiel, 2014) and nutrients to the lake (Borrelli et al., 2016, 2017). These effects, in turn, can impact the internal phosphorus loading from sediments, as well as the cycling of phosphorus within the water column (Radosavljevic et al., 2022). Additionally, land cover changes can alter the delivery of organic matter (Silliman et al., 1996), which is often a large pool of P in lakes (Slomp & Van Cappellen, 2007). Therefore, understanding the interconnections between land cover changes and the P cycle in lakes is essential for developing effective management strategies to preserve these vital freshwater ecosystems, especially in the era of intensive urban development.

1.4. Thermal stratification in lakes and impact on P cycling

Thermal stratification is a phenomenon that occurs in many lakes or reservoirs which can persist for extended periods of time (Boehrer & Schultze, 2008; Ladwig et al., 2021). This stratification is primarily a result of density differences that occur within the water bodies, leading to the development of potentially distinct chemical gradients with significant ecological implications. Temperature and dissolved substances are major contributors to these density differences (Figure 1.5) (Beohrer & Schultze, 2008). During the warm season, the lake surface is subjected to a temperature signal from the atmosphere, resulting in the establishment of thermal stratification, particularly in deeper lakes. Conversely, during the cold period, surface cooling induces vertical circulation of water masses, leading to the removal of gradients of water properties (Dake & Harleman, 1969).

Nevertheless, gradients of dissolved substances may persist for considerably longer than one annual cycle, leading to sustained stratification that precludes complete overturning of the lake water masses (Boehrer & Schultze, 2008; Bubeck & Burton, 1989; Ladwig et al., 2021).

Furthermore, the introduction of anthropogenic salts into a lake or reservoir system can result in the accumulation of salts and a subsequent increase in density gradients within the water column, ultimately leading to delayed, reduced, or even disrupted lake mixing (Ladwig et al., 2021). For instance, the case of Woods Lake in Michigan, which has a depth of 12 meters, serves as an illustrative example of this phenomenon. Specifically, sustained inputs of deicers were found to have contributed to the transition of the lake from a state of holomixis to meromixis, as documented in studies conducted by Koretsky et al. (2012) and Sibert et al. (2015). This shift in the lake's mixing regime resulted in persistent anoxia in the bottom water layer, and this highlights the significant and widespread effects of human-induced salt inputs in aquatic ecosystems, which are not yet fully understood.

There is a close relationship between P cycling in lakes and thermal stratification in lakes. Thermal stratification creates distinct layers of water with different temperature and oxygen profiles (Cott et al., 2008), which can lead to the development of anoxic conditions in the hypolimnion (Boehrer & Schultze, 2008; Soranno et al., 1997). These anoxic conditions can promote the release of redox-sensitive P pools from the sediment, which then diffuses upwards into the overlying water column, resulting in internal P loading (O'Connell et al., 2020). Additionally, the density differences created by thermal stratification can lead to reduced mixing between the hypolimnion and the epilimnion (Ladwig et al., 2021), which further exacerbates the accumulation of P in the hypolimnion (Riley & Prepas, 1984). Thus, thermal stratification plays a crucial role in disturbing P cycling in lakes, and understanding this relationship is important for effective lake management and restoration efforts.

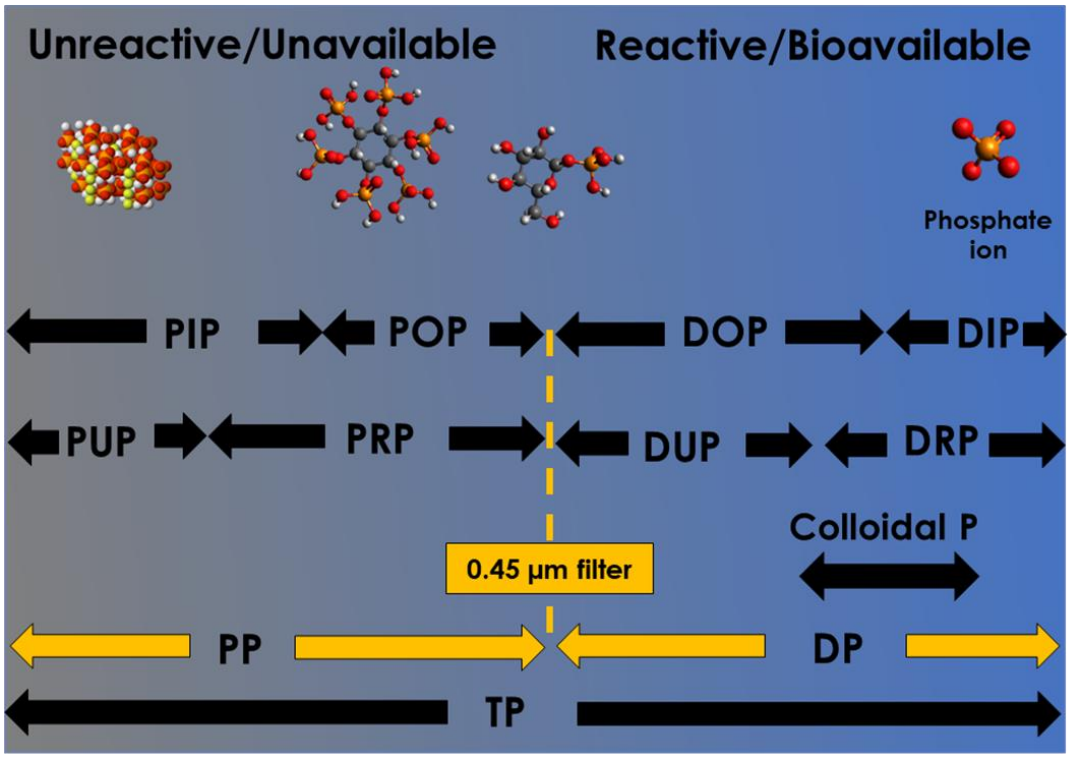

Figure 1.4. Diagram of different P species in water (unpublished figure of C. Parsons).

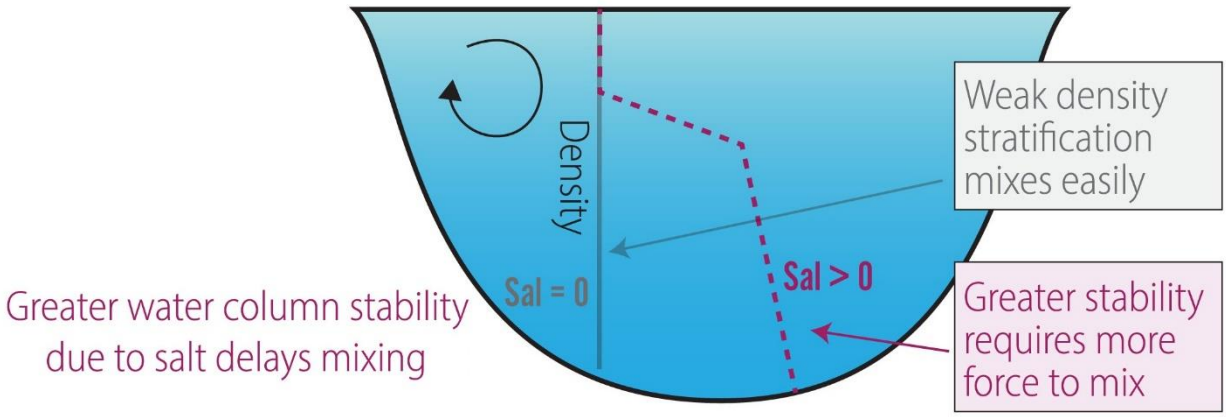

Figure 1.5. Thermal stratification with temperature (a) and dissolved solids (b) as contributors to its strengthening (adapted from Ladwig et al., 2021)

1.5. Salinization as an additional stressor for urban freshwater lakes

Salinity refers to the collective concentration of dissolved ions in water, which is often expressed as electrical conductivity (EC) (Cañedo-Argüelles et al., 2013, 2016; Williams & Sherwood, 1994) or measured using chloride (Cl^-) as a proxy for salinization in regions of cold climate (Mazumder et al., 2021). In recent decades, the salinization of freshwater has become an increasingly pressing issue in many regions of the world (Figure 1.6), with significant implications for both human health and the environment (Iglesias, 2020; Kaushal et al., 2017, 2018; 2021).

While salinization was once primarily associated with agricultural areas in semi-arid and arid regions (Singh, 2018; Zhang et al., 2020), it has now become a global concern (Kaushal et al., 2005; Utz et al., 2022), particularly in urban regions with cold climate lakes (Cooper et al., 2014; Haq et al., 2018; Jamshidi et al., 2020; Kaushal et al., 2005; Laceby et al., 2019; Miron et al., 2022; Novotny et al., 2008). While there are numerous natural sources of freshwater salinization, including evaporation, geothermal activity, rock dissolution, weathering, seawater intrusion, and seawater spray (Mirzavand et al., 2020), the negative impact of anthropogenic sources has become increasingly significant in the 21st century. Key anthropogenic sources of freshwater salinization include agriculture, resource extraction (including land clearing), wastewater effluents, including detergents, and the use of deicers such as road salt (Kaushal et al., 2018). As a result, effective management of these systems has become increasingly important to ensure the preservation of freshwater ecosystems and the protection of human health and the environment (Utz et al., 2022).

In recent decades, the use of road salt has been increasingly recognized as a significant anthropogenic source of freshwater salinization, which has become a global phenomenon (Hintz et al., 2016, 2022; Kaushal et al., 2005, 2019), particularly in urbanized areas (Kaushal et al., 2005; Mazumder et al., 2021). Although the full extent of the global spread of freshwater salinization remains unknown, recent research (Chen et al., 2019; Estévez et al., 2019; Kaushal et al., 2018) and comprehensive published data (Thorslund & van Vliet, 2020) indicate that salinization is on the rise throughout the world, including North America (US, Canada), S. America, Russia, China, S. Africa, Australia, Europe (Sweden, Germany).

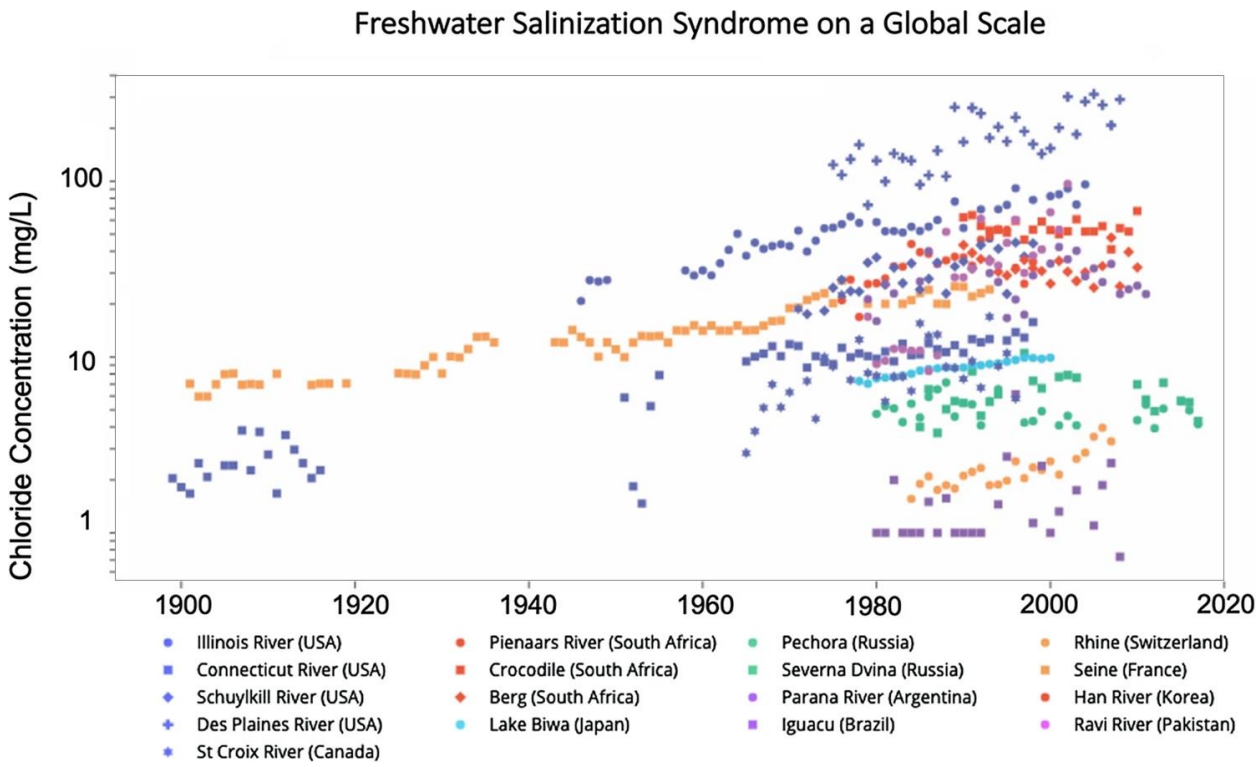

Figure 1.6. Regions affected by freshwater salinization (from: Kaushal et al., 2021)

In particular, freshwater salinization has been increasing in cold climate urban areas due to the excessive use of deicers, such as road salt and brine (Hinitz et al., 2022; Kaushal et al., 2005; Miron et al., 2022). Studies focusing on cold urban regions have reported that 37% of the contiguous United States has been affected by salinization due to the excessive use of road salt (Kaushal et al., 2018). In North America, 44% of freshwater lakes have experienced long-term salinization (Dugan et al., 2017), while Le et al. (2019) found that 80% of streams and rivers in Germany have undergone increasing salinity (Le et al., 2019). Moreover, Novotny et al. (2008) observed an increase in salinization in Swedish lakes, while Löfgren (2001) demonstrated the impact of deicers on soil and stream water in five catchments in southeast Sweden.

In urbanized watersheds with a high proportion of impervious land cover, Cl^- concentrations in water bodies often exceed environmental guidelines set by the Canadian Council of Ministers of the Environment (chronic: 120 mg L^{-1}) (Wallace et al., 2016) The highest concentrations of Cl^- in freshwater lakes occurs when meltwater containing deicers runs off impervious surfaces and travels to receiving waters (Meriano et al., 2009). In some watersheds, elevated Cl^- concentrations persist throughout the year (Robinson and Hasenmueller, 2017), posing a growing threat to aquatic ecosystems and freshwater health. The distribution of road salt within a watershed remains uncertain (Figure 1.7), with some of the deicers reaching receiving water bodies and others being retained in the watershed (Oswald et al., 2019). Quantifying the spatiotemporal variability in annual watershed-scale salt ions retention and exploring the magnitude of their retention represents a crucial first step towards disentangling the complex processes underlying the increasing lake salinization in urban areas. While the overall increase in salinity is undeniable, especially with the increase in urbanization, the long-term effects of salinization in lake ecosystems and its impact on biogeochemical cycling remain poorly understood, as do comprehensive solutions to this rising issue.

1.6. Thesis structure

This thesis addresses the following research questions:

1. How do shifts in watershed land use/land cover (LULC) - from forested to agricultural to urban - impact external P loadings and in-lake P cycling in a downstream lake (i.e., Lake Wilcox)?
2. How does a rapid increase in imperviousness impact the water chemistry, especially the symptoms of eutrophication, when external P inputs to the lake are lowered by various best management practices?
3. How does an increase in salinization impact (1) the mixing regimes and (2) the water chemistry of a cold climate urban lake? On what timescale will the lake's salinity and mixing regime recover if road salt ion loads to the lake are reduced?
4. What is the fate of road salt ions in an urban watershed once they are applied to maintain winter conditions? To what extent are they retained in watershed compartments such as soil and groundwater? How does the extent of impervious cover impact their retention?
5. While the analysis of the Lake Wilcox case study site indicates that salinization causes a change in lake mixing regime and an increase in eutrophication symptoms, does this happen in other North American cold climate urban lakes?

The research segment of the thesis comprises four chapters, wherein Chapter 2 presents an analysis based on a sediment core obtained from an urban lake (i.e., Lake Wilcox, Ontario). Along with the dated sediment core, this chapter utilizes water chemistry data and historical information to reconstruct the post-1920 trajectories of P loadings and cycling, which occurred concurrently with the land-use and land-cover (LULC) changes in the watershed. The study illustrates the disparities in P budgets resulting from the progression of the watershed's LULC changes and presents the hypothesis that different LULCs impacted P loading to and cycling within the lake (research question 1).

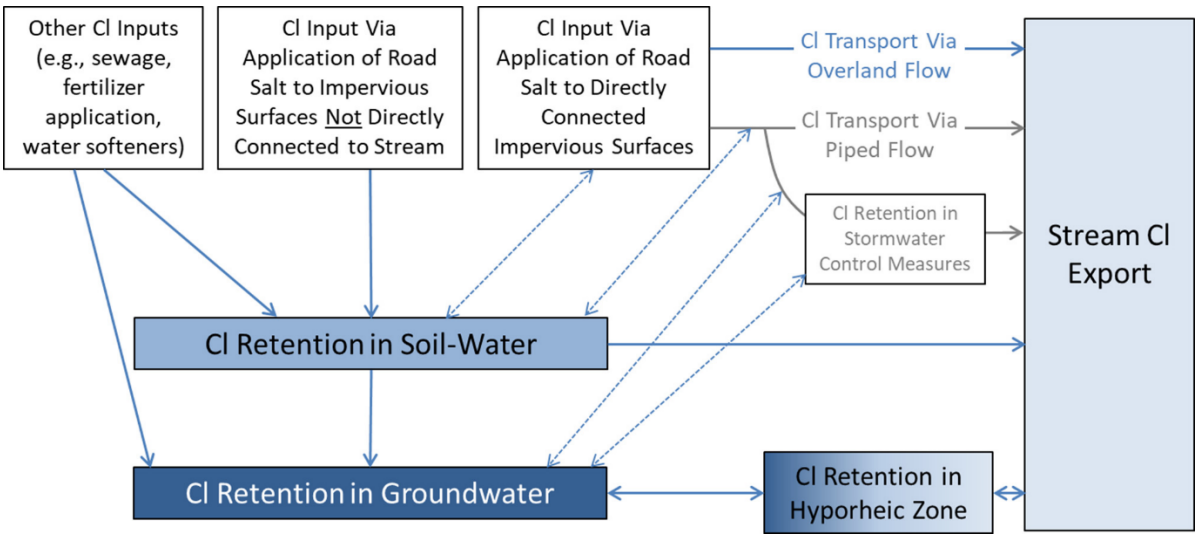

Figure 1.7. conceptual diagram of distribution of salty runoff in the watershed of urban area (from Oswald et al., 2019)

In accordance with Chapter 2, Chapter 3 aims to address the subsequent research question (2) through an in-depth analysis of a comprehensive data set of water chemistry parameters spanning over 20 years for the epilimnion and hypolimnion zones of the lake. The findings presented in this chapter outline crucial factors contributing to the degradation of water quality in an urban lake, particularly in areas with high levels of impervious surfaces in cold climate regions.

Based on the findings presented in the preceding chapters, Chapter 4 provides an analysis of the impact of road salt on the mixing regimes of Lake Wilcox. This analysis employs an analytical and mass balance modelling approach to evaluate the effects of salinization resulting from road salt application, as well as the impact of excessive salt use on the geochemical type of the lake water (research question 3). Furthermore, this chapter employs a mass balance approach and utilizes water chemistry data to assess the distribution of salt ions, specifically Cl^- and sodium (Na^+), within the urban watershed (research question 4).

Chapter 5 expands on the insights gleaned in the prior chapters for the Lake Wilcox case study to undertake a comprehensive analysis of multiple urban lakes across North America. The main goal of this chapter is to ascertain whether eutrophication symptoms have increased in other lakes despite reductions in external P inputs. In doing so, the Lake Wilcox case study findings are extended to a broader context, by upscaling the analysis to investigate the impact of salinization on the promotion of eutrophication symptoms in urban lakes of cold climate regions.

Chapter 6 provides a comprehensive overview of the main findings pertaining to the five Research Question posed in this thesis. Moreover, it delineates the key research avenues that warrant further exploration in light of the findings of this thesis. Finally, a succinct summary of recommended best management practices and the challenges associated with managing road salt application in cold climate regions is presented, along with a discussion of the broader implications of salinization on freshwater ecosystems.

Chapter 2

Contrasting impacts of agricultural intensification and urbanization on lake phosphorus cycling and implications for managing eutrophication

Modified from:

Slowinski S., Radosavljevic J., Graham A., Ippolito I, Thomas K., Rezanezhad F., Shafii M., Parsons C.T., Basu N. B., Wiklund J., Hall R., Van Cappellen P. (2023). Contrasting impacts of agricultural intensification and urbanization on lake phosphorus cycling and implications for managing eutrophication. *JGR: Biogeosciences*. (Submitted and in review)

2.1. Summary

A dated sediment core from Lake Wilcox (southern Ontario, Canada) was used to reconstruct the post-1920 trajectories of phosphorus (P) loading and cycling that accompanied changes in land use of the watershed. The progressive conversion of the initially forested watershed to farmland was followed by agricultural intensification after World War II and by rapid urbanization since the turn of the century. The watershed now comprises 60% urban land cover and has become integrated into the sprawling Toronto metropolitan area. The post-1950 agricultural intensification was accompanied by a 2.5-times increase in the sedimentation rate. Since the early 1980s, however, the sedimentation rate has dropped to values below those observed before 1940 because of better soil conservation, spreading impermeable land cover and, after 2000, effective stormwater management. While urbanization is marked by significant upcore increases of the concentration of total P (TP) and the fraction of organic P (P_{org}), the TP burial rate decreased by around 60% from its peak value in the early 1970s. Post-2000 water quality monitoring data further implies that the expansion of anoxic conditions in the hypolimnion are not caused by increasing watershed P loading but rather by rapid salinization that strengthens the lake's summer stratification. Longer periods of summer anoxia, in turn, enhance internal P loading from the sediments which, in recent years, represents about 13% of the total (external plus internal) P loading to the water column. Reconstructed TP budgets for Lake Wilcox highlight the shifts in the lake's P cycle driven by the land use changes.

2.2. Introduction

Land use/land cover, or LULC, exerts a major control on the material flows exported from watersheds to downstream water bodies. Around the world, watershed loadings of sediment and nutrients have undergone massive changes because of human settlement and conversion of natural land cover to agricultural use and urban development (Duda, 1993; Jenny et al., 2016; Soranno et al., 1996;). The increased watershed export of anthropogenic nutrients to lakes, especially the limiting nutrient phosphorus (P), is a major driver of eutrophication and accompanying water quality and ecosystem degradation (Carpenter et al., 2015; Schindler, 1977).

Agricultural P enrichment of lakes and reservoirs has been extensively studied (Carpenter et al., 2015; Sharpley et al. 2011). Agricultural LULC is a source of excess P because of the application of mineral fertilizer and manure that supply essential nutrients, including P, for crop growth (Van Meter et al., 2021; Van Staden et al., 2022). Soil erosion and surface runoff then transfer P from agricultural landscapes to water bodies (Sharpley et al., 2000). Cities import large amounts of P via food, fuel, fertilizers, industrial minerals, and other construction materials and produce P-containing waste materials (Metson et al., 2012). Hence, urban landscapes release P from multiple sources, including pet waste, construction sites, leaky sanitary sewers and septic systems, and tree leaf litter decomposition, to downstream aquatic environments (Baker and Brezonik 2007; Bernhardt et al. 2008; Carey et al., 2013; Carpenter et al., 1998; Hobbie et al., 2017;).

During the past decades, many efforts have been made to improve lake water quality by implementing strict measures to abate external total P (TP) loads from agricultural and urban landscapes (Jeppesen et al., 2005; Van der Molen and Boers, 1994). In agricultural landscapes, practices including buffer strips, cover crops, and conservation tillage are used to reduce P export (Sharpley et al., 2000). A common approach to mitigate excess TP loads from urban landscapes to downstream water bodies is the implementation of stormwater management infrastructure, which can reduce peak water flows and nutrient runoff, including that of P (Carey et al., 2013; Garnier et al., 2013; Jacobson, 2011; Shuster et al., 2005).

Even after the abatement of the external P loading, eutrophic conditions have been observed to persist in certain lakes (Carpenter et al., 2005; Schindler et al., 2016). This may be related to the role of internal P loading as a source of bioavailable P to the water column (Robertson et al., 2018; Sondergaard et al., 2003; Van der Molen and Boers, 1994). Under high external total P (TP) loads, sediments can accumulate significant amounts of P in relatively reactive chemical forms (O'Connell et al., 2020). When the external loading decreases, the degradation of these reactive P phases may continue to release dissolved P back to the overlying water column over time scales of decades (O'Connell et al., 2020) or even centuries (Markelov et al., 2019). Moreover, recent studies have shown that salinization may amplify internal P loading due to a strengthening

of the water column density stratification, which in turn enhances dissolved oxygen depletion of the bottom waters (Ladwig et al., 2021; Radosavljevic et al., 2022).

Phosphorus is transported to lakes in a variety of chemical forms with different reactivities (O'Connell et al., 2020; Wang et al., 2013). After entering a lake, the supplied P undergoes further biogeochemical transformations in the water column and bottom sediments, including uptake into biomass, mineralization, adsorption-desorption, and dissolution-precipitation reactions (Katsev et al., 2006; Markelov et al., 2019; Orihel et al., 2017; Van Cappellen and Berner, 1988). A lake's sediment core can therefore serve as a historical archive of the changes in external P loading and in-lake cycling (Bhattacharya et al., 2022; O'Connell et al., 2020; Wang et al., 2013). In addition, sediment accumulation rates measured using dating techniques, such as the ^{210}Pb method, provide information about historical changes in soil erosion and runoff (Dearing, 1991).

In this study, we analyze the impact of watershed LULC changes on the P cycle of a lake in southern Ontario based on chemical profiles in a dated sediment core and, for the more recent past, water quality monitoring data. These data, plus ancillary historical information, delineate four phases of watershed development: (1) early conversion of forest to farmland, (2) agricultural intensification, (3) implementation of agricultural best management practices (BMPs) and initial urban encroachment, and (4) rapid urbanization. We reconstruct lake P budgets representative of the four phases to highlight the impact of LULC changes on the lake's P loading, cycling, productivity and bottom water hypoxia.

2.3. Materials and Methods

2.3.1. Study site: Lake Wilcox and the watershed development

Lake Wilcox (LW) is a kettle lake located in Richmond Hill, along the northern edge of the greater Toronto metropolitan area in Ontario, Canada (Figure A1). The lake has a surface area of 55.6 ha, and a mean and maximum depth of 5.6 and 17.4 m, respectively (Reports 4, 5 and 6 in Table A1; Table A2). The average water residence time of LW is around two years (Reports 4 and 5 in Table A1). The lake has two basins separated by a ridge topping out at around 8 m water depth. The maximum depth of the west basin is 14 m, that of the east basin 17.4 m (see Table A2 for more detailed bathymetric data). The lake's

morphometric ratio is 7.6 m km^{-2} (Report 5 in Table A1). The area of the LW watershed is 2.39 km^2.

The LULC of LW's watershed has changed substantially since the first arrival of European settlers in the Richmond Hill region. The watershed was initially entirely forested. In the late 19th century, deforestation began to open land for farming, continuing after the turn of the century. At the same time, construction of cottages near the lake started (Robinson and Clark, 2000). After World War II, agricultural LULC dominated the watershed. In the 1950s and 1960s, cottages with individual septic tanks and tile beds were built along the lake's shoreline (Robinson and Clark, 2000). Leakage from septic systems likely represented a source of nutrients, especially P and N, to the lake. Municipal sanitary sewer infrastructure was installed in the mid to late 1980s, at which time the septic systems were decommissioned (Report 4 in Table A1). By 1995, almost all homes in the watershed had been connected to the city's sanitary sewer system (Report 4 in Table A1). Since the 1980s, urbanization steadily expanded in the watershed with a rapid growth of impervious land cover since the early 2000s (Figure 2.1).

Concern about eutrophication of LW mounted in the 1980s due to the recurrent incidences of algal blooms and longer periods of deepwater hypoxia (Nürnberg et al., 2003). To combat the blooms, the City of Richmond Hill (CRH; known as the Town of Richmond Hill until 2019) installed a lake aerator in 1998 to lower the efflux of dissolved P from the bottom sediments to the water column, that is, the "internal P loading" (Report 5 in Table A1). Activation of the aerator in 1999, however, coincided with a large, and unexpected, cyanobacterial bloom of *Planktothrix* sp. (Nürnberg, 2003). The aerator was removed after only one year of service.

2.3.2. Coring and sample preservation

Two sediment cores were collected next to each other in the deeper part of LW's east basin (N43°56'58.6" W079°25'57.9") on October 19, 2019, using a Uwitec Hammer corer (Figure A1). Core 1 was 76 cm long and used for geochemical analyses; core 2 was 88 cm long and used for age dating and chlorophyll-*a* analysis. The cores were sectioned in the field into 1-cm intervals using a vertical extruder (Telford et al., 2021). Each sample from core 1 was placed in a Whirl-Pak© bag and frozen at -20 ºC and later freeze dried.

Following freeze drying, a sub-sample of the sediment was ground with a mortar and pestle and sieved to <125 µm. The core 2 depth segments were stored at -4°C in the dark prior to the analyses. Select samples that had been freeze-dried but had not been ground and sieved were analyzed for their grain size distributions using the pipette method (Gee et al., 1986).

2.3.3. Radiometric core dating and areal burial rates

Sediment ages were derived from depth profiles of ^{210}Pb, ^{137}Cs and ^{226}Ra (via daughters ^{214}Pb and ^{214}Bi) activities. Thirty-one 1-cm freeze-dried sections spanning the length of core 2 were analyzed for 23 to 95 hours for radioisotope activity using a co-axial HPGe Digital Gamma Ray Spectrometer (Ortec GWL-120-15) interfaced with Maestro 32 software. Depth-dependent sedimentation rates were obtained with the ^{210}Pb constant rate of supply age model (Appleby and Oldfield, 1978; Appleby et al., 2001). The ^{210}Pb ages from core 2 were transferred to core 1 by aligning the Loss on Ignition (LOI) depth profiles (Thompson et al., 2012). LOI was measured by sub-sampling (0.5 ± 0.05 g) well-mixed wet sediment into a pre-weighted dry crucible and then sequentially heating the sample at 90° (24 hours), 550°C (2 hours), and 950° (2 hours) with 2 hours of cooling in between. Weighing after each heating step yielded the water, organic matter, and carbonate contents (Heiri et al., 2001).

The measured bulk density was used to relate the sediment accumulation rate at a given depth, expressed in units of g cm^{-2} yr^{-1}, to the linear sedimentation rate following Appleby et al. (2001) and Aba et al. (2014) (Figure A2). The depth-dependent areal burial fluxes of TP and other sediment-bound chemical constituents were then calculated by multiplying the sediment accumulation rate by the concentration of the analyte of interest measured in the same core segment.

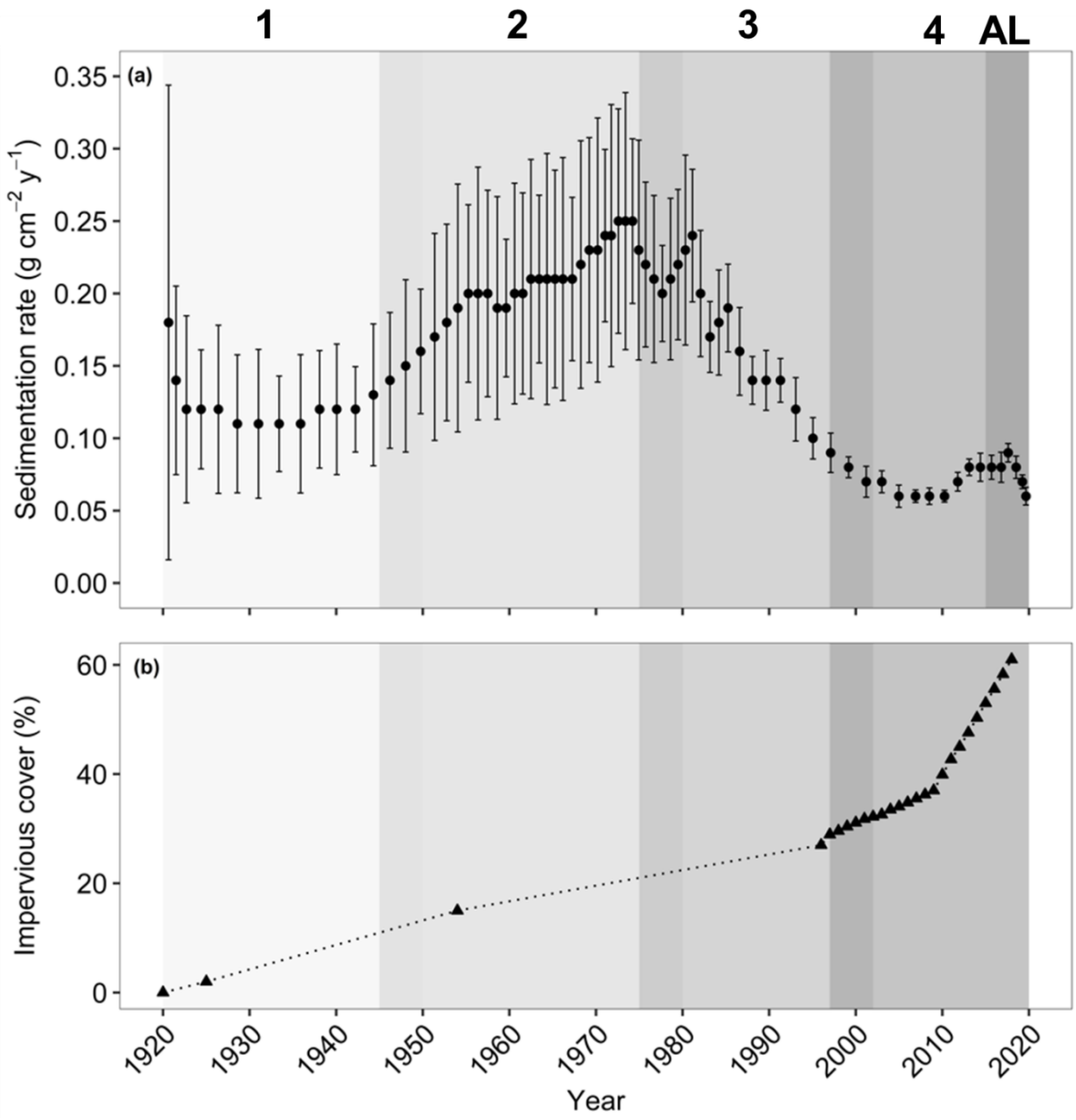

Figure 2.1. (a) Sediment accumulation rate as a function of time calculated using the ^{210}Pb constant rate of supply model with error bars showing standard deviations, (b) percentage of impervious land cover in Lake Wilcox' catchment versus time. Numerals 1 to 4 at the top and the corresponding color shadings indicate the four catchment development phases separated by five-year buffer periods between phases; AL stands for the active (or early diagenetic) surface sediment layer.

2.3.4. Geochemical analyses

Samples for total sediment P, aluminum (Al), calcium (Ca), iron (Fe), potassium (K), sodium (Na), manganese (Mn), and sulfur (S) analysis were extracted according to Aspila et al. (1976) by adding 1 mL of 50% w/v $Mg(NO_3)_2$ to 0.1 g of freeze-dried sediment, then ashing at 550 °C in a muffle furnace for 2 hours. Next, 10 mL of 1M HCl was mixed with the sediment for 16 hours before filtering the extract through a 0.45 µm pore size nylon membrane syringe filter. The HCl extracts were diluted 1:10 in a 2% nitric acid matrix and analyzed by inductively coupled plasma optical emission spectrometry (ICP-OES). The TP detection limit for the overall extraction procedure was 1.7 µmol g^{-1}. A certified reference material for TP, European Commission Community Bureau of Reference BCR Reference Material No. 684 "River sediment (extractable phosphorous)," was included for every series of 15 TP samples being extracted, resulting in 5 replicate analyses. All CRM extractions resulted in TP values within 4% of the certified value with an average recovery of 96% and a precision of <11% RSD among the replicates. The method detection limits for the overall extraction procedure for the elements other than TP were: 76.0, 208, 3.6, 7.3, 3.9 and 19.9 µmol g^{-1} for sediment Al, K, Mn, Fe, S, Na and Ca, respectively. Note that the method of Aspila et al. (1976) does not extract forms of elements strongly bound in crystalline mineral phases.

Total organic carbon (TOC) and total nitrogen (TN) were analyzed by combustion at 600 °C on an elemental analyzer (Elementar vario EL cube). While the combustion method may release some inorganic N, TN is mostly composed of N bound in organic compounds. Approximately 30 mg of freeze-dried, ground, and sieved sediment were weighed and put into a tin wrap. The detection limits were 0.1 and 0.14 mmol g^{-1} for TOC and TN, respectively. Sulfanilamide was used as an internal standard, and its measured organic C and N contents were within 10% and 20% error, and were detected with a precision of <3% and <9% RSD among the replicates, respectively. X-ray diffraction (XRD) and scanning electron microscopy-electron dispersive spectroscopy (SEM-EDS) analyses were performed on a subset of core sections spanning the four watershed development phases for identification of crystalline minerals (XRD) and analysis of morphology and elemental composition of areas of interest in the sediment samples (SEM-EDS). Details on the XRD and SEM-EDS methods are provided in the Supporting Information (Text A2).

2.3.5. SEDEX: Sequential extractions of sediment P

The SEDEX sequential extraction method of Ruttenberg et al. (2009) was applied to separate the following operationally defined sediment P pools: easily exchangeable (P_{Ex}), humic-bound (P_{Hum}), redox-labile (P_{Fe}), calcium-bound (i.e., carbonate- and apatite-bound) (P_{Ca}), detrital apatite and other inorganic mineral-bound P (P_{Det}), and organic (P_{Org}) P pools. The successive extractants were: 1 M $MgCl_2$, 1 M $NaHCO_3$, citrate-dithionite (CDB), 1 M acetate at pH 4, 1 M HCl, and 1 M HCl after ashing at 550ºC (see Figure A3). Note that the original SEDEX method of Ruttenberg was modified by the addition of the 1 M $NaHCO_3$ extraction step of Baldwin (1996) to release P bound to humic substances (Audette et al., 2020; O'Connell et al., 2020; Parsons et al., 2017).

Extractions were performed on 0.1 g of freeze-dried sediment with the manifold system of Ruttenberg (2009). For each extraction step the supernatant was diluted 1:10 in a 2% nitric acid matrix and the P concentration measured by ICP-OES. Matrix-matched standards for each sequential extraction reagent were analyzed to correct for matrix effects. Each sample was extracted in duplicate. The sum of the sequentially extracted chemical P pools compared well with the TP values obtained with the Aspila et al. (1976) method, with a mean percent error of 4.5%. The same certified reference material (European Commission Community Bureau of Reference BCR Reference Material No. 684) used to validate the Aspila et al. (1976) TP extraction method was added in duplicate for each batch of 8 samples being extracted in duplicate. The TP extracted by SEDEX (i.e., the sum of all the SEDEX fractions) in the certified reference material were within 5% of the certified TP value.

2.3.6. Pigments: chlorophyll-a and pheophytin

Chlorophyll-*a* and pheophytin were analyzed by High-Performance Liquid Chromatography (HPLC). Approximately 3.0-4.0 g of wet sediment was subsampled from each 1-cm core segment and transferred to a 20 mL glass scintillation vial and freeze-dried in the dark. The freeze-dried samples were extracted in a mixture of acetone and methanol (80:20) for 24 hours then dried under inert N_2 gas and re-eluted in calibration solvent consisting of a mixture of methanol and ion-pairing reagent (7.5 g L^{-1} tetrabutyl ammonium acetate mixed with 77 g L^{-1} ammonium acetate) and an internal standard

(Sudan II). Samples were analyzed on a Waters Alliance HPLC following standard methods (Leavitt et al., 1989; Mantoura and Llewellyn 1983). The chlorophyll-*a* and pheophytin concentrations were determined from the chromatographs according to Jeffrey et al. (1997). Algal pigment concentrations were expressed in µg chlorophyll-*a* and µg pheophytin per g organic matter (OM from the LOI measurement). For each core segment, the areal chlorophyll-*a* burial rate (ng cm^{-2} yr^{-1}) was then calculated by multiplying the chlorophyll-*a* concentration by the organic matter burial rate.

2.4. Results

2.4.1. Watershed development phases

Four phases of watershed development were identified based on a break point analysis of the core-derived sediment accumulation rate time series. The breakpoint analysis was conducted using the Davies test using the Segmented Package in R (Muggeo, 2008) (for additional details on the breakpoint analysis, see Supplementary Information: Text A3 and Figure A4). The resulting temporal definitions of the phases were consistent with historical LULC information, historical accounts and, for more recent decades, direct water quality monitoring data (Table 2.1). The phases are shown by shading in the time series figures (Figures 2.1-2.4). Because the transitions between successive development phases are gradual, we separated the phases by 5-year buffer periods.

Phase 1, which saw the continuation of growing European settlement and farming, began before the earliest date reached by the sediment core (i.e., around 1920) and lasted until the end of World War II (1945). Phase 2 corresponds to the period of agricultural intensification of the watershed and lasted for about 25 years (from 1951 to 1975). Introduction of agricultural BMPs and inroads by urban LULC define Phase 3 (1981-1997). In Phase 4 (2003-2019), urban development greatly accelerated. Although Phase 4 is still ongoing, here it extends until 2019 when the sediment core was collected.

The topmost 5 cm of the core were identified as the biogeochemically active layer, that is, the depth interval where most of the physical, geochemical, and biological transformation processes of the deposited sediments are concentrated. The processes in this so-called early diagenetic layer largely control the chemical exchanges between the bottom sediments and the water column, including internal nutrient loading (Wang et

al., 2003). The active layer is indicated in the figures showing sediment core results by the darker shading at the far right of the panels and the label AL (short for active layer). The variations in the chemical depth profiles below the active layer are assumed to record historical changes in the watershed-lake system.

2.4.2. Sedimentation rates and grain size distributions

The sediment at the bottom of core 1 was deposited circa 1920 based on the ^{210}Pb dating (Figure A2). The ^{210}Pb CRS model further yielded sedimentation rates ranging from 0.05 to 0.25 g cm^{-2} y^{-1} (Figure 2.1). In Phase 1, the sediment accumulation rate was around 0.12 g cm^{-2} y^{-1}. After 1950, the rate increased to peak values of about 0.25 g cm^{-2} y^{-1} by the mid-1970s (Phase 2). From 1980 on, the sediment accumulation rate dropped and since the mid-1990s has remained below 0.1 g cm^{-2} y^{-1} in Phases 3 and 4. Throughout Phases 1, 2 and 3, the sediment comprised on average 6% sand, 62% silt, and 32% clay (Figure A11). The most notable feature in the grain size depth distribution is the decrease in the proportion of silt and the corresponding increase in the proportion of clay in Phase 4 relative to the preceding 3 phases.

2.4.3. TP sediment concentrations and burial rates

The average sediment TP concentration in the core was 35 µmol g^{-1}. The TP concentration declined gradually between 1920 and 1990, followed by an increase from 33 to 49 µmol g^{-1} in sediments deposited between 1991 and 1999 (Figure 2.2). A subsequent sharp increase occurred between 2016 and 2019, from 40 µmol g^{-1} to a core-top concentration of 55 µmol g^{-1}. Concentrations of the other elements extracted by the Aspila et al. (1976) method used to extract TP are given in Table A3.

The areal TP burial rate followed a very different trajectory than the sediment TP concentration, roughly paralleling the sedimentation rate (Figure 2.2). The TP burial rate increased from 5.0 µmol cm^{-2} y^{-1} in 1951 to a maximum of 8.5 µmol cm^{-2} y^{-1} in 1973, that is, during the period of agricultural intensification (Phase 2). After the early 1980s, the TP burial rate dropped to values below those observed prior to 1940. After reaching a minimum of 2.3 µmol cm^{-2} y^{-1}, the burial rate increased slightly during 2010-2019.

Table 2.1. The four watershed development phases of Lake Wilcox, southern Ontario, Canada. The percentages indicate the average contributions of natural (Nat), agricultural (Ag) and urban (Urb) land cover during each period.

Phase	Period	LULC development	% Nat	%Ag	%Urb
1	1920-1945	Significant conversion of forested to agricultural land; country cottages	75	25	0
2	1951-1975	Agricultural intensification; nearshore cottages with septic systems	40	50	10
3	1981-1997	Agricultural BMPs and urban transition	40	35	25
4	2003-2019	Urban intensification; stormwater management infrastructure	35	20	45

2.4.4. Sediment P speciation

The relative contributions to TP of P_{Ex} and P_{Org} decreased between 2019 and 2015 (i.e., from depth 0 to 5 cm) from 21.5% to 5% and from 38% to 33%, respectively. At the same time, the relative contributions of P_{Fe}, P_{Hum}, P_{Detr} and P_{Ca} increased from 14% to 19%, from 18% to 22%, from 4 to 9%, and from 4.5 to 12%, respectively (Figure 2.2, Figure A5). Sediments deposited in 1999 showed peak concentrations of P_{Ex}, P_{Org}, P_{Fe} and P_{Hum} relative to the adjacent sediments, that is, those deposited in the early 1990s and around 2002. Aside from the pronounced increases between 2015 and 2019 plus the peak values of 1999, the concentration and relative contribution of P_{Org} progressively increased from Phase 2 to Phase 4 (i.e., between the late 1970s and 2015). The fractions of P_{Hum}, P_{Fe} and P_{Ca} remained relatively unchanged throughout the core, while that of P_{Detr} decreased between 2000 and 2019. The concentrations of P_{Hum} and P_{Org} exhibited significant ($p<0.05$) positive correlations with the TOC concentration (Figures A6, A7).

2.4.5. Burial rates of Al, Fe, Ca and K

The burial rates of the mineral-associated elements Al, Fe, Ca and K all showed temporal trends very similar to that of the sediment accumulation rate (Figure A10, Figure 2.2a). In short, the burial rates of these elements remained relatively constant throughout Phase 1, rose during Phase 2, then decreased from their peak values in Phase 3, and reached their minimum values in Phase 4 (Figure A10). Thus, as for TP, the lowest burial rates for all four of the mineral-associated elements were observed in Phase 4.

2.4.6. Sediment geochemistry: XRD and SEM

Pyrite was detected by XRD in sediment deposited during Phase 2 and Phase 4 but not during Phases 1 and 3 (Table A4). This did not mean that pyrite was absent from sediments in Phases 1 and 3, but rather that the mineral's abundance was lower than the XRD detection limit (~1 % by volume). In fact, SEM images identified iron- and sulfur-rich framboidal structures consistent with pyrite or greigite throughout the entire length of the core (Figure A8).

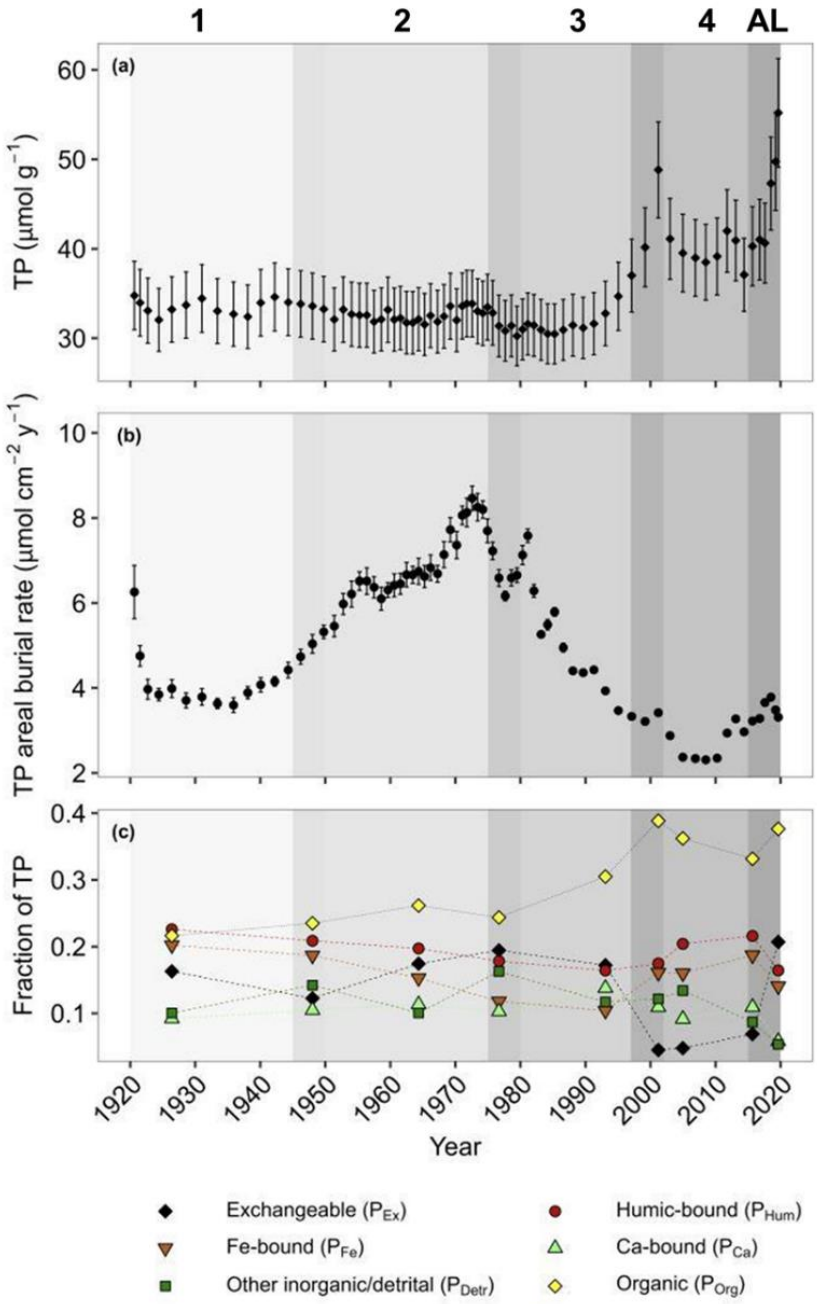

Figure 2.2. Sediment phosphorus versus year of deposition: (a) total phosphorus (TP) concentration, (b) TP areal burial rate (or mass accumulation rate), (c) fractions of the different sediment P pools determined by sequential chemical extractions. Numerals and color shading as in Figure 2.1. Note that the broken lines in panel (c) are only intended to guide the eye – they have no theoretical meaning.

2.4.7. Concentrations of TOC, TON, and TOC:TON and TOC:TP ratios

The TOC and TN concentrations exhibited similar temporal trends with a pronounced maximum between 1960 and 1970, followed by a drop and minimum values during the late 1980s and early 1990s (Figure 2.3). In the late 1990s, the TOC and TN concentrations rose again to values comparable to those between 1960 and 1970. Phase 4 saw slight decreases in the TOC and TN concentrations, while the active sediment layer (top 5 cm) was characterized by steep gradients with the highest concentrations at the sediment-water interface.

Prior to 1980, most molar TOC:TN ratios were above 10, with a slightly increasing trend during Phase 2 (Figure 2.3). During Phase 3, TOC:TN values dropped to about 9.5, remaining between 9.5 and 10 in Phase 4. The molar TOC:TP ratios ranged from 203 to 319 with a mean of 240 (Figure 2.3). The general trend of TOC:TP resembled that of the TOC concentration. The peak TOC:TP values in the 1960-1970 period were entirely due to changes in the TOC concentration. Between 1960 and 1965, both the TOC:TP ratio and the TOC concentration increased by a factor of 1.4, while the TP concentration hardly changed. By contrast, the approximately 25% increase of the TOC:TP ratio from Phase 3 to Phase 4 was substantially lower than the corresponding 60% rise in TOC concentration because of the increasing TP concentration from Phase 3 to Phase 4 (Figure 2.3).

The TOC burial rate (or TOC mass accumulation rate) experienced its greatest rise during Phase 2, from 1.2 to 2.3 mmol cm^{-2} y^{-1} between 1951 and 1970 (Figure 2.4). After 1980, the combined decreases of both the sedimentation rate and the TOC concentration caused the TOC burial rate to drop to 0.7 mmol cm^{-2} y^{-1} by the end of the 20^{th} century. In Phase 4, the magnitude of the TOC burial rate remained below values observed in Phase 1 (excluding the topmost 5 cm AL).

2.4.8. Pigments

The pheophytin burial rates increased during Phase 2 (1951-1975), reaching their highest values (range 0.06–0.34 µg cm^{-2} $year^{-1}$) toward the end of Phase 2 and during the transition between Phases 2 and 3. Following the maximum pheophytin burial rates of the 1975-1981 period, the values decreased during Phase 3 and reached a relatively

constant value in Phase 4 (excluding the 0-5 cm AL layer) (Figure 2.4). The near constant chlorophyll-*a*:pheophytin ratios throughout the core suggested that the depth-dependent changes in the chlorophyll-*a* and pheophytin concentrations and burial rates likely reflected variations in the lake's algal productivity and not differences in the extent of early diagenetic processing.

The chlorophyll-*a*:pheophytin ratio did not exhibit any systematic trends except in the most recent 4 years (i.e., in the 0-5 cm AL layer), when the ratio decreased sharply down-core, confirming that this depth interval is the active layer of the sediment where the degradation of deposited organic matter drives biogeochemical activity (Van Cappellen and Gaillard, 2018) (Figure 2.4).

2.5. Phosphorus budget calculations

To link watershed LULC changes and the lake's TP budget, we constructed a steady state lake TP budget (see conceptual diagram in Figure A8) for each of the four development phases. The derivation of the TP fluxes in Phases 3 and 4 was informed by the relatively large abundance of monitoring data. In the absence of similar data for Phases 1 and 2, additional assumptions had to be made. For Phases 1, 3 and 4 the budgets are representative for the average, mid-phase lake conditions. For Phase 2, the fluxes are illustrative of the late-phase conditions when the sediment core data suggest the lake reached its most eutrophic state. The following sections describe the various estimation methods used, based on the sediment core data reported in section 3 and additional details provided in the Supplementary Information (Tables A5 and A6).

2.5.1. TP burial fluxes

At steady state, the external TP influx to the lake (F_{ext}), supplied by the watershed inflow plus atmospheric deposition, is balanced by the TP permanently buried in the lake's bottom sediments (F_{bur}) plus the outflux of TP through the outflow channel (F_{out}):

$$F_{ext} = F_{bur} + F_{out} \quad (2.1)$$

Areal TP burial fluxes (in units of μmol cm^{-2} yr^{-1}) for Phases 1, 3, and 4 were the arithmetic means of the TP burial rates calculated as the product of the sediment TP concentration [μmol g^{-1}] and the sediment mass accumulation rate [g cm^{-2} y^{-1}] for all the core segments

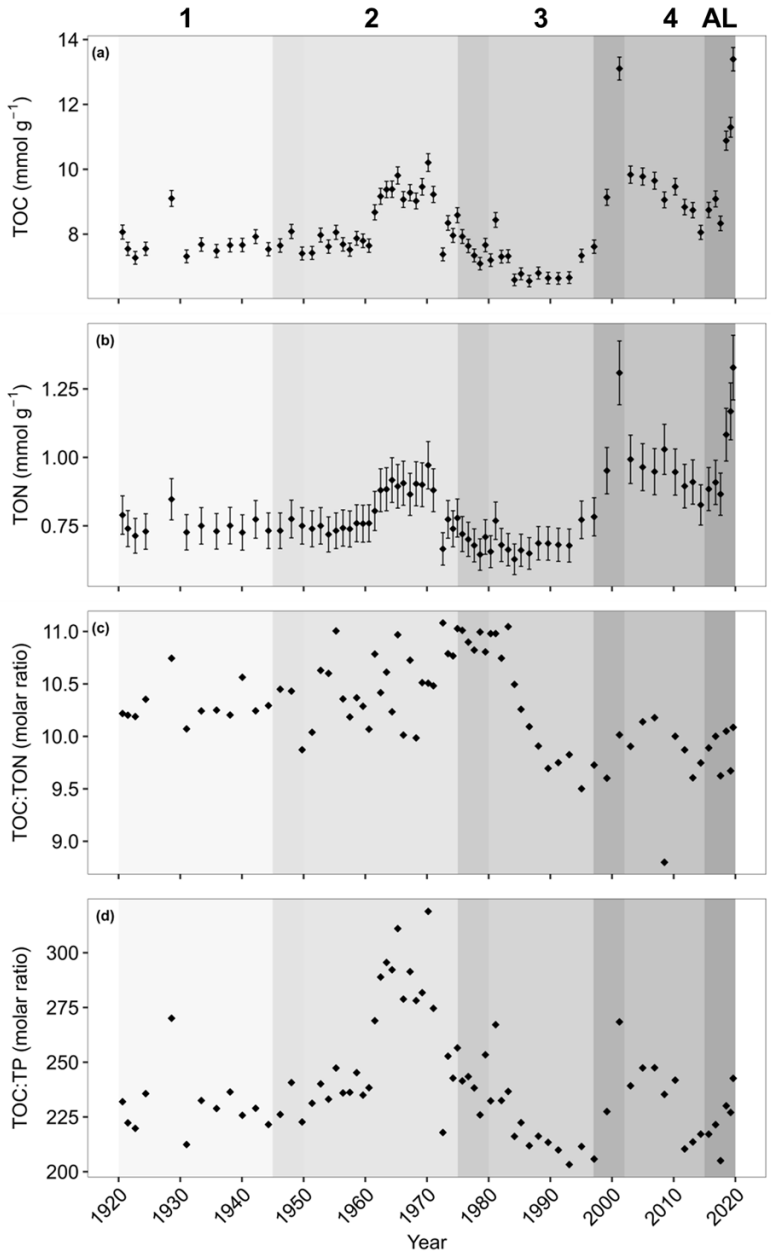

Figure 2.3. Sediment organic matter composition versus year of deposition: (a) total organic carbon (TOC) concentration, (b) total organic nitrogen (TON) concentration, (c) TOC:TON ratio, and (d) TOC:TP ratio. Numerals and color shading as in Figure 2.1.

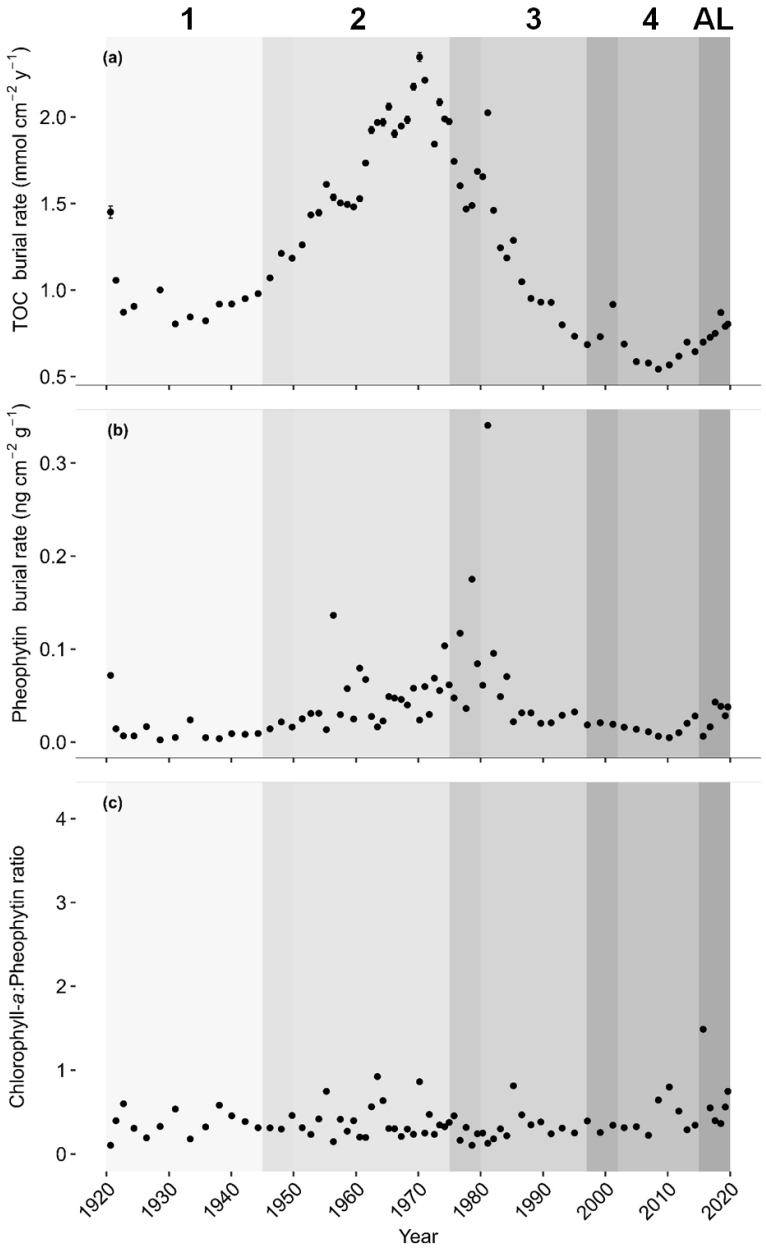

Figure 2.4. Organic matter burial versus year of deposition: (a) total organic carbon (TOC) burial rate (or mass accumulation rate), (b) pheophytin burial rate, (c) chlorophyll-*a*:pheophytin ratio. Numerals and color shading as in Figure 2.1.

within that phase. Data from the topmost 0-5 cm active layer of sediment were excluded from the areal TP burial flux calculation for Phase 4. The areal TP burial flux of the Phase 2 TP budget was the average for the 1970-1975 period during which the maximum TOC and chlorophyll-*a* accumulation rates were observed to represent the most severe eutrophic state of the lake (Figure 2.4).

To estimate whole-lake TP burial fluxes (F_{bur} in units of kmol yr^{-1}) the area of active sediment deposition (ASD) needed to be determined. In lakes with steep bathymetry, such as kettle lakes, sediment tends to accumulate in the deepest areas (Lehman, 1975; Carpenter, 1983) and ASD is therefore expected to be smaller than the total surface area of the lake. For Phases 3 and 4, ASD values were obtained by calculating F_{bur} as the difference $F_{ext} - F_{out}$ and then dividing F_{bur} by the areal TP burial flux obtained from the core data. Average values of F_{ext} and F_{out} were derived from TP concentration and discharge data measured by CRH at the lake inlets and outlet. Flow-weighted TP fluxes were calculated following Walling and Webb (1985) and Moatar and Meybeck (2005). Table A1 summarizes the CRH reports containing the relevant data. Atmospheric TP input to the lake was estimated from deposition rates in the literature (Table A6). For Phases 3 and 4, atmospheric deposition accounted for 8 and 6% of the total TP input to the lake, respectively.

For both Phases 3 and 4, the resulting ASD area was found to be 6.05 ha or about 11% of LW's open water surface area (Table A2). In addition to LW's low depth ratio (i.e., the ratio of mean depth to maximum depth) of 0.32, the relatively small ASD value also reflected the fact that the sediment core was retrieved from the deepest part of the lake, therefore, yielding higher than whole-lake average areal sediment accumulation rates. The same ASD value of 6.05 ha was assumed to apply to Phases 1 and 2, enabling the calculation of the corresponding F_{bur} values from the areal TP burial fluxes derived from the sediment core data.

2.5.2. Lake TP budgets: Phases 3 and 4

The steep concentration depth gradients of chemical compounds resulting from microbially mediated degradation, such as TOC, TON, TP and chlorophyll-*a*, identified the topmost 5 cm of sediment as the active layer of post-depositional biogeochemical

processing (Van Cappellen and Gaillard, 2018). The TP concentration dropped from ~55 μmol g^{-1} at the SWI to ~40 μmol g^{-1} at 5 cm depth. Based on the radiometric dating, the 0-5 cm depth interval was found to represent about 4 years of deposition. We attributed this drop in TP to the early diagenetic release of solid-bound P to the pore water, from which it then returns to the water column (Van Cappellen and Berner, 1988). Below the top 5 cm, the sediment TP stabilized at a value of ~40 μmol g^{-1} between 2000 and 2015, which we assumed represented P preserved through burial in Phase 4. The P deposition flux at the sediment surface was then estimated by multiplying the P burial flux at 5 cm by a factor of 1.375 (= 55:40). Assuming steady state, the difference between the deposition and burial fluxes equals the internal P loading flux. This approach yielded a value of the whole-lake internal loading flux (F_{int}) of 0.62 kmol yr^{-1} and an areal loading flux of about 1.0 μmol cm^{-2} yr^{-1} for Phase 4.

Our previous analysis of LW's post-1990 water chemistry data revealed an intensification of internal P loading caused by the rapid increase in the lake's salinity that stabilizes the water column's summer stratification (Radosavljevic et al., 2022). The latter promotes longer periods of bottom water hypoxia during which the sediments release dissolved P (Figure 2.5), mostly as inorganic P or DIP, to the hypolimnion (Markelov et al., 2019; Nürnberg, 1987). As a result, the DIP to TP molar ratio (DIP:TP) in the hypolimnion also exhibited an increasing trend with time, with an average DIP:TP value of 0.76 in Phase 4 and 0.55 in Phase 3 (Radosavljevic et al., 2022). Assuming that the increase in the DIP:TP ratio from Phase 3 to Phase 4 was proportional to the increase of the internal P load from the sediments, a value for F_{int} in Phase 3 of 0.45 kmol y^{-1} was estimated.

Equation (2.1) expresses the steady state mass balance of TP for the lake's water column plus the topmost 0-5 cm depth interval of sediment in which post-depositional biogeochemical reactions drive the internal P loading (Figure A8). Alternatively, one can consider the TP mass balance for the water column alone, hence explicitly accounting for the whole-lake TP internal loading (F_{int}) and deposition (F_{dep}) fluxes:

$$F_{dep} = F_{bur} + F_{int}. \qquad (2.2)$$

For Phases 3 and 4, the previously estimated F_{bur} and F_{int} values then yielded the F_{dep} values.

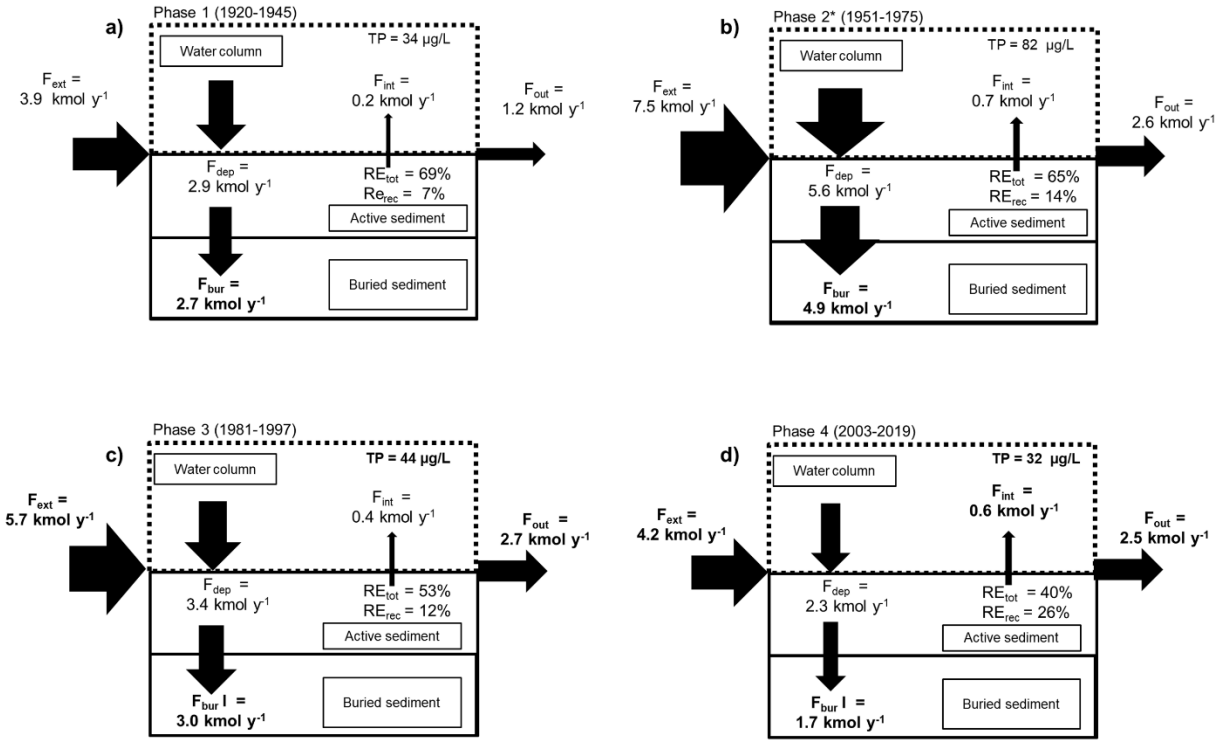

Figure 2.5. Total phosphorus (TP) budgets for the four development phases of Lake Wilcox' watershed. For Phases 1, 3 and 4, the budgets are representative of mid-phase conditions. For Phase 2*, the budget is representative of late-phase conditions, when the lake reached peak eutrophication intensity. The concentrations and fluxes indicated **in bold** on the panels are those that are directly constrained by observational data.

2.5.3. Lake TP budgets: Phases 1 and 2

For Phases 1 and 2, we first estimated average water column TP concentrations based on the chlorophyll-*a* burial rates. Changes in chlorophyll-*a* burial rates track changes in water column chlorophyll-*a* concentrations (Routh et al., 2009; Szymczak-Żyła et al., 2011) that, in turn, have been shown to correlate linearly with water column TP concentrations (Jones and Bachmann, 1983). Hence, water column TP concentrations for Phases 1 and 2 were derived by multiplying the TP concentration of Phase 3 (44 µg L^{-1}) by the chlorophyll-*a* burial rates in Phases 1 and 2 normalized to that in Phase 3. As for the TP burial flux (section 4.1), the Phase 2 chlorophyll-*a* burial rate used was representative of the late-phase eutrophic maximum.

Next, values of F_{out} were calculated by multiplying the estimated TP concentrations for Phases 1 and 2 (34 and 82 µg L^{-1}, respectively) with the lake's annual volumetric outflow discharge, Q_{out}. The latter was adjusted to account for the increased surface runoff due to urbanization (Brabec et al., 2002; Fletcher et al., 2013; Li et al., 2018). Hence, for Phases 1 and 2 we used the reported Q_{out} value of 2816 m^3 d^{-1}, that is, 46% lower than the 5175 m^3 d^{-1} value of Phase 3 and 60% lower than the 6998 m^3 d^{-1} of Phase 4 (Table A1). The values of F_{out} were used with the previously estimated F_{bur} values to derive the input fluxes F_{ext} (Equation 1). These F_{ext} values fall within the ranges calculated using reported TP export coefficients of the major LULC types (i.e., forested, agricultural, and urban) under similar climate conditions (Table A5) weighted by the estimated surface areas of the LULC types in each development phase (Table A6).

Values of F_{dep} were obtained with the relationship proposed by Nürnberg (1984) describing the efficiency with which TP is removed from the water column in stratified lakes by sediment deposition at the lake floor (RE_{dep}):

$$RE_{dep} = \frac{F_{dep}}{F_{ext}} = \frac{15}{18 + q_s} \tag{2.3}$$

where q_s [m y^{-1}] is the outflow Q_{out} from the lake divided by the lake surface area. For Phases 1 and 2, the value of q_s is 1.87 m y^{-1}, hence, resulting in an RE_{dep} value of 0.75 (i.e., 75% of TP entering the lake is deposited). Combining the estimates of RE_{dep} and

F_{ext} provided the F_{dep} values, while the differences between F_{dep} and F_{bur} yielded the internal loads, F_{int}. For further discussion of empirical relationships such as Equation (2.3), the reader is referred to the extensive work on this topic by Nürnberg (2009).

Additional metrics used to describe changes in P cycling in the lake included the sediment TP recycling efficiency (RE_{rec}) and the whole-lake TP retention efficiency (RE_{tot}) defined as (Figure A8):

$$RE_{rec} = \frac{F_{int}}{F_{dep}} \tag{2.4}$$

and

$$RE_{tot} = \frac{F_{ext} - F_{out}}{F_{ext}} = \frac{F_{bur}}{F_{ext}} \tag{2.5}$$

The reconstructed lake TP budgets for all four watershed development phases are summarized in Figure 2.5.

2.6. Discussion

2.6.1. Sedimentation rate as indicator of changing LULC

The changes in sedimentation rate in the lake over time reflect the changes in watershed LULC and the resulting changes in soil erosion and sediment runoff. Historical records indicate that the initial European settlement in LW's watershed and surrounding areas took place in the early 1800s. Phase 1 (1920-1945) represents the continuation of settlement, land clearance and other land use developments of the watershed, including the construction of lakeshore cottages that began around 1912. During this phase, the sedimentation rate remained relatively steady. A distinct increase in sedimentation accumulation signals the post-World War II agricultural intensification and the start of Phase 2 (1951-1975) (Figure 2.1). Agricultural land use, especially when it involves soil tilling, can contribute high sediment yields because of high soil erosion (Matisoff et al., 2002; Fu et al., 2006). Superimposed on the steady rise of the sediment accumulation rate of Phase 2 there is a small local peak in the mid-1950s (Figure 2.1), which may have recorded a surge in sediment yields due to the extreme rainfall during the passage of Hurricane Hazel in October 1954 (Nirupama et al., 2014).

The mid-1970s and onwards decrease in the sedimentation rate (Figure 2.1) is best explained by the generalized adoption of no-till and other BMPs by farmers in southern Ontario (Smith, 2015). A decrease in soil erosion and, hence, in terrestrial organic matter input to the lake is also consistent with the observed drop of the TOC:TN ratio in Phase 3 (Figure 2.3), which points to an increasing fraction of in-lake produced algal organic matter in the sediments (Meyers, 2003). Another contributing factor may have been the channelization of the lake's outlet. The outlet channel was built in 1978 to control the water level by increasing the flushing rate of the lake (Reports from table A1) that, at the same time, may have allowed more of the suspended sediment load to wash out of the lake.

In addition to the implementation of agricultural BMPs, LW's watershed during Phase 3 experienced a slow transition from agricultural to urban LULC. The 1980s ushered in a period of cottage development and population growth in the watershed. Consequently, impervious land cover rose above 15%, reaching 25% by the end of Phase 3. Previous work has shown 15% impervious cover to represent a threshold beyond which significant changes in watershed suspended sediment and TP loads are usually observed (Brabec et al., 2002; Jacobson, 2011; Schindler et al., 2016). Despite the increase in impervious land cover, the sedimentation rates and TP burial rates kept decreasing in Phase 3 and further in Phase 4. We attribute this to the implementation of stormwater management infrastructure.

Even during Phase 4 (2003-2019), when urbanization greatly accelerated and impervious land cover increased to 60%, the sedimentation rate remained near its lowest levels. The latter part of Phase 3 and Phase 4 saw the systematic expansion of the storm sewer system in LW's watershed, while stormwater management ponds and bioswales were installed to manage the increases in stormwater peak volumes and flow rates. Stormwater management ponds are known to significantly reduce sediment yields from urban areas (Verstraeten and Poesen, 2000), thus explaining why sedimentation rates in the lake have remained low in Phase 4. Further evidence for sediment retention by the stormwater ponds is the finer grain size of lake sediments in Phase 4 (Figure A11), consistent with a preferential retention of coarser silt-sized suspended matter over clay-sized suspended matter.

2.6.2. Sediment TP, speciation, and burial rates

The top 5 cm of sediment represents the active layer (section 2.4.2). From the sediment surface down to 5 cm depth (i.e., in the most recent 4 years in the time series figures), the TP concentration exhibits a large drop, which is mostly accounted for by decreases in the concentrations of P_{Ex}, P_{Fe}, P_{Hum} and P_{Org} (Figures 2.2 and A5), that is, the more labile P pools that undergo post-depositional remobilization by biogeochemical processes including desorption, (reductive) dissolution, and mineralization (Hyacinthe and Van Cappellen, 2004; Joshi et al., 2015; Quiquampoix and Mousain, 2005; Syers et al., 1973; Zhu et al., 2016). The release of P from these sediment pools drives the internal P loading flux from the sediments (Katsev et al., 2006; Orihel et al., 2017; Markelov et al., 2019). Note that, in addition to P desorption from mineral surfaces, P release by lysis of deposited algal cells may contribute to P_{Ex} because of the high ionic strength and osmotic pressure of the 1 M $MgCl_2$ extraction solution (Ruttenberg, 1992). Furthermore, salinization can alter P speciation by decreasing P_{Fe} and P_{Ex}. Dissolved phosphate ions can be displaced from sorption sites by competing anions, in particular chloride, hence reducing P_{Ex} (McCarter et al., 2019), while the intensification of hypolimnion hypoxia accompanying the salinization of LW (Radosavljevic et al. 2022) enhances the release of P_{Fe} to solution due to the reductive dissolution of ferric iron oxyhydroxides (Parsons et al., 2017).

The transition from Phase 1 to Phase 2 marks the onset of the intensive use of synthetic fertilizers in southern Ontario (Van Staden et al., 2022). The production of synthetic fertilizers significantly increased after the conclusion of the Second World War (Raven and Wagner, 2021). In southern Ontario, this led to a rapid rise in the use of these fertilizers starting in the early 1950s and peaking around 1980 (Van Staden et al., 2022). The transition from Phase 1 to Phase 2 marks the onset of agricultural intensification enabled by the greatly expanded availability of fertilizers to farmers. In addition, in the 1960s and 1970s new cottages with septic systems were built close to the shoreline. Together, this would have increased the input of P to the lake and stimulated in-lake biological productivity.

The rising TP burial rates in Phase 2 are accompanied by increases in the fractions of P_{Ex} and P_{Org}, balanced by decreases in those of P_{Fe} and P_{Hum} (Figure 2.2). Faster sediment accumulation rates enhance the preservation of relatively reactive P pools, such as P_{Ex} and P_{Org}, that would otherwise be more extensively remobilized by early diagenetic processes (Ingall and Van Cappellen, 1990; Sobek et al., 2009). As also implied by the TOC and chlorophyll-*a* burial rates, the increasing external P input to the lake during Phase 2 would have stimulated the lake's primary productivity, in turn enhancing the degradation of organic debris and intensifying bottom water hypoxia. Hence, conditions would have been less favorable for the burial of phosphate ions associated with ferric iron oxyhydroxides and those forming ternary complexes with humic matter and ferric iron as the bridging cation (O'Connell et al., 2020). Note, however, that because of the large increase in the TP burial rate, the burial rates of all sediment P pools increase during Phase 2 (Figure 2.1 and 2.2).

The most distinct change in sediment P speciation seen in Phases 3 and 4 is the pronounced increase of the P_{Org} fraction (Figure 2.2). At first glance, this could be interpreted as signaling a worsening eutrophication of the lake. However, because of the large drop of the sediment accumulation rate, the burial rate of P_{Org} decreases despite its increased concentration. We attribute the dominant contribution to sediment TP of the P_{Org} fraction during Phase 4 to the implementation of stormwater ponds in LW's watershed and the efficient retention of particulate inorganic P phases in these ponds, especially P_{Detr}, P_{Ca}, and P_{Ex} (Greb and Bannerman, 1997). That is, the stormwater ponds reduce the dilution of in-lake produced P_{Org} by land-derived P. This interpretation is further supported by Phase 4 having the lowest burial rates of the geogenic elements Al, Fe, Ca, and K (Figure A10) and the decrease in the fraction of silt in the lake sediments (Figure A11), indicating the preferential retention of silt-sized land-derived inorganic material in the stormwater ponds.

Our previous analysis of water quality monitoring data available for the mid-1990s onwards confirms that the TP loading from the watershed has been on a declining trajectory during the past decades (Radosavljevic et al., 2022). At the same time, the progressive salinization of the lake, primarily due to the significant use of road salt in winter (on average 52 g m^{-2} of road salt are applied per snow event according to Report

6 in Table A1), has resulted in longer periods of summer stratification (Radosavljevic et al., 2022). With the ongoing salinization of LW, the water density has been steadily increasing. This has further been strengthening the thermal stratification during summer, hence, expanding the annual period of hypoxia in the hypolimnion (Ladwig et al., 2021; Radosavljevic et al., 2022). The longer period of oxygen-depleted bottom waters, in turn, enhances internal P loading and explains the increasing trend of the DIP:TP ratio observed in the hypolimnion (Radosavljevic et al., 2022). An additional mechanism explaining the increase in internal loading in Phase 4 could be the enhanced retention in stormwater ponds of the mineral elements Fe, Al and Ca (Figure A10), hence, decreasing the sediment accumulation of P by mineral adsorption and co-precipitation (Markovic et al., 2019).

The inferred lower urban TP loads of Phase 4 diverge from other studies that found urban TP loads to be of comparable magnitude to those from agricultural areas (Janke et al., 2014; Petrone, 2010; Wollheim et al., 2005). These contrasting findings indicate that while P wash-off from urban areas is an important source of P (Zhou et al., 2023), stormwater management can significantly attenuate the export of urban P to downstream aquatic ecosystems.

Overall, the sediment TP concentration and the TP burial rate depth profiles exhibit distinctly different trends (Figure 2. 2). This is particularly evident when comparing Phase 2 to Phase 4. During Phase 2, the TP burial rate exhibits a steep increase while the TP concentration stays roughly constant. In Phase 4, the sediment TP concentration reaches its maximum level while, at the same time, the TP burial rate drops to its lowest level. Thus, when only considering the temporal variations of the sediment TP concentration, one might erroneously conclude that urban growth in the watershed may result in greater P enrichment of LW compared to the pre-1980s period of agricultural intensification. A completely opposite storyline emerges, however, when the changes in the sediment TP burial rate that accompany the changes in LULC are taken into account.

2.6.3. Lake productivity and hypoxia

Multiple parameters in the sediment core data imply that LW's primary productivity was highest during the second half of Phase 2, that is, from ~1960 to the mid-1970s, similar

to other lakes in southern Ontario (Meyers, 2003). During this period, the burial rates of TOC, TN, TP, and chlorophyll-*a* all reached their peak values (Figures 2.2, 2.3 and 2.4). In addition, the sediment TOC:TP molar ratios attained their maximum values (Figure 2.3), which we attribute to an intensification of bottom water hypoxia due to the increased degradation of organic detritus (Müller et al., 2012) following seasonal periods of high algal productivity (Adams et al., 2022). Bottom water hypoxia is known to enhance the preservation efficiency of sediment TOC while decreasing that of TP (Ingall and Jahnke, 1996).

Hypoxia during Phase 2 is also supported by the detection by XRD of pyrite in the corresponding sediments, but not in the sediments from Phases 1 and 3 (Table A4). Pyrite is an indicator of bottom water redox conditions (Roychoudhury et al., 2003; Wilkin et al., 1996). The XRD results therefore point to more intense hypoxia during the second half of Phase 2, relative to Phases 1 and 3. Like Phase 2, the sediments from Phase 4 exhibit pyrite concentrations above the XRD detection limit (Table A4), as well as a peak in the TOC:TP ratio (Figure 2.3). Water column monitoring data for Phase 4 further show a growing number of yearly anoxic days during which the hypolimnion's dissolved oxygen concentration falls below 2 mg L^{-1} (Radosavljevic et al., 2022). The available evidence thus identifies both Phases 2 and 4 as periods of increased bottom water hypoxia. However, while hypoxia in Phase 2 is clearly linked to increasing eutrophication in response to the high TP loads from the catchment, in Phase 4 the stabilization of water column stratification by salinization appears to be the main driver of intensifying hypoxia.

From Phase 3 to Phase 4, the estimated average contribution of internal TP loading increases by 50% (Figure 2.5). Yet, even then, internal loading in Phase 4 only contributes on average 13% of the total (external plus internal) TP loading to the water column. This moderate contribution of internal P loading, together with a relatively low external TP input and a short water residence time (about 2 years), helps explain why algal productivity has remained relatively low during Phase 4. It further implies that to mitigate eutrophication symptoms in LW, especially the expanding summer hypoxia of the hypolimnion, measures should be taken to attenuate rising salinization and ensure the continued effectiveness of on-land P retention by proper maintenance and monitoring of the stormwater management infrastructure.

A further noteworthy feature is the 1999 peak values of the TP, P_{Org}, TOC, and TN concentrations. These probably correspond to the large cyanobacterial bloom event linked to the starting up of the sediment aerator in that year (section 2.2.1). The aerator was removed and, to our knowledge, there has not been an algal bloom event of similar magnitude since 1999. Note that the mechanism(s) linking the aerator's operation and the cyanobacterial bloom has yet to be resolved (Nürnberg, 2003). Possibly, the aeration caused resuspension of bottom sediment that then released dissolved phosphate to the water column, which fueled additional algal growth.

2.6.4. Comparative TP budgets

The TP budgets in Figure 5 illustrate some of the main features of the lake's P cycle response to the evolving LULC of the watershed. The external TP input to the lake, F_{ext}, nearly doubled throughout agricultural intensification. This was accompanied by correspondingly large increases in the deposition (F_{dep}) and burial (F_{bur}) fluxes of TP, with the TP burial rate culminating in the 1970s. The maximum estimated water column TP concentration (82 µg L^{-1}) was also reached during Phase 2. Taken together, the evidence implies that LW experienced its highest biological productivity at the end of Phase 2, driven by the high TP input from the watershed. With the implementation of agricultural BMPs, the TP input dropped during Phase 3.

The external TP loading (F_{ext}) was close to its lowest level during the rapid urbanization of the watershed in Phase 4, because of the efficient retention of urban P emissions by the stormwater management infrastructure. The low watershed TP input in Phase 4 has in part been offset by an increase in the sediment TP recycling efficiency (RE_{rec}), from 7-14 % in the previous Phases to 26% in Phase 4, and a drop in the whole-lake TP retention efficiency (RE_{tot}), from 53-69% down to 40%. Because of the reduction in the whole-lake mean TP retention efficiency, the TP outflow flux, F_{out}, in Phase 4 is only around 7% lower than in Phase 3, although the external TP input (F_{ext}) in Phase 4 is estimated to be on average 26% lower than in Phase 3.

2.7. Conclusions

The watershed of Lake Wilcox has undergone major LULC transformations since the early 1900s. The initially forested watershed underwent land clearing for farming, followed by agricultural intensification and, in recent decades, rapid urban growth. Here, we use sediment composition data and burial rates from a dated core going back to about 1920, plus historical records and water quality data from the 1990s onwards, to reconstruct the temporal changes in sediment and TP loading to the lake and the accompanying changes in the lake's TP budget.

The post-WWII agricultural intensification period of LW's watershed saw large increases in the sediment, TP, TOC, TON, and chlorophyll-a accumulation rates, indicative of the escalating cultural eutrophication of the lake. Increased sediment TOC:TP ratios and X-Ray detectable pyrite concentrations during this period further point to expanding bottom water hypoxia driven by the high agricultural TP loads. The sediment and TP loads from the watershed were greatly reduced from circa 1970 to 1990 as the result of the implementation of agricultural BMPs, the removal of septic tanks along the shoreline, and the decreasing agricultural land area.

Rapid urban expansion beginning in the late 1990s was accompanied by a further reduction of the TP burial rate while, at the same time, the sediment TP concentration and the relative contribution of organic P to sediment TP increased. These findings are explained by the efficient interception of suspended sediment by urban stormwater management infrastructure that caused large decreases in the supply of land-derived sediment and TP to the lake. The decrease in external TP loading has been partly compensated by increased TP recycling from the sediments (i.e., internal loading) that, in turn, appears to be driven by the salinization-driven upward trend of the duration of summer stratification of the water column and, possibly, also due to reduced mineral-bound P sinks in the sediments.

Our results provide insights not only into the impacts of changes in watershed land cover on the lake's TP cycle, trophic state and hypoxia, but also into the effectiveness of P abatement measures. During both the period of intensive agriculture and that of rapid urban expansion, the implementation of soil conservation and stormwater management

practices have successfully reduced the TP loading to the lake. In addition, our analysis indicates that the current eutrophication symptoms affecting LW, especially the expanding summer hypoxia in the hypolimnion, are linked to the ongoing salinization of the lake waters. Further lowering the watershed TP loading alone is therefore unlikely to revert these symptoms without additionally managing the salt input to the lake. Given worldwide freshwater salinization trends, this conclusion likely applies to many lakes and reservoirs.

Chapter 3

Salinization as a driver of eutrophication symptoms in an urban lake (Lake Wilcox, Ontario, Canada)

Modified from:

Radosavljevic, J., Slowinski, S., Shafii, M., Akbarzadeh, Z., Rezanezhad, F., Parsons, C. T., Withers W., & Van Cappellen, P. (2022). Salinization as a driver of eutrophication symptoms in an urban lake (Lake Wilcox, Ontario, Canada). *Science of The Total Environment*, 846, 157336.

3.1. Summary

Lake Wilcox (LW), a shallow kettle lake located in southern Ontario, has experienced multiple phases of land use change associated with human settlement and residential development in its watershed since the early 1900s. Urban growth has coincided with water quality deterioration, including the occurrence of algal blooms and depletion of dissolved oxygen (DO) in the water column. We analyzed 22 years of water chemistry, land use, and climate data (1996–2018) using principal component analysis (PCA) and multiple linear regression (MLR) to identify the contributions of climate, urbanization, and nutrient loading to the changes in water chemistry. Variations in water column stratification, phosphorus (P) speciation, and algal abundance (*chl-a*) explain 76% of the observed temporal trends of the four main PCA components derived from water chemistry data. MLR results further imply that the intensity of stratification, quantified by the Brunt-Väisälä frequency, is a major predictor of the changes in water quality. Other important factors explaining the variations in nitrogen (N) and P speciation, and the DO concentrations, are watershed imperviousness and lake chloride concentrations that, in turn, are closely correlated. We conclude that the observed in-lake water quality trends over the past two decades are linked to urbanization via increased salinization associated with expanding impervious land cover rather than increasing external P loading. The rising salinity promotes water column stratification, which reduces the oxygenation of the hypolimnion and enhances internal P loading to the water column. Thus, stricter controls on the application and runoff of de-icing salt should be considered as part of managing eutrophication symptoms in lakes of cold climate regions.

3.2. Introduction

Urbanization is a global phenomenon. In 2007, half of the world's population lived in urbanized area and this fraction is expected to exceed more than 65% by 2050 (McGrane, 2016). Urbanization negatively impacts biodiversity, water quality and air quality (McDonald et al., 2014; Zhao et al., 2006). Regardless of the magnitude of urban development, these impacts are generally significant (Brabec et al., 2002; Paul & Meyer, 2001; Walsh et al., 2005, 2012). Increased imperviousness in urban areas can enhance the mobility of contaminants (Garnier et al., 2013; McGrane, 2016; Pringle, 2001) that

cause the deterioration of downstream water quality (Jacobson, 2011; Shuster et al., 2005; Walsh et al., 2005). Examples of common urban contaminants include toxic metals, such as zinc, lead, cadmium, and nickel (Floresrodrîguez et al., 1994; Mansoor et al., 2018) and polycyclic aromatic hydrocarbons (PAHs) (Zehetner et al., 2009), which negatively impact water quality and aquatic life of urban lakes and streams. Along with heavy metals (Pastor & Hernández, 2012) and thermal pollution (Wang et al., 2008), nutrients represent an important class of urban contaminants (Carey et al., 2013; Garnier et al., 2013) that may result in eutrophication of the receiving water bodies (Carpenter, 2005; Carpenter et al., 1998; Filippelli, 2008; Frossard et al., 2014; Jenny et al., 2016; Tromboni & Dodds, 2017).

Phosphorus (P) is often considered to be the main limiting nutrient responsible for eutrophication in freshwater lakes (Schindler et al., 2016). Excessive nutrient P loading leads to increased primary productivity and oxygen (O_2) depletion, especially during periods of water column stratification. Jenny et al. (2016) reported that intensification of hypoxic conditions in European lakes is historically correlated with the growth of nearby urban areas and the export of P from urban point sources. In addition to the increased frequency of algal blooms and hypoxic conditions caused by algae decomposition (Carey et al., 2013; Heisler et al., 2008), eutrophication may also be accompanied by the demise of submerged vegetation and the release of toxins by harmful algal species that negatively impact fish, wildlife, pets and even humans (Carey et al., 2013; Yang et al., 2008).

In cold temperate regions, direct road salt runoff is a growing and multi-faceted problem for lentic ecosystems. Elevated chloride (Cl^-) and other dissolved ion concentrations from de-icing agents impact biodiversity and food webs, alter base cation balances, and modify the mixing regime of lakes that, in turn, can cause oxygen depletion of the hypolimnion (Corsi et al. 2015; Dugan et al., 2017; Kortesky et al., 2012; Ladwig et al., 2021).

Urban stormwater management (SWM) systems are implemented to control peak runoff and mitigate contaminant export, including that of nutrients, to surface and groundwater (Hathaway et al., 2012; Khan et al., 2021; Song et al., 2015, 2017). These systems include both grey infrastructure, such as stormwater ponds, and green infrastructure such

as bioretention cells. These facilities help restore more natural hydrological conditions that are considered more efficient for the mitigation of urban contaminants (Goh et al., 2019; Hathaway et al., 2012, 2016; Kratky et al., 2017; Song et al., 2015, 2017; Yang & Toor, 2017, 2018). Despite their success in reducing runoff (Jefferson et al., 2017), it is still unclear known whether an existing SWM facilities permanently immobilize P (Perry et al., 2009). In fact, some stormwater ponds have been found to increase the export of the more bioavailable forms of P (Frost et al., 2019; Song et al., 2015, 2017).

Along with urbanization, climate change represents a potential stressor on water quality and aquatic ecosystem health. Cold and cold-temperate regions, including Canada, are warming rapidly, and this trend is expected to continue in the future, both at annual and seasonal scales (Jennings et al., 2009; Lemieux et al., 2011; Lemieux & Scott, 2011; Vincent et al., 2018). Climate change is accompanied by hydrological changes, such as more frequent high-intensity precipitation events (Clifton et al., 2018; Stocker, 2014; Tebaldi et al., 2006; Whan et al., 2016). Extreme events, such as heavy rainfall, windstorms, heat and cold waves, and droughts are forecasted to become the new normal in the coming decades (Emilsson & Sang, 2017; Forzieri et al., 2018; Kaushal et al., 2014; Whan and Zwiers, 2016; Zhang et al., 2008). In urban landscapes, heavy rainfall events create higher peak runoff flows with high pollutant loads of total suspended solids (TSS), nutrients, and toxic metals (Alamdari et al., 2020; Ekness & Randhir, 2015). Longer dry periods between precipitation events (Stocker, 2014) can favor sediment buildup in urban landscapes and cause the flushing of high TSS concentrations during subsequent runoff events (Sharma et al., 2016).

To understand the impacts of land use and climate change on water quality, previous studies have focused on individual lakes (Patterson et al., 2002) or groups of lakes (Seilheimer et al., 2007; Tomer & Schilling, 2009; Yang & Chang, 2007) using modeling (Carpenter, 2005) and data analyses (O'Reilly et al., 2015; Taranu & Gregory-Eaves, 2008; Yang et al., 2020). These studies typically rely on comprehensive but relatively short data time series, usually covering a year or two. Here, we investigate water quality changes in a lake using a multi-variate dataset collected over two decades. Lake Wilcox (LW) in southern Ontario, Canada is a kettle lake within an urbanizing watershed. Our

goals are to assess the changes in water quality in LW during the period 1996–2018 and identify drivers of these changes using statistical analysis methods.

3.3. Methods

3.3.1. Study site: Lake Wilcox

Lake Wilcox (LW) is a small kettle lake located in the city of Richmond Hill in Ontario, Canada, along the northern edge of the greater Toronto metropolitan area (Figure 3.1). It is divided into an east and west basin that are 17 m and 14 m deep, respectively. The two basins are separated by a ridge which peaks at ~8 m water depth (Reports number 4, 5 and 6 in Table A1). The lake's surface area is 0.56 km^2 and its watershed area is 2.39 km^2. Nearby Lake St. George (watershed area: 2.5 km^2) drains into LW via a connecting channel. The high morphometric ratio (7.6 m/km) promotes stratification of LW during the summer (Report number 5 in Table A1). The lake has one outflow and seven inflow points, of which the St. George and North Shore inflows contribute the highest flows (~85±5%) to the lake (Report number 6 in Table A1). Based on discharge measurements for the period 1998-2010, the average annual surface inflow is on the order of $7x10^5$ m^3 and the water retention time is approximately 2 years (Reports number 4 and 5 in Table A1).

The lake's watershed experiences a continental climate moderated by the Laurentian Great Lakes. The watershed is influenced by warm, moist air masses from the south and cold, dry air masses from the north (TRCA, 2008). The average total annual precipitation is about 853 mm (range: 700 to 1,000 mm) and the average daily temperature 7.7°C (Government of Canada, 2019). The majority of precipitation occurs during the summer months (June, July, and August). The mean annual evapotranspiration is approximately 517 mm per year (TRCA, 2018).

The originally forested watershed of LW has undergone significant development since the early 1900s when the land was converted to agriculture. This was followed by the construction in the 1940s of nearshore cottages on septic systems. The latter were decommissioned in the 1960s when monitoring revealed rising eutrophication of the lake (Reports number 1, 2 and 3 in Table A1). Sub-urban and urban development took off in the 1980s, further accelerating in the early 2000s. As a result of development, land surface imperviousness increased to over 60% at present (Figure 3.2a).

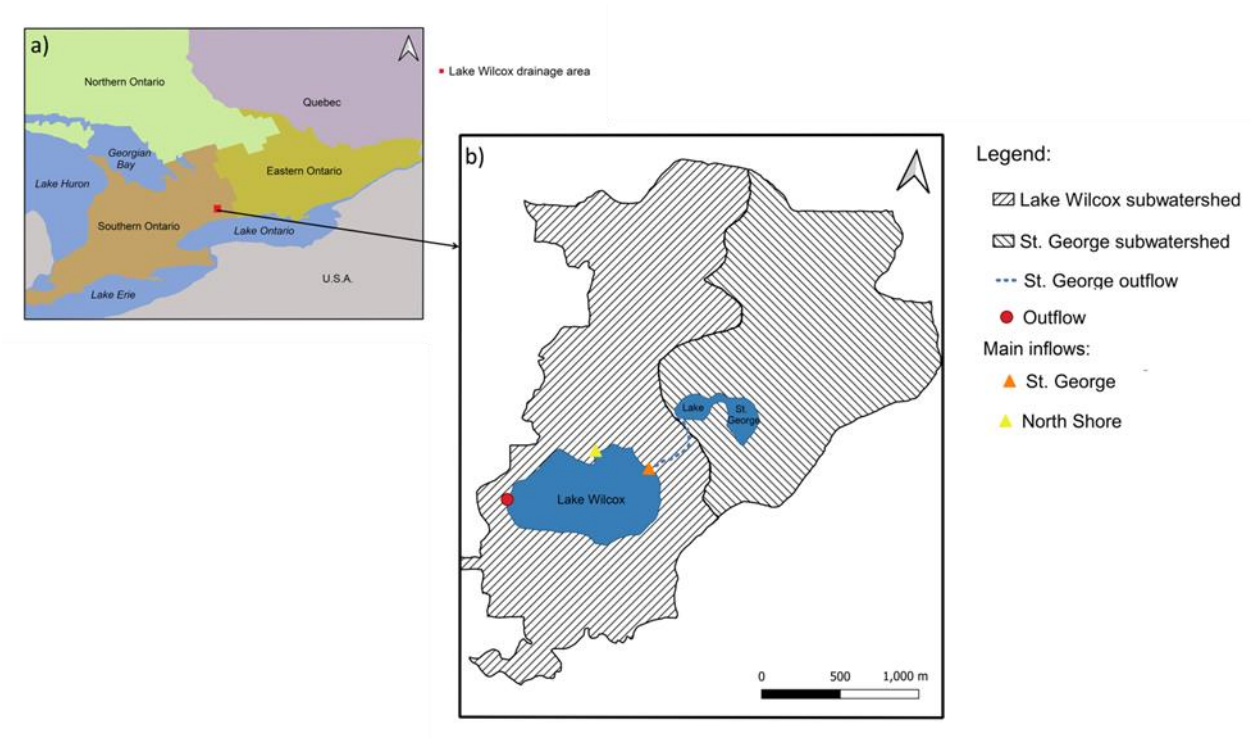

Figure 3.1. Location of Lake Wilcox in Ontario, Canada (a), and sketch of its drainage area (b).

The imperviousness values (in % watershed land cover) from 1996 to 2018 shown in Figure 3.2a are based on estimates reported in previous studies for the years 1996, 2009, 2012, and 2018 (Reports number 1-6 in Table A1; Baker et al., 2017; Doyle & Macpherson, 2017; OMAFRA, 2019), complemented with our own estimates obtained manually from aerial images. Values for the other years were interpolated as done in previous studies (Exum et al., 2005; Li & Wu, 2016; Wu & Hung, 2016). Note that Figure 3.2a shows the total imperviousness, that is, it corresponds to the sum of all impervious land parcels in Lake Wilcox's watershed. Thus, it comprises both the disconnected and directly connected impervious land cover. The directly connected imperviousness is the sum of impervious land parcels that are connected to the storm sewer network.

By the 1980s, worsening eutrophication, including declining dissolved oxygen (DO) levels and the appearance of cyanobacteria, had become a major issue, with the lake becoming meso-eutrophic (Reports number 4 and 5 in Table A1; Nürnberg, 1997; Nürnberg, 1996). To combat increasing algal productivity and avoid harmful algal blooms (HABs) an aeration system was installed in 1998 with the goal of slowing down internal P loading from the lake sediments to the water column – a process known to be a major driver of algal growth (Olding, 2012; Report number 5 in Table A1). The aerator, however, broke down in early 2001 and was never reactivated (Olding, 2012). Due to the lack of improvement in LW's water quality, a suite of SWM systems, notably wet ponds, were constructed in the watershed, starting in the early 2000s. To add more SWM systems, more of the urban and suburban developments were connected to the storm sewer system, and as a result, the expansion of imperviousness from around 2010 till today saw an increase in the fraction of directly connected imperviousness (William Withers, personal communication, September 2020).

3.3.2. Datasets

A variety of datasets were collected from different sources, including water quality monitoring data provided by the City of Richmond Hill (CRH), climate data downloaded from the Environment and Climate Change Canada (ECCC) and Toronto and Region Conservation Authority (TRCA) websites (Table B1), as well as satellite images obtained from Esri's Wayback Living Atlas Google Earth Pro and USGS Land Look.

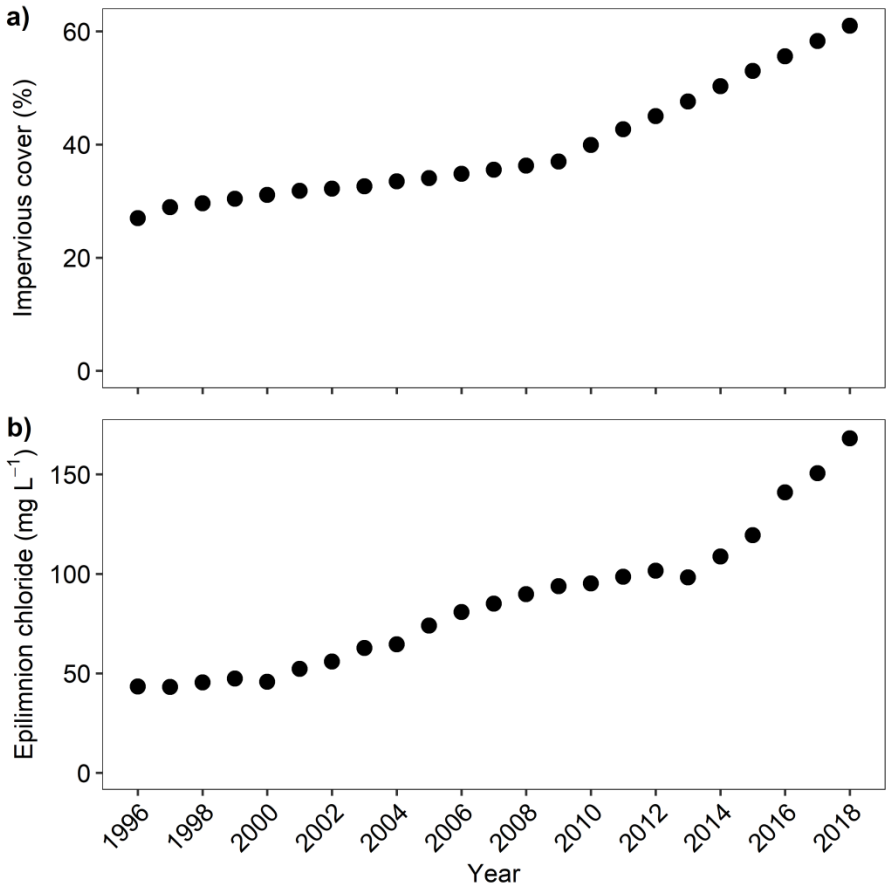

Figure 3.2. Fraction of impervious land cover in Lake Wilcox's watershed (a) and in-lake surface water chloride concentrations (b) from 1996 to 2018.

Data were synthesized for the period 1996 to 2018. From the climate records we derived values for the mean daily temperature, average yearly temperature, mean daily and yearly precipitation, and the 95th percentile of rainfall (calculated following U.S. Environmental Protection Agency guidelines (USEPA 2009)), as described in Shrestha et al., 2013).

The CRH water quality dataset comprised results of bi-weekly sampling from May to November, from 1996 to 2018. Included were concentrations of dissolved oxygen (DO), total P (TP), dissolved inorganic P (DIP), nitrate (NO_3^-), ammonium (NH_4^+), dissolved inorganic nitrogen (DIN), and chloride (Cl^-) in both the epilimnion and hypolimnion, plus the concentrations of chlorophyll-a (*chl-a*) in the epilimnion. The annual TP loadings to the lake were derived from the discharge and TP concentration values in the CRH reports following the flow-weighted averaging method described in Walling & Webb (1985) and Moatar & Meybeck (2005).

With the availability of more than 20 years of continuous data on water chemistry that overlap with the period during which the watershed experienced a significant increase in impervious cover, Lake Wilcox is unique site to study impact of land use change on water chemistry and eutrophication-like symptoms.

Anoxic factor (AF)

The DO time series data served to calculate anoxic factor values following the method proposed by Nürnberg (1995, 2004):

$$AF = \frac{\sum_{i=1}^{n} t_i * a_i}{Ao} \quad (3.1)$$

where *AF* is the anoxic factor (in days) for a given year, t_i is the number of days of anoxia during that year or season, a_i is the hypolimnetic surface area (m^2), and Ao is lake surface area (m^2). The appearance of Ao in the denominator of Equation (3.1) accounts for the variable lateral extent of anoxic bottom waters. The annual AF value thus corresponds to the number of days in a year during which a sediment area equal to the lake surface area is overlain by anoxic water. Annual AF values are a proxy for changes in the intensity of deoxygenation of the hypolimnion.

Brunt-Väisälä frequency (BVF)

The Brunt-Väisälä or buoyancy frequency (BVF) represents the amount of work required against gravity to break down thermal stratification in the water column (Mortimer, 1974). It is calculated as follows:

$$N^2 = \frac{-g}{\bar{\rho}} * \frac{\partial \rho}{\partial z} \quad (3.2)$$

where N is the BVF (s^{-1}), g is the gravitational acceleration (m s^{-2}), $\bar{\rho}$ is the average water density over the entire water depth considered (kg m^{-3}), ρ is the water density (kg m^{-3}) at a given depth z (m) (Mortimer, 1974; Zadereev & Tolomeyev, 2007). Note that the use of Equation (2) yields a depth profile of BVF.

The density of water was calculated from the corresponding temperature and salinity values with the Javascript calculator developed by the collaborative Computer Support Group (CSG) Network of University of Michigan and National Oceanic and Atmospheric Administration (NOAA). For those sampling times where Cl^- concentrations were reported for both the epilimnion and hypolimnion, little vertical difference in the Cl^- concentrations was observed. Because Cl^- concentrations were measured systematically in the epilimnion, but not the hypolimnion, only the epilimnion Cl^- concentrations were used and converted to salinity values (Dugan et al., 2017; Shambaugh, 2008). For the calculation of the BVF depth profile at a given sampling time, the same salinity value was then applied to all depths while the measured depth-dependent temperature profiles were imposed. For details on the water density calculation, see Gill (1986).

In order to assess interannual variability in the intensity of stratification, we compared BVF depth profiles calculated for the month of August for each year. In southern Ontario, July-August exhibit the highest monthly air temperatures and water column stratification is most pronounced. In addition, by August, the lake's temperature distribution retains negligible memory from the preceding spring mixing event.

3.3.3. Statistical Analyses

We relied on multiple statistical methods to describe and interpret water quality changes. We used the Mann-Kendall (MK) test to assess the statistical significance of temporal trends in water quality variables (with $p<0.1$ as threshold). We further employed Principal

Component Analysis (PCA) to reduce the dimensionality of the large water quality data set (section *2.5.2*). We also developed Multiple Linear Regression (MLR) models to explore the relationships between the principal components (PCs) and potential predictor variables (*e.g.,* degree of urbanization, salinization, temperature, nutrient concentrations and speciation, etc.).

3.3.3.1. Mann-Kendall test (MK) and Kendall's τ

The MK tests were carried out with the XLSTAT software (Addinsoft, version 2022). Positive values of the MK statistic indicate an upward trend, negative values a downward trend, and a zero value no change over time. The larger the MK statistic deviates from zero, the greater the evidence for a significant temporal trend in the data series (Hirsch et al., 1982; Kendall, 1975; Lettenmaier, 1988; Şen, 2014, 2017). Here, we report the closely related Kendall's τ (tau) values that rescale the MK statistic values within the range –1 to +1, which facilitates the comparison of data series with variable numbers of observations (Helsel & Hirsch, 1992; Meals et al., 2011). More details about the MK test can be found in Hirsch et al., 1982; Kendall, 1975; and Zhang et al., 2004.

3.3.3.2. Principal Components Analysis (PCA)

To identify the drivers of water chemistry changes it is often helpful to group variables that are correlated. We selected PCA, which has been widely applied to environmental data time series (Arslan, 2013; Parinet et al., 2004; Sahoo et al., 2020; Wold et al., 1987; Yang et al., 2020). The emerging groupings then create a new and smaller set of presumably uncorrelated variables, that is, the principal components (PCs). Details about PCA can be found in many previous works (Liu et al., 2019; Zou & Xue, 2018). The 13 water chemistry variables included in the PCA were epilimnion and hypolimnion concentrations of DIP, TP, NH_4^+, NO_3^-, DIN, and DO, plus the *chl-a* concentration in the epilimnion.

As required in PCA, we first filtered the dataset to remove missing data points. Water quality parameters that had non-existing values for more than 25% of the sampling dates were removed. We further excluded data from 1997 to 2000 because during that time the DO concentrations were artificially manipulated by using an aerator (section 3.3.*1*). The

PCA was performed and visualized in R 4.1.2 (R Core Team, 2021) using the factoextra package (Kassambara and Mundt, 2020).

3.3.3.3. Multiple Linear Regression (MLR)

In the MLR analyses, the water chemistry PCs were treated as the dependent (or *y*) variables. The goal was to identify the (independent) explanatory variables that most contribute to the temporal trends of the water chemistry PCs. To compare the regression coefficients from the MLR analyses, we first normalized the values of each explanatory variable by that variable's mean value to make them unitless. The MLR analysis was performed with the JMP statistical software (SAS Institute Inc.) based on the following formulation:

$$y = b_0 + b_1 x_1 + b_2 x_2 + \cdots + b_i x_i \quad (3.3)$$

where y is the dependent variable, x_i the i^{th} explanatory (or predictor) variable, b_o the regression constant, and b_i the i^{th} coefficient of the corresponding explanatory variable (Brix et al., 2017; Liu et al., 2015; Weisberg, 2005).

The predictors included in the MLR analyses were: watershed imperviousness (as a measure of urbanization), lake Cl^- concentration (as a measure of deicing salt usage), external P loading to the lake, water column stratification (using the Brunt-Väisälä frequency), and the following climate parameters: 14-day average temperature and 14-day total rainfall prior to sampling, average yearly temperature and rainfall, and yearly 95% percentile of rainfall. The latter is used as a measure of a year's extreme precipitation events that can play an important role in pollutant wash-off in urban areas (Carpenter et al., 2018; Knapp et al., 2008; Rahimi et al., 2021; Ummenhofer & Meehl, 2017; Vincent et al., 2018; Whan & Zwiers, 2016).

The explanatory variables selected are known drivers of water quality changes (Carey et al., 2013; Garnier et al., 2013; McGrane, 2016; Pringle, 2001; Pickett et al., 2011; Walsh et al., 2005). Obviously, the analyses can only provide insights into the roles of the selected explanatory variables. Other variables, such as lake ice cover and duration, are likely responsible for part of the temporal variability of the PCs (Carey et al., 2012;

Cavaliere & Baulch, 2018; Rodgers & Salisbury, 1981), however, they are not included here because of the lack of a corresponding data time series.

3.4. Results

3.4.1. Time series trends

3.4.1.1. Dissolved oxygen (DO) and anoxic factor (AF)

Hypoxic conditions were first recorded in LW in the 1980s (Reports number 4 and 5 in Table A1). For the observation period considered here (1996-2018), average DO concentrations were 10.2 and 1.1 mg L^{-1} in the epilimnion and hypolimnion, respectively. Maximum and minimum DO concentrations were 17.8 and 2.4 mg L^{-1} in the epilimnion, and 12.0 and 0 mg L^{-1} in the hypolimnion. The time series DO depth profiles shown in Figure 3.3 indicate a transition around the year 2005 characterized by a lengthening of the annual periods of DO deficient conditions in the hypolimnion (*i.e.,* the dark blue color in the figure), sometimes extending throughout the entire year. The depth of the redoxcline also increased, from around 4 m at the beginning of the data series to around 6 m in the most recent years. The DO trend analysis for LW revealed a statistically significant (p<0.1) decrease in DO concentrations, especially in the hypolimnion (Kendall's τ = -0.35) (Figure 3.4). The average value of AF for the entire period (excluding years with artificial aeration) was 72 days per year. The annual AF exceeded 80 days in 2005, 2008 and 2015. As expected from the DO trend analysis, Figure 3.4 shows an increasing trend of AF with time (Kendall's τ= +0.42).

3.4.1.2. Chloride

The average Cl^- concentration in the epilimnion increased from 43 mg L^{-1} in 1996 to 175 mg L^{-1} in 2018 at which time the watershed's imperviousness exceeded 60% (Figure 3.2b, Table B2). Of all the water quality variables tested, the Cl^- time series showed the strongest positive trend with time (Kendall's τ = 0.94, Figure 4). Several distinct phases of Cl^- increase can be distinguished (Figure 2.2b, Table B2). From 1996 to the turn of the century only a small increase of the Cl^- concentration was observed. This was followed by a much faster increase up to ~90 mg L^{-1} by the year 2008, while the watershed's imperviousness rose to 36%. The next phase, from 2008 to 2012, was again

characterized by a relatively slow growth of the Cl^- concentration as the imperviousness reached 45%. The last phase saw the most rapid rise of the Cl^- concentration to about 175 mg L^{-1} in just six years. During that same period, major efforts were undertaken to expand directly connected imperviousness (section 3.3.1).

3.4.1.3. Brunt-Väisälä frequency (BVF)

August BVF depth profiles are shown in Figure 3.5 for the beginning and end of the observation period (1996 and 2018) plus intermediate year 2007. Overall, the shape of the profile became wider over the years while the maximum BVF values moved to deeper depths. The latter is consistent with the generally downward trend observed for the redoxcline (Figure 3.3). As for Cl^-, maximum BVF values exhibited an increasing trend with time (Kendall's τ = +0.12, Figure 3.4).

3.4.1.4. Phosphorus: concentrations and speciation

Over the entire time period considered, the TP and DIP concentrations in the hypolimnion were about 10 and 30 times higher than those measured in the epilimnion, respectively. In the epilimnion the DIP varied from 0.001 to 0.059 mg L^{-1} with an average value of 0.005 mg L^{-1}, while TP concentrations ranged from 0.003 to 0.116 mg L^{-1} with an average value of 0.032 mg L^{-1}. The hypolimnion concentrations of DIP ranged from 0.001 to 0.513 mg L^{-1} with an average value of 0.175 mg L^{-1}, while TP varied from 0.017 to 1.33 mg L^{-1} and averaging at 0.249 mg L^{-1}. The epilimnion TP concentration showed a decreasing trend over time (Kendall's τ = -0.27, Figure 3.4 and 3.6, Table B2). The hypolimnion TP concentration similarly exhibited a decreasing trend, although less pronounced than that in the epilimnion (Kendall's τ = -0.24, Figures 3.4 and 3.6, Table B2). Since 2000, the DIP concentrations in the epilimnion and hypolimnion have experienced slight declines (Table B2).

The DIP:TP ratios in the epilimnion and hypolimnion exhibited statistically significant increasing trends over time (Kendall's τ = +0.13 and +0.23, respectively in the epilimnion and hypolimnion, Figure 3.4). As can be seen in Figure B1, a relatively large increase in DIP:TP occurred after 2010, particularly in the epilimnion. Further note that the minimum hypolimnion DIP:TP value of 1998 coincided with the time the aerator was in operation.

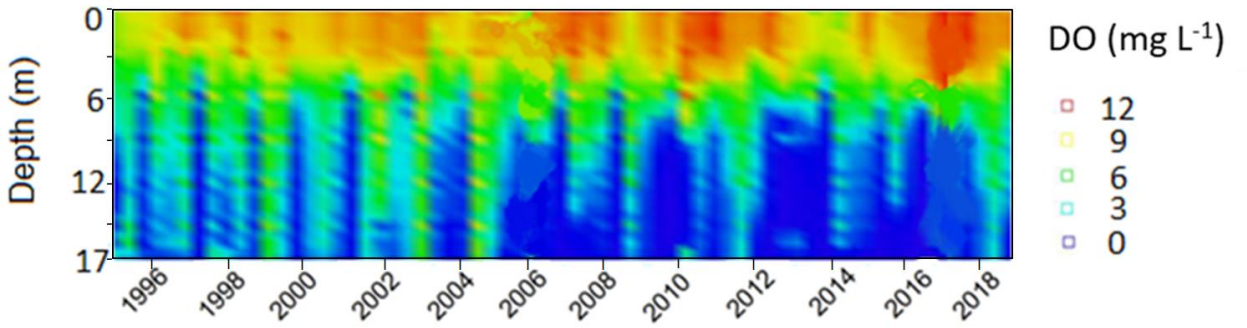

Figure 3.3. Mid-lake depth distributions of dissolved oxygen concentrations (DO) between 1996 and 2018. Note the lengthening of the yearly period of anoxia (blue color) after 2003.

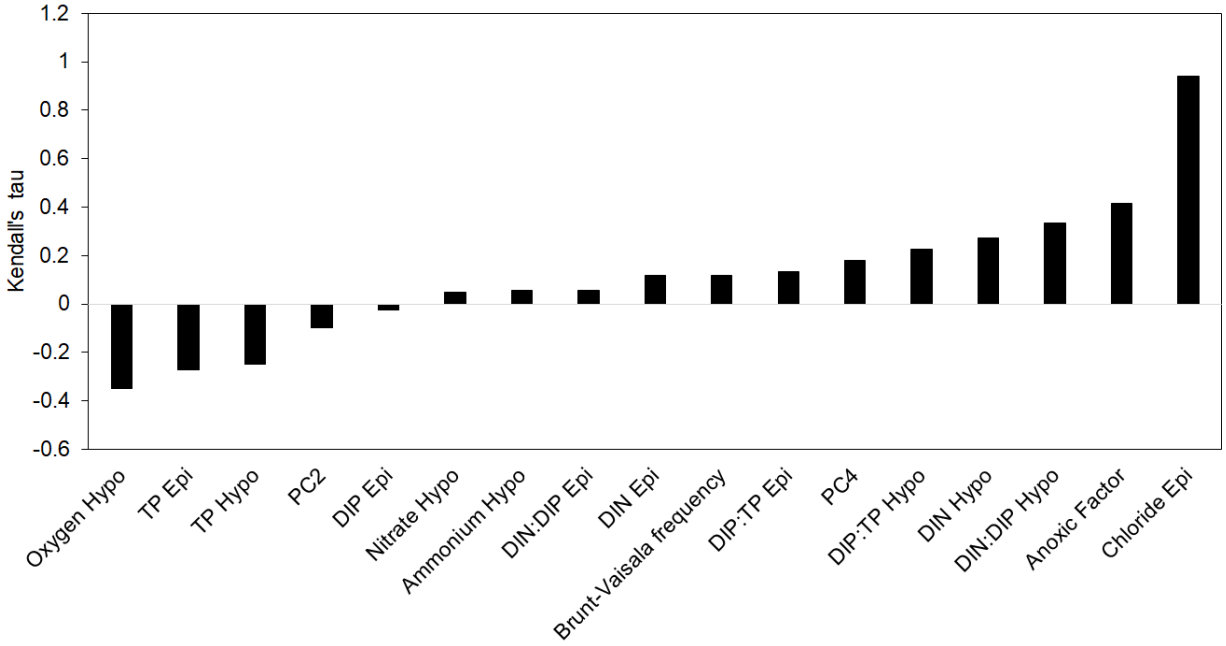

Figure 3.4. Kendall's tau values for Mann-Kendall trend analyses. The figure includes the results for the water quality parameters, MLR explanatory variables, and principal components (PCs) that show a statistically significant ($p \leq 0.1$) trend with time over the period 1996 to 2018. Hypo = hypolimnion, Epi = epilimnion.

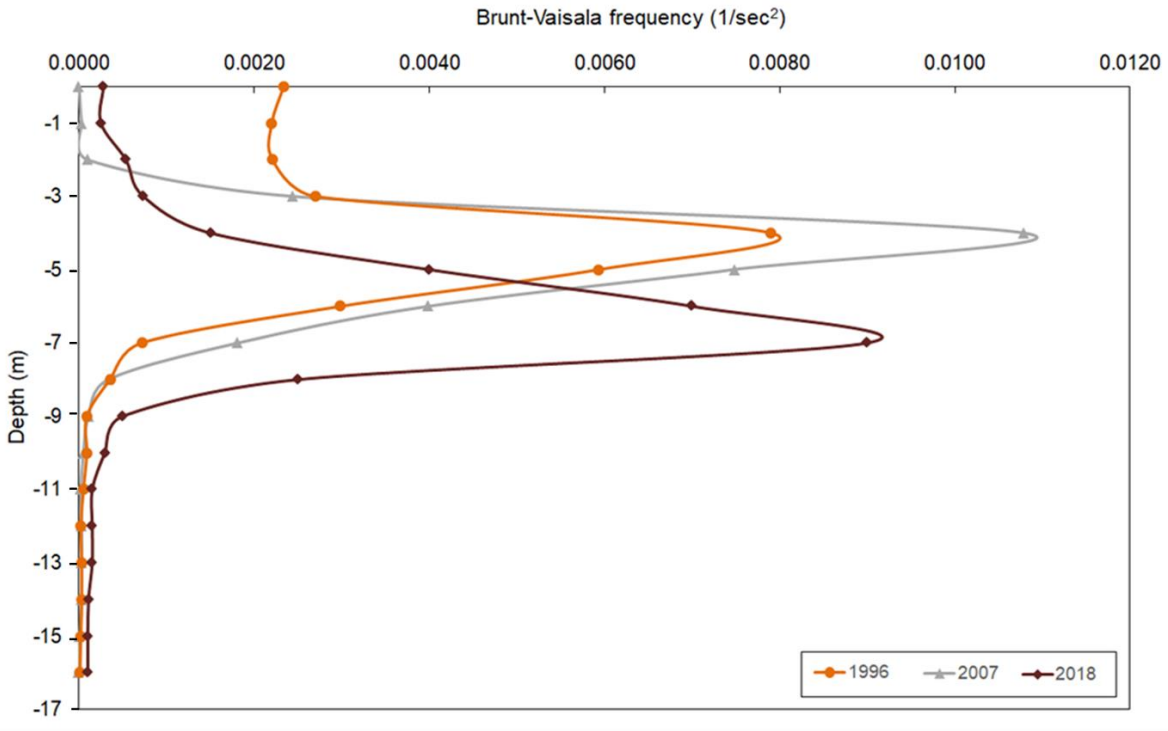

Figure 3.5. Mid-lake Brunt-Vaisala frequency (BVF) depth profiles for the month of August in 1996, 2007, and 2018.

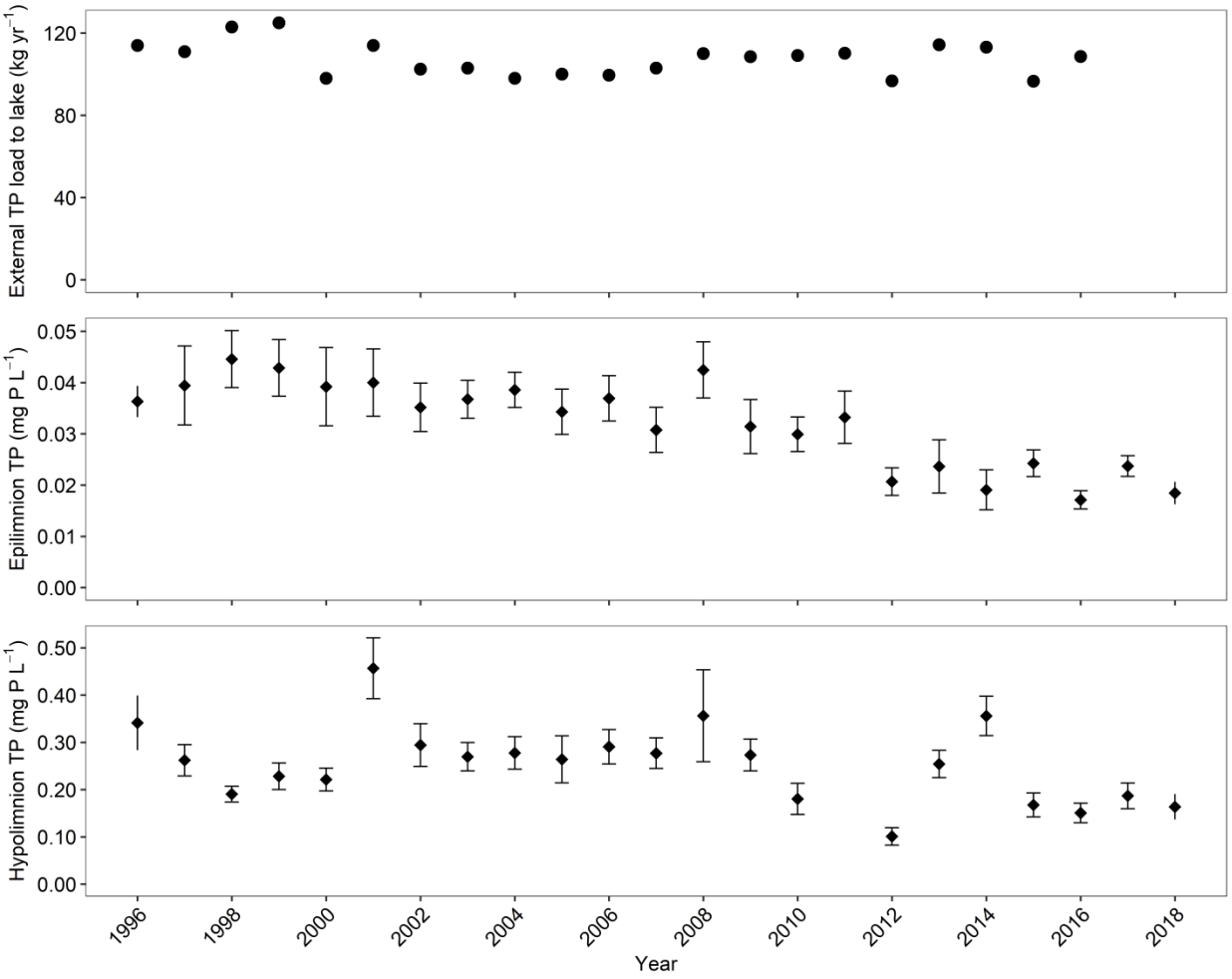

Figure 3.6. Time series of total phosphorus (TP) external loads to Lake Wilcox, and in-lake TP concentrations in epilimnion and hypolimnion. The error bars represent standard deviation.

3.4.4.5. Nitrogen: concentrations and speciation

As for TP and DIP, the DIN (= sum of ammonium, nitrite and nitrate) concentrations in the hypolimnion were much higher than for the epilimnion (Table B2). The maximum DIN concentration in the epilimnion was 1.64 mg L^{-1} and the average value was 0.15 mg L^{-1}. The DIN concentrations in the hypolimnion reached a maximum value of 6.71 mg L^{-1}, with an average concentration of 1.54 mg L^{-1}. In both epilimnion and hypolimnion, the DIN concentrations showed increasing trends (Kendall's τ = +0.12 and +0.27 for epilimnion and hypolimnion, respectively) (Figure 3.4).

The speciation of DIN also differed markedly between the epilimnion and hypolimnion (Table B2). In the hypolimnion, nearly all DIN was under the form of NH_4^+. The average NO_3^- concentration in the hypolimnion was 0.04 mg L^{-1} while the average concentration of NH_4^+ was 1.50 mg L^{-1}. In the epilimnion, the average concentrations of NO_3^- and NH_4^+ were 0.05 and 0.10 mg L^{-1}, respectively. The epilimnion was also more depleted in DIP relative to DIN, compared to the hypolimnion (Table B2). The yearly average DIN:DIP and DIN:TP mass ratios in the epilimnion were 32.7 and 5.3, respectively, and 9.3 and 6.8 for the corresponding values in the hypolimnion (Figure B2). (Note: to convert to molar N:P ratios, the mass N:P ratios are multiplied by 2.21.)

3.4.4.6. Chlorophyll-a

The *chl*-a concentration is commonly used as a measure of the abundance of algal biomass in lakes (Jones & Bachmann, 1976; Quinlan et al., 2021; Reynolds & Descy, 1996). The long-term average value of *chl-a* for LW was 9.8 µg L^{-1} indicating eutrophic conditions. The concentrations, however, varied widely between years, in the range 0.2 - 41 µg L^{-1}. The average *chl-a* concentration in fall (11.4 µg L^{-1}) was higher than that observed in summer (9.3 µg L^{-1}). The *chl-a* time series data did not exhibit a statistically significant temporal trend ($p>0.1$).

3.4.2. Principal Components Analysis

The percentages of the variations across the entire 13-dimensional water chemistry dataset that are explained by the PCs are presented in Figure B3. The results indicate that 76% of the variation in the data was explained by the first four PCs that, in descending

order, contributed 33.3%, 20.2%, 11.7% and 10.8%. In the following section, we focus on these four PCs. Given their relative contributions, we refer to PC1 and PC2 as the major PCs and PC3 and PC4 as the minor PCs. The PC1 versus PC2 biplot is shown in Figure 3.7. The three variables that most strongly correlated with PC1 were the concentrations of the reactive forms of N and P in the hypolimnion: DIN, DIP, and NH_4^+ (Figure 3.7, see also Figure A4). Additionally, the correlations were all positive (Figure 3.7, see also Figure 3.8). For PC2 the three strongest, also positive, correlations were with the concentrations of DIN, DIP, and NH_4^+ in the epilimnion (Figure 3.7 and Figure 3.8, see also Figure B4). The main three variables correlating with PC3 and PC4 were the concentrations of NO_3^-, DIP and *chl*-a in the epilimnion (for PC3), and *chl*-a and DO in the epilimnion plus NO_3^- in the hypolimnion (for PC4) (Figure B4). These variables only weakly contributed to PC1 and PC2 (Figure B4) and therefore plotted relatively close to the center of the PC1-PC2 biplot (Figure 3.7).

The major cluster of variables that correlated positively with PC1 (hypolimnion DIN, DIP, NH_4^+, and TP) also correlated positively with PC2 (Figure 3.7 and 3.8). In contrast, the major cluster that correlated positively with PC2 (epilimnion DIN, DIP, NH_4^+, and TP) correlated negatively with PC1. Moreover, the DO concentrations in epilimnion and hypolimnion were negatively correlated with PC1 but showed little connection to PC2.

3.4.3. Multiple Linear Regression (MLR)

We used MLR to delineate which of the 9 selected predictor variables (see section *3.3.3.3.*) most impacted the temporal variations of the PCs. During the stepwise development and assessment of the MLR models, variables that had no impact on the PCs were discarded while the others remained in the pool of significant predictors (using a p-value of 0.1 as the cut-off). The remaining predictor variables are those in the grey shaded cells in Table 3.1. The table further identifies in bold text the predictor variable(s) with the largest regression coefficient(s) for a given PC. The value of a regression coefficient is a measure of the sensitivity of the PCs to the predictor variable. Note that because the predictor variables were normalized to their mean values, the relative magnitudes of the coefficients also provide a first-order indication of the relative importance of the predictor variables in explaining the variability of the PCs.

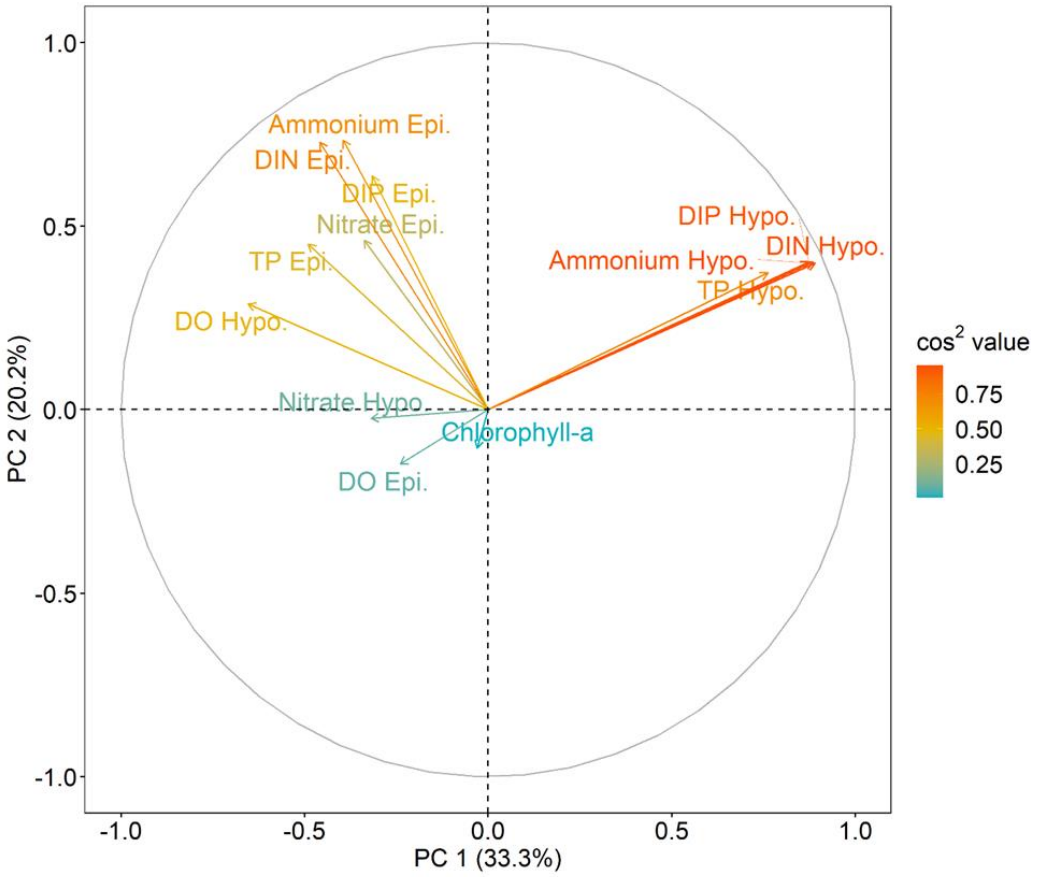

Figure 3.7. PC1 versus PC2 biplot of variables included in PCA. The color of the arrows indicates how well the variable is represented by PC1 and PC2. Arrow length and direction show the extent and direction (positive or negative) of the variable's correlation with PC1 and PC2. Variables with arrows closest to the outer grey circle are best represented by PC1 and PC2.

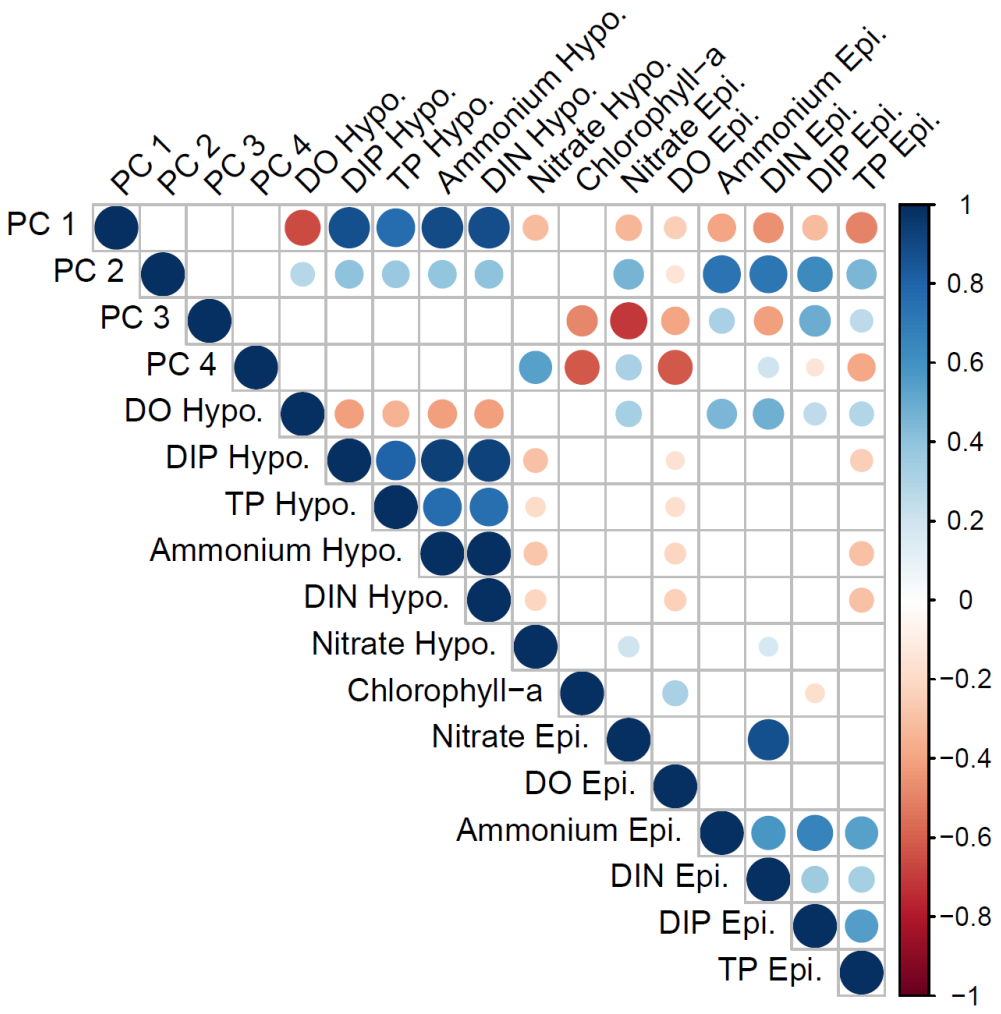

Figure 3.8: Pearson's correlation between the PCs and variables included in the analysis ($p<0.1$). Size and color of a circle indicate the strength and direction (blue is positive, red is negative) of the correlation, respectively.

Table 3.1: Results of the MLR analysis. Significant variables ($p \leq 0.1$) are identified by the shaded boxes with **bold** marking the most important explanatory variables.

	Urbanization		Climate					Loadings	Stratification
	Urbanization	Chloride	Mean temperature 14 days prior sampling	Average yearly temperature	Total rainfall 14 days prior sampling	Total yearly rainfall	>95% of the events	P loadings	BVF
PC1 (mixing/stratification)	0.87	3.05	3.30	0.99	-1.36	0.81	-0.66	0.56	**4.08**
PC2 (nutrient state and trophic conditions)	0.44	0.08	**2.97**	1.36	0.68	-1.21	-0.43	0.42	-0.78
PC3 (SWM infrastructure)	**2.52**	-1.53	-0.62	0.61	0.38	**-3.37**	1.22	0.75	-1.57
PC4 (extreme events)	1.18	-0.60	-0.68	0.63	-0.37	0.84	**1.70**	0.89	-1.38

3.5. Discussion

3.5.1. Water chemistry trends

The 22 years of water chemistry parameters were analyzed for factors that are known to play a role in the lake eutrophication - symptoms. A numerous literature shows that excessive nutrient inputs, primarily phosphorus (P), are the most important driver of eutrophication of freshwater lakes (Gurkan et al., 2006; Smith et al., 1999; Vollenweider, 1968). Previous studies have also shown that eutrophication can be managed by reducing nutrient P inputs to lakes (Bhagowati & Ahamad, 2019; Carpenter et al., 1998, Smith et al., 1999). Although P inputs have been reduced, the eutrophic conditions have persisted in LW. We explored Cl^-/salinity as potential explanatory variables for such conditions due to high increase in the Cl^- concentrations (Figure 3.2b) in the lake during the period that hypoxia in the hypolimnion intensified (Figure 3.3). From the variables for which data series could be obtained, the two major macronutrients (P and nitrogen, N), dissolved oxygen (DO) and chlorophyll-a have all been linked to lake eutrophication and were therefore considered in the statistical analyses (see section 3.5.2).

During the period 1996-2018, the water chemistry of LW underwent significant changes, especially in terms of the concentrations of Cl^-, DO, TP, DIP, plus the DIP:TP and DIN:DIP ratios (Figure 3.4). The chloride concentration increased by a factor of 4, likely due to the increasing application of deicing agents as the watershed became increasingly urbanized (Figure 3.2a). At the same time, however, the % imperviousness grew by only a factor of 2.3. Thus, the relative increase in LW's Cl^- concentration outpaced that of urbanization, as also noted by Corsi et al. (2010) for rivers in the northern United States. In addition, the changes in slope on Figure 3.2b indicate that the expansion of urban cover alone does not explain the pace at which the Cl^- concentration has been building up in the lake. Additional factors can include the type of deicing agent used (e.g., road salt versus brine) and the development of, and connectivity to, the stormwater management (SWM) infrastructure (Sorchetti et al., 2022). In particular, the rapid increase in Cl^- between 1996 and 2010 possibly reflects the expansion of the total imperviousness in LW's catchment, while the development of directly connected imperviousness may explain the switch to a faster rise of the Cl^- concentration after 2010. Directly connected imperviousness tends

to accelerate the transfer of contaminants, including Cl^-, to streams and lakes (Brabec et al., 2002; Duan & Kaushal, 2015; Walsh et al., 2005). Spatial distribution of impervious surfaces in the watershed could be an important factor controlling contaminant loads (Brabec et al., 2002; McGrane, 2016), including that of chloride (Richardson & Tripp, 2006), to the lake. Detailed reconstructions over time of the spatial distribution of impervious land cover (Luo et al., 2018), as well as the types and application rates of de-icing agents, would provide further insights into the salinization trajectory of the lake (Ramakrishna & Viraraghavan, 2005), and more research on these are needed.

Rising Cl^- concentrations in lakes negatively impact water quality and drinking water supply (Kaushal et al., 2005, 2018), as well as aquatic ecosystem health (MacLeod et al., 2011; Tiquia et al., 2007). They can further cause changes in a lake's mixing regime (Bubeck et al., 1971; Novotny et al., 2007, 2008). With increasing Cl^- concentrations and, hence, increasing density of the water, more energy is required to overcome the thermal stratification (Mortimer, 1974). In turn, reduced vertical mixing causes the expansion of DO depleted conditions in the hypolimnion (Figure 3.3) and is consistent with the broadening of the depth interval of positive BVF values (Figure 3.5) plus the increasing trend of the maximum BVF value over the time period considered (Figure 3.4).

The external TP loads to LW, as well as the TP concentrations of both epilimnion and hypolimnion, have been generally declining (Figures 3.4 and 3.6). A possible reason is increasing TP retention by SWM infrastructure, especially stormwater ponds, in the urbanizing watershed of LW (Goh et al., 2019; Kratky et al., 2017, 2021) (Goh et al., 2019; Kratky et al., 2017, 2021). In contrast to TP, however, DIP concentrations exhibit negligible, or only very slightly decreasing, trends during the 1996-2018 period (Figure 3.4). As a result, the DIP:TP ratios in the lake have been on the rise (Figures 3.4 and B1). Also worth noting are the minimum DIP concentrations measured in 1998 and 1999 in the hypolimnion, which occurred during the short-lived operation of the aerator in the lake (see section *3.3.1*). Oxygenation of the bottom waters by the aerator likely inhibited the internal DIP loading from sediments to the water column.

Although the ultimate retention of P in sediment is dependent on a variety of factors, including the flux of organic matter to sediment and the relative concentrations of iron and

sulfur (Orihel et al., 2017), the influence of dissolved oxygen at the sediment-water interface on internal DIP loading is well established (Markelov et al., 2019; O'Connell et al., 2020; Orihel et al., 2017; Parsons et al., 2017). When the hypolimnion remains fully oxygenated, P tends to be retained in the sediments, while the sediments tend to release DIP when the bottom waters become anoxic. Thus, the general trend toward longer annual periods of DO depletion of the hypolimnion (Figure 3.3) and the corresponding increase of the AF has likely promoted internal P loading in LW. This is consistent with generally increasing trends of the DIP:TP ratios (Figure B1). In the epilimnion, the most pronounced increase in the DIP:TP ratio occurred after 2012, that is, when LW's Cl^- concentration rose above 100 mg L^{-1}.

The DIP:TP ratio provides a rough indicator of the relative bioavailability of P, given that DIP represents the fraction of TP that is most easily assimilated by biota (Kao et al., 2022). Thus, the decreasing trends of the average TP concentrations in both the epilimnion and hypolimnion are in part being offset by the increase of the DIP:TP ratios. In addition to in-lake internal loading, SWM infrastructure in the watershed may also cause changes in the lake's DIP:TP ratio. Stormwater ponds, which are the dominant SWM structures in LW's watershed, generally reduce downstream TP loadings (Goh et al., 2019; Jefferson et al., 2017; Kratky et al., 2017). However, they also modify P speciation, often preferentially accumulating particulate P or even becoming net sources of DIP (Duan et al., 2012; Frost et al., 2019; Marvin et al., 2020; Song et al., 2015, 2017).

The relative roles of internal and external P loading in modulating the trends in LW's DIP:TP ratios will need to be further investigated. The available data show that despite the decreasing average TP concentrations in LW, there has been no detectable improvement in the DO concentrations in the hypolimnion. We hypothesize that the rising salinity of LW is responsible for strengthening water column stratification, hence reducing the DO supply to the hypolimnion while enhancing internal P loading.

3.5.2. Statistical analyses

The first principal component (PC1), which explains around 33% of the water chemistry trends, is positively correlated with the hypolimnion DIP, DIN and NH_4^+ concentrations and inversely with the hypolimnion DO (Figure 3.7, Figure 3.8 and B4). Thus, we propose

that PC1 encapsulates the water column stratification, the redox state in the hypolimnion and the mixing regime of LW. As PC1 increases, stratification strengthens, DO in the hypolimnion decreases and the concentrations of DIP and NH_4^+ increase while as PC1 decreases, mixing increases resulting in higher hypolimnetic DO, lower DIP and decreased NH_4^+. This is supported by the observed seasonality of PC1 (Figure B5). In southern Ontario lakes, thermal stratification typically starts in May and then increases until late summer (Kao et al., 2022) . As expected, PC1 shows an increasing trend from May to September-October. The drop in PC1 between October and November can then be attributed to the breakdown of the summer stratification during fall turnover. Moreover, the trend analysis of PC1 shows a positive, admittedly weak (p = 0.38), temporal trend during the period of observation potentially suggesting a strengthening of the summer thermal stratification over time (Figure B6).

The results of the MLR analysis indicate that BVF is the top predictor of PC1 (Table 3.1), hence confirming that the variability in the data explained by PC1 is closely related to the lake's stratification and vertical mixing regime. PC1 also correlates positively with the Cl^- concentration (Table 3.1), which is attributed to the stabilization of the water column stratification by the increasing water density. The other significant predictor for PC1 is the average air temperature (positive correlation) during the two weeks preceding a given sampling date. The latter likely reflects the steeper thermocline during warmer summer months.

The depth distributions of DO indicate a deepening of the redoxcline by approximately 2 m between 1996 and 2018 (Figure 3.3). A comparable observation has been made by Kraemer et al. (2015) based on data from 26 lakes around the world. These authors found that, from 1970 to 2010, stratification in most of the lakes became more stable while also experiencing a deepening of the thermocline. Jane and Rose, 2021 report widespread declines of DO concentrations in both the surface and deep waters of temperate lakes. These authors invoke warmer air temperatures for lowering the O_2 solubility in surface waters and a strengthening of the thermal stratification for causing DO loss in the deeper waters. We propose that, in regions where the use of deicing agents is extensive, salinization is an additional driver of the intensification of lake stratification and, hence, the lowering of hypolimnetic DO concentrations.

While PC1 correlates negatively with the DIP, DIN and NH_4^+ concentrations in the epilimnion, PC2 is positively correlated with the DIP, DIN and NH_4^+ concentrations in both the epilimnion and hypolimnion (Figures 3.7 and 3.8). The decreasing trend of PC2 (Figure 3.4, Figure B6) over the period 1996-2018, further parallels that of the TP concentration in the epilimnion (Figure 3.6). Also, in contrast to PC1, the monthly average PC2 values do not experience a distinct drop in November (Figure B5). This points to a link between the long-term changes of PC2 and the overall trophic and nutrient state of the lake, rather than to internal loading processes. The dependence of PC2 on the air temperature, both during the two-week period preceding sampling as well as averaged over the year (Table 3.1), could reflect the enhanced transfer of biomass-associated N and P produced in the watershed during warmer years (Butturini & Sabater, 1988), but additionally it could reflect trophic state of the lake. We therefore tentatively relate PC2 to the overall trophic and nutrient state of the LW.

The interpretations of PC3 and PC4 are less straightforward. The epilimnion *chl-a*, NO_3^-, and DO concentrations contribute most to both PC3 and PC4 (Figure B4). The correlations between *chl-a* and DO are negative, however (Figure 8). Also, in contrast to PC1, PC3 and PC4 are inversely related to BVF (Table 3.1). For PC3, the strongest predictor variables are the extent of urbanization (positive) and the yearly precipitation (negative). Hence, PC3 may in part reflect nutrient processing and movement of nutrients within the SWM infrastructure in the lake's watershed. We speculate that, during drier years, longer water residence times and the accompanying more stagnant conditions in SWM ponds promote the mobilization of DIP and the elimination of NO_3^- by denitrification as seen in dammed reservoirs and during anoxic conditions in wetlands (Parsons et al., 2017). The proposed impact of variable water residence time in the SWM ponds is consistent with the negative and positive correlations of PC3 with the epilimnion NO_3^- and DIP concentrations, respectively (Figure 3.8). Drier years likely also result in less flushing out of deicing salt applied during preceding winters, hence, providing a possible explanation for the inverse relationship between PC3 and the Cl^- concentration in the lake (Table 3.1).

The rather similar correlation and regression coefficients for PC3 and PC4 seen in Figure 8 and Table 3.1 imply a closeness of the two principal components. The most notable

differences include the statistically significant increasing trend of PC4 with time (τ = 0.18, p = 1.6e-05), compared to little change in PC3 (τ =-0.0063, p = 0.88) (Figure 3.4, Figure B6), and the importance of the yearly 95% percentile of rainfall as a predictor of PC4 rather than the yearly rainfall for PC3 (Table 3.1). Therefore, PC4 could record the impact of more extreme precipitation events on the transfer of N and P to the lake. Intense rainfall tends to cause more direct runoff from surrounding soils. Thus, the inverse relationships of PC4 with *chl-a* and DO could be attributed to increased turbidity that negatively impacts photosynthetic activity while enhancing heterotrophic activity in the lake's surface waters. Nutrient loads exported from soils also tends to be characterized by high N:P ratios (Downing and McCauley, 1992), consistent with the positive correlation of PC4 with the epilimnion nitrate concentration but a negative one with the epilimnion TP concentration (Figure 3.8).

3.5.3. Implications

Seasonal stratification plays a key role in the biogeochemical functioning of lakes. With the establishment of a stable thermocline, the hypolimnion becomes increasingly isolated from the atmosphere thereby causing deoxygenation and the build-up of reduced chemical species, such as ammonium. It also activates the recycling of DIP from the sediments. That is, internal P loading gains in importance relative to the external P loading of the lake (Markelov et al., 2019).

According to our results, a key impact of urbanization on the biogeochemistry of LW is related to the growing impervious land cover and the accompanying increase in road salt application, which leads to a strengthening of the lake's water column stratification. Lake eutrophication is usually attributed to excessive P enrichment fueling enhanced algal growth (Schindler, 1971). Since the year 2000, however, the concentrations of TP and DIP in LW exhibit downward trajectories, while the *chl-a* data series imply little change in primary productivity of the lake. Thus, the symptoms of eutrophication, in particular the lengthening of the annual period of low hypolimnion DO concentrations, could be caused mainly by the progressive salinization of the lake.

Many temperate lakes experience declining DO concentrations and more intense stratification, changes that tend to be ascribed to climate warming (Jane et al., 2017). Our

results suggest that, in cold and cold-temperate regions, salinization may be an additional driver of these changes. As shown by Dugan et al. (2017), in the past decade the Cl^- concentrations of lakes in urban watersheds in North America and Europe have been exhibiting generally increasing trends (Sorichetti et al., 2022), like the one observed in LW. Thus, the proposed salinization-driven water column stratification may be widespread. Efforts to control the external nutrient loading to such lakes may therefore be offset by the enhanced internal P loading caused by growing DO depletion of bottom waters (Søndergaard et al., 2003).

Historical use of road salt in urban watersheds has also likely created chloride legacies in groundwater and soils (Mazumder et al., 2021). These legacies could continue to supply excess Cl^- to the lakes in these watersheds, even if winter salt applications were reduced or altogether halted. Protecting the health of urban lakes therefore calls for integrated management strategies that account for the impacts of past and ongoing road deicing practices on a lake's mixing regime. This, however, will require further work to better understand the relative contributions of climate change, urbanization, and salinization to changes in lake water quality.

3.6. Conclusions

The impervious urban land cover increased significantly in LW's watershed during the period (1996-2018) for which water quality data are analyzed in this study. The growing impervious and directly connected impervious land covers have been accompanied by an increase in the annual duration of anoxic conditions in the hypolimnion, as well as an increase in the DIP:TP ratio. The increasing anoxia and intensification of the water column stratification have been occurring despite stable, even slightly decreasing, external TP loads to the lake, likely because of the expansion of stormwater management infrastructure in the watershed since the early 2000s. At the same time, in-lake TP concentrations have declined, while *chl-a* concentrations show no evidence of increasing algal productivity.

Statistical analyses (PCA and MLR) of the water chemistry time series data shed light on the mechanism(s) responsible for the intensification of eutrophication-like symptoms in LW. The progressive salinization of the lake emerges as a major driver of the

strengthening of water column stratification and the accompanying changes in water quality, in particular the expansion of hypolimnion anoxia and the enhancement of internal P loading. The latter contributes to maintaining LW in its eutrophic state. To our knowledge, this is the first study that links salinization with lake eutrophication symptoms. Lake management in regions where the use of de-icing agents is widespread therefore needs to consider the multi-faceted role of salinization in changes lake water quality, including those that traditionally are associated to increasing external nutrient loading. Further research on the water quality impacts of de-icing agents will require reliable data on their types and application rates.

Chapter 4

Road salt-induced salinization impacts water geochemistry and mixing regime of a Canadian urban lake

Modified from:

Radosavljevic J., Slowinski S., Rezanezhad F., Shafii M., Gharabaghi B., and Van Cappellen P. (2023). Road salt application is reducing vertical mixing and degrading water quality in a Canadian cold-temperate urban lake water. Submitted to *Applied Geochemistry.*

4.1. Summary

The extensive use of road salts as deicers during winter months is causing the salinization of freshwater systems in cold climate regions worldwide. We analyzed 20 years (2001-2020) of data on lake water chemistry, land cover changes, and road salt application for the Lake Wilcox (LW) located in southern Ontario, Canada. The lake is situated within a rapidly urbanizing watershed in which, during the period of observation, on average 785 tons of road salt were applied annually. However, only about a quarter of this salt has reached the lake so far. That is, most salt has been retained in the watershed, likely through accumulation in soils and groundwater. Despite the high watershed salt retention, time series trend analyses for LW show significant increases in the dissolved concentrations of sodium (Na^+) and chloride (Cl^-), as well as those of sulfate (SO_4^{2-}), calcium (Ca^{2+}), and magnesium (Mg^{2+}). The relative changes in the major ion concentrations indicate a shift of the lake water chemistry from the mixed SO_4^{2-}-Cl^--Ca^{2+}-Mg^{2+} type to the Na^+-Cl^- type. Salinization of LW has further been strengthening and lengthening the summer stratification of the lake, which, in turn, has been enhancing hypoxia of the hypolimnion and increasing the internal loading of the limiting nutrient phosphorus. The theoretical salinity threshold at which fall overturn would become increasingly unlikely was estimated at around 1.23 g kg^{-1}. A simple chloride mass balance model predicts that, under the current trend of impermeable land cover expansion, LW could reach this salinity threshold by mid-century. Our results also highlight the need for additional research on the accruing salt legacies in watersheds because they represent potential long-term threats to water quality for receiving freshwater ecosystems and regional groundwater resources.

4.2. Introduction

Salinization of inland freshwaters is a rising problem globally (Kaushal et al. 2005, 2021; Novotny and Stefan, 2010; Perera et al., 2013). It is driven by domestic and industrial effluents, human-augmented chemical rock weathering, mine drainage, agricultural runoff, seawater intrusion, and road salt application (Kaushal et al., 2018, 2019, 2021). Salinization usually results in increasing trends in the concentrations of chloride (Cl^-), sodium (Na^+), calcium (Ca^{2+}), magnesium (Mg^{2+}), potassium (K^+), sulfate (SO_4^{2-}) and

dissolved inorganic carbon (DIC) of streams, lakes, wetlands, and aquifers (Corsi et al., 2015; Dugan et al., 2017; Ladwig et al., 2021; Trenouth et al., 2015). Elevated salinity impairs freshwater ecosystem health by diminishing habitability for sensitive biota, altering the food web community structure, changing the base cation composition, increasing heavy metal mobilization, and modifying the mixing regime (Cañedo-Argüelles et al. 2016; Couture et al., 2015; Koretsky et al., 2012; Ladwig et al., 2021; Norrström et al., 2001; Scott et al., 2018).

Many recent salinization trends have been reported for lakes in urban areas of cold winter regions, primarily related to the runoff of salts applied on roads, sidewalks, and parking lots as deicing agents in the winter (Dugan et al., 2017; Haake & Knouft, 2019; Kaushal et al., 2005, 2017; Meriano et al., 2009; Trenouth et al., 2015). According to Dugan et al. (2021), current trends in de-icing salt application practices have put more than 7,000 lakes in North America at risk of water quality impairment due to salinization. Urban runoff enriched in ions contained in deicers can alter the natural ion balance in receiving water bodies (Rhodes and Guswa; 2016; Sutherland et al., 2019) and, hence, change the geochemical water type. The latter is essential when assessing impacts on water quality because water type is linked to alkalinity and pH buffering capacity. Road salt application can mobilize the base cations Ca^{2+}, Mg^{2+}, and K^{+} from soils via displacement by Na^{+} (Eimers et al., 2015; Norrstrom and Bergstedt, 2001; Rhodes and Guswa, 2016; Rose, 2012; Rosfjord et al., 2007; Sutherland et al., 2018). However, changes in geochemical water type caused by road salt application have received limited attention thus far.

Impervious surfaces in urban landscapes (*e.g.,* roads) and stormwater sewers serve as direct pathways for the transport of salt to downstream water bodies (Foley et al., 2005; Kaushal et al., 2017; Corsi et al., 2015; Dugan et al., 2017, 2021; Haake & Knouft, 2019; Meriano et al., 2009; Wyman et al., 2018; Tabrizi et al., 2021). Enhanced salt transport with stormwater runoff reduces the watershed retention of salt ions that would otherwise infiltrate in the soils and further into groundwater (Perera et al., 2013). Chloride watershed retention efficiencies in the range 30-90% have been reported for various watersheds (Oswald et al., 2019; Meriano et al., 2009). Moreover, Oswald et al. (2019) showed that watershed Cl^{-} retention efficiency decreases with increasing impervious land cover across a series of watersheds in southern Ontario, Canada. To our knowledge, the changes in

watershed Cl^- retention during periods of rapid urbanization have not yet been reported in the literature.

Lake water column stratification and the associated lake mixing regime are also modified by salinization. Intensification of stratification, in turn, may adversely affect lake bottom water oxygenation and enhance the in-lake recycling of oxygen-sensitive species, such as nutrients and trace metals (Ladwig et al., 2021; Markelov et al., 2019; Orihel et al., 2017; Parsons et al., 2017; Straile et al., 2003). Temperate lakes are typically dimictic with turnover occurring two times per year in spring and fall, while stratifying in summer (Lewis, 1983; Spigel & Imberger, 1980). The water density profile is the determinant of vertical mixing dynamics in lakes; it is modulated by both temperature and salinity (Boehrer and Schultze, 2008; Boehrer et al., 2013, 2017; Eklund, 1965; Ladwig et al., 2021; Woolway et al., 2019, 2022). In freshwater lakes, the temperature is the dominant variable controlling water density variations. In some lakes, however, salinization has become an important driver of changes in water density (Ladwig et al., 2021; Millero & Poisson, 1981) that, in turn, can lead to disrupted, delayed, or even ceased vertical water column mixing (Ladwig et al., 2021).

In this study, we assess the impact of road salt applications on the water chemistry and mixing regime of Lake Wilcox (LW) in southern Ontario, Canada. Rapid urbanization of LW's watershed has resulted in rising loads of salt ions to the lake through stormwater runoff. Harmful algal blooms (HABs), high dissolved phosphorus concentrations, and expanding periods of bottom-water hypoxia in LW became growing concerns in the 1980s (Reports 5 and 6 in Table A1; Radosavljevic et al., 2022). Even though the total phosphorus loading to the lake decreased after the implementation of stormwater ponds, eutrophication-like symptoms have persisted. In a previous study, we showed that these symptoms are caused by the rising salinity of the lake (Radosavljevic et al., 2022). Here, we hypothesized that salinization is driving coupled changes in LW's water chemistry and stratification regime. We analyzed lake water chemistry data available for 20 years (2001-2020) to delineate the trajectories of the major dissolved ion concentrations (Cl^-, Na^+, Ca^{2+}, Mg^{2+}, SO_4^{2-} and DIC) and determine how the lake's geochemical water type has been changing during salinization. Moreover, to predict how lake Cl^- and Na^+ concentrations, water density, and the lake's vertical mixing regime may further evolve

under different future road salt management scenarios, we developed mass balance models to quantify the accumulation of Cl^- and Na^+ in the watershed versus in the lake.

4.3. Material and methods

4.3.1. Water quality dataset

Water quality data used in this study, provided by CRH, consisted of bi-weekly measured concentrations of major ions and other physicochemical parameters in LW's epilimnion and hypolimnion for the period 2001 to 2020. The data included water temperature, pH, alkalinity (as $CaCO_3$), and the aqueous concentrations of Na^+, potassium (K^+), Ca^{2+}, Mg^{2+}, and Cl^-, SO_4^{2-} and DIC.

4.3.2. Water quality data analyses

4.3.2.1. Geochemical water type: Piper diagram

Piper diagrams are a common graphical representation of the major chemical ion composition of natural waters and are used to classify water geochemical types (Piper, 1944). A Piper diagram shows a water chemical composition as percentages of cations and anions. It was used here to display the trajectory of LW's water geochemistry over the period of 2000 to 2020.

4.3.2.2. Salinity threshold for meromixis

Imberger & Patterson (1989) introduced the "*lake number*" (*LN*) concept to estimate the hypolimnetic salinity threshold above which lake turnover becomes increasingly unlikely. The concept has been successfully applied in several studies (e.g., Ladwig et al. 2021; Lindenschmidt & Chorus, 1998; Robertson & Imberger, 1994). The lake number is a dimensionless parameter describing the balance between a lake's mass moment and the wind moment, formulated as:

$$LN = \frac{g \cdot \left(St \cdot \frac{Ao}{g}\right) \cdot \beta}{\rho_z \cdot u^2 \cdot Ao \cdot z_{vol}} \quad (4.1)$$

where St is the Schmidt stability (Schmidt, 1928), which represents the amount of energy needed to mix the entire water column or, equivalently, the potential energy of the water column [J m^{-2}], g is the gravitational acceleration [m s^{-2}], Ao the surface area of the lake

[m^2], β the angle between the metalimnion surface to the lake bottom [-], ρ_z the bottom water density [kg m^{-3}], u the wind friction velocity [m s^{-1}], and z_{vol} the depth of the center of volume [m]. Note that by multiplying St in eq (1) by $g\frac{A_z}{g}$ the potential energy is obtained in units of J. When $LN > 1$, the water column is stable and whole water column vertical mixing is unlikely. When $LN < 1$, vertical mixing is expected to occur (Ficker et al., 2017; Lindenschmidt & Chorus, 1998).

Here, we estimated the threshold salinity for dynamic stability, $LN = 1$, under average conditions for the 2016-2020 period. Like other lakes in southern Ontario, LW experiences peak stratification during summer, followed by turnover during fall (Boehrer & Schultze, 2008; Woolway & Merchant, 2018). Hence, we calculated the threshold salinity for fall turnover using the average August-September temperature profile as representative of late summer stratification and the average September-October wind velocity as representative for fall turnover. The wind velocity data were measured 10 m above ground surface at the Richmond Hill meteorological station of Environment and Climate Change Canada. Because wind velocity is highly variable, we also calculated the threshold salinities for the lower and upper boundaries of the range that contains 90% of wind velocities measured during the 2016-2020 period for which extensive data is available. Other data needed to calculate the various terms on the RHS of Eq. (4.1) is provided in Reports 4, 5 and 6, and in Table A1. Detailed information about *LN* and the threshold salinity can be found in the Supplementary Information, section C2.

4.3.2.3. Trend analysis

The Mann-Kendall (MK) trend analyses were performed using the XLSTAT software (Addinsoft, version 2022). Positive values of the MK statistic indicate an increasing trend, negative values suggest a decreasing trend, and a zero value signifies no change over time. The magnitude of the MK statistic's deviation from zero serves as evidence for the presence of a significant temporal trend in the data series (Hirsch et al., 1982). To enhance comparability between data series with varying numbers of observations, we present the Kendall's-τ (tau) values alongside the MK statistic. These τ values rescale the MK results within the range of -1 to +1 (Helsel and Hirsch, 1992). More insights into the MK test could be found in Hirsch et al. (1982) and Kendall (1975).

4.3.3. Mass balance modeling

We developed simple lake mass balance models for Cl^- and Na^+ to assess the impact of watershed de-icing salt management scenarios on water column salinity and stability (*i.e.,* stratification). The model, inspired by previous studies of Sutherland et al. (2018), Doerr et al. (1994), and Sonzogni et al. (1983), predicts how the lake water column Cl^- and Na^+ concentrations change as a function of the external watershed Cl^- and Na^+ loads. Assumptions in the model include: (i) the lake is a perfectly mixed system, and (ii) Cl^- and Na^+ are conservative ions, that is, no reaction terms were considered that removed or added Cl^- or Na^+ from or to the water column (Sonzogni et al., 1983; Sutherland et al., 2018; Doerr et al., 1994). The model steps forward in time on a yearly time scale:

$$C_{i+1} = (C_i + \Delta C_{i+1}) \tag{4.2a}$$

$$\Delta C_{i+1} = (\sigma_{i+1} \cdot n_{i+1} - \gamma \cdot C_i) \cdot \Delta t \tag{4.2b}$$

where C_i is the average annual Cl^- (or Na^+) lake water concentration in the *i*-th year, ΔC_{i+1} is the change in the lake's mean annual Cl^- (or Na^+) concentration from year *i* to year *i*+1, σ_{i+1} represents the contribution to ΔC_{i+1} of the change in external loading from year *i* to year *i*+1 [mg L^{-1} y^{-1}], n_i is the number of years [unitless] since 2000, which was the first year for which a complete set of water column Cl^- (and Na^+) data were available (n_i = 1, 2, 3…, for i = 1, 2, 3…), γ is the lake's flushing rate constant that controls the removal rate of Cl^- (or Na^+) from the lake via the outlet [y^{-1}]; and Δt is the time step (here 1 y).

Equations (2a) and (2b) were fitted to the observed Cl^- and Na^+ concentration data for the period 2001-2020, hence retrieving the yearly values of σ_{i+1}. The Supplementary Information, section C3 provides details of the fitting procedure. For any given year, the external load of Cl^- (or Na^+) normalized to the volume of the lake, L_E [mg L^{-1} y^{-1}], was then given by:

$$L_E = \sigma_{i+1} \cdot n_{i+1} \tag{4.3}$$

For 2016, 2017, 2018, and 2019, CRH reports annual Cl^- load estimates based on measured discharge and chemistry data for the various inflows to LW. (Note: the available

data were insufficient for the other years to calculate annual loads.) The CRH load estimates agreed with the model-derived values obtained here.

The model was run for several future Cl^- and Na^+ loading scenarios from 2020 till 2050. In the business-as-usual scenario, the areal salt application rates in the watershed were kept the same as in 2020, but the imperviousness continued to increase linearly to 80% by 2050, which is a realistic endpoint under current regional urban development planning (W. Withers, personal communication). In the two mitigation scenarios, the external load changes rates (i.e., σ_{i+1}) dropped instantaneously from their 2020 values (σ_{i+1}= 5.3 and 2.8 mg L^{-1} y^{-1} for Cl^- and Na^+, respectively) by 50% or 75% and then remained constant at their new values from 2021 to 2050.

4.3.4. Watershed salt application and retention rates

The road salt, and therefore Cl^- and Na^+, application rates to the watershed were derived from CRH's 2011 and 2016 Salt Management Plans plus Report 6 in Table A1, according to which event-based salt type and application rates are adjusted to reflect projected air temperature, snow depth, and ice conditions (see Table C2). As a result, areal application rates during salting events may range from 40 to 110 g m^{-2} depending on the weather conditions (Report 6 in Table A1). However, because total annual road salt usage was not available for each individual year during the period 2000-2020, we used the average salt application rate of 52 g m^{-2} reported by CRH, a value close to the average value of 58.1 g m^{-2} estimated previously for the same region (Lembcke et al., 2017; Fu et al., 2013). The average application rate was then combined with the average number of salting events per year to estimate the total amount of road salt applied annually. Based on the Road Operations and Data Analysis (ROADA) GPS Truck data, the number of weather events requiring road salt application during the period of observation (2001-2020) ranged from 58 to 63 per year, with an average of 61.

For each year from 2001 to 2020, the annual salt loading to the watershed (L_{total}) was calculated by multiplying the average salt application rate (52 g m^{-2}) with the average yearly number of salting events (61), LW's watershed surface area, and the fraction of imperviousness where road salt is applied (sidewalks, roads, school property and parking lots). Thus, the growing imperviousness was the only variable that changed from year to

year (see Supplementary Information, section C3, for more details). Given that clear road salt (NaCl), was the main deicing agent used in the watershed during the 2001 to 2021 period, the road salt application rates were converted to Na^+ and Cl^- application rates using the mass ratios of 0.6:1 and 0.4:1 of Cl^- and Na^+ in NaCl.

The yearly amounts of Cl^- and Na^+ retained in the watershed (L_R) were calculated as:

$$L_R = L_{total} - L_E \tag{4.4}$$

where the value of L_E was obtained with Eq. (4.3). The retention efficiency (RE) of Cl^- or Na^+ in the watershed, expressed as a percentage, was then obtained as:

$$RE = \frac{L_R}{L_{total}} * 100\% \tag{4.5}$$

Upper and lower bounds for the watershed loads and retention efficiencies of Cl^- or Na^+ were assigned using the highest and lowest reported application rates of road salt (i.e., 110 and 40 g m^{-2}), as well as the highest and lowest reported number of yearly salting events (63 and 58). Our approach may underestimate the total road salt application rates in the watershed because it does not account for blasting (locally higher application rates on curves or steep slopes) or multiple salt truck crossings at wide intersections after an event. Underestimations of the watershed salt applications would translate into underestimations of the retention efficiencies. However, the associated uncertainties are likely well within the calculated upper and lower bounds.

4.4. Results

4.4.1. Water chemistry trends and geochemical water type

The Mann-Kendall (MK) analyses showed significant increasing trends in both epilimnion and hypolimnion for the major dissolved ions, DIC, and alkalinity (Figure 4.1 and Table 4.1), except for K^+. Some of the concentration time series are illustrated in Figures 2. Minimum, maximum, and average values for the various water geochemical variables are given in Table 4.1.

As seen also on the Piper diagram (Figure 4.3) the main cation in the epilimnion of LW were Na^+ and K^+, followed by Ca^{2+} and Mg^{2+} (bottom left triangle in Figure 4.3), while Cl^-

was the main anion followed by SO_4^{2-} and DIC (bottom right triangle in Figure 4.3). The hypolimnion exhibited the same trends with the water geochemistry evolving from the mixed Ca^{2+}-Mg^{2+}-Cl^- -HCO_3^- type (zone 3 in Figure 4.3) to the Na^+-Cl type (zone 2 in Figure 4.3; note that Figure 4.3 only shows the results for the epilimnion, however, the results are identical for the hypolimnion). Moreover, the epilimnion concentrations of Na^+ and Cl^- (in molar units) exhibited a strong positive relationship with a slope of 0.902 (Figure C2).

4.4.2. Critical salinity threshold for fall meromixis

The average wind speed in September-October during the 2016-2020 period was 4.8 m s^{-1}, with 90% of the measurements comprised between 3.1 and 5.0 m s^{-1} (Figure 4.4). According to Eq. (4.1), the salinity threshold for the average wind velocity was 1.23 g kg^{-1}, which corresponds to a Cl^- concentration of 385 mg L^{-1}. The fall turnover would be inhibited at higher salinities, hence turning LW from a dimictic to a monomictic lake. The present salinity of 0.55 g kg^{-1} is below the threshold value for the average wind velocity (4.8 m s^{-1}) and at the lower end of the 0.49 and 1.34 g kg^{-1} salinity range for the 90% wind velocity range (3.1-5.0 m s^{-1}). The rapidly rising salinization of LW therefore implies that fall turnover may increasingly be bypassed in the years ahead (see section 3.3.2).

4.4.3. Mass balance modelling

4.4.3.1. External Cl^- and Na^+ loads

The estimated yearly external loads of Cl^- and Na^+ from 2001 to 2020 ranged from 44 to 229 t yr^{-1} and 26 to 146 t yr^{-1}, respectively (Figure 4.5), with an average of 120 t yr^{-1} for Cl^- and 62 t yr^{-1} for Na^+. The model-predicted external Cl^- load averaged from 2016 to 2019 was 227 t yr^{-1}, which compared very well with the observed average load of 221 t yr^{-1} derived from inflow concentration and discharge data measured at LW's inflow point during the same 4 years.

4.4.3.2. Future road salt management scenarios

In the business-as-usual scenario, by 2050, lake Cl^- and Na^+ concentrations would reach 395 and 245 mg L^{-1} values, respectively. Note that the 2050 Cl^- concentration (as well as the salinity) would then exceed the threshold value of 385 mg L^{-1} for fall turnover under

the average wind velocity of 4.8 m s^{-1}. In the mitigation scenarios, the Cl^- concentrations in the lake would decline to 45 mg L^{-1} (50% reduction of σ_{i+1}) and 30 mg L^{-1} (75% reduction of σ_{i+1}) by mid-century (Figure 4.6). Moreover, the Cl^- and Na^+ concentrations would reach their new steady state values within about 10 years (i.e., around 2030).

4.4.4. Cl^- and Na^+ watershed application and retention efficiencies

On average 758 t yr^{-1} (range: 545-1078 t yr^{-1}) of road salt was applied to LW's watershed during the 2001-2020 period (Figure 4.7). The corresponding average amounts of Cl^- and Na^+ were 454 t yr^{-1} (range: 327 to 628 t yr^{-1}) and 302 t yr^{-1} (range: 218-418 t yr^{-1}) respectively (Figure 4.8). The cumulative mass of Cl^- applied as road salt in the watershed for the period 2001 to 2020 was 9101 t and for Na^+ 6067 t (Figure 4.8). For comparison, the cumulative masses of Cl^- and Na^+ retained in the watershed between 2001 and 2020 were 6480 t and 4655 t, respectively (Figure 4.8).

Table 4.1. Minimum, maximum and average values and Kendall-T values of major cation and anion concentrations, alkalinity, electrical conductivity, and calcite saturation index (SI) in the hypolimnion (Hypo.) and epilimnion (Epi.) of Lake Wilcox for the 2001-2020 period.

	Minimum value	Maximum value	Average value	Kendall-T (p<0.001)	*n*
Alk. Epi ($CaCO_3$ L^{-1})	56	223	107	0.235	176
Alk. Hypo. ($CaCO_3$ L^{-1})	99	206	142	0.671	161
EC Epi. (µS cm^{-1})	213	963	551	0.925	324
EC Hypo. (µS cm^{-1})	231	1506	561	0.941	324
Na^+ Epi. (mg L^{-1})	19	122	58	0.889	176
Na^+ Hypo. (mg L^{-1})	6	210	61	0.792	214
Cl^- Epi. (mg L^{-1})	50	198	109	0.938	320
Cl^- Hypo. (mg L^{-1})	49	301	90	0.731	176
DIC Epi (mg L^{-1})	3.7	41	23	NS	251
DIC Hypo. (mg L^{-1})	31	55	38	0.660	103
SO_4^{2-} Epi. (mg L^{-1})	0.3	20	16	0.405	299
SO_4^{2-} Hypo. (mg L^{-1})	1	14	13	0.186	167
Ca^{2+} Epi. (mg L^{-1})	21	74	41	0.393	218
Ca^{2+} Hypo. (mg L^{-1})	32	77	52	0.541	214
Calcite SI Epi.	-1.8	0.03	-0.33	0.092	165
Calcite SI Hypo.	-1.10	0.003	-0.59	0.095	165

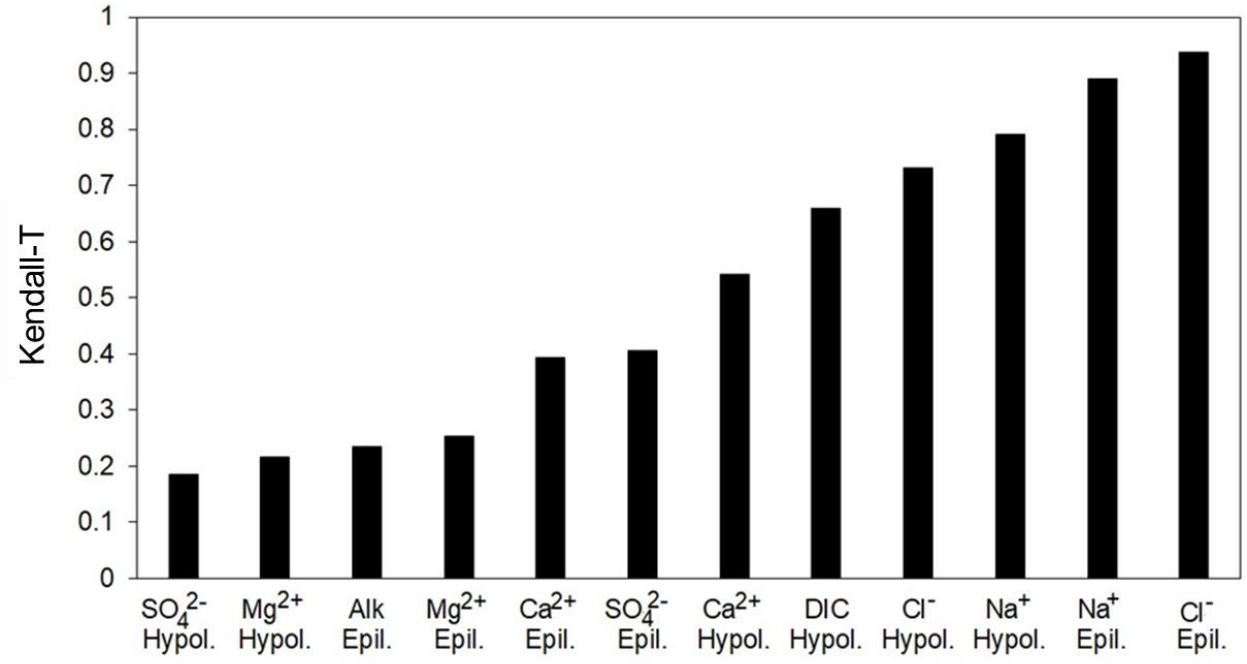

Figure 4.1. Kendall's tau values for the Mann-Kendall trend analyses of water chemistry variables that show a statistically significant ($p \leq 0.01$) trend in the hypolimnion (Hypo.) and epilimnion (Epi.) of Lake Wilcox for the 2001-2020 period.

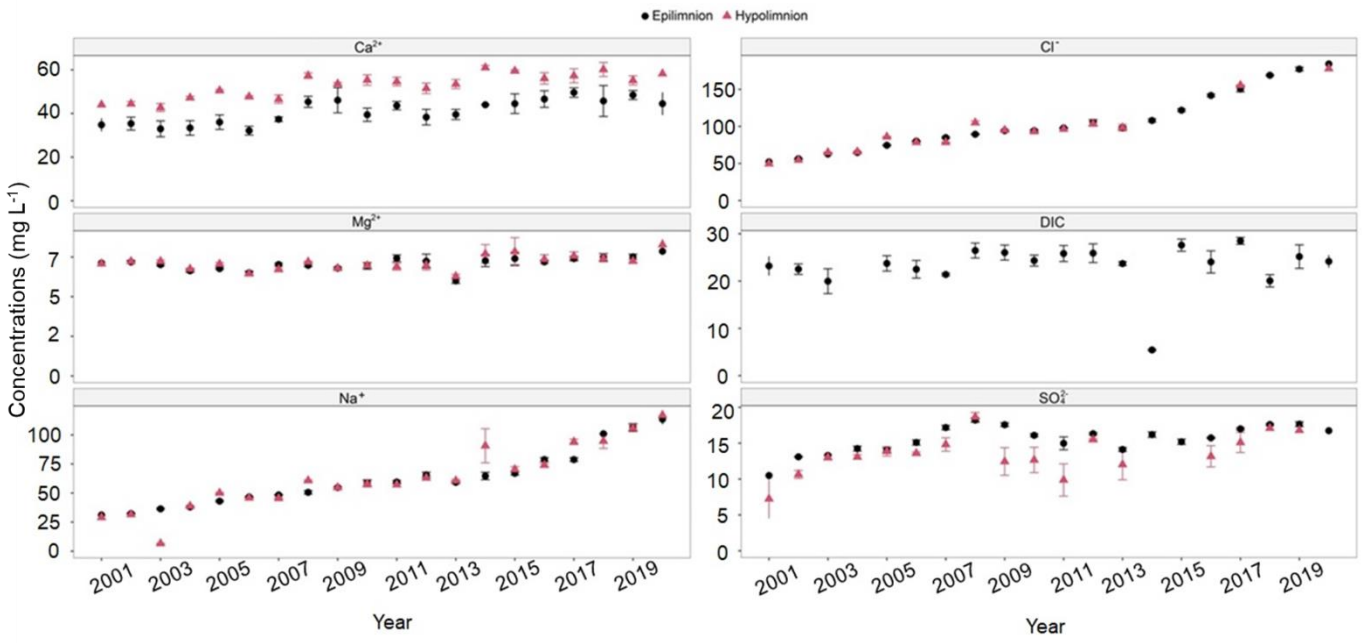

Figure 4.2. Concentration time series of calcium (Ca^{2+}), magnesium (Mg^{2+}), sodium (Na^{+}), chloride (Cl^{-}), dissolved inorganic carbon (DIC), and sulphate (SO_4^{2-}) for both epilimnion and hypolimnion over the period 2001 to 2020.

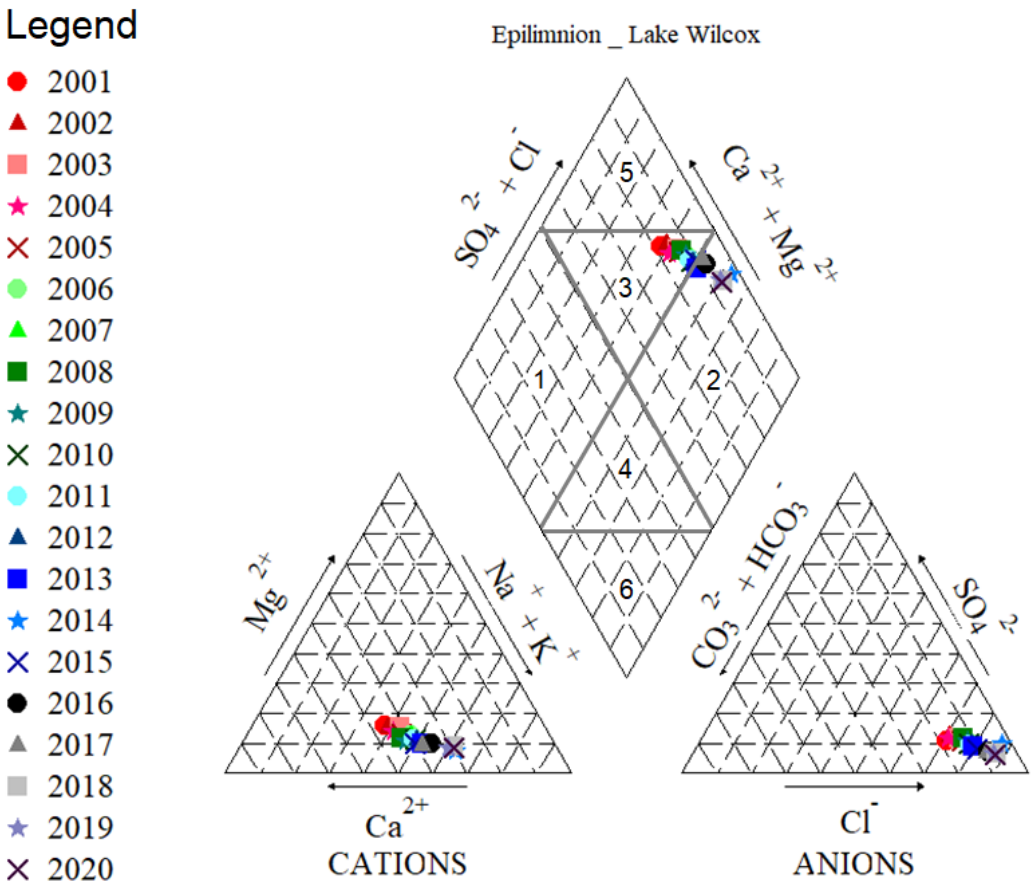

Figure 4.3. Piper diagram for LW's epilimnion major ion water chemistry, for the period 2001 to 2020.

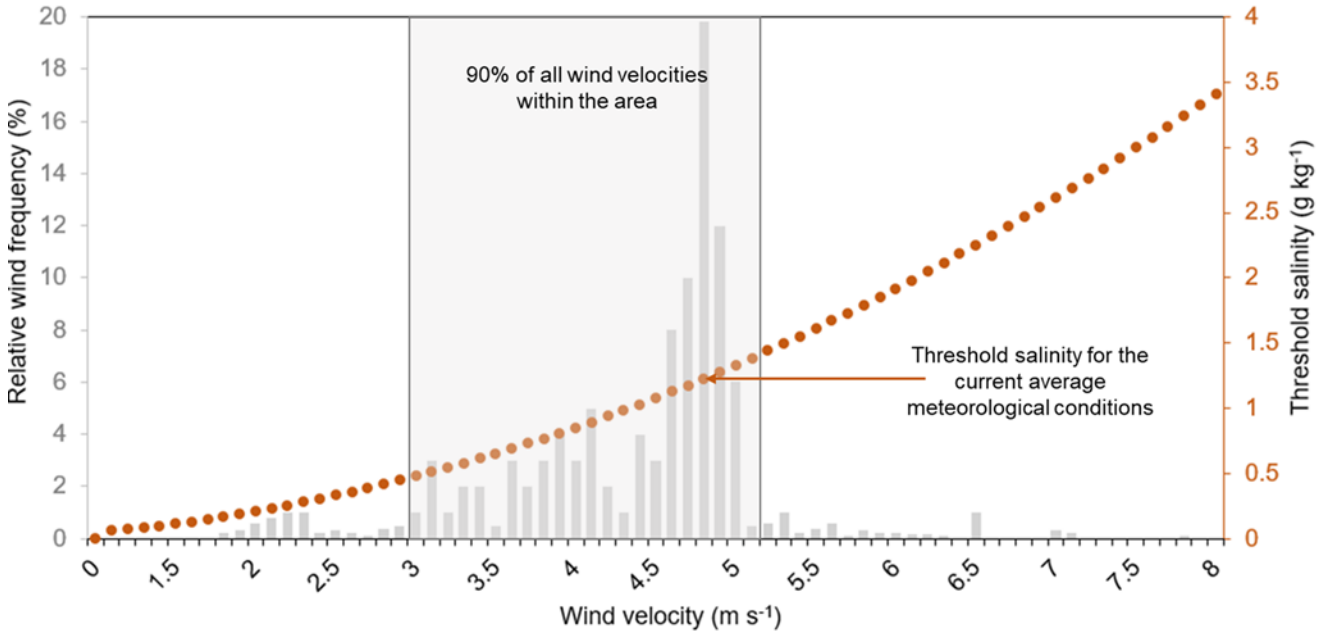

Figure 4.4. Frequency distribution of wind velocity at the Richmond Hill meteorological station at 10 m above the land surface (grey bars). Also shown are the threshold salinity values calculated with Eq. (4.1) as a function of the wind velocity (red circles). The mean wind velocity is 4.8 m s^{-1}.

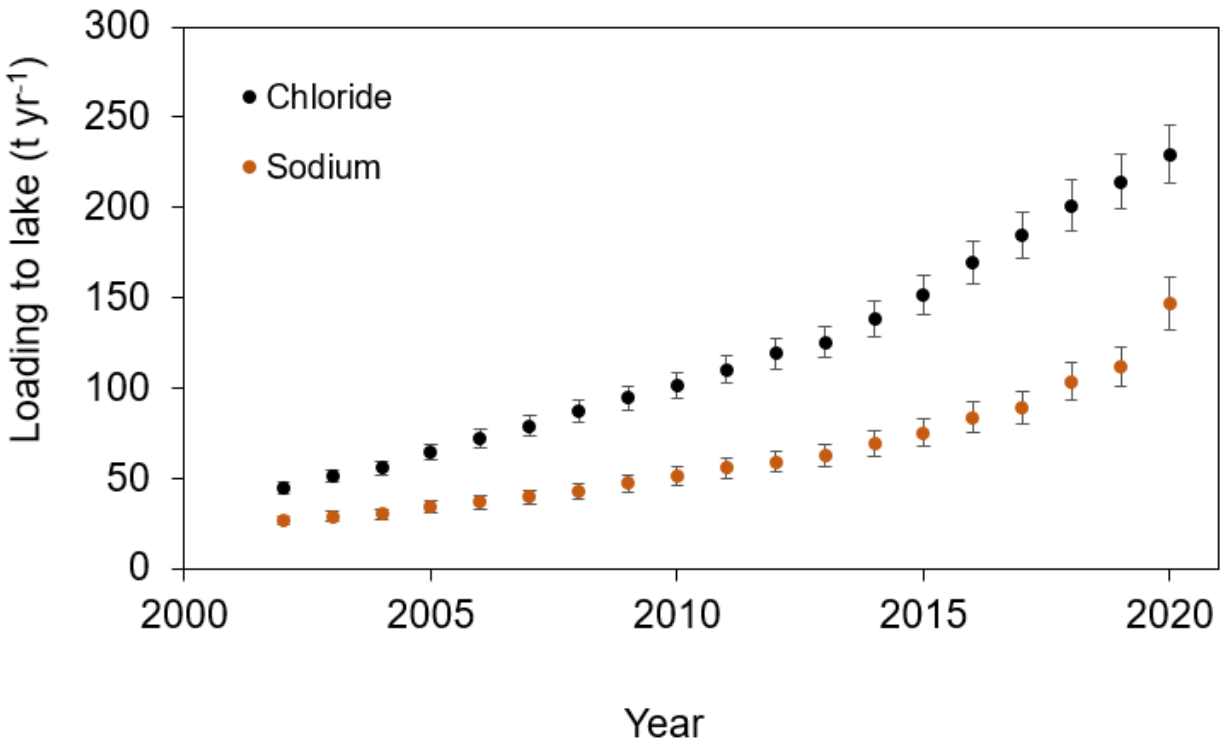

Figure 4.5. Annual mass loadings of Na^+ and Cl^- to LW during the period of observation (2001-2020), where the error bars represent the standard deviation.

4.5. Discussion

4.5.1. Salinization correlates with urbanization

Electrical conductivity and major ion concentrations have been on the rise in LW over the past two decades (Figures 4.2, C3, C4). Similar temporal trends have been observed in other cold and cold-temperate lakes (Dugan et al., 2017; Kaushal et al., 2013, 2017). In LW, these trends correlate with the increase in imperviousness of the watershed that, in turn, correlates with increasing amounts of road salt applied during the winter season (Radosavljevic et al., 2022). The lake mass balance models for Cl^- and Na^+ presented here corroborate this finding. While LW road salt is the main driver of salinization, other sources of excess ions may contribute to salinization in other lakes, including those not experiencing cold winters. In urban and urbanizing watersheds, these additional sources comprise fertilizer applications, detergent inputs, domestic sewage, industrial waste, and runoff from construction sites (Lind et al., 2018; MacLeod et al., 2011; Haq et al., 2018). Therefore, the effects of salinization associated with urbanization on water chemistry and mixing dynamics seen in LW may be widespread around the globe.

The most significant increasing trends in ion concentrations are those observed for Cl^- and Na^+ (Kendall's-τ of 0.938 and 0.889, respectively, Figure 4.1). The correlation of these trends with watershed imperviousness (p<0.001) is the result of the increased runoff of stormwater to the lake plus the growing amounts of de-icing salts applied as the fraction of urban area in the watershed expands (Scott et al., 2019). The simultaneous increases in lake water Ca^{2+} and Mg^{2+} concentrations may in part reflect the presence of these ions in the deicing salts used in LW's watershed (Table C2). The main source of Ca^{2+} and Mg^{2+}, however, is likely cation exchange with Na^+ as observed in previous studies (Norrstrom and Bergstedt, 2001; Rhodes and Guswa, 2016; Rose, 2012; Rosfjord et al., 2007; Sutherland et al., 2018).

4.5.2. Changing geochemical water type

As a result of the road salt applications, the water chemistry of LW is evolving from the mixed Ca^{2+}-Mg^{2+}-Cl^- -HCO_3^- type to the Na^+-Cl^- type (Figure 4.3). The excess Na^+ ions delivered to the lake are reducing the relative contribution of base cations (Mg^{2+} and Ca^{2+}) that would generally dominate under pristine conditions. The Piper plot also shows that

strongly acidic anions (Cl^- + SO_4^{2-}) overtake amphoteric anions (i.e., DIC). Over time, LW's pH buffering capacity is therefore decreasing making it more sensitive to pH perturbations due to, for example, increasing atmospheric CO_2 concentrations, warmer air temperatures, and shifts in algal growth (Hasler et al., 2018, Raven et al., 2020). Therefore, the concern is that lowering pH buffering capacity due to salinization may reduce the resiliency of the lake ecosystem toward climate change. Changes in water geochemistry like those reported here are expected to occur in other urban lakes where salinization is disproportionally increasing the Na^+ and Cl^- ion concentrations.

4.5.3. Watershed salt ion retention

The retention efficiencies of Cl^- and Na^+ decrease with the increasing imperviousness of the watershed (Figure 4.9). This trend in salt ion retention has also been observed in other watersheds (Oswald et al., 2019; Perera et al., 2013). It reflects the decline in transit time of stormwater with increasing expansion of the urban land cover and, hence, leaving less time for solutes to infiltrate into the subsurface (McGrane et al., 2016; Morales and Oswald, 2020). The annual watershed Cl^- retention efficiencies for LW during the 2001-2020 period fall within the previously reported range of 30 to 90% (Novotny, 2009; Oswald et al., 2019).

The relationship between the Cl^- (and Na^+) retention efficiency and the fraction of total impervious land cover shows an inflection around 2011 (Figure 4.9). One possible reason is that, prior to 2011, road salt management changed from applying a salt-sand mixture while only salt has been applied since 2011. Another, likely more important, reason is the increase in the connected impervious cover near the lake that occurred around 2011. Connected impervious cover decreases the overall water travel time. In addition, impervious areas close to, and directly discharging into, a receiving water body more strongly impacts water quality than more upland impervious area not connected directly with the receiving water body (Brabec et al., 2002). Oswald et al. (2019) similarly showed that, in addition to the total impervious land cover, the spatial distribution of imperviousness, especially the proximity of the impervious areas to the watershed outlets to the lake, is an important control on the salt ion retention efficiency.

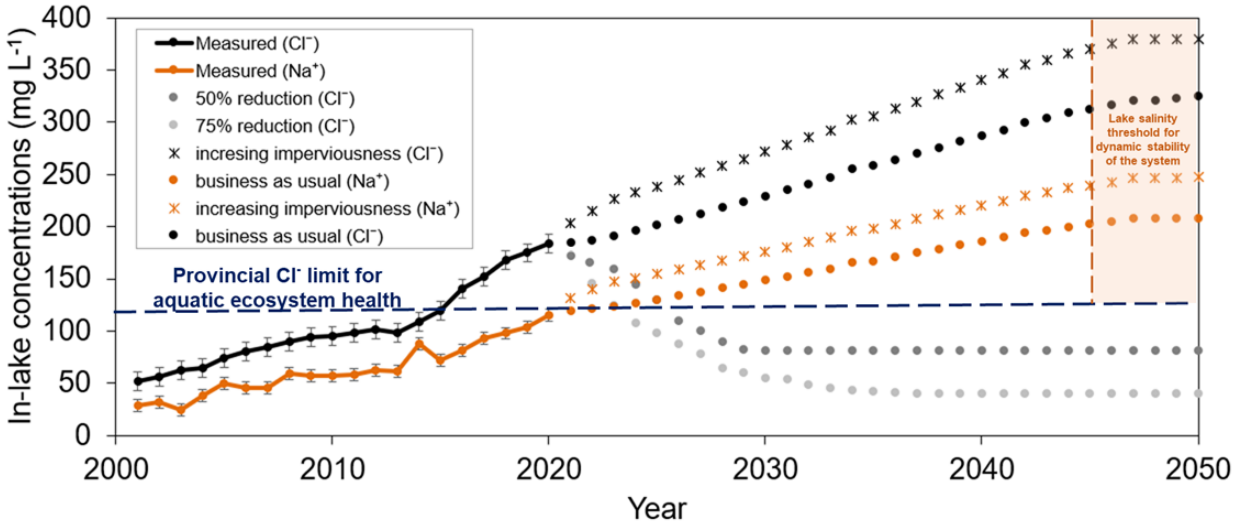

Figure 4.6. Results of mass balance modeling of in-lake Na^+ and Cl^- concentrations under different future salt loadings scenarios (see section 4.3.3 for details). For each scenario, results for only one of the ions, Na^+ or Cl^-, are shown. See text for detailed descriptions of the scenarios.

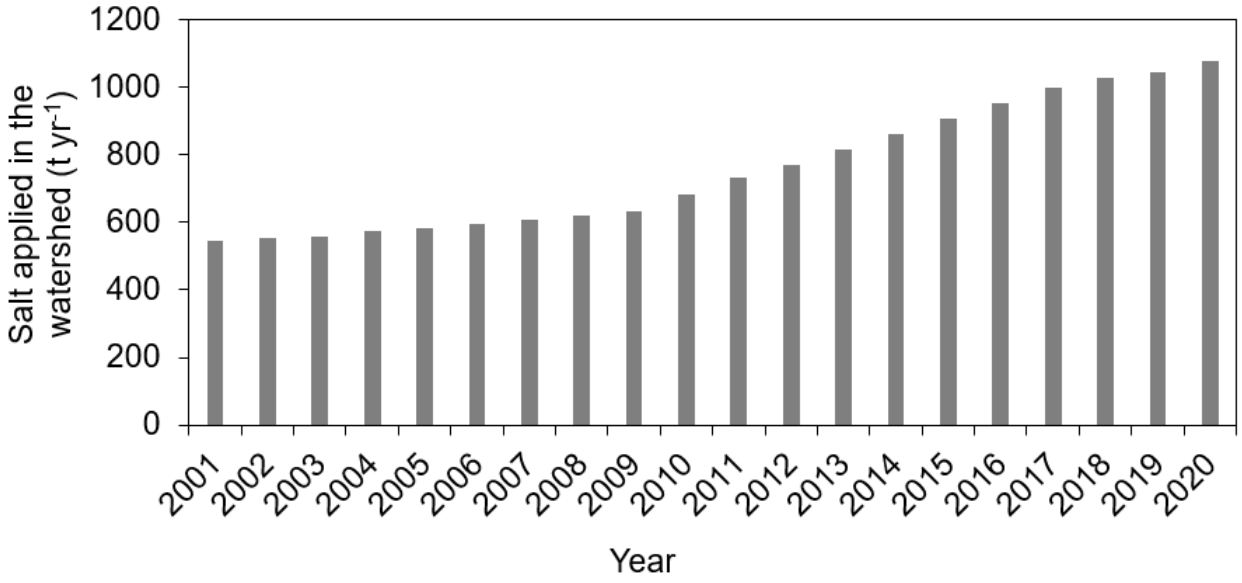

Figure 4.7. Annual amounts of the road salt applied in LW's watershed from 2001 to 2020.

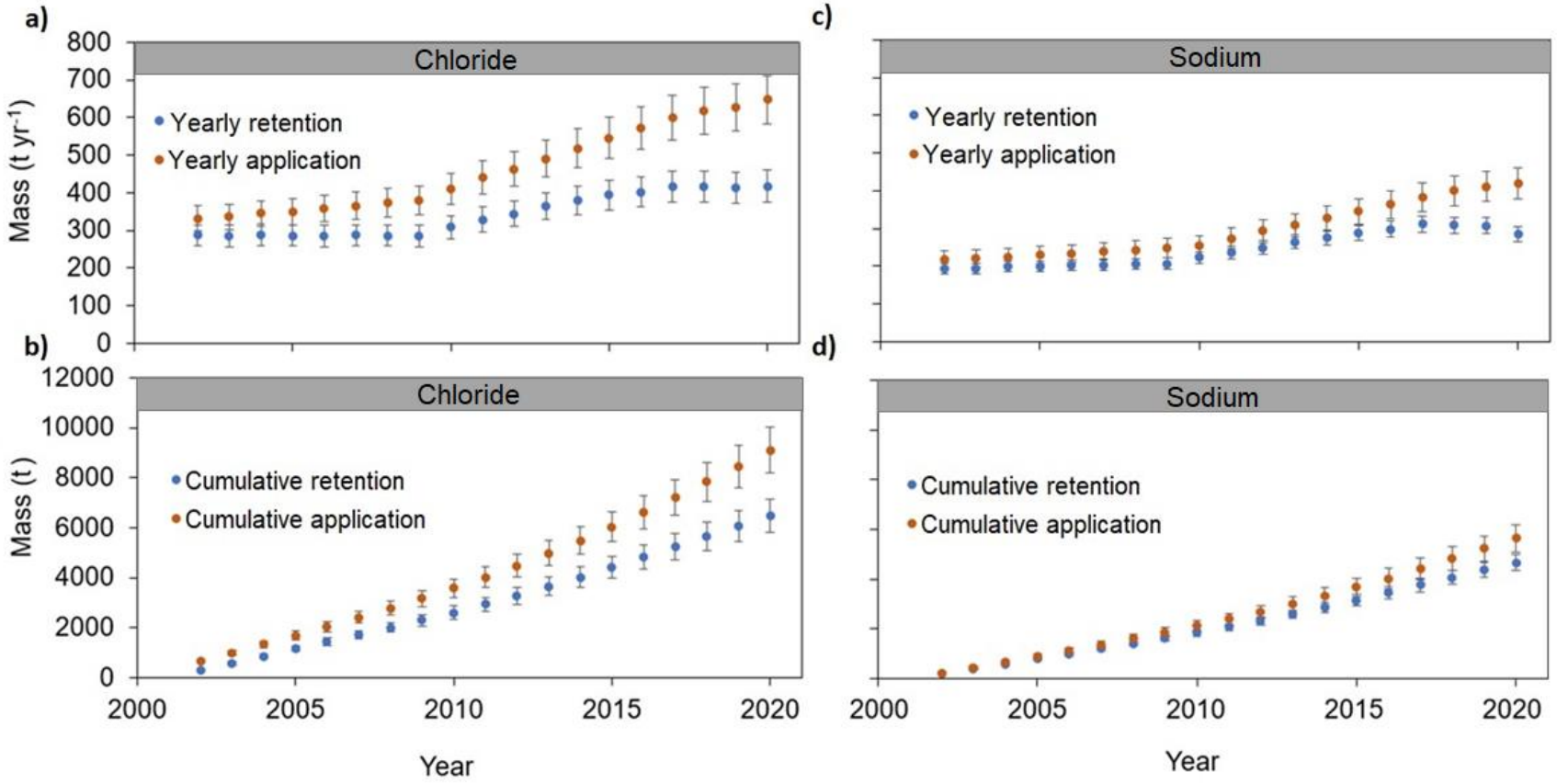

Figure 4.8. Annual (upper panels) and cumulative (bottom panels) amounts of Cl^- (a and b) and Na^+ (c and d) applied to and retained in LW's watershed from 2001-2020. The error bars represent standard deviations.

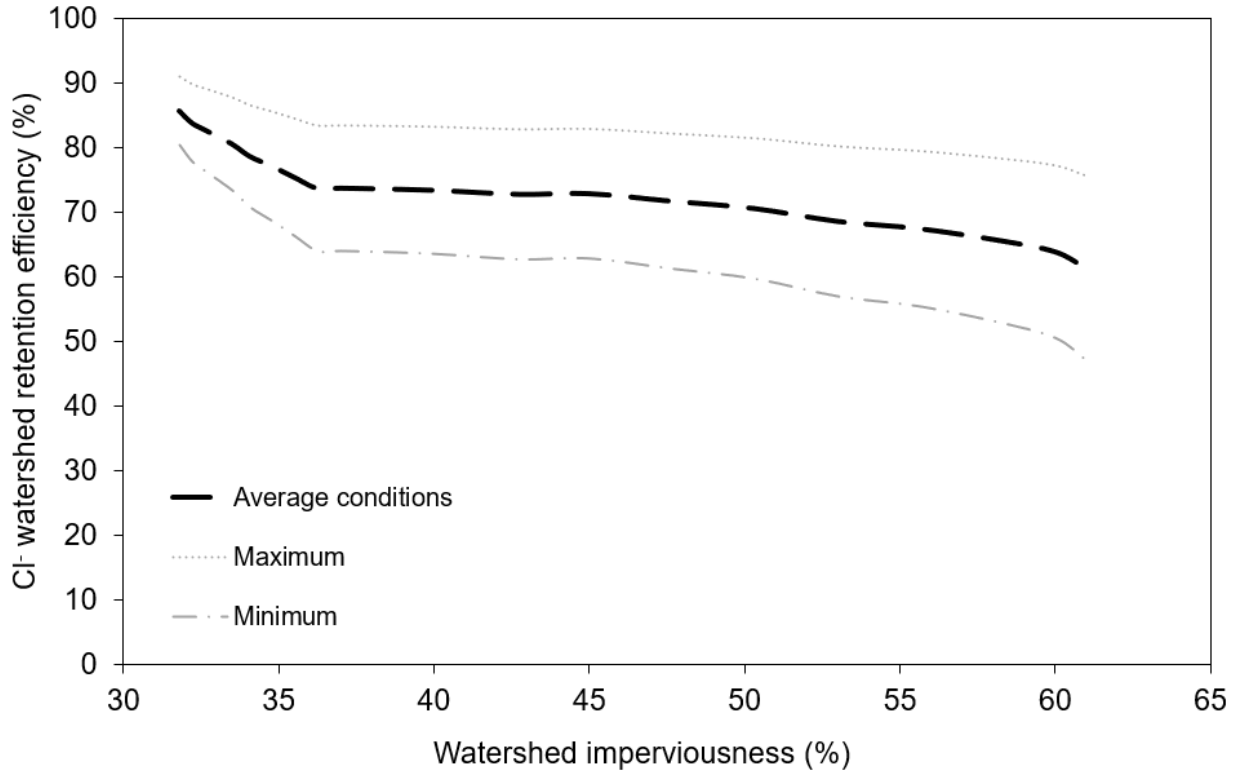

Figure 4.9. Watershed retention efficiency of Cl^- plotted versus watershed imperviousness from 2001 to 2020. The black line corresponds to average weather conditions (i.e., average road salt application rates and number of salting events). The "maximum" and "minimum" lines correspond to, respectively, the highest and the lowest values for the road salt application rate plus those for the yearly number of salting events. The watershed retention efficiency of Na^+ shows a trend similar to that of Cl^-, but with absolute values about 10% higher.

Our mass balance calculations do not include Cl^- and Na^+ ions other than those added with winter road salt applications. Additional sources of Cl^-, Na^+, and other major ions include water softeners (Kaushal et al., 2016) and runoff from construction sites (Neave & Rayburg, 2006). Thus, the Cl^- and Na^+ loads to LW's watershed and, hence, their retention efficiencies may be somewhat higher than estimated here.

4.5.4. Watershed salt legacies

The estimated Na^+ and Cl^- retention efficiencies imply that significant amounts of salt ions are accumulating in the watershed. The fate of these ion legacies should receive further attention. Given its high mobility, Cl^- will likely reach the groundwater and be transported away from the surface source areas (Mackie et al., 2022). By contrast, more Na^+ is expected to accumulate in the soil compartment, where it can occupy cation exchange sites (Rhodes et al., 2017; Sun et al., 2012;). Note that the less than 1:1 molar Na^+:Cl^- ratio in the lake water (Figure C2) is consistent with the lower mobility of Na^+ in the watershed compared to Cl^-. Future research on the spatial and temporal subsurface distributions of Na^+ and Cl^- in urbanizing watersheds may help delineate possible long-term risks to water resources and aquatic ecosystems associated with salt legacies. For example, significant unknowns remain about how the transport pathways and timing of Cl^- may be affected by reactive processes (Asplund and Grimvall, 1991; McCarter et al., 2019; Öberg, 2002; Snodgrass et al., 2008, 2017).

4.5.5. Salinization and lake mixing

The 2020 salinity of 0.55 g kg^{-1} in LW indicates the lake may still be relatively far from the salinity threshold of 1.23 g kg^{-1} where, in principle, salinization may prevent fall turnover (Bubeck & Burton, 1989; Ladwig et al., 2021; Sibert et al., 2015). The business-as-usual scenario suggests that LW could reach the salinity threshold by mid-century (Figure 4.9). Nonetheless, even at the current level of salinization, the vertical mixing regime of LW has already been significantly affected (Radosavljevic et al., 2022). The last two decades have seen a strengthening and lengthening of the summer stratification of the water column, together with a deepening of the thermocline and the expansion of hypoxia of the hypolimnion. As shown in our previous work, these changes are driven by increasing salinity, rather than nutrient enrichment or climate warming (Radosavljevic et al., 2022).

The salinity threshold of 1.23 g kg^{-1} is calculated for the average fall wind velocity for the 2016-2020 period. Wind velocity patterns, however, are inherently variable and unpredictable. Figure 4.4 shows that even wind velocities slightly lower than the average of 4.8 m s^{-1} can significantly decrease the salinity threshold for whole-lake mixing. Given the current upward salinization trajectory (Figure 4.6), LW is increasingly at risk of experiencing severe curtailment of seasonal mixing events. The resulting decrease in ventilation of the deeper waters could further deteriorate the water quality and ecological functions of the lake (Cunillera-Montcusí et al., 2022).

In the 50% and 75% salt load reduction scenarios, lake Cl^- concentrations by 2050 would be 75 and 32 mg L^{-1}, that is, concentrations well below the 120 mg L^{-1} Canadian guideline for sustainable freshwater ecosystem health (Wallace et al., 2016). The mitigation scenarios also show a rapid stabilization of the Cl^- concentrations following an instantaneous external load reduction to the lake. This is expected given the relatively short water residence time (and therefore fast flushing rate) of LW of ~2 years. Achieving a given target external salt load reduction to the lake will require adaptive management strategies that adjust road salt applications in the watershed as urban land cover, stormwater management, and hydrological connectivity of impervious areas continue to evolve. In addition, climate change and the fate and pathways of legacy salt ions remain largely unknown factors that will likely modulate future salinization and water column stratification trends of the lake.

4.5.6. Environmental implications

Our results consistently point to salinization of LW as being the result of increasing road salt applications to impervious areas in its urbanizing watershed, consistent with findings for other cold climate lakes (Dugan et al., 2017). Salinization reduces the vertical mixing of the water column and therefore causes longer periods of deoxygenation of the deeper waters. This can lead to further deterioration of water quality, for instance, by releasing toxic solutes from sediments under oxygen-depleted bottom waters. In addition to solutes such as ammonium, hydrogen sulfide and trace metals (Torres et al., 2015), hypoxic and anoxic conditions also promote the benthic release of dissolved phosphate (O'Connell et al., 2020). The latter process, known as internal phosphorus loading, can fuel excess

algal growth and thus contribute to worsening lake eutrophication (Hintz et al., 2017; Jenny et al., 2016; Radosavljevic et al., 2022).

Mitigating lake salinization in urban watersheds requires integrated and adaptive management strategies. Salt emissions, including road salt applications and other anthropogenic sources, should be reduced. In regions with cold winters, areal salt application rates can be optimized by better aligning salt application rates with event-specific temperature and icing intensity conditions (Kaushal et al, 2016; Snodgrass et al., 2017), for example, by investing in intelligent salt trucks equipped with mobile weather stations that map a city's microclimate and continually update winter storm and road pavement temperature forecasts (Tabirizi et al., 2021).

The implementation of infiltration-based low-impact development options (LIDs), such as bioretention cells, permeable pavement, and green roofs, can further help reduce the direct surface salt runoff from urban areas. However, these LIDs may facilitate salt intrusion into underlying aquifers and, hence, threaten drinking water source areas (Granato et al., 1995; Snodgrass et al., 2017). Other approaches include the implementation of traffic-calming measures that help reduce salt application rates without jeopardizing road traffic safety (Trenouth et al., 2015), and the installation of enhanced roadside drainage systems to protect salt-sensitive areas (Tabrizi et al., 2021). Given the complex nature of the freshwater salinization problem, solutions developed through collaboration of researchers, watershed managers, and the public hold the greatest promise.

Our mass balance calculations imply that the majority of Na^+ and Cl^- applied to LW's watershed accumulates in the watershed, likely in soil and groundwater compartments. The salt legacies could thus act as long-term sources of Cl^- and Na^+ to LW even after salt application rates are greatly decreased (Mackie et al., 2022; Oswald et al., 2019). The build-up of soil and groundwater salt legacies also affects soil fertility and drinking water supply. Thus, overall, the findings in our study call for consistent water quality monitoring programs that enable the simultaneous determination of salinization trajectories along the whole watershed-lake-groundwater continuum. For instance, the trajectories of salt ion

concentration measured in stream baseflow during summer may help characterize salt ion legacies in shallow groundwater (Mazumder et al., 2019; Perera et al., 2013).

4.6. Conclusions

Two decades of water chemistry time series data for Lake Wilcox (LW) illustrate the impacts of urbanization-driven salinization on the water geochemistry of the lake. A simple mass balance modeling is used to reconstruct the historical salt loadings to LW, and to forecast the future trajectories of lake water column Cl^- and Na^+ concentrations under different watershed salt application scenarios. The mass balance calculations imply that most of the Na^+ and Cl^- ions applied as road salt are being retained in the watershed, likely accumulating in, and thus contaminating, soil and groundwater compartments. The accumulation of Na^+ and Cl^- legacies in the watershed could act as a source of these ions to the lake in the future. The calculations further show that the watershed retention efficiencies of Cl^- and Na^+ have been decreasing with expanding impervious land cover, thus increasing the risk of accelerating lake salinization in the future. Under the current salinization trajectory, vertical mixing of LW would be impaired by mid-century, hence, fundamentally altering the physical, biogeochemical and ecological functioning of the lake.

Chapter 5

Increase in salinity amplifies eutrophication symptoms in freshwater lakes of North America

Modified from:

Radosavljevic J., Shahvaran A.R., Slowinski S., Alcott L., Nandita B. Basu, Parsons C.T., Rezanezhad F. & Van Cappellen P. (2023). Increase in salinity amplifies eutrophication symptoms in freshwater lakes of North America. *In prep.*

5.1. Summary

The acceleration of global urbanization continues to fuel concerns surrounding water quality impairments in urban lakes, particularly their eutrophication. Cultural eutrophication of freshwater environments is generally assumed to be driven by the anthropogenic augmentation of phosphorus (P) inputs which can alleviate limitations on primary production. Salinization is also recognized as a stressor on urban freshwater quality, particularly in cold climate regions in which salts are applied to road surfaces as de-icing agents. While the ecological damages caused by P enrichment and salinization to freshwaters are both well established, thus far, their impacts on water quality have only been considered independently. Although improvements to the management of urban stormwater and wastewater have decreased P inputs to freshwater systems in recent decades, many lakes worldwide remain eutrophic, as indicated by declining dissolved oxygen (DO) concentrations and rising dissolved inorganic P (DIP) concentrations in their hypolimnions. Our previous study of an urban freshwater lake in Ontario, Canada, showed that persistent eutrophication symptoms can be linked to salinization associated with impervious land cover expansion, rather than high external P loading. In this research, we present multiple decades of water chemistry data analyses for several North American urban lakes to study how increased lake salinization rates intersect with water temperature and lake morphometry to promote stratification, thus, increasing eutrophication symptoms. Our trend analysis shows progressive salinization (observed through significant increases in chloride or electrical conductivity) of all the lakes investigated. Calculation of Brunt Väisälä frequency, as an index of stratification over time showed that, on average, lake stratification is becoming more stable, and increased salinity plays a greater role in enhancing lake stratification, than temperature. The increasing salinity trends are accompanied by increasing hypolimnion hypoxia and increasing DIP:TP in all lakes, thereby demonstrating the mechanistic link between salinization and eutrophication. Rising salinity intensifies water column stratification, in turn, reducing the oxygenation of the hypolimnion and enhancing internal P loading from the sediments. These results highlight that stricter management of de-icing salt application rates should be considered to control lake eutrophication symptoms in cold climate regions.

5.2. Introduction

Human impacts on freshwater quality have been recognized for decades (e.g., Dodds et al., 2013). Cultural eutrophication has led to the increased incidence of harmful algal blooms, declines in bottom water oxygen concentrations, and numerous other detrimental impacts (e.g., Paerl, 1999). Lake eutrophication is primarily driven by the excess supply of phosphorus (P), the limiting nutrient for primary production in most freshwater lakes (Worsfold et al., 2016). The source of this excess P can be both external watershed loading as well as the diffusion of P from lake bottom sediments (i.e., internal loading). The accumulation of legacy P in bottom sediments in many eutrophic lakes results in significant internal P loading even after external P loads are reduced, impeding recovery of lakes (Orihel et al., 2017; O'Connell et al., 2020). This phenomenon has recently received increased attention in temperate and cold regions (Cyr et al., 2009; Nürnberg et al., 2018) where seasonal thermal stratification leads to efficient sediment P recycling (Lepori and Roberts, 2017; Tu et al., 2019).

Whilst every effort has been made to reduce external lake P inputs via the implementation of best management practices (BMPs), laws, and regulations, many lakes continue to suffer from persistent hypoxia (oxygen depletion) and anoxia (absence of oxygen) (Jane et al., 2023; Carey et al., 2022), as well as elevated and increasing internal P loading fluxes (Nürnberg et al., 2018; Carey et al., 2022). This has led to an increasing interest in understanding the underlying causes of lake bottom-water oxygen depletion and internal P loading, in order to better develop effective management strategies (Markelov et al., 2019; Parsons et al., 2017).

Indirect drivers related to land use and land use change can also play a significant role in causing eutrophication-like symptoms (e.g., lake hypoxia or anoxia) (Jenny et al., 2016). A seasonal example is the adverse impacts of the excessive use of road salt deicers, which elevate water density via increasing the water column salinity, strengthening lake stratification (Ladwig et al., 2021; Radosavljevic et al., 2022), resulting in longer hypoxia and anoxia in deep lakes (Jenny et al., 2016), and in turn, increasing internal P loading (Nürnberg et al., 2023). Temperate urban lakes are more susceptible to road salt-driven

salinization and the associated intensification of these eutrophication symptoms (Kortesky et al., 2012; Radosavljevic et al., 2022).

While the impact of temperature on lake stratification and mixing is relatively well studied, the potential for water column salinity to affect lake stratification has received less attention. The density profile of a lake water column is the determinant of mixing dynamics (Boehrer and Schultze, 2008). In freshwater lakes, temperature effects on water density are typically the dominant control on lake stratification, and the adverse effects of increasing air and water temperatures on on lake stratification have been recognized (Coats et al., 2006; Saulnier-Talbot et al., 2014). However, the addition of salt ions to freshwater increases water density, and salinity can in some cases become a stronger regulator of water density than temperature (Millero and Poisson, 1981; Ladwig et al., 2021).

Given the global ongoing challenge of water quality deterioration despite the regulatory efforts, it is crucial to understand the drivers to be able to identify potential solutions. Here, we investigate the temporal trends in bottom water dissolved oxygen and P remobilization from sediments (i.e., internal P loading) along with changes in water column salinity in multiple freshwater urban lakes in North America using a multi-variate dataset spanning over two decades. We assessed the change in water column stability using the Brunt–Väisälä frequency (BVF) which is a common approach to quantify the strength of thermal stratification in lakes. Using these comprehensive data and statistical trend-analysis approaches, we identified drivers of change in water chemistry and water column stability trends. All lakes experienced a decrease in P external loadings, and all researched lakes are affected by road salt due to the presence of typical winter conditions. The established link between salinization and eutrophication symptoms (i.e., DO depletion and P remobilization) is clearly seen on this continental scale. This research has the potential to inform the development of effective strategies for water quality management in the face of global land use and climate change. However, addressing this complex issue will require a shift away from a dichotomous view of the environment versus human safety in temperate regions. Such an approach can help to create a more sustainable and resilient future for both people and the planet.

5.3. Methods

5.3.1. Research sites and data availability

We synthesized available data from 9 lakes (in the U.S.A, and in Canada) located in urban, cold temperate regions (Figure 5.1, Table 5.1) spanning the last two to four decades (see table 5.1 for the time span when data were available for each lake). The lakes we examined had varying characteristics, including surface area ranging from 0.05 to 744 km^2, maximum depth of 4.3 to 41 m, and mean depth of 2.7 to 15 m (Table 5.1).

A variety of datasets were collected from different sources, including water quality monitoring data downloaded from the North Temperate Lakes US Long-Term Ecological Research Network (NTL LTER); Freshwater Society; Minnesota Pollution Control Agency; Lake Simcoe Region Conservation Authority and data provided by the City of Richmond Hill (CRH) (Table D1), as well as satellite images obtained from Esri's Wayback Living Atlas, Google Earth Pro and USGS Land Look.

There were a limited number of urban lakes that had the necessary data for the analyses required in this study. The water chemistry of the epilimnion of lakes, including urban lakes, is often monitored whereas the hypolimnion water chemistry is not often available, which excludes those lakes with only epilimnion data from this analysis.

Thus, the lakes were selected because of the availability of the long-term data on needed water chemistry that overlap with the period during which the watershed experienced urban development and excessive road salt application. Those lakes provide a unique setting to relate the temporal changes in eutrophication symptoms to the salinization-caused disturbance of water column stratification, as hypothesized.

The water quality dataset was in the most cases comprised of bi-weekly or monthly sampling from March to October during the period of observation for each lake (exception is L8, which has yearly data from 2012-2017 yearly data, but before that monthly data were available). All lakes are freshwater lakes that underwent change in land cover towards more urbanized, located in North America, and had already reported increased salinity gradients, observed through increase in Cl^-, due to the excessive use of road salt (data sources: Table D1).

Data included in each lake's dataset were dissolved oxygen (DO) concentration depth profiles, concentrations of total P (TP) and dissolved inorganic P (DIP) of hypolimnion, and chloride (Cl^-) or electrical conductivity (EC).

Furthermore, according to the reports of Clean Water Alliance from 2021, lakes in Wisconsin experienced decreasing trends in TP (L1-L4, L7) due to erosion controls implementations. According to Environmental Indicators Initiative, the lakes in Minnesota (L8, L9) experienced decreasing TP inputs due to improving wastewater treatment facilities. The same case is for Lake Simcoe and Lake Wilcox, where retention ponds were implemented (Radosavljevic et al., 2022). Those lakes provide a unique setting to relate the temporal changes in eutrophication symptoms to the salinization-caused disturbance of water column stratification, as hypothesized.

5.3.2. Water density and stratification analysis

For each lake, we determined the average whole-lake temperature and bottom water temperature from temperature profiles or data collected at 1 m above the lake bottom. Further, we calculated water density for each lake using widely accepted methods (I) using given temperature (in °C), assuming negligible effects of any solutes on density, as detailed described in Martin and McCutcheon (1999) and (II) according to the combined effects of salinity and water temperature based on the methods of Millero and Poisson (1981). Water density values are needed to quantify the strength of thermal stratification using the Brunt-Väisälä frequency (BVF). The densities calculated using both temperature and salinity are more realistic, especially for those lakes with significant salinity (Ladwig et al., 2021).

The BVF is the angular frequency of oscillation of a water parcel if displaced from its original position in the water column. Further, it represents the amount of work required against gravity to break down thermal stratification in the water column (Mortimer, 1974). High BVF values indicate a stronger resistance to vertical mixing at the thermocline. In order to assess interannual variability in the intensity of stratification, we compared BVF depth profiles calculated for the month of August for each year. In North American lakes, July–August exhibit the highest monthly air temperatures and water column stratification is most pronounced. In addition, by August, the lake's temperature distribution retains

negligible memory from the preceding spring mixing event. The BVF values were calculated for every 2 m depth, forming unique BVF profiles for each lake. Details on calculation could be found in Radosavljevic et al., 2022, as well as in methods section of chapter 3 of this thesis.

Using rLakeAnalyzer (Read et al., 2011; Ladwig et al., 2021), we were able to compute multiple values of the BVF. rLakeAnalyzer employs widely accepted methods for calculating lake stratification indices from in situ temperature profiles, salinity, and hypsographic data (Ladwig et al., 2021).

5.3.3. Trend analysis and correlation test

Mann-Kendall (MK) trend tests were carried out to determine the temporal trends for each lake for all the variables of interest using the XLSTAT software (Addinsoft, Version 2022). The MK tests were done separately for each lake: for DO concentrations and DIP:DP ratios of hypolimnion; for Cl^- concentrations or EC values for the water column, as well as for the temperature; and for BVF maximum values with density derived with and without imposed salinity (as described above).

Relationships among the considered variables (DO and DIP:TP data of hypolimnion, Cl- and BVF values; and two morphometric predictors (see in next section)) were tested using Pearson's correlation with statistical significance at $p<0.01$.

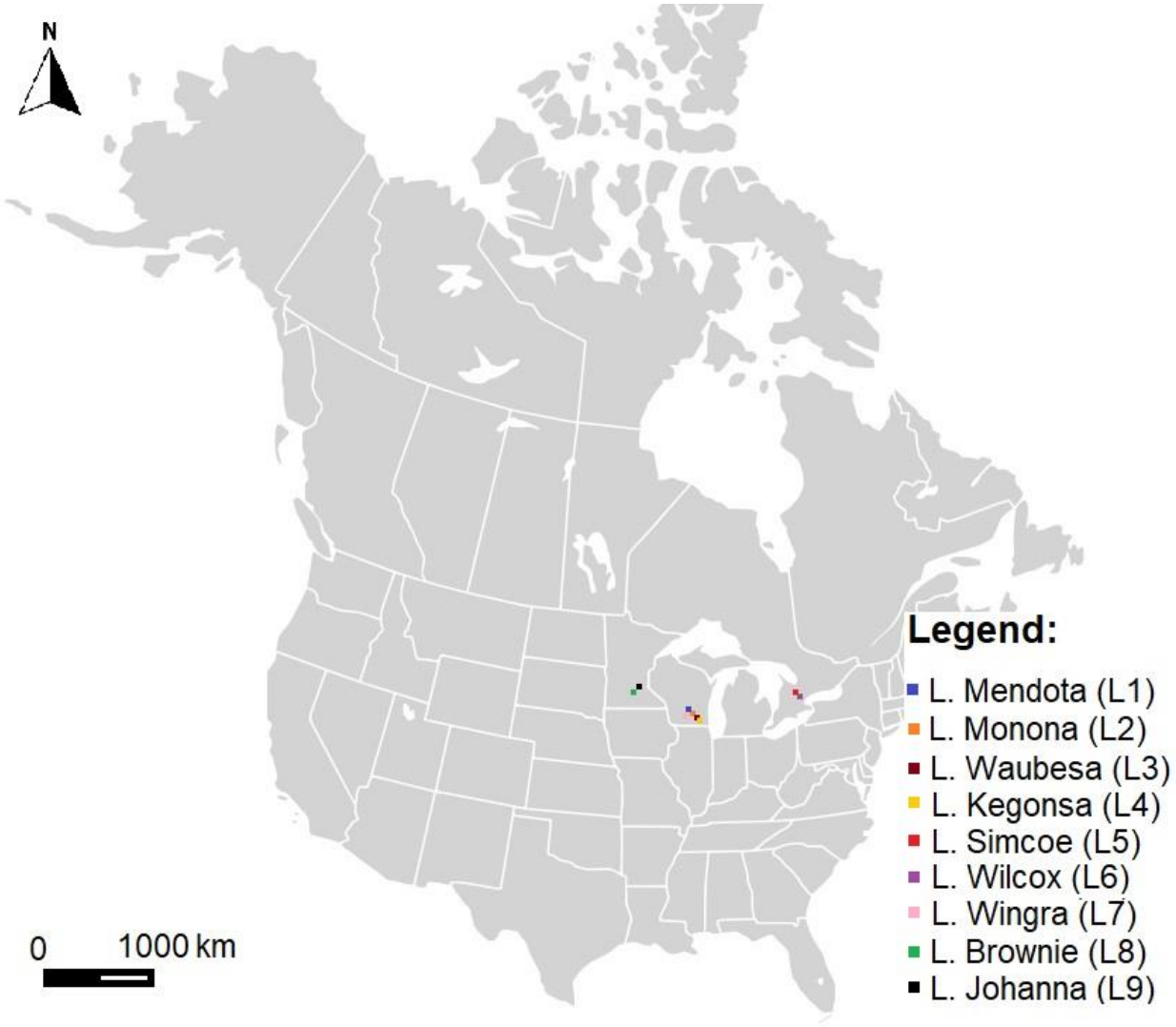

Figure 5.1. Location of research sites.

Table 5.1. Summary of the lakes' characteristics.

Lake symbol	Name of the lake	Surface area (km^2)	Mean depth (m)	Maximum depth (m)	Country	Period of data availability
L1	Mendota	39.4	12.8	25.3	Wisconsin, US	1990-2018
L2	Monona	13.0	8.2	23.0	Wisconsin, US	1990-2018
L3	Waubesa	8.1	4.8	12.0	Wisconsin, US	1992-2019
L4	Kegonsa	12.9	5.2	9.1	Wisconsin, US	1992-2019
L5	Simcoe	744	15.0	41.0	Ontario, CA	1980-2018
L6	Wilcox	0.55	5.6	17.4	Ontario, CA	1996-2020
L7	Wingra	1.3	2.7	4.3	Wisconsin, US	1990-2018
L8	Brownie	0.05	5.9	14.0	Minnesota, US	2005-2017
L9	Johanna	0.8	5.2	13.1	Minnesota, US	1998-2018

5.3.4. Predictors of stratification trends

To analyze the relative contribution of different predictor variables to the trends in the BVF values in the lakes, we used a multiple linear regression model (MLR). First, we calculated BVF values for each lake, and in the MLR analyses, the BVF values were treated as the dependent variables in order to identify the (independent) explanatory variables that most contribute to the strength in stratification. To compare the regression coefficients from the MLR analyses, we first normalized the values of each explanatory variable by that variable's mean value to make them unitless. The MLR analysis was performed with the JMP statistical software (SAS Institute Inc.) based on the formulation described in Brix et al., 2017; Liu et al., 2015; Radosavljevic et al., 2022, as well as in Chapter 3 of this thesis. Further, we calculated absolute values of normalized coefficients, to be able to show the relative importance of each predictor as a percentage. The predictors included in the MLR analyses were grouped into two categories: lake morphometric predictors and density predictors. The lake morphometric predictors were: (i) the depth ratio, the ratio between mean (z_{mean}) and maximum depth (z_{max}) ($r_d = \frac{z_{mean}}{z_{max}}$); and (ii) the morphometric ratio, the ratio between the mean depth and the surface area (A_o) ($r_m = \frac{z_{mean}}{A_o}$). The density predictors were the (iii) average temperature and the (iv) average salinity.

5.4. Results

5.4.1. Stratification and water chemistry trends

Dissolved oxygen in hypolimnion ranges from 0 to 4.1 mg L^{-1}, and in general, the lakes' bottom waters became more DO depleted through time. In all but one of the lakes (L5), this decreasing DO trend was significant ($p<0.05$). (Figure 5.2). DIP in hypoliimnion in all lakes increased ($p<0.05$). DIP to TP ratios vary from 0.4-0.9, and in all lakes, it has a significant increasing trend (Figure 5.2, Table D2). Salinity (observed through concentrations of Cl^-) in all lakes underwent significant increasing trends during the period of observation (Figure 5.3).

The surface water temperature in all lakes varies between 6.7 and 24°C, while bottom temperature ranges from 1.5 to 6°C. On average, lake surface temperatures warmed by 0.54°C during 15 to 30 years, however, the bottom temperatures experienced no

statistically significant trend (p=0.478) with increases less than 0.05°C in most of the lakes. Slight bottom water temperature decreases were observed in two lakes (L3 and L6, p<0.05), and one experienced a slight increase (L4). The average density of the water column in all lakes was between 996.8 and 1001.51 kg m^{-3}, with an average increasing rate of 0.15-0.23 per year. Subsequentially, lake stratification is becoming more stable, with deeper and steeper thermoclines (Figure 5.4). The maximum values of the BVF varies from 0.0012 to 0.0058 sec^{-2}, with almost all of the investigated lakes experiencing significant increases in BVF (p<0.05). Only one lake (L5) had no significant trend in BVF (p >0.1). Trend test for the BVF, when density of the water column is obtained just from the temperature data, showed no statistically significant trend (Table D3).

Pearson correlation indicated a high positive correlation between DIP:TP ratios with both concentrations of Cl^- and BVF (+0.71 and +0.84, respectively), while DO was negatively correlated with them (with -0.51 for Cl^- and -0.81 for BVF). Depth ratios (r_d) were also positively correlated with BVF (+0.65).

5.4.2. Predictors of stratification trends

Whole-lake salinity, together with depths ratios (r_d) explained a high percentage of the variance in stratification trends, followed by average lake temperature, whilst morphometric ratios comparatively were unimportant. In sum, whole-lake salinity, depths ratios and water temperature account for 82% of the explained variation in the BVF trend (Figure 5.5). On average, water salinity, depth ratios and temperature explain 31, 27 and 24% of changes, respectively.

From the beginning to the end of the period of observation, the importance of the explanatory variables changed. On average, the importance of salinity in the first 10 years of available data for almost all lakes (except L8), when increase in Cl^- was not extremely rapid, importance of salinity was around 26%, while temperature had around 29% importance (Figure D1). Furthermore, according to the BVF profiles, the thermocline deepened in almost all the lakes (Figure 5.4). Here, we defined thermocline depth as the depth at which the water column has the highest density gradient (Cantin et al., 2011; Ladwig et al., 2021).

5.5. Discussion

Our analysis of the change in North American lakes provides evidence that pollution from road salts can have a significant impact on the mixing dynamics of freshwater lakes in temperate regions where TP best management practices are implemented to reduce TP loads to the lakes. We conducted separate calculations to evaluate the contribution of temperature-induced density gradients and salinity-induced density gradients to lake stratification. When considering density values without taking salinity into account, changes in buoyancy frequency (BVF) were not statistically significant ($p>0.1$) in most lakes. However, when salinity was included in the calculations, significant increases in BVF ($p<0.05$) were observed, indicating that salinity plays a crucial role in enhancing density, thus, stratification in urban temperate lakes in North America.

While BVF is sensitive to temperature changes, and according to literature, tropical regions are more responsive to temperature changes compared to temperate and arctic regions (Kraemer et al., 2015; Lewis, 1996), particularly due to climate change, in this research we showed that changes in the stratification patters in lakes impacted by increased salinity, BVF is more likely to be responsive to changes in salinity (compare figures 5.5 and D1).

Furthermore, our multiple linear regression (MLR) model indicates that increasing salinity is the primary driver of changes in stratification indices (also observed in Ladwig et al., 2021) once lakes reach chloride concentrations above 60 mg L^{-1}. Many lakes in North America are exhibiting increasing trends in chloride concentrations due to the excessive use of road salt (Dugan et al., 2017), with further projected increases in the future (Kaushal et al., 2021).

In the context of the lakes observed in this study, some of the findings (Koretsky et al. 2012; Sibert et al. 2015) suggest that the runoff of salt during winter months may already be causing a delay in the mixing process. However, further research is required to establish a conclusive link between winter salt runoff and the observed delay in mixing. Although it is not anticipated that these lakes will reach a salinity threshold that would impede lake fall turnover within the next decade (Ladwig et al., 2021), thereby hindering

the mixing process, the long-term trend of increasing salinization and strengthening of thermal stratification is a cause for concern.

In the case of the lakes studied here, as well as potentially many other temperate North American lakes, the use of road salts should be reduced to prevent unwanted changes in the mixing regimes of urban lakes.

In addition to salinization, the depth ratios are positively correlated with the BVF values, as has also been shown at the regional scale (Butcher et al., 2015). This finding suggests that the extension of the stratified season in lakes that fully mix or the reduction in the spatial extent of mixing in lakes that partially mix will be most common in relatively deep lakes (Gorham and Boyce, 1989). Thus, global patterns in the responses of lake stability to salinization (or climate change) will, in part, depend on global patterns of lake depth.

Biogeochemical processes, primarily driven by microbial activity, play a crucial role in the uptake of dissolved oxygen (DO) at the interface between lake sediments and the water column. This uptake removes DO from the water, and typically, diffusive transport from the water above replenishes the DO levels (Novotny et al., 2012). However, when the supply of DO from convective or wind mixing from the water above becomes insufficient, the bottom waters of lakes and the underlying sediments become depleted of oxygen, leading to anaerobic conditions (Ladwig et al., 2021). This situation is exacerbated by increased water density resulting from thermal stratification (Verburg et al., 2003).

Over the past two to three decades, there has been a significant and abrupt increase in water density in the North American lakes studied here, primarily due to the rising salinity levels caused by the excessive use of road salt (Dugan et al., 2017; Kaushal et al, 2021). This rise in density has been accompanied by notable changes in the mixing patterns of the lakes (Ladwig et al., 2021), impairing the replenishment of DO to the hypolimnion, consequently leading to an increase in the extent and duration of seasonal hypoxia (Jenny et al., 2016).

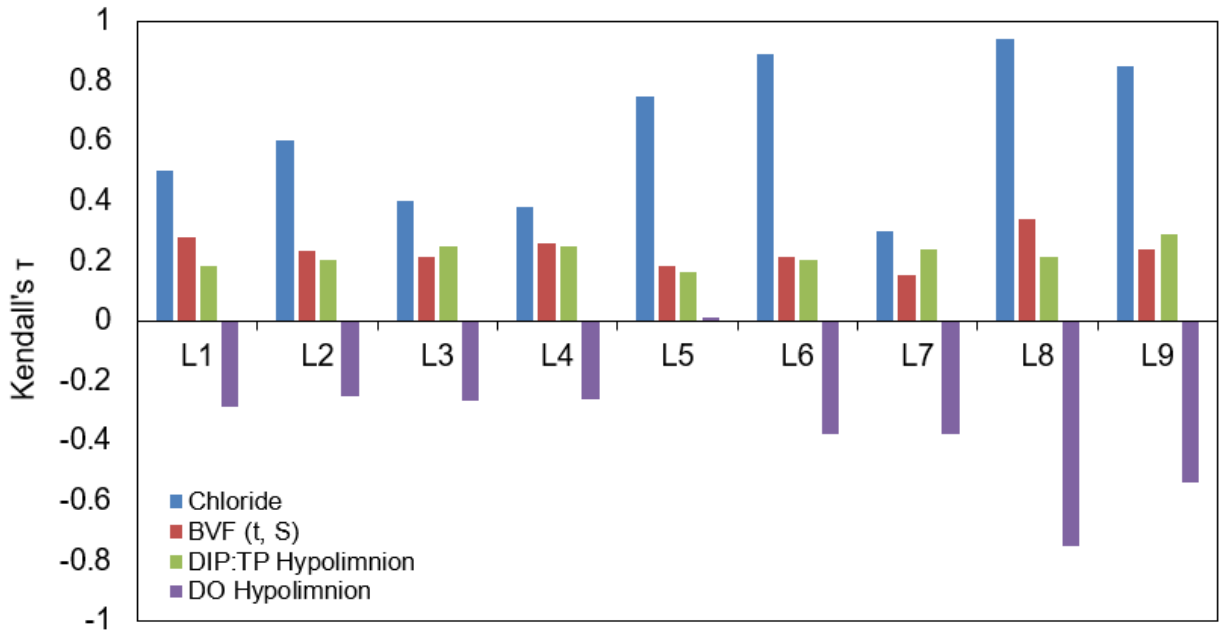

Figure 5.2. Trend test results for the chloride concentrations, strength of stratification (BVF) and eutrophication symptoms parameters (dissolved oxygen (DO)) and dissolved inorganic phosphorus to total phosphorus ratios (DIP:TP)).

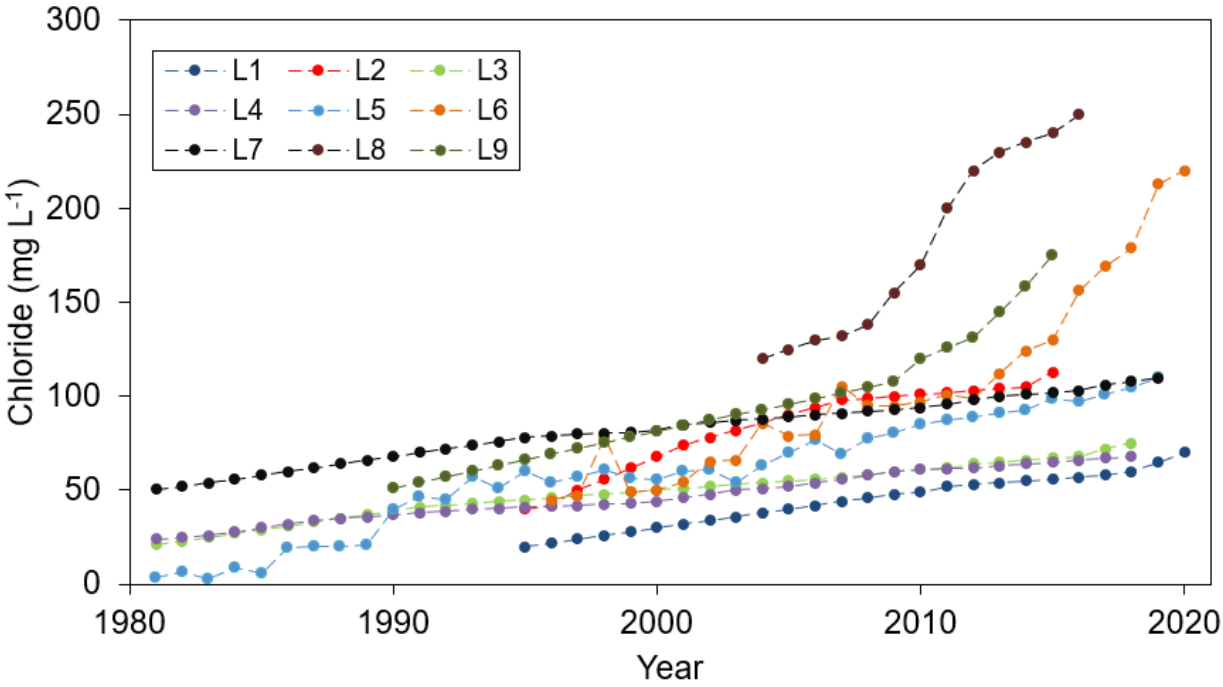

Figure 5.3. Chloride concentration trends in selected lakes.

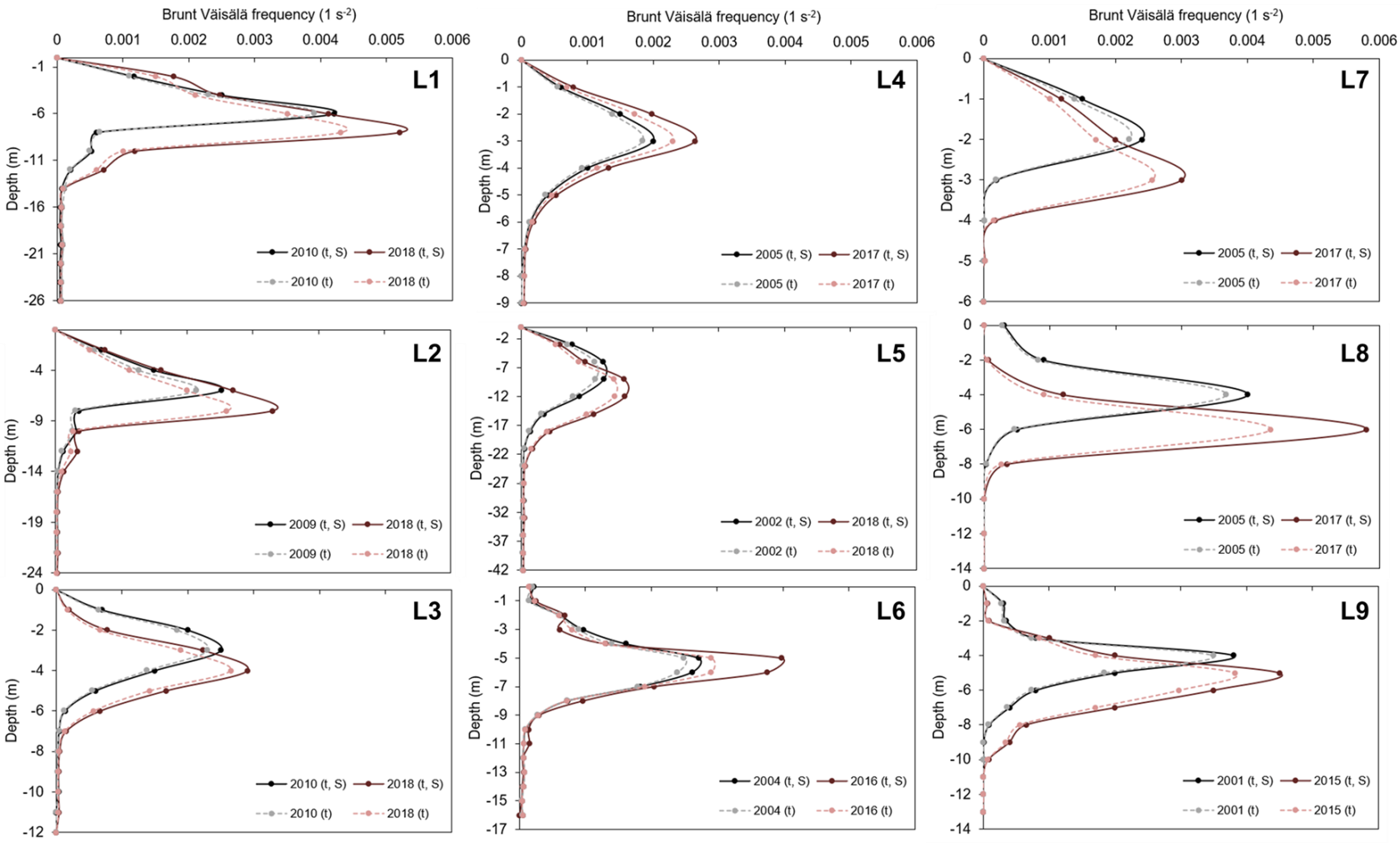

Figure 5.4. Profiles of Brunt-Väisäla frequency (BVF) values, where dashed lines represent values when just temperatures were included, while full lines represent the BVF values obtained with including salinity data.

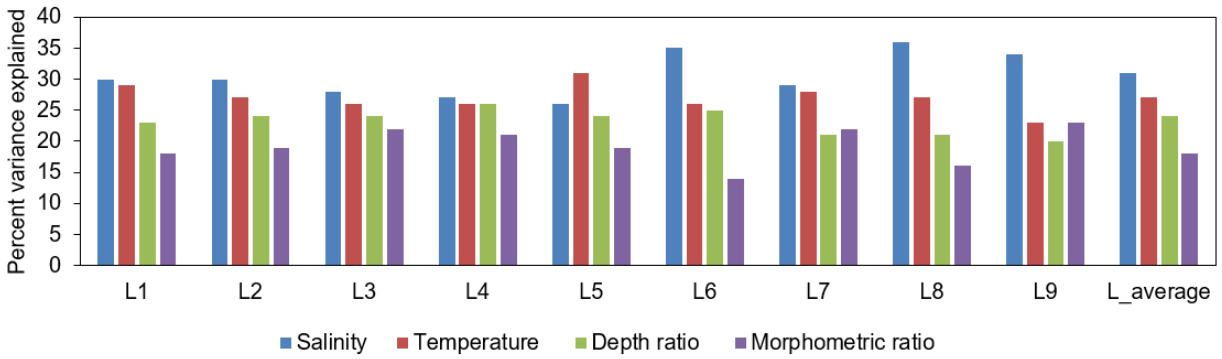

Figure 5.5. The variance in long-term trends in lakes BVF explained by four predictor variables as a percentage of variance explained by the MRL model. L_average represents the average conditions for all lakes.

Furthermore, the period of consistent seasonal hypoxia coincided with an increase in deep-water ratios of DP:TP. This increase is primarily attributed to increased internal P loading within the lakes, despite a reduction of TP inputs due to the implementation of various best management practices (BMPs) aimed at reducing P loading to the lakes (Yang & Lusk, 2018).

The findings of our study highlight that salinization is the primary driver behind increasing thermal stratification, which ultimately leads to oxygen depletion in the hypolimnion of temperate lakes in North America. Oxygen depletion (i.e., hypoxic and anoxic conditions) further leads to disturbed P cycling in lakes of North America. Although in our study the temperature is not the main driver of changes in water stability, this deleterious effect on lake oxygen levels can also be observed, albeit to a lesser degree, as a result of climate warming, as indicated in some previous studies (e.g., Sahoo et al., 2015; Schwefel et al., 2016; Ficker et al., 2017, 2019).

The prolonged occurrence of hypoxia or anoxia in urban lakes worldwide is a pervasive phenomenon which has been reported in numerous studies (e.g., Jenny et al., 2016). Furthermore, emerging research has shown that anoxia persists even in cases where external inputs of total P (TP) to lakes have decreased (Tong et al., 2020). Interestingly, many of these lakes have experienced a simultaneous increase in both eutrophication symptoms, namely oxygen depletion and internal P loading fluxes, alongside a rise in water column salinization. However, it is important to note that the reasons for increased salinization may not be uniform across all cases, unlike the excessive use of road salt observed in North American lakes. Consequently, there is a pressing need to expand this line of inquiry from a continental to a global scale and delve deeper into the underlying mechanisms driving these changes.

5.6. Conclusions

Here, the long-term water chemistry and temperature data from lakes in North America are used to study the impact of salinization on increasing eutrophication symptoms of lakes. Further, it is determined how increased lake salinization rates intersect with lake temperature and morphometry to alter its stratification. Calculations of lakes mixing indices over time showed that, on average, a lakes' stratification becomes more stable

with deeper thermoclines. Increasing salinity plays a crucial role in enhancing lake stratification, becoming a stronger regulator of water density than temperature in the temperate urban freshwater lakes studied here. The addition of salt ions increasing water density, modifying the mixing dynamics and stability of lake water columns. This, in turn, leads to the promotion of eutrophication symptoms i.e., decrease availability of oxygen exacerbating internal P loading, thus, further impairing water quality.

It is essential to consider the implications of salinization for in-lake P cycling dynamics when developing management strategies for urban lake ecosystems. Proactive measures aimed at mitigating the impact of salinization and controlling P inputs are crucial for the preservation and restoration of freshwater quality in these environments.

Whilst the link between salinization and eutrophication symptoms (i.e., oxygen depletion and internal P loading), is evident in North American lakes, this study highlights the need for a global perspective on understanding the underlying mechanisms, regardless of the driver of the salinization.

Chapter 6

Conclusions and Perspectives

6.1. Summary of major findings

This thesis presents a comprehensive analysis of water quality data, sediment core data, and modelling work that examines the impact of land use/land cover changes and salinization on urban lake systems and the cycling of P within them. Specifically, using a dated sediment core (Chapter 2), I demonstrate that the shift from agricultural to urban land use resulted in reduced sediment and TP loading to the lake, which can be attributed to the implementation of best management practices (BMPs). Furthermore, this shift in land use also influenced productivity and P cycling within the lake. Notably, despite the observed reduction in TP loadings, my results reveal a surprising increase (of around 15%) in P recycling on the sediment-water interface (i.e., internal loading) within the lake.

This thesis employs a case study approach, focusing on Lake Wilcox (Chapters 2, 3, and 4) and several cold-climate lakes in North America (Chapter 5), to illustrate how the urbanization and the accompanying salinization of downstream lakes can impact the lakes' mixing regimes, resulting in oxygen depletion in the hypolimnion and increased cycling of P within the lake (i.e., promotion of internal P loading). Specifically, Chapter 3 provides clear evidence that salinization, that correlates with urbanization, strengthens thermal stratification, which contributes to the ongoing symptoms of apparent eutrophication in the lake, even when TP inputs to the lake have decreased.

In addition, Chapter 4 highlights the potential negative impacts of salinization resulting from the use of deicers, which can extend beyond thermal stratification and hypolimnetic anoxia. Specifically, my findings suggest that a dimictic lake can become monomictic if the water column salinity continues to increase. The salinization of the lake is also characterized by a shift in the geochemical composition of the water from mixed hydro carbonate-sulphate to sodium-chloride. Furthermore, a mass balance model was developed in Chapter 4 to assess various road-salt management scenarios and predict changes in Cl^- and Na^+ concentrations in the lake. This model can be a valuable tool for management practices for other lakes and provide initial estimations of water salinization levels to practitioners under different winter management practices. Additionally, the

model allows for estimations of the Na^+ and Cl^- loading to the lake from the watershed and the retention of Na^+ and Cl^- in the watershed. I found that urbanization reduces salt retention in the watershed, resulting in more salt runoff being flushed to the lake. Specifically, my results indicate that a 30% increase in impervious cover from 2001 to 2020 resulted in a decrease in salt ion retention in soil and groundwater from 86% to 65%.

In Chapter 5 of the thesis, I investigated the impact of excessive use of deicers, primarily road salt, on urban lakes situated in cold climatic regions of North America. My results revealed that urban lakes in such areas experience the promotion of eutrophication symptoms, including increased levels of DIP (from internal loading) and bottom water anoxia, due to the increase in salinization and affected lakes' mixing regimes. This research represents a significant advancement in my understanding of the complex interactions between salinization and eutrophication in lakes. Through the use of multiple case studies and comprehensive data analyses, this study has successfully demonstrated the interconnectedness of these two previously considered separate issues. This novel scientific insight highlights the need for a more integrated approach to lake management, as the effects of one problem on the lake ecosystem cannot be fully understood without considering the influence of other related factors.

6.2. Future work

Overall, the research presented in this thesis provides new insight into the interrelationship between salinization and eutrophication symptoms in lakes and into the influence of land use changes on P loading to and cycling within lakes. Further, it highlights the importance of reducing road salt application in urban areas to mitigate the impacts on lake stratification and ecosystem health. Further investigation is needed to develop and evaluate effective management strategies for mitigating the negative impacts of salinization and the accompanying increase in internal P loading. To further advance the research presented in this thesis, several areas should be the focus of the future investigation.

6.2.1. Advancing the understanding and quantifying the importance of the stressors to changes in thermal stratification

Thermal stratification plays a crucial role in controlling the biogeochemical processes in lakes. In this thesis, I demonstrated that salinization increases water density, resulting in stronger thermal stratification, which has significant implications for P cycling in lakes. Despite significant advances in the understanding of lake stratification and its impact on P cycling presented in this thesis, several directions could enhance the comprehension of the principal stressors affecting lake mixing. The research in this thesis further highlights the impact of human activities such as urbanization and the excessive use of road salt on thermal stratification in lakes. I recommend that future studies investigate the cumulative effect of multiple stressors, including salinization, to quantify the contribution of each stressor to the strength of thermal stratification. The changes in temperature, precipitation, and wind patterns that are anticipated with climate change will alter lake stratification patterns. Future research should explore how these changes will interact to affect lake stratification and the ecological functioning of lakes. Moreover, the influence of the physical characteristics of lakes, such as altered flushing rates resulting from the dynamic climate and the disturbed hydrological cycling triggered by urbanization, on thermal stratification, remains inadequately studied. Hence, it necessitates further inquiry to ascertain their significance in importance for disrupting thermal stratification. To gain a better understanding of the cumulative effects of salinization, climate change, and physical characteristics of lakes on thermal stratification, I suggest the development of a novel modelling approach that takes into consideration all the above-mentioned variables. This would provide a more comprehensive understanding of the potential consequences of biogeochemical cycling in lakes and improve overall water quality management.

Furthermore, a comprehensive understanding of changes in stratification regimes induced by urbanization and climate change is critical in predicting the potential development of anoxia in lakes. This knowledge would significantly enhance existing models of P internal loading fluxes. Integrated research that considers physical, biogeochemical, and ecological aspects of lake stratification changes and how they are influenced by natural and human-induced factors is necessary. Further research is required to evaluate the effectiveness of various management strategies aimed at

mitigating the negative impacts of salinization and internal and external P loadings on lake ecosystems. These management strategies may include nutrient management practices, land-use planning, stormwater management practices, and lake restoration or remediation approaches.

6.2.2. Advancing the understanding of LULC change impacts on lake P cycling

This thesis highlights the significance of using a detailed sediment core analysis approach to unveil the impact of historic LULC changes on P cycling, algal productivity, and bottom water oxygen conditions. To enhance the reconstruction of past lake conditions, research could focus on the comprehensive analysis of sediment cores from other lakes around the world that have undergone different phases of LULC change and should be merged with historical records of the particular watershed. The sediment coring process should yield a core of sufficient length to capture the pre-developed or pristine conditions of the lake.

Furthermore, this research provides new insights into the importance of both accumulation rates and concentrations of elements. Thus, future studies on a similar topic should consider both factors to avoid misinterpreting the obtained data. Furthermore, to gain a better understanding of the impacts of different land use changes on P biogeochemical cycling and processes within the lake, further analyses should include P speciation analysis, which contributed significantly to the discussion in this thesis. However, to provide a more comprehensive understanding of the anoxic and oxic cycles of lakes, which are crucial for the P remobilization from sediments, as well as the critical mechanisms driving changes in P cycling, iron and sulfur species analysis should be conducted additionally. Adopting this approach in research would enable the documentation and quantification of the magnitude and timing of shifts in algal productivity, bottom water oxygenation, and P cycling. Current sediment core studies are restricted to specific lakes or regions, and there are few studies (Bhattacharya et al. (2022) is one example) that analyze temporal trends in multiple sediment cores to generalize patterns in historical changes across lakes and regions.

6.2.3. The emerging relationship between the impact of salinization and eutrophication symptoms in lakes

The research presented in Chapters 2-5 has established a clear link between salinization and the development of bottom water anoxia, leading to increased internal P loading. Therefore, the development of a process-based model that accounts for both thermal stratification and salinization is a logical next step. Such a process-based model would be capable of predicting the impact of these factors on internal P-loading fluxes associated with P biogeochemical processes, while also considering the reinforcement of thermal stratification.

In Chapter 5, I demonstrated the occurrence of similar trends in internal loading fluxes and oxygen depletion in road-salt-affected urban lakes in North America as observed in my Chapter 3 case study on LW. Additionally, more lakes in cold regions should be taken into consideration if data are available. This phenomenon may be observed globally, regardless of the source of salinization. For instance, in Southern China, despite a reduction in TP due to improved wastewater treatment facilities and/or the implementation of best management practices (BMPs), many lakes have still been maintained in a eutrophic state (Tong et a., 2020). These lakes also experienced an increase in electrical conductivity (salinization) in the water column due to excessive urbanization (Chen et al., 2019; Jia et al., 2021; Tao et al., 2013; Wang et al., 2018; Xu et al., 2010). Further analysis is required to determine whether this phenomenon is a result of increased lake stratification and anoxic conditions. Therefore, the findings of this thesis have the potential to be expanded globally.

Furthermore, in the analysis of lakes in North America affected by road-salt use, it is observed that some lakes (such as Lake Simcoe) experienced an increase in internal P loading, despite the fact that thermal stratification was not affected by salinization and P loadings to the lake were reduced. This finding underscores the need to expand this study to investigate the additional impact of salinization on P internal loading fluxes, specifically ion exchange at the sediment-water interface. The proposed research in this sub-chapter is necessary to evaluate the effectiveness of various management strategies aimed at mitigating the adverse effects of salinization and internal and external P loadings on lake ecosystems. Such management strategies would include nutrient management practices, land use planning, stormwater management practices, and lake restoration/remediation approaches.

6.2.4. Recommendations for considering salinization to mitigate eutrophication symptoms of the lakes

In light of the comprehensive findings presented in this thesis, a significant and innovative relationship emerges between two huge challenges in water quality management: (1) eutrophication symptoms and (2) salinization. Prior to this study, these two huge water quality concerns were conventionally addressed separately. However, this research underscores the compelling link between salinization and lake water quality deterioration (i.e., eutrophication symptoms such as oxygen depletion), shedding new light on their interconnectedness. Negative effects of salinization on lake water quality and eutrophication symptoms have been highlighted throughout the entire thesis, with Chapter 2 and 3 particularly highlighting the newly established connection. In chapter 5, it is shown that the issue might be applicable on a broader scale –particularly to those lakes significantly impacted by salinization arising from road salt application.

The urge to integrate salinization into freshwater protection policies emerges as an essential approach from the findings in this thesis. Traditionally, the focus is solely on phosphorus as the principal driver of eutrophication and consequent water quality deterioration symptoms (i.e., anoxia) (Jenny et al., 2016). However, this perspective has now decisively shifted to recognize the crucial influence of salinity. The detailed interaction between salinization and eutrophication, carefully explained in this research, emphasizes the pressing need to take a comprehensive approach when developing strategies for water management (Radosavljevic et al., 2022). Disregarding salinity would regrettably dilute the efficacy of policy interventions, given that this research firmly establishes salinization as a potent amplifier of eutrophication symptoms, further impacting lake water quality. Understanding how salinity acts as a catalyst in the amplifying eutrophication symptoms, policies should be carefully designed to reflect the complex challenges that freshwater ecosystems have been undergoing. Integrating salinity considerations into protective measures enhances their effectiveness and significance, leading to a coherent and sustainable approach in protecting freshwater resources.

6.2.5. Recommendations for mitigating the use of road salt in urban areas of cold climate

In this thesis, the negative effects of excessive road salt use have been highlighted, with Chapter 4 particularly elucidating this issue. Despite widespread recognition among governmental entities, municipalities, researchers, and citizens of the negative impact of road salt on freshwater ecosystems and the environment at large, the reduction or cessation of its use remains a distant possibility. This reluctance can be attributed to the prioritization of public safety and the indispensable role of road salt in winter maintenance. As such, persuading the responsible parties to adopt alternative measures presents a formidable challenge.

To address the issue of excessive salt usage, several strategies may be employed. Some of the most important could include (1) enhancing current management practices at the municipal and regional levels could lead to effective control and reduction of salt usage (Hintz et al., 2022); (2) raising public awareness through education campaigns could encourage individuals to make informed choices regarding their salt intake (Stone & Marsalek, 2011); (3) the development of innovative techniques and technologies could provide alternative solutions for reducing salt usage (Trenouth et al., 2015); (4) a collaborative effort between government bodies, municipalities, researchers, and practitioners may be necessary to coordinate and implement effective solutions (Imperail, 2005). Lastly, (5) considering the success of different approaches used in other countries may offer valuable insights and potential solutions to this issue (Hassall, 2014).

Improving management practices could include several measures that can be implemented (Stone & Marsalek, 2011). Improving de-icing management practices through real-time weather forecasting and the use of smart sensors can optimize application rates and enable the use of alternative deicers when needed, reducing salt usage while maintaining road safety (Gillis et al., 2021). Additionally, the calibration of salt spreaders is one of the key factors that can contribute to minimizing excessive salt usage while ensuring public safety, as well as improving snow and ice removal. Careful placement of snow collectors is an important factor in reducing the runoff of melted snow containing high levels of road salt from entering water bodies or aquifers, along with

protecting salt storage year-round and ensuring that it is properly covered can play a significant role in minimizing environmental runoff of salt (Kelly et al., 2019).

Effective public education and outreach initiatives hold immense potential to enhance knowledge and promote behavioral change towards sustainable practices that can significantly mitigate the adverse effects of salt on water quality. These initiatives can sensitize individuals to the grave ecological and health consequences associated with salt runoff from sidewalks, driveways, and roads, including the contamination of freshwater sources, degradation of aquatic ecosystems, and potential harm to human health. Through targeted educational campaigns and outreach programs, communities can be empowered to embrace alternative de-icing agents and reduce their reliance on excessive salt usage (Rafieifar et al., 2016; Wentzel-Viljoen et al., 2017). This, in turn, can help to reduce salt runoff into water bodies, protect natural habitats, and promote a cleaner and healthier environment for future generations. Such public education and outreach programs can be developed and implemented through a range of approaches, including online learning modules, community workshops, and engagement with schools, businesses, and civic groups. By encouraging individuals to adopt more sustainable practices and promoting awareness of the impacts of salt on water quality, public education and outreach initiatives hold immense potential to bring about lasting positive change for the environment and society as a whole (Wentzel-Viljoen et al., 2017).

New technologies and techniques are needed that reduce or switch the use of road salt, and they should be environmentally friendly, cost-effective, and efficient (Tabrizi et al., 2021). Potential deicer materials should be effective in melting ice and snow while minimizing their impact on water bodies, vegetation, and wildlife. Smart infrastructure can be developed to improve the efficiency and safety of winter road maintenance. For example, heated pavements can be installed to melt snow and ice, reducing the need for deicing materials (Li et al., 2022). Additionally, advanced sensor networks should be deployed on roads and bridges to monitor weather conditions, pavement temperatures, and other variables. This information can be used to predict icing conditions and optimize the application of deicing materials (Hernandez Gonzalez et al., 2020).

Collaboration between government, municipalities, researchers, and practitioners is essential for developing effective solutions to reduce the use of road salt (Sparacino et al., 2022). A targeted monitoring program is a critical component of any effort to reduce road salt use. Such a program can help identify areas where excessive salt is being applied and monitor the effectiveness of salt reduction measures. By analyzing data on salt use and runoff, researchers and practitioners can gain a better understanding of the impacts of road salt and develop more effective solutions. The cause-effect analysis is another essential element in reducing the use of road salt for which collaboration is necessary. It involves identifying the root causes of excessive salt use and developing strategies to address them (Fay et al., 2013; Hull, 2008). For example, some municipalities may be using excessive salt due to outdated equipment or insufficient training. By addressing these underlying causes, governments and practitioners can reduce salt use while maintaining safe and effective road conditions. Finally, the development and optimization of solutions to reduce salt use are crucial for achieving long-term success. Researchers and practitioners can work together to identify and test innovative approaches to snow and ice removal that reduce salt use without compromising safety (Sparacino et al., 2022). These solutions may include new technologies for spreading salt more efficiently or alternative materials such as beet juice or cheese brine (Parker & Tatum, 2021).

The countries that have freshwater salinization as a huge problem, could implement some of the good management practices used or proposed by other countries. Salt runoff could be collected, processed if necessary and reused as brine (Alleman et al., 2004; Garg et al., 2018). Another way to manage salty runoff is by injecting it into aquitards, and that can help reduce the risk of contamination of nearby groundwater resources and surface water (Foley, 1994). It is important to note that the collection and reuse of salty runoff requires careful planning and management to ensure that the water is properly treated and disposed of. Additionally, proper monitoring and regulation are essential to prevent any adverse impacts on the environment and human health (Equiza et al., 2017).

6.2.6. Recommendation for stormwater management infrastructure implementation and maintenance

The Lake Wilcox watershed, the focus study site of this thesis, has undergone significant changes in land cover since the beginning of the 20th century, including the implementation of stormwater management systems (SWMs), including ponds, trenches, and bioretention cells. This is also the case for many areas all around the world (Schroer et al., 2018). Optimal SWMs implementation, maintenance and improvement are crucial to preserve and improve the water quality of receiving water systems (e.g., lakes). In this thesis, I highlighted the importance of not just the absolute quantity of P coming to the lake, but also the relative amount of different P species. Urbanization followed by water quality degradation has led to the constant upgrading and retrofitting of stormwater management systems worldwide (Taguchi, et al., 2020). Optimal stormwater management system implementation in urban areas involves a combination of traditional and innovative techniques. While stormwater management ponds were initially designed for peak flow reduction and sediment settling, they are now also retrofitted to retain nutrients and contaminants by increasing the water residence time, a crucial variable that enhances the retention of dissolved and particulate contaminants (Ellison & Brett, 2006). Low-impact development (LID) infrastructures, such as the above-mentioned bioretention cells, have also been developed to address the export of P from urban catchments with substantial impervious area fractions (Zhou et al., 2023).

The maintenance of SMWs is crucial for ensuring their optimal performance, and to therefore prevent harm to downstream receiving water bodies. Regular inspections of the SWM infrastructure can help identify any issues early on and address them before they become more serious. Inspections should include checking the condition of the SWMs liner, checking for signs of erosion, and ensuring that the inlet and outlet structure is functioning properly (Pedretti et al., 2012; Tahvonen, 2018). Additionally, vegetation management and choosing plants that can uptake significant amounts of nutrients are important as well as ensuring that vegetation does not impede the flow of water in the SWM systems (ponds in particular) (Muerdter et al., 2016; Paus & BrasKerud, 2014). It is also important to prevent invasive plant species from taking over the SWM structure (Li, 2015). Sediment accumulation can reduce the effectiveness of the pond in treating

stormwater runoff. Sediment removal should be performed periodically to maintain the pond's capacity and effectiveness (Gu et al., 2017; Heal et al., 2006). Nutrient management is another important aspect of SWMs maintenance (Adhikari, 2003). Regular monitoring of nutrient levels can help identify when nutrient removal practices are needed, and when is the point that SWMs do not work as designed (Rosenzweig et al., 2011).

Moreover, the P retention performance of SWM ponds could be improved by adding Ca-rich compounds to form stable calcium-associated P species that are effectively retained in the sediments (Babin et al., 1994; Dunne et al., 2005) One way to enhance this process is by adding calcium carbonate-containing materials, commonly referred to as "liming," such as calcinated egg shells, spent lime, or steel slag, to increase both the pH and dissolved calcium concentrations. These materials have been successfully used in the past to remove P in experimental column systems (Christianson et al., 2017), batch studies with wastewater (Yin et al., 2013), simulated stormwater (Prabhukumar et al., 2015), and at the field-scale to treat stormwater (Kuster et al., 2022) and agricultural runoff (Kirkkala et al., 2012). While the use of iron-containing materials can also enhance phosphorus retention (Prabhukumar et al., 2015), the phosphorus species formed via associations with iron are often phosphate ions and/or organic phosphorus forms sorbed to iron oxides/hydroxides (Orihel et al., 2017), which are redox-sensitive and not stable long-term phosphorus sinks. In contrast, calcium phosphate minerals are redox-stable sinks for P (Slomp & Van Cappellen, 2007).

In addition to improving the performance of SWM systems, other recommended measures for stormwater management in urban areas could include (1) installing green roofs on buildings that help reduce the volume of runoff, improve water quality, and enhance the thermal performance of buildings (Palla et al., 2010); (2) implementing permeable pavement for roads, sidewalks, and parking lots that would allow water to infiltrate the ground, reducing runoff and improving the water quality of receiving water bodies (Imran et al., 2013; Zhu et al., 2019) and (3) educating the public on the importance of stormwater management and ways to reduce their impact on runoff can lead to greater community involvement in stormwater management efforts (Barclay & Klotz, 2019).

Overall, an effective stormwater management system in urban areas should involve a combination of traditional and innovative techniques tailored to the specific needs of the surrounding environment and community. In that way, the optimal water quality of receiving water bodies (i.e., lakes) could be ensured.

Bibliography

Aba, A., Uddin, S., Bahbahani, M., & Al-Ghadban, A. (2014). Radiometric dating of sediment records in Kuwait's marine area. *Journal of Radioanalytical and Nuclear Chemistry*, *301*, 247-255.

Adams, H., Ye, J., Persaud, B. D., Slowinski, S., Kheyrollah Pour, H., & Van Cappellen, P. (2022). Rates and timing of chlorophyll-a increases and related environmental variables in global temperate and cold-temperate lakes. *Earth System Science Data*, *14*, 5139-5156.

Adhikari, S. (2003). Fertilization, soil and water quality management in small-scale ponds. *The Gher Revolution, 6,* 6-8.

Alamdari, N., Sample, D. J., Ross, A. C., & Easton, Z. M. (2020). Evaluating the impact of climate change on water quality and quantity in an urban watershed using an ensemble approach. *Estuaries and Coasts*, *43*, 56-72.

Allan, J. D. (2004). Landscapes and riverscapes: the influence of land use on stream ecosystems. *Annual Review of Ecology, Evolution, and Systematics*, *35*, 257-284.

Alleman, J. E., Partridge, B. K., & Yeung, L. (2004). Innovative environmental management of winter salt runoff problems at INDOT yards, *1*, 1-60.

Appleby, P. G., Birks, H. H., Flower, R. J., Rose, N., Peglar, S. M., Ramdani, M., Fathi, A. A. (2001). Radiometrically determined dates and sedimentation rates for recent sediments in nine North African wetland lakes. *Aquatic Ecology*, *35*, 347-367.

Appleby, P. G., & Oldfield, F. (1978). The calculation of lead-210 dates assuming a constant rate of supply of unsupported 210Pb to the sediment. *Catena*, *5*, 1-8.

Arslan, O. (2013). Spatially weighted principal component analysis (PCA) method for water quality analysis. *Water Resources*, *40*, 315-324.

Aspila, K. I., Agemian, H., & Chau, A. S. Y. (1976). A semi-automated method for the determination of inorganic, organic and total phosphate in sediments. *Analyst*, *101*, 187-197.

Asplund, G., & Grimvall, A. (1991). Organohalogens in nature. *Environmental Science & Technology*, *25*, 1346-1350.

Audette, Y., Smith, D. S., Parsons, C. T., Chen, W., Rezanezhad, F., & Van Cappellen, P. (2020). Phosphorus binding to soil organic matter via ternary complexes with calcium. *Chemosphere*, *260*, 127624.

Babin, J., Prepas, E. E., Murphy, T. P., Serediak, M., Curtis, P. J., Zhang, Y., & Chambers, P. A. (1994). Impact of lime on sediment phosphorus release in hard water lakes: the case of hypereutrophic Halfmoon Lake, Alberta. *Lake and Reservoir Management*, *8*, 131-142.

Baker, L. A., & Brezonik, P. L. (2007). Using whole-system mass balances to craft novel approaches for pollution reduction: examples at scales from households to urban regions. *Cities of the Future: Green Cities Blue Waters. Wingspan Center, Racine, Wisconsin, 1,* 92-104.

Baker, M. J. E., Gillies, M., Liu, R., Maynard, K., Williams, S., & Yee, E. (2017). The effects and implications of urbanization on the environmental integrity of the Oak Ridges Moraine in Ontario, Canada. *The International Journal for Geographic Information and Geovisualization*, *52*, 132-141.

Baldwin, D. S. (1996). The phosphorus composition of a diverse series of Australian sediments. *Hydrobiologia*, *335*, 63-73.

Barclay, N., & Klotz, L. (2019). Role of community participation for green stormwater infrastructure development. *Journal of environmental management, 251*, 109620.

Bennett, E. M., Carpenter, S. R., & Caraco, N. F. (2001). Human impact on erodable phosphorus and eutrophication: a global perspective: increasing accumulation of phosphorus in soil threatens rivers, lakes, and coastal oceans with eutrophication. *BioScience*, *51*, 227-234.

Bernhardt, E. S., Band, L. E., Walsh, C. J., & Berke, P. E. (2008). Understanding, managing, and minimizing urban impacts on surface water nitrogen loading. *Annals of the New York Academy of Sciences*, *1134*, 61-96.

Bhagowati, B., & Ahamad, K. U. (2019). A review on lake eutrophication dynamics and recent developments in lake modeling. *Ecohydrology & Hydrobiology*, *19*, 155-166.

Bhattacharya, R., Lin, S. G. M., & Basu, N. B. (2022). Windows into the past: lake sediment phosphorus trajectories act as integrated archives of watershed disturbance legacies over centennial scales. *Environmental Research Letters*, *17*, 034005.

Boehrer, B., Golmen, L., Løvik, J. E., Rahn, K., & Klaveness, D. (2013). Thermobaric stratification in very deep Norwegian freshwater lakes. *Journal of Great Lakes Research*, *39*, 690-695.

Boehrer, B., & Schultze, M. (2008). Stratification of lakes. *Reviews of Geophysics*, *46*, RG2005.

Boehrer, B., von Rohden, C., & Schultze, M. (2017). Physical features of meromictic lakes: stratification and circulation. *Ecology of Meromictic Lakes, 15,* 15-34.

Borrelli, P., Lugato, E., Montanarella, L., & Panagos, P. (2017). A new assessment of soil loss due to wind erosion in European agricultural soils using a quantitative spatially distributed modelling approach. *Land Degradation & Development, 28*, 335-344.

Borrelli, P., Panagos, P., Ballabio, C., Lugato, E., Weynants, M., & Montanarella, L. (2016). Towards a pan-European assessment of land susceptibility to wind erosion. *Land Degradation & Development*, *27*, 1093-1105.

Boström, B., Persson, G., & Broberg, B. (1988). Bioavailability of different phosphorus forms in freshwater systems. In *Phosphorus in Freshwater Ecosystems: Proceedings of a Symposium held in Uppsala, Sweden, 25–28 September 1985*). Springer, 133-155.

Bouraï, L., Logez, M., Laplace-Treyture, C., & Argillier, C. (2020). How do eutrophication and temperature interact to shape the community structures of phytoplankton and fish in Lakes? *Water (Switzerland)*, *12*, 779.

Brabec, E., Schulte, S., & Richards, P. L. (2002). Impervious surfaces and water quality: a review of current literature and its implications for watershed planning. *Journal of Planning Literature*, *16*, 499-514.

Bratt, A. R., Finlay, J. C., Hobbie, S. E., Janke, B. D., Worm, A. C., & Kemmitt, K. L. (2017). Contribution of leaf litter to nutrient export during winter months in an urban residential watershed. *Environmental Science and Technology*, *51*, 3138-3147.

Brix, K. V., Deforest, D. K., Tear, L., Grosell, M., & Adams, W. J. (2017). Use of multiple linear regression models for setting water quality criteria for copper: a complementary approach to the biotic ligand model. *Environmental Science and Technology*, *51*, 5182-5192.

Brown, R. G. (1988). Effects of precipitation and land use on storm runoff. *Water Resources Bulletin, 24*, 421-426.

Bubeck, R. C., & Burton, R. S. (1989). Changes in chloride concentrations, mixing patterns, and stratification characteristics of Irondequoit Bay, Monroe County, New York, after decreased use of road-deicing salts, 1974-1984 (Vol. 87). Department of the Interior, US Geological Survey.

Bubeck, R., Diment, W., Deck, B., Baldwin, A., & Lipton, S. (1971). Runoff of deicing salt: effect on Irondequoit Bay, Rochester, New York. *Science*, *172,* 1128-1132.

Burns, M. J., Fletcher, T. D., Walsh, C. J., Ladson, A. R., & Hatt, B. E. (2012). Hydrologic shortcomings of conventional urban stormwater management and opportunities for reform. *Landscape and Urban Planning*, *105*, 230-240.

Butcher, J. B., Nover, D., Johnson, T. E., & Clark, C. M. (2015). Sensitivity of lake thermal and mixing dynamics to climate change. *Climatic Change*, *129*, 295-305.

Butturini, A., & Sabater, F. (1998). Ammonium and phosphate retention in a Mediterranean stream: hydrological versus temperature control. *Canadian Journal of Fisheries and Aquatic Sciences*, *55*, 1938-1945.

Campbell, J., Rihn, A., & Khachatryan, H. (2020). Factors influencing home lawn fertilizer choice in the United States. *Hortico Technology*, *30*, 296-305.

Cañedo-Argüelles, M., Hawkins, C. P., Kefford, B. J., Schäfer, R. B., Dyack, B. J., Brucet, S., Lazorchak, J. (2016). Saving freshwater from salts. *Science*, *351*, 914-916.

Cañedo-Argüelles, M., Kefford, B. J., Piscart, C., Prat, N., Schäfer, R. B., & Schulz, C.-J. (2013). Salinisation of rivers: an urgent ecological issue. *Environmental Pollution*, *173*, 157-167.

Cantin, A., Beisner, B. E., Gunn, J. M., Prairie, Y. T., & Winter, J. G. (2011). Effects of thermocline deepening on lake plankton communities. *Canadian Journal of Fisheries and Aquatic Sciences*, *68*, 260-276.

Carey, C. C., Hanson, P. C., Thomas, R. Q., Gerling, A. B., Hounshell, A. G., Lewis, A. S. L., Woelmer, W. M. (2022). Anoxia decreases the magnitude of the carbon, nitrogen, and phosphorus sink in freshwaters. *Global Change Biology*, *28*, 4861-4881.

Carey, R. O., Hochmuth, G. J., Martinez, C. J., Boyer, T. H., Dukes, M. D., Toor, G. S., & Cisar, J. L. (2013). Evaluating nutrient impacts in urban watersheds: challenges and research opportunities. *Environmental Pollution, 173*, 138-149.

Carey, R. O., Hochmuth, G. J., Martinez, C. J., Boyer, T. H., Nair, V. D., Dukes, M. D., Sartain, J. B. (2012). A review of turfgrass fertilizer management practices: implications for urban water quality. *Hortico Technology*, *22*, 280-291.

Carlton, R. G., & Wetzel, R. G. (1988). Phosphorus flux from lake sediments: effect of epipelic algal oxygen production. *Limnology and Oceanography*, *33*, 562-570.

Carpenter, S. R., Caraco, N. F., Correll, D. L., Howarth, R. W., Sharpley, A. N., & Smith, V. H. (1998). Nonpoint pollution of surface waters with phosphorus and nitrogen. *Ecological Applications*, *8*, 559-568.

Carpenter, S. R. (1983). Lake geometry: implications for production and sediment accretion rates. *Journal of Theoretical Biology*, *105*, 273-286.

Carpenter, S. R. (2005). Eutrophication of aquatic ecosystems: Bistability and soil phosphorus. *National Academy of Science*, *102,* 10002-10005.

Carpenter, S. R., Booth, E. G., & Kucharik, C. J. (2018). Extreme precipitation and phosphorus loads from two agricultural watersheds. *Limnology and Oceanography*, *63*, 1221-1233.

Carpenter, S. R., Booth, E. G., Kucharik, C. J., & Lathrop, R. C. (2015). Extreme daily loads: role in annual phosphorus input to a north temperate lake. *Aquatic Sciences*, *77*, 71-79.

Cavaliere, E., & Baulch, H. M. (2018). Denitrification under lake ice. *Biogeochemistry*, *137*, 285-295.

Chiandet, A. S., & Xenopoulos, M. A. (2016). Landscape and morphometric controls on water quality in stormwater management ponds. *Urban Ecosystems, 19*, 1645-1663.

Chen, X., Liu, X., Peng, W., Dong, F., Chen, Q., Sun, Y., & Wang, R. (2019). Hydroclimatic influence on the salinity and water volume of a plateau lake in southwest China. *Science of the Total Environment*, *659*, 746-755.

Chen, Y., Xie, Q., & Saeedi, A. (2019). Role of ion exchange, surface complexation, and albite dissolution in low salinity water flooding in sandstone. *Journal of Petroleum Science and Engineering*, *176*, 126-131.

Chowdhury, R. B., & Chakraborty, P. (2016). Magnitude of anthropogenic phosphorus storage in the agricultural production and the waste management systems at the regional and country scales. *Environmental Science and Pollution Research*, *23*, 15929-15940.

Christianson, L. E., Lepine, C., Sibrell, P. L., Penn, C., & Summerfelt, S. T. (2017). Denitrifying woodchip bioreactor and phosphorus filter pairing to minimize pollution swapping. *Water Research*, *121*, 129-139.

Clifton, C. F., Day, K. T., Luce, C. H., Grant, G. E., Safeeq, M., Halofsky, J. E., & Staab, B. P. (2018). Effects of climate change on hydrology and water resources in the Blue Mountains, Oregon, USA. *Climate Services*, *10*, 9-19.

Coats, R., Perez-Losada, J., Schladow, G., Richards, R., & Goldman, C. (2006). The warming of lake Tahoe. *Climatic Change*, *76*, 121-148.

Cooper, C. A., Mayer, P. M., & Faulkner, B. R. (2014). Effects of road salts on groundwater and surface water dynamics of sodium and chloride in an urban restored stream. *Biogeochemistry*, *121*, 149-166.

Cordell, D., Drangert, J.-O., & White, S. (2009). The story of phosphorus: global food security and food for thought. *Global Environmental Change*, *19*, 292-305.

Correll, D. L. (1999). Phosphorus: a rate limiting nutrient in surface waters. *Poultry Science*, *78*, 674-682.

Correll, D. L., Jordan, T. E., & Weller, D. E. (1999). Precipitation effects on sediment and associated nutrient discharges from Rhode river watersheds. *Journal of Environmental Quality*, *28*.

Corsi, S. R., Graczyk, D. J., Geis, S. W., Booth, N. L., & Richards, K. D. (2010). A fresh look at road salt: aquatic toxicity and water-quality impacts on local, regional, and national scales. *Environmental Science and Technology*, *44*, 1897-1907.

Corsi, S. R., De Cicco, L. A., Lutz, M. A., & Hirsch, R. M. (2015). River chloride trends in snow-affected urban watersheds: increasing concentrations outpace urban growth rate and are common among all seasons. *Science of the Total Environment*, *508*, 488-497.

Cott, P. A., Sibley, P. K., Gordon, A. M., Bodaly, R. A., Mills, K. H., Somers, W. M., & Fillatre, G. A. (2008). Effects of water withdrawal from ice-covered lakes on oxygen, temperature, and fish. *Journal of the American Water Resources Association*, *44*, 328-342.

Couture, R.-M., Charlet, L., Markelova, E., Madé, B., & Parsons, C. T. (2015). On–off mobilization of contaminants in soils during redox oscillations. *Environmental Science & Technology*, *49*, 3015-3023.

Cunillera-Montcusí, D., Beklioğlu, M., Cañedo-Argüelles, M., Jeppesen, E., Ptacnik, R., Amorim, C. A., Dugan, H. A. (2022). Freshwater salinisation: a research agenda for a saltier world. *Trends in Ecology & Evolution, 37*, 440-453.

Cyr, H., McCabe, S. K., & Nürnberg, G. K. (2009). Phosphorus sorption experiments and the potential for internal phosphorus loading in littoral areas of a stratified lake. *Water Research*, *43*, 1654-1666.

Czemiel Berndtsson, J. (2014). Storm water quality of first flush urban runoff in relation to different traffic characteristics. *Urban Water Journal*, *11*, 284-296.

Dake, J. M. K., & Harleman, D. R. F. (1969). Thermal stratification in lakes: analytical and laboratory studies. *Water Resources Research*, *5*, 484-495.

Dearing, J. A. (1991). Lake sediment records of erosional processes. In *Environmental History and Palaeolimnology: Proceedings of the Vth International Symposium on Palaeolimnology, held in Cumbria, UK*, Springer, *214*, 1-7.

Dodds, W. K., Perkin, J. S., & Gerken, J. E. (2013). Human impact on freshwater ecosystem services: a global perspective. *Environmental Science & Technology*, *47*, 9061-9068.

Doerr, S. M., Effler, S. W., Whitehead, K. A., Auer, M. T., Perkins, M., & Heidtke, T. M. (1994). Chloride model for polluted Onondaga Lake. *Water Research*, *28*, 849-861.

Doyle, V., & Macpherson, K. (2017). Oak Ridges moraine conservation plan case study (Ontario). *Canadian Council on Ecological Areas (CCEA) Occasional Paper, 123*.

Downing, J. A., & McCauley, E. (1992). The nitrogen: phosphorus relationship in lakes. *Limnology and Oceanography, 37*, 936-945.

Duan, S., & Kaushal, S. S. (2015). Salinization alters fluxes of bioreactive elements from stream ecosystems across land use. *Biogeosciences*, *12*, 7331-7347.

Duan, S., Kaushal, S. S., Groffman, P. M., Band, L. E., & Belt, K. T. (2012). Phosphorus export across an urban to rural gradient in the Chesapeake Bay watershed. *Journal of Geophysical Research: Biogeosciences*, *117*, G1.

Duda, A. M. (1993). Addressing nonpoint sources of water pollution must become an international priority. *Water Science and Technology*, *28*, 1-11.

Dugan, H. A., & Rock, L. A. (2021). The slow and steady salinization of Sparkling Lake, Wisconsin. *Limnology And Oceanography Letters, 8*, 74-82.

Dugan, H. A., Summers, J. C., Skaff, N. K., Krivak-Tetley, F. E., Doubek, J. P., Burke, S. M., Weathers, K. C. (2017). Long-term chloride concentrations in North American and European freshwater lakes. *Scientific Data*, *4*, 1-11.

Dugan, H. A., Bartlett, S. L., Burke, S. M., Doubek, J. P., Krivak-Tetley, F. E., Skaff, N. K., Weathers, K. C. (2017). *Proceedings of the National Academy of Sciences, 114,* 4453-4458.

Dunne, E. J., Culleton, N., O'Donovan, G., Harrington, R., & Daly, K. (2005). Phosphorus retention and sorption by constructed wetland soils in Southeast Ireland. *Water Research*, *39*, 4355-4362.

Eklund, H. (1965). Stability of lakes near the temperature of maximum density. *Science*, *149*, 632-633.

Ekness, P., & Randhir, T. O. (2015). Effect of climate and land cover changes on watershed runoff: a multivariate assessment for storm water management. *Journal of Geophysical Research: Biogeosciences*, *120*, 1785-1796.

Ellison, M. E., & Brett, M. T. (2006). Particulate phosphorus bioavailability as a function of stream flow and land cover. *Water Research*, *40*, 1258-1268.

Emilsson, T., & Sang, Å. O. (2017). Impacts of climate change on urban areas and nature-based solutions for adaptation. *Nature-Based Solutions to Climate Change Adaptation in Urban Areas, Springer*, *1,* 15-27.

Environment Canada, Canadian Council of Ministers (2001). *Canadian Water Quality Guidelines for the Protection of Aquatic Life: CCME Water Quality Index 1.0 User's Manual.* Canadian Environmental Quality Guidelines, Canadian Council of Ministers of the Environment Edmonton, AB, Canada.

Equiza, M. A., Calvo-Polanco, M., Cirelli, D., Señorans, J., Wartenbe, M., Saunders, C., & Zwiazek, J. J. (2017). Long-term impact of road salt (NaCl) on soil and urban trees in Edmonton, Canada. *Urban Forestry & Urban Greening*, *21*, 16-28.

Estévez, E., Rodriguez-Castillo, T., González-Ferreras, A. M., Cañedo-Argüelles, M., & Barquin, J. (2019). Drivers of spatio-temporal patterns of salinity in Spanish rivers: a nationwide assessment. *Philosophical Transactions of the Royal Society B*, *374*, 20180022.

Exum, L. R., Bird, S. L., Harrison, J., & Perkins, C. A. (2005). Estimating and projecting impervious cover in the southeastern United States. *Ecosystems Research Division, 133,* 1-37.

Fay, L., Shi, X., & Huang, J. (2013). *Strategies to mitigate the impacts of chloride roadway deicers on the natural environment* (Vol. 449). Transportation Research Board Washington, DC.

Ferreira, C. S. S., Walsh, R. P. D., & Ferreira, A. J. D. (2018). Degradation in urban areas. *Current Opinion in Environmental Science and Health*, *5,* 19-25.

Ferreira, C. S. S., Walsh, R. P. D., de Lourdes Costa, M., Coelho, C. O. A., & Ferreira, A. J. D. (2016). Dynamics of surface water quality driven by distinct urbanization patterns and storms in a Portuguese peri-urban catchment. *Journal of Soils and Sediments*, *16*, 2606-2621.

Ficker, H., Luger, M., & Gassner, H. (2017). From dimictic to monomictic: empirical evidence of thermal regime transitions in three deep alpine lakes in Austria induced by climate change. *Freshwater Biology*, *62*, 1335-1345.

Ficker, H., Luger, M., Pamminger-Lahnsteiner, B., Achleitner, D., Jagsch, A., & Gassner, H. (2019). Diluting a salty soup: impact of long-lasting salt pollution on a deep Alpine lake (Traunsee, Austria) and the downside of recent recovery from salinization. *Aquatic Sciences*, *81*, 7.

Filippelli, G. M. (2008). The Global Phosphorus Cycle: Past, Present, and Future. *Elements*, *4,* 89-95.

Fletcher, T. D., Andrieu, H., & Hamel, P. (2013). Understanding, management and modelling of urban hydrology and its consequences for receiving waters: a state of the art. *Advances in Water Resources*, *51*, 261-279.

Flores-Rodrîguez, J., Bussy, A.-L., & Thévenot, D. R. (1994). Toxic metals in urban runoff: physico-chemical mobility assessment using speciation schemes. *Water Science and Technology*, *29*, 83-93.

Foley, J. A., DeFries, R., Asner, G. P., Barford, C., Bonan, G., Carpenter, S. R., Gibbs, H. K. (2005). Global consequences of land use. *Science*, *309*, 570-574.

Foley, M. G. (1994). *West Siberian basin hydrogeology-regional framework for contaminant migration from injected wastes*. Battelle Pacific Northwest Lab, PNL-SA—24157.

Forzieri, G., Bianchi, A., Silva, F. B. e., Marin Herrera, M. A., Leblois, A., Lavalle, C., Feyen, L. (2018). Escalating impacts of climate extremes on critical infrastructures in Europe. *Global Environmental Change*, *48*, 97-107.

Frossard, V., Millet, L., Verneaux, V., Jenny, J. P., Arnaud, F., Magny, M., & Perga, M. E. (2014). Depth-specific responses of a chironomid assemblage to contrasting anthropogenic pressures: a palaeolimnological perspective from the last 150 years. *Freshwater Biology*, *59*, 26-40.

Frost, P. C., Prater, C., Scott, A. B., Song, K., & Xenopoulos, M. A. (2019). Mobility and bioavailability of sediment phosphorus in urban stormwater ponds. *Water Resources Research*, *55*, 3680-3688.

Fu, G., Chen, S., & McCool, D. K. (2006). Modeling the impacts of no-till practice on soil erosion and sediment yield with rusle seed, and ArcView GIS. *Soil and Tillage Research*, *85*, 38-49.

Fu, L., Omer, R., & Jiang, C. (2012). Field test of organic deicers as prewetting and anti-icing agents for winter road maintenance. *Transportation Research Record*, *2272*, 130-135.

Garg, K., Khullar, V., Das, S. K., & Tyagi, H. (2018). Performance evaluation of a brine-recirculation multistage flash desalination system coupled with nanofluid-based direct absorption solar collector. *Renewable Energy*, *122*, 140-151.

Garnier, J., Brion, N., Callens, J., Passy, P., Deligne, C., Billen, G., Billen, C. (2013). Modeling historical changes in nutrient delivery and water quality of the Zenne River (1790s–2010): the role of land use, waterscape and urban wastewater management. *Journal of Marine Systems*, *128*, 62-76.

Gee, G. W., Bauder, J. W., & Klute, A. (1986). Methods of soil analysis, part 1, physical and mineralogical methods. *Soil Science Society of America, American Society of Agronomy*, 5.

Gill, A. (1986). *The Dynamic of Atmosphere and Ocean*, *2*. Moscow: Mir.

Gillis, P. L., Salerno, J., Bennett, C. J., Kudla, Y., & Smith, M. (2021). The relative toxicity of road salt alternatives to freshwater mussels; examining the potential risk of eco-friendly de-icing products to sensitive aquatic species. *ACS ES&T Water*, *1*, 1628-1636.

Goh, H. W., Lem, K. S., Azizan, N. A., Chang, C. K., Talei, A., Leow, C. S., & Zakaria, N. A. (2019). A review of bioretention components and nutrient removal under different climates—future directions for tropics. *Environmental Science and Pollution Research, 26*, 14904-14919.

Gorham, E., & Boyce, F. M. (1989). Influence of lake surface area and depth upon thermal stratification and the depth of the summer thermocline. *Journal of Great Lakes Research*, *15*, 233-245.

Government of Canada. (2019). *Canadian climate normals 1981-2010 station data*.

Government of Canada. (2013). *Soil Survey of York County*.

Granato, G. E., Church, P. E., & Stone, V. J. (1995). Mobilization of major and trace constituents of highway runoff in groundwater potentially caused by deicing chemical migration. *Transportation Research Record*, *1483*, 92-104.

Greb, S. R., & Bannerman, R. T. (1997). Influence of particle size on wet pond effectiveness. *Water Environment Research*, *69*, 1134-1138.

Gu, L., Dai, B., Zhu, D. Z., Hua, Z., Liu, X., van Duin, B., & Mahmood, K. (2017). Sediment modelling and design optimization for stormwater ponds. *Canadian Water Resources Journal/Revue Canadienne Des Ressources Hydriques*, *42*, 70-87.

Gurkan, Z., Zhang, J., & Jørgensen, S. E. (2006). Development of a structurally dynamic model for forecasting the effects of restoration of Lake Fure, Denmark. *Ecological Modelling*, *197*, 89-102.

Haake, D. M., & Knouft, J. H. (2019). Comparison of contributions to chloride in urban stormwater from winter brine and rock salt application. *Environmental Science & Technology*, *53*, 11888-11895.

Haq, S., Kaushal, S. S., & Duan, S. (2018). Episodic salinization and freshwater salinization syndrome mobilize base cations, carbon, and nutrients to streams across urban regions. *Biogeochemistry*, *141*, 463-486.

Hasler, C. T., Jeffrey, J. D., Schneider, E. V. C., Hannan, K. D., Tix, J. A., & Suski, C. D. (2018). Biological consequences of weak acidification caused by elevated carbon dioxide in freshwater ecosystems. *Hydrobiologia*, *806*, 1-12.

Hassall, C. (2014). The ecology and biodiversity of urban ponds. *Wiley Interdisciplinary Reviews: Water*, *1*, 187-206.

Hathaway, J. M., Tucker, R. S., Spooner, J. M., & Hunt, W. F. (2012). A traditional analysis of the first flush effect for nutrients in stormwater runoff from two small urban catchments. *Water, Air, and Soil Pollution*, *223*, 5903-5915.

Hathaway, J. M., Winston, R. J., Brown, R. A., Hunt, W. F., & McCarthy, D. T. (2016). Temperature dynamics of stormwater runoff in Australia and the USA. *Science of the Total Environment*, *559*, 141-150.

Heal, K. V, Hepburn, D. A., & Lunn, R. J. (2006). Sediment management in sustainable urban drainage system ponds. *Water Science and Technology*, *53*, 219-227.

Heino, J., Bini, L. M., Andersson, J., Bergsten, J., Bjelke, U., & Johansson, F. (2017). Unravelling the correlates of species richness and ecological uniqueness in a metacommunity of urban pond insects. *Ecological Indicators*, *73*, 422-431.

Heiri, O., Lotter, A. F., & Lemcke, G. (2001). Loss on ignition as a method for estimating organic and carbonate content in sediments: reproducibility and comparability of results. *Journal of Paleolimnology*, *25*, 101-110.

Heisler, J., Glibert, P. M., Burkholder, J. M., Anderson, D. M., Cochlan, W., Dennison, W. C., Suddleson, M. (2008). Eutrophication and harmful algal blooms: a scientific consensus. *Harmful Algae*, *8*, 3-13.

Helsel, D., & Hirsch, R. (1992). Statistical methods in water resources. *Elsevier*, *49*.

Hernandez Gonzalez, L. M., Rivera, V. A., Phillips, C. B., Miller, W. M., & Packman, A. I. (2020). Road salt intrusion dynamics in a midwestern prairie-wetland complex. In *AGU Fall Meeting Abstracts*, *2020*, H069-04.

Hintz, W. D., Arnott, S. E., Symons, C. C., Greco, D. A., McClymont, A., Brentrup, J. A., Gray, D. K. (2022). Current water quality guidelines across North America and Europe do not protect lakes from salinization. *Proceedings of the National Academy of Sciences*, *119*, e2115033119.

Hintz, W. D., Fay, L., & Relyea, R. A. (2022). Road salts, human safety, and the rising salinity of our fresh waters. *Frontiers in Ecology and the Environment*, *20*, 22-30.

Hintz, W. D., Mattes, B. M., Schuler, M. S., Jones, D. K., Stoler, Lovisa Lind, A. B., & Relyea, R. A. (2016). Salinization triggers a trophic cascade in experimental freshwater communities with varying food-chain length. *Exological Applications*, *27*, 833-844.

Hirsch, R. M., Slack, J. R., & Smith, R. A. (1982). techniques of trend analysis for monthly water quality data. *Water Resources Research*, *18,* 107-121.

Hobbie, S. E., Finlay, J. C., Janke, B. D., Nidzgorski, D. A., Millet, D. B., & Baker, L. A. (2017). Contrasting nitrogen and phosphorus budgets in urban watersheds and implications for managing urban water pollution. *Proceedings of the National Academy of Sciences of the United States of America*, *114*, 4177-4182.

Hull, A. (2008). Policy integration: what will it take to achieve more sustainable transport solutions in cities? *Transport Policy*, *15*, 94-103.

Hyacinthe, C., & Van Cappellen, P. (2004). An authigenic iron phosphate phase in estuarine sediments: composition, formation and chemical reactivity. *Marine Chemistry*, *91*, 227-251.

Iglesias, M. C.-A. (2020). A review of recent advances and future challenges in freshwater salinization. *Limnetica*, *39*, 185-211.

Imberger, J., & Patterson, J. C. (1989). Physical limnology. *Advances in Applied Mechanics*, *27*, 303-475.

Imran, H. M., Akib, S., & Karim, M. R. (2013). Permeable pavement and stormwater management systems: a review. *Environmental Technology*, *34*, 2649-2656.

Indris, S. N., Rudolph, D. L., Glass, B. K., & Van Cappellen P. (2020). Evaluating phosphorous from vehicular emissions as a potential source of contamination to ground and surface water. *Cogent Environmental Science*, *6*, 1794702.

Ingall, E. D., & Van Cappellen, P. (1990). Relation between sedimentation rate and burial of organic phosphorus and organic carbon in marine sediments. *Geochimica et Cosmochimica Acta*, *54*, 373-386.

Ingall, E., & Jahnke, R. (1997). Influence of water-column anoxia on the elemental fractionation of carbon and phosphorus during sediment diagenesis. *Marine Geology*, *139*, 219-229.

IPCC Climate Change. (2007). The Physical Science Basis. *Contribution of Working Group I to the 4th Assessment Report of the Intergovernmental Panel on Climate Change*.

Jacobson, C. R. (2011, June). Identification and quantification of the hydrological impacts of imperviousness in urban catchments: a review. *Journal of Environmental Management, 92,* 1438-1448.

Jamshidi, A., Goodarzi, A. R., & Razmara, P. (2020). Long-term impacts of road salt application on the groundwater contamination in urban environments. *Environmental Science and Pollution Research*, *27*, 30162-30177.

Jane, S. F., Hansen, G. J. A., Kraemer, B. M., Leavitt, P. R., Mincer, J. L., North, R. L., Rose, K. C. (2021). Widespread deoxygenation of temperate lakes. *Nature*, *594*, 66-70.

Jane, S. F., & Rose, K. C. (2021). Predicting arctic-alpine lake dissolved oxygen responses to future tree line advance at the Swedish forest-tundra transition zone. *Global Change Biology, 27*, 4238-4253.

Jane, S. F., Mincer, J. L., Lau, M. P., Lewis, A. S. L., Stetler, J. T., & Rose, K. C. (2023). Longer duration of seasonal stratification contributes to widespread increases in lake hypoxia and anoxia. *Global Change Biology*, *29*, 1009-1023.

Janke, B. D., Finlay, J. C., Hobbie, S. E., Baker, L. A., Sterner, R. W., Nidzgorski, D., & Wilson, B. N. (2014). Contrasting influences of stormflow and baseflow pathways on nitrogen and phosphorus export from an urban watershed. *Biogeochemistry*, *121*, 209-228.

Jefferson, A. J., Bhaskar, A. S., Hopkins, K. G., Fanelli, R., Avellaneda, P. M., & McMillan, S. K. (2017). Stormwater management network effectiveness and implications for urban watershed function: a critical review. *Hydrological Processes*, *31*, 4056-4080.

Jennings, E., Allott, N., Pierson, D. C., Schneiderman, E. M., Lenihan, D., Samuelsson, P., & Taylor, D. (2009). Impacts of climate change on phosphorus loading from a grassland catchment: Implications for future management. *Water Research*, *43*, 4316-4326.

Jenny, J. P., Francus, P., Normandeau, A., Lapointe, F., Perga, M. E., Ojala, A., Zolitschka, B. (2016). Global spread of hypoxia in freshwater ecosystems during the last three centuries is caused by rising local human pressure. *Global Change Biology*, *22*, 1481-1489.

Jeppesen, E., Meerhoff, M., Davidson, T. A., Trolle, D., SondergaarD, M., Lauridsen, T. L., González-Bergonzoni, I. (2014). Climate change impacts on lakes: an integrated ecological perspective based on a multi-faceted approach, with special focus on shallow lakes. *Journal of Limnology, 73*, 88-111.

Jeppesen, E., Søndergaard, M., Jensen, J. P., Havens, K. E., Anneville, O., Carvalho, L., Foy, B. O. B. (2005). Lake responses to reduced nutrient loading–an analysis of contemporary long-term data from 35 case studies. *Freshwater Biology*, *50*, 1747-1771.

Jia, B., Si, J., Xi, H., & Qin, J. (2021). A Characterization of the Hydrochemistry and Main Controlling Factors of Lakes in the Badain Jaran Desert, China. *Water*, *13*, 2931.

Jones, J. R., & Bachmann, R. W. (1976). Prediction of phosphorus and chlorophyll levels in lakes. *Journal of Water Pollution Control Federation, 1,* 2186-2182.

Joshi, S. R., Kukkadapu, R. K., Burdige, D. J., Bowden, M. E., Sparks, D. L., & Jaisi, D. P. (2015). Organic matter remineralization predominates phosphorus cycling in the mid-bay sediments in the Chesapeake Bay. *Environmental Science & Technology*, *49*, 5887-5896.

Kalmykova, Y., Harder, R., Borgestedt, H., & Svanäng, I. (2012). Pathways and management of phosphorus in urban areas. *Journal of Industrial Ecology*, *16*, 928-939.

Kao, N., Mohamed, M., Sorichetti, R. J., Niederkorn, A., Van Cappellen, P., & Parsons, C. T. (2021). Phosphorus retention and transformation in a dammed reservoir of the Thames River, Ontario: impacts on phosphorus load and speciation. *Journal of Great Lakes Research, 48,* 84-96.

Kassambara, A. & Mundit (2016). Factoextra: extract and visualize the results of multivariate data analyses. *R Package Version*, *1*.

Katsev, S., Tsandev, I., L'Heureux, I., & Rancourt, D. G. (2006). Factors controlling long-term phosphorus efflux from lake sediments: Exploratory reactive-transport modeling. *Chemical Geology*, *234*, 127-147.

Kaushal, S. S., Duan, S., Doody, T. R., Haq, S., Smith, R. M., Newcomer Johnson, T. A., Stack, W. P. (2017). Human-accelerated weathering increases salinization, major ions, and alkalinization in fresh water across land use. *Applied Geochemistry*, *83*, 121-135.

Kaushal, S. S., Likens, G. E., Pace, M. L., Haq, S., Wood, K. L., Galella, J. G., Utz, R. (2019). Novel 'chemical cocktails' in inland waters are a consequence of the freshwater salinization syndrome. *Philosophical Transactions of the Royal Society B: Biological Sciences*, *374*, 20180017.

Kaushal, S. S., Likens, G. E., Pace, M. L., Reimer, J. E., Maas, C. M., Galella, J. G., Woglo, S. A. (2021). Freshwater salinization syndrome: from emerging global problem to managing risks. *Biogeochemistry*, *154*, 255-292.

Kaushal, S. S., Likens, G. E., Pace, M. L., Utz, R. M., Haq, S., Gorman, J., & Grese, M. (2018). Freshwater salinization syndrome on a continental scale. *Proceedings of the National Academy of Sciences of the United States of America*, *115*, E574-E583.

Kaushal, S. S., Likens, G. E., Utz, R. M., Pace, M. L., Grese, M., & Yepsen, M. (2013). Increased river alkalinization in the eastern U.S. *Environmental Science and Technology*, *47*, 10302-10311.

Kaushal, S. S., Mayer, P. M., Vidon, P. G., Smith, R. M., Pennino, M. J., Newcomer, T. A., Belt, K. T. (2014). Land use and climate variability amplify carbon, nutrient, and contaminant pulses: a review with management implications. *Journal of the American Water Resources Association*, *50*, 585-614.

Kaushal, S. S., McDowell, W. H., & Wollheim, W. M. (2014). Tracking evolution of urban biogeochemical cycles: past, present, and future. *Biogeochemistry*, *121*, 1-21.

Kaushal, S. S., Groffman, P. M., Likens, G. E., Belt, K. T., Stack, W. P., Kelly, V. R., Fisher, G. T. (2005). Increased salinization of fresh water in the northeastern United States. *Proceedings of the National Academy of Sciences 102,* 13517-13520*.*

Kelly, V. R., Findlay, S. E., Hamilton, S. K., Lovett, G. M., & Weathers, K. C. (2019). Seasonal and long-term dynamics in stream water sodium chloride concentrations and the effectiveness of road salt best management practices. *Water, Air, & Soil Pollution*, *230*, 1-9.

Kendall, M. G. (1975). Rank Correlation Methods. *Griffin, London*.

Khan, S. T., Edward Beighley, R., VanHoven, D., & Watkins, K. (2021). Dynamic stormwater management to mitigate phosphorous export. *Science of the Total Environment*, *787*, 147506.

Kirkkala, T., Ventelä, A., & Tarvainen, M. (2012). Long-term field-scale experiment on using lime filters in an agricultural catchment. *Journal of Environmental Quality*, *41*, 410-419.

Knapp, A. K., Beier, C., Briske, D., Aimee, C. T., Yiqi, L., Reichstein, M., Fay, P. A. (2008). Consequences of more extreme precipitation regimes for terrestrial ecosystems. *Bioscience*, *58*, 811-821.

Koretsky, C. M., MacLeod, A., Sibert, R. J., & Snyder, C. (2012). Redox stratification and salinization of three kettle lakes in southwest Michigan, USA. *Water, Air, and Soil Pollution*, *223*, 1415-1427.

Kraemer, B. M., Anneville, O., Chandra, S., Dix, M., Kuusisto, E., Livingstone, D. M., McIntyre, P. B. (2015). Morphometry and average temperature affect lake stratification responses to climate change. *Geophysical Research Letters*, *42*, 4981-4988.

Kratky, H., Li, Z., Chen, Y., Wang, C., Li, X., & Yu, T. (2017). A critical literature review of bioretention research for stormwater management in cold climate and future research recommendations. *Frontiers of Environmental Science and Engineering, 48*, 1-15.

Kratky, H., Li, Z., Yu, T., Li, X., & Jia, H. (2021). Study on bioretention for stormwater management in cold climate, part II: water quality. *Journal of Water and Climate Change, 12*, 25-34.

Kuster, A. C., Pilgrim, K. M., Kuster, A. T., & Huser, B. J. (2022). field application of spent lime water treatment residual for the removal of phosphorus and other pollutants in urban stormwater runoff. *Water*, *14*, 2135.

Laceby, J. P., Kerr, J. G., Zhu, D., Chung, C., Situ, Q., Abbasi, S., & Orwin, J. F. (2019). Chloride inputs to the North Saskatchewan River watershed: the role of road salts as a potential driver of salinization downstream of North America's northern most major city (Edmonton, Canada). *Science of the Total Environment*, *688*, 1056-1068.

Ladwig, R., Rock, L. A., & Dugan, H. A. (2021). Impact of salinization on lake stratification and spring mixing. *Limnology and Oceanography Letters*, *8*, 93-102.

Le, T. D. H., Kattwinkel, M., Schützenmeister, K., Olson, J. R., Hawkins, C. P., & Schäfer, R. B. (2019). Predicting current and future background ion concentrations in German surface water under climate change. *Philosophical Transactions of the Royal Society B, 374*, 20180004.

Leavitt, P. R., Carpenter, S. R., & Kitchell, J. F. (1989). Whole-lake experiments: the annual record of fossil pigments and zooplankton. *Limnology and Oceanography*, *34*, 700-717.

Leeson, G. W. (2018). The growth, ageing and urbanisation of our world. *Journal of Population Ageing*, *11*, 107-115.

Lehman, J. T. (1975). Reconstructing the rate of accumulation of lake sediment: the effect of sediment focusing. *Quaternary Research*, *5*, 541-550.

Lemieux, C. J., Jacob, A. L., Gray, P. A., & Canadian Council on Ecological Areas. (2011). Implementing connectivity conservation in Canada. *Environmental Management*, *48*, 17-208.

Lemieux, C. J., & Scott, D. J. (2011). Changing climate, challenging choices: identifying and evaluating climate change adaptation options for protected areas management in Ontario, Canada. *Environmental Management*, *48*, 675-690.

Lembcke, D., Thompson, B., Read, K., Betts, A., & Singaraja, D. (2017). Reducing road salt application by considering winter maintenance needs in parking lot design. *Journal of Green Building, 12*, 1-12.

Lepori, F., & Roberts, J. J. (2017). Effects of internal phosphorus loadings and food-web structure on the recovery of a deep lake from eutrophication. *Journal of Great Lakes Research*, *43*, 255-264.

Lettenmaier, D. P. (1988). Multivariate nonparametric tests for trend in water quality. *Journal of the American Water Resources Association*, *24*, 505-512.

Lewis Jr, W. M. (1996). Tropical lakes: how latitude makes a difference. *Perspectives in Tropical Limnology*, *4364*, 43-64.

Lewis Jr, W. M. (1983). A revised classification of lakes based on mixing. *Canadian Journal of Fisheries and Aquatic Sciences*, *40*, 1779-1787.

Li, C., Liu, M., Hu, Y., Shi, T., Qu, X., & Walter, M. T. (2018). Effects of urbanization on direct runoff characteristics in urban functional zones. *Science of the Total Environment*, *643*, 301-311.

Li, H. (2015). Green infrastructure for highway stormwater management: field investigation for future design, maintenance, and management needs. *Journal of Infrastructure Systems*, *21*, 05015001.

Li, W., Dong, W., Guo, Y., Wang, K., & Shah, S. P. (2022). Advances in multifunctional cementitious composites with conductive carbon nanomaterials for smart infrastructure. *Cement and Concrete Composites*, *128*, 104454.

Li, W., & Wu, C. (2016). A geostatistical temporal mixture analysis approach to addresses endmember variability for estimating regional impervious surface distributions. *GIScience and Remote Sensing*, *53*, 102-121.

Lin, J., Huang, J., Prell, C., & Bryan, B. A. (2021). Changes in supply and demand mediate the effects of land-use change on freshwater ecosystem services flows. *Science of the Total Environment*, *763*, 143012.

Lind, L., Schuler, M. S., Hintz, W. D., Stoler, A. B., Jones, D. K., Mattes, B. M., & Relyea, R. A. (2018). Salty fertile lakes: how salinization and eutrophication alter the structure of freshwater communities. *Ecosphere*, *9*, e02383.

Lindenschmidt, K.-E., & Chorus, I. (1998). The effect of water column mixing on phytoplankton succession, diversity and similarity. *Journal of Plankton Research*, *20*, 1927-1951.

Lindh, G. (1972). Urbanization: a hydrological headache. *Ambio*, *1*, 185-201.

Liu, K., Chen, X., Li, L., Chen, H., Ruan, X., & Liu, W. (2015). A consensus successive projections algorithm - multiple linear regression method for analyzing near infrared spectra. *Analytica Chimica Acta*, *858*, 16-23.

Liu, Y., Gao, X., Gao, Q., Shao, L., & Han, J. (2019). Adaptive robust principal component analysis. *Neural Networks*, *119*, 85-92.

Löfgren, S. (2001). The chemical effects of deicing salt on soil and stream water of five catchments in southeast Sweden. *Water, Air, and Soil Pollution*, *130*, 863-868.

Luo, Y., Zhao, Y., Yang, K., Chen, K., Pan, M., & Zhou, X. (2018). Dianchi lake watershed impervious surface area dynamics and their impact on lake water quality from 1988 to 2017. *Environmental Science and Pollution Research*, *25*, 29643-29653.

Maavara, T., Parsons, C. T., Ridenour, C., Stojanovic, S., Dürr, H. H., Powley, H. R., & Van Cappellen, P. (2015). Global phosphorus retention by river damming. *Proceedings of the National Academy of Sciences*, *112*, 15603-15608.

Macintosh, K. A., Mayer, B. K., McDowell, R. W., Powers, S. M., Baker, L. A., Boyer, T. H., & Rittmann, B. E. (2018). Managing diffuse phosphorus at the source versus at the sink. *Environmental Science & Technology*, *52*, 11995-12009.

Mackie, C., Lackey, R., Levison, J., & Rodrigues, L. (2022). Groundwater as a source and pathway for road salt contamination of surface water in the Lake Ontario basin: a review. *Journal of Great Lakes Research*, *48*, 24-36.

MacLeod, A., Sibert, R., Snyder, C., & Koretsky, C. M. (2011). Eutrophication and salinization of urban and rural kettle lakes in Kalamazoo and Barry Counties, Michigan, USA. *Applied Geochemistry*, *26*, S214-S217.

Mansoor, S. Z., Louie, S., Lima, A. T., Van Cappellen, P., & MacVicar, B. (2018). The spatial and temporal distribution of metals in an urban stream: A case study of the Don River in Toronto, Canada. *Journal of Great Lakes Research*, *44*, 1314-1326.

Mantoura, R. F. C., & Llewellyn, C. A. (1983). The rapid determination of algal chlorophyll and carotenoid pigments and their breakdown products in natural waters by reverse-phase high-performance liquid chromatography. *Analytica Chimica Acta*, *151,* 297-314.

Markelov, I., Couture, R., Fischer, R., Haande, S., & Van Cappellen, P. (2019). Coupling Water Column and Sediment Biogeochemical Dynamics: Modeling Internal Phosphorus Loading, Climate Change Responses, and Mitigation Measures in Lake Vansjø, Norway. *Journal of Geophysical Research: Biogeosciences*, *124*, 3847-3866.

Markovic, S., Liang, A., Watson, S. B., Depew, D., Zastepa, A., Surana, P., Dittrich, M. (2019). Reduction of industrial iron pollution promotes phosphorus internal loading in eutrophic Hamilton Harbour, Lake Ontario, Canada. *Environmental Pollution*, *252*, 697-705.

Marvin, J. T., Passeport, E., & Drake, J. (2020). State-of-the-Art Review of Phosphorus Sorption Amendments in Bioretention Media: A Systematic Literature Review. *Journal of Sustainable Water in the Built Environment*, *6*, 03119001.

Matisoff, G., Bonniwell, E. C., & Whiting, P. J. (2002). Radionuclides as indicators of sediment transport in agricultural watersheds that drain to Lake Erie. *Journal of Environmental Quality*, *31*, 62-72.

Mazumder, B., Wellen, C., Kaltenecker, G., Sorichetti, R. J., & Oswald, C. J. (2021). Trends and legacy of freshwater salinization: untangling over 50 years of stream chloride monitoring. *Environmental Research Letters*, *16*, 095001.

McCarter, C. P. R., Rezanezhad, F., Gharedaghloo, B., Price, J. S., & Van Cappellen, P. (2019). Transport of chloride and deuterated water in peat: The role of anion exclusion, diffusion, and anion adsorption in a dual porosity organic media. *Journal of Contaminant Hydrology*, *225,* 103497.

McDonald, R. I., Weber, K., Padowski, J., Flörke, M., Schneider, C., Green, P. A., Montgomery, M. (2014). Water on an urban planet: Urbanization and the reach of urban water infrastructure. *Global Environmental Change*, *27*, 96-105.

McGrane, S. J. (2016). Impacts of urbanisation on hydrological and water quality dynamics, and urban water management: a review. *Hydrological Sciences Journal*, *61*, 2295-2311.

Meals, W. D., Spooner, J., Dressing, A. C., & Harcum, B. J. (2011). Statistical analysis for monotonic trends. *Department for US Environmental Protection Agency*, *1*, 1-23.

Meriano, M., Eyles, N., & Howard, K. W. F. (2009). Hydrogeological impacts of road salt from Canada's busiest highway on a Lake Ontario watershed (Frenchman's Bay) and lagoon, City of Pickering. *Journal of Contaminant Hydrology*, *107*, 66-81.

Metson, G. S., Hale, R. L., Iwaniec, D. M., Cook, E. M., Corman, J. R., Galletti, C. S., & Childers, D. L. (2012). Phosphorus in Phoenix: a budget and spatial representation of phosphorus in an urban ecosystem. *Ecological Applications*, *22*.

Meyers, P. A. (2003). Applications of organic geochemistry to paleolimnological reconstructions: a summary of examples from the Laurentian Great Lakes. *Organic Geochemistry*, *34*, 705-721.

Miller, J. D., & Hess, T. (2017). Urbanization impacts on storm runoff along a rural-urban gradient. *Journal of Hydrology*, *552*, 474-489.

Millero, F. J., & Poisson, A. (1981). International one-atmosphere equation of state of seawater. *Deep Sea Research Part A. Oceanographic Research Papers*, *28*, 625-629.

Miron, J., Millward, A. A., Vaziriyeganeh, M., Zwiazek, J. J., & Urban, J. (2022). Winter Climate Variability, De-Icing Salt and Streetside Tree Vitality. *Frontiers in Ecology and Evolution*, *10*, 749168.

Mirzavand, M., Ghasemieh, H., Sadatinejad, S. J., & Bagheri, R. (2020). An overview on source, mechanism and investigation approaches in groundwater salinization studies. *International Journal of Environmental Science and Technology*, *17*, 2463-2476.

Moatar, F., & Meybeck, M. (2005). Compared performances of different algorithms for estimating annual nutrient loads discharged by the eutrophic River Loire. *Hydrological Processes: An International Journal*, *19*, 429-444.

Montgomery, M. (2007). United Nations Population Fund: State of world population 2007: Unleashing the potential of urban growth. *Population and Development Review*, *33*, 639-641.

Morales, K., & Oswald, C. (2020). Water age in stormwater management ponds and stormwater management pond-treated catchments. *Hydrological Processes*, *34*, 1854-1867.

Mortimer, C. H. (1974). Lake hydrodynamics. *SIL Communications, 20*, 60-72.

Muggeo, V. M. (2008). Segmented: an R package to fit regression models with broken-line relationships. *R news, 8*, 20-25.

Muerdter, C., Özkök, E., Li, L., & Davis, A. P. (2016). Vegetation and media characteristics of an effective bioretention cell. *Journal of Sustainable Water in the Built Environment*, *2*, 04015008.

Müller, B., Bryant, L. D., Matzinger, A., & Wüest, A. (2012). Hypolimnetic oxygen depletion in eutrophic lakes. *Environmental Science & Technology*, *46*, 9964-9971.

Neave, M., & Rayburg, S. (2006). Salinity and erosion: a preliminary investigation of soil erosion on a salinized hillslope. *IAHA Publication*, *306*, 531.

Nirupama, N., Armenakis, C., & Montpetit, M. (2014). Is flooding in Toronto a concern? *Natural Hazards*, *72*, 1259-1264.

Norrström, A.-C., & Bergstedt, E. (2001). The impact of road de-icing salts (NaCl) on colloid dispersion and base cation pools in roadside soils. *Water, Air, and Soil Pollution*, *127*, 281-299.

Novotny, E. V., Murphy, D., & Stefan, H. G. (2008). Increase of urban lake salinity by road deicing salt. *Science of the Total Environment*, *406*, 131-144.

Novotny, E. V, & Stefan, H. G. (2012). Road salt impact on lake stratification and water quality. *Journal of Hydraulic Engineering*, *138*, 1069-1080.

Novotny, E. V. (2009). Road deicing salt impacts on urban water quality. Retrieved from the *University of Minnesota Digital Conservancy.*

Novotny, E. V., & Stefan, H. G. (2010). Projections of chloride concentrations in urban lakes receiving road de-icing salt. *Water, Air, and Soil Pollution*, *211*, 261-271.

Novotny, E., Murphy, D., & Stefan, H. (2007). Road Salt Effects on the Water Quality of Lakes in the Twin Cities Metropolitan Area. St. Anthony Falls Laboratory. Retrieved from the *University of Minnesota Digital Conservancy.*

Nürnberg, G. (1997). Coping with water quality problems due to hypolimnetic anoxia in Central Ontario Lakes. *Water Quality Research Journal*, *32*, 391-405.

Nürnberg, G. K. (1984). The prediction of internal phosphorus load in lakes with anoxic hypolimnia 1. *Limnology and Oceanography*, *29*, 111-124.

Nürnberg, G. K. (1987). Hypolimnetic withdrawal as lake restoration technique. *Journal of Environmental Engineering*, *113*, 1006-1017.

Nürnberg, G. K. (1995). *Quantifying anoxia in lakes*. *Limnology and Oceanography, 40*, 1100-1111.

Nürnberg, G. K. (2009). Assessing internal phosphorus load–problems to be solved. *Lake and Reservoir Management*, *25*, 419-432.

Nürnberg, G. K. (2004). Quantified Hypoxia and Anoxia in Lakes and Reservoirs. *The Scientific World*, *4*, 42-54.

Nürnberg, G. K. (1996). Trophic state of clear and colored, soft- and hardwater lakes with special consideration of nutrients, anoxia, phytoplankton and fish. *Lake and Reservoir Management*, *12*, 432-447.

Nürnberg, G. K., LaZerte, B. D., & Olding, D. D. (2003). An artificially induced planktothrix rubescens surface bloom in a small kettle lake in Southern Ontario compared to blooms world-wide. *Lake and Reservoir Management*, *19*, 307-322.

Öberg, G. (2002). The natural chlorine cycle–fitting the scattered pieces. *Applied Microbiology and Biotechnology*, *58*, 565-581.

O'Connell, D. W., Ansems, N., Kukkadapu, R. K., Jaisi, D., Orihel, D. M., Cade-Menun, B. J., Chessell, H., Behrends, T., Van Cappellen, P. (2020). Changes in sedimentary phosphorus burial following artificial eutrophication of Lake 227, Experimental Lakes Area, Ontario, Canada. *Journal of Geophysical Research: Biogeosciences*, *125*, e2020JG005713.

Oertli, B., & Parris, K. M. (2019). Review: Toward management of urban ponds for freshwater biodiversity. *Ecosphere*, *10*, e02810.

Olding, D. (2012). Water Quality and Remediation Options for Lake Wilcox. *Town of Richmond Hill, Ontario*.

OMAFRA. (2019). Land use maps. Retrieved February 2, 2019, from http://www.omafra.gov.on.ca/english/landuse/gis/mapgallery.ht,

O'Reilly, C. M., Sharma, S., Gray, D. K., Hampton, S. E., Read, J. S., Rowley, R. J., Zhang, G. (2015). Rapid and highly variable warming of lake surface waters around the globe. *Geophysical Research Letters*, *42*, 10-773.

Orihel, D. M., Baulch, H. M., Casson, N. J., North, R. L., Parsons, C. T., Seckar, D. C. M., & Venkiteswaran, J. J. (2017). Internal phosphorus loading in Canadian fresh waters: a critical review and data analysis. *Canadian Journal of Fisheries and Aquatic Sciences*, *74*, 2005-2029.

Oswald, C. J., Giberson, G., Nicholls, E., Wellen, C., & Oni, S. (2019). Spatial distribution and extent of urban land cover control watershed-scale chloride retention. *Science of the Total Environment*, *652*, 278-288.

Paerl, H. W. (1999). Cultural eutrophication of shallow coastal waters: Coupling changing anthropogenic nutrient inputs to regional management approaches. *Limnologica*, *29*, 249-254.

Palla, A., Gnecco, I., & Lanza, L. G. (2010). Hydrologic restoration in the urban environment using green roofs. *Water*, *2*, 140-154.

Parinet, B., Lhote, A., & Legube, B. (2004). Principal component analysis: An appropriate tool for water quality evaluation and management - Application to a tropical lake system. *Ecological Modelling*, *178*, 295-311.

Parker, D. M., & Tatum, T. C. (2021). Is the Use of Road Salt and Chemical Deicers Worth the Costs? A Call for Environmentally Sustainable Winter Road Operations. *Journal of Strategic Innovation & Sustainability*, *16*, 139-144.

Parsons, C. T., Rezanezhad, F., O'Connell, D. W., & Van Cappellen, P. (2017). Sediment phosphorus speciation and mobility under dynamic redox conditions. *Biogeosciences*, *14*, 3585-3602.

Pastor, J., & Hernández, A. J. (2012). Heavy metals, salts and organic residues in old solid urban waste landfills and surface waters in their discharge areas: Determinants for restoring their impact. *Journal of Environmental Management*, *95*, S42-S49.

Patterson T., R., Dalby, A., Kumar, A., Henderson, L. A., & Boudreau, E. (2002). Arcellaceans (thecamoebians) as indicators of land-use change: settlement history of the Swan Lake area, Ontario as a case study. *Journal of Paleolimnology 28*, 297-316.

Paul, M. J., & Meyer, J. L. (2001). Streams in the urban landscape. *Annual Review of Ecology and Systematics*, *32*, 333-365.

Paus, K. H., & BrasKerud, B. C. (2014). Suggestions for designing and constructing bioretention cells for a nordic climate. *Journal of Water Management and Research*, *3*, 139-150.

Pedretti, D., Barahona-Palomo, M., Bolster, D., Fernàndez-Garcia, D., Sanchez-Vila, X., & Tartakovsky, D. M. (2012). Probabilistic analysis of maintenance and operation of artificial recharge ponds. *Advances in Water Resources*, *36*, 23-35.

Penn, M. R., Auer, M. T., Doerr, S. M., Driscoll, C. T., Brooks, C. M., & Effler, S. W. (2000). Seasonality in phosphorus release rates from the sediments of a hypereutrophic lake

under a matrix of pH and redox conditions. *Canadian Journal of Fisheries and Aquatic Sciences*, *57*, 1033-1041.

Perera, N., Gharabaghi, B., & Howard, K. (2013). Groundwater chloride response in the Highland Creek watershed due to road salt application: A re-assessment after 20 years. *Journal of Hydrology*, *479*, 159-168.

Perry, S., Garbon, J., & Lee, B. (2009). Urban Stormwater Runoff Phosphorus Loading and BMP Treatment Capabilities. *Imbrium Systems*, *1*, 1-13.

Petrone, K. C. (2010). Catchment export of carbon, nitrogen, and phosphorus across an agro-urban land use gradient, Swan-Canning River system, southwestern Australia. *Journal of Geophysical Research: Biogeosciences*, *115*, G1.

Pham, H. V., Sperotto, A., Torresan, S., Acuña, V., Jorda-Capdevila, D., Rianna, G., Critto, A. (2019). Coupling scenarios of climate and land-use change with assessments of potential ecosystem services at the river basin scale. *Ecosystem Services*, *40*, 101045.

Pickett, S. T. A., Cadenasso, M. L., Grove, J. M., Boone, C. G., Groffman, P. M., Irwin, E., Warren, P. (2011). Urban ecological systems: Scientific foundations and a decade of progress. *Journal of Environmental Management, 92*, 331-362.

Piper, A. M. (1944). A graphic procedure in the geochemical interpretation of water-analyses. *Eos, Transactions American Geophysical Union*, *25,* 914-928.

Prabhukumar, G., Bhupal, G. S., & Pagilla, K. R. (2015). Laboratory evaluation of sorptive filtration media mixtures for targeted pollutant removals from simulated stormwater. *Water Environment Research*, *87*, 789-795.

Pringle, C. M. (2001). Hydrologic connectivity and the management of biological reserves: a global perspective. *Ecological* Applica*tions, 11,* 981-998.

Quinlan, R., Filazzola, A., Mahdiyan, O., Shuvo, A., Blagrave, K., Ewins, C., Sharma, S. (2021). Relationships of total phosphorus and chlorophyll in lakes worldwide. *Limnology and Oceanography*, *66*, 392-404.

Quiquampoix, H., & Mousain, D. (2005). Enzymatic hydrolysis of organic phosphorus. In *Organic phosphorus in the environment*, *1*, 89-112.

Radosavljevic, J., Slowinski, S., Shafii, M., Akbarzadeh, Z., Rezanezhad, F., Parsons, C. T., Withers W., and Van Cappellen, P. (2022). Salinization as a driver of eutrophication symptoms in an urban lake (Lake Wilcox, Ontario, Canada). *Science of The Total Environment*, *846*, 157336.

Rafieifar, S., Pouraram, H., Djazayery, A., Siassi, F., Abdollahi, Z., Dorosty, A. R., Farzadfar, F. (2016). Strategies and opportunities ahead to reduce salt intake. *Archives of Iranian Medicine*, *19*, 729-734.

Rahimi, L., Deidda, C., & De Michele, C. (2021). Origin and variability of statistical dependencies between peak, volume, and duration of rainfall-driven flood events. *Scientific Reports*, *11*, 5182.

Ramakrishna, D. M., & Viraraghavan, T. (2005). Environmental impact of chemical deicers–a review. *Water, Air, and Soil Pollution*, *166*, 49-63.

Raven, P. H., & Wagner, D. L. (2021). Agricultural intensification and climate change are rapidly decreasing insect biodiversity. *Proceedings of the National Academy of Sciences*, *118*, e2002548117.

Raven, J. A., Gobler, C. J., & Hansen, P. J. (2020). Dynamic CO2 and pH levels in coastal, estuarine, and inland waters: Theoretical and observed effects on harmful algal blooms. *Harmful Algae*, *91*, 101594.

Read, J. S., Hamilton, D. P., Jones, I. D., Muraoka, K., Winslow, L. A., Kroiss, R., Gaiser, E. (2011). Derivation of lake mixing and stratification indices from high-resolution lake buoy data. *Environmental Modelling & Software*, *26,* 1325-1336.

Reynolds, C. S., & Descy, J.-P. (1996). The production, biomass and structure of phytoplankton in large rivers. *River Systems*, *10*, 161-187.

Rhodes, A. L., & Guswa, A. J. (2016). Storage and release of road-salt contamination from a calcareous lake-basin fen, western Massachusetts, USA. *Science of the Total Environment*, *545*, 525-545.

Rhodes, J., Hetzenauer, H., Frassl, M. A., Rothhaupt, K.-O., & Rinke, K. (2017). Long-term development of hypolimnetic oxygen depletion rates in the large Lake Constance. *Ambio*, *46*, 554-565.

Richardson, C. P., & Tripp, G. A. (2006). Investigation of boundary shear stress and pollutant detachment from impervious surface during simulated urban storm runoff. *Journal of Environmental Engineering*, *132*, 85-92.

Riley, E. T., & Prepas, E. E. (1984). Role of internal phosphorus loading in two shallow, productive lakes in Alberta, Canada. *Canadian Journal of Fisheries and Aquatic Sciences*, *41*, 845-855.

Robertson, D. M., & Imberger, J. (1994). Lake number, a quantitative indicator of mixing used to estimate changes in dissolved oxygen. *Internationale Revue Der Gesamten Hydrobiologie Und Hydrographie*, *79*, 159-176.

Robertson, D. M., Siebers, B. J., Diebel, M. W., & Somor, A. J. (2018). *Water-quality response to changes in phosphorus loading of the Winnebago Pool Lakes, Wisconsin, with special emphasis on the effects of internal loading in a chain of shallow lakes*. US Geological Survey.

Robinson, H. K., & Hasenmueller, E. A. (2017). Transport of road salt contamination in karst aquifers and soils over multiple timescales. *Science of the Total Environment*, *603*, 94-108.

Robinson, M. B., & Clark, M. J. (2000). *A History of the Community from 1930 to 1999.* Town of Richmond Hill: Richmond Hill Public Library Board.

Rodgers, P., & Salisbury, D. (1981). Water Quality Modeling of Lake Michigan and Consideration of the Anomalous Ice Cover of 1976–1977. *Journal of Great Lakes Research*, *7*, 467-480.

Rose, S. (2012). Comparative major ion geochemistry of Piedmont streams in the Atlanta, Georgia region: possible effects of urbanization. *Environmental Geology*, *42*, 102-113.

Rosenzweig, B. R., Smith, J. A., Baeck, M. L., & Jaffé, P. R. (2011). Monitoring nitrogen loading and retention in an urban stormwater detention pond. *Journal of Environmental Quality*, *40*(2), 598–609.

Rosfjord, C. H., Webster, K. E., Kahl, J. S., Norton, S. A., Fernandez, I. J., & Herlihy, A. T. (2007). Anthropogenically driven changes in chloride complicate interpretation of base cation trends in lakes recovering from acidic deposition. *Environmental Science and Technology*, *41*, 7688-7693.

Routh, J., Choudhary, P., Meyers, P. A., & Kumar, B. (2009). A sediment record of recent nutrient loading and trophic state change in Lake Norrviken, Sweden. *Journal of Paleolimnology*, *42*, 325-341.

Roychoudhury, A. N., Kostka, J. E., & Van Cappellen, P. (2003). Pyritization: a palaeoenvironmental and redox proxy reevaluated. *Estuarine, Coastal and Shelf Science*, *57*, 1183-1193.

Ruttenberg, K. C. (2003). The global phosphorus cycle. *Treatise on Geochemistry*, *8*, 585-643.

Ruttenberg, K. C., Ogawa, N. O., Tamburini, F., Briggs, R. A., Colasacco, N. D., & Joyce, E. (2009). Improved, high-throughput approach for phosphorus speciation in natural sediments via the SEDEX sequential extraction method. *Limnology and Oceanography: Methods*, *7*, 319-333.

Ruttenberg, K. C. (1992). Development of a sequential extraction method for different forms of phosphorus in marine sediments. *Limnology and Oceanography*, *37*, 1460-1482.

Sahoo, G. B., Forrest, A. L., Schladow, S. G., Reuter, J. E., Coats, R., & Dettinger, M. (2015). Climate change impacts on lake thermal dynamics and ecosystem vulnerabilities. *Limnology and Oceanography*, *61*, 496-507.

Sahoo, T. K., Banka, H., & Negi, A. (2020). Novel approaches to one-directional two-dimensional principal component analysis in hybrid pattern framework. *Neural Computing and Applications*, *32*, 4897-4918.

Saulnier-Talbot, É., Gregory-Eaves, I., Simpson, K. G., Efitre, J., Nowlan, T. E., Taranu, Z. E., & Chapman, L. J. (2014). Small changes in climate can profoundly alter the dynamics and ecosystem services of tropical crater lakes. *PloS One*, *9*, 4897-4918.

Schindler, D. W. (1971). Carbon, nitrogen, and phosphorus and the eutrophication of freshwater lakes 1. *Journal of Phycology*, *7*, 321-329.

Schindler, D. E., Kitchell, J. F., He, X., Carpenter, S. R., Hodgson, J. R., & Cottingham, K. L. (1993). Food web structure and phosphorus cycling in lakes. *Transactions of the American Fisheries Society*, *122*, 756-772.

Schindler, D. W. (1977). Evolution of phosphorus limitation in lakes: natural mechanisms compensate for deficiencies of nitrogen and carbon in eutrophied lakes. *Science*, *195*, 260-262.

Schindler, D. W., Carpenter, S. R., Chapra, S. C., Hecky, R. E., & Orihel, D. M. (2016). Reducing phosphorus to curb lake eutrophication is a success. *Environmental Science & Technology*, *50*, 8923-8929.

Schmidt, W. (1928). Über Die Temperatur-Und Stabili-Tätsverhältnisse Von Seen. *Geografiska Annaler*, *10*, 145-177.

Schroer, W. F., Benitez-Nelson, C. R., Smith, E. M., & Ziolkowski, L. A. (2018). Drivers of sediment accumulation and nutrient burial in coastal stormwater detention ponds, South Carolina, USA. *Ecosystems*, *21*, 1118-1138.

Schwefel, R., Gaudard, A., Wüest, A., & Bouffard, D. (2016). Effects of climate change on deepwater oxygen and winter mixing in a deep lake (L ake G eneva): Comparing observational findings and modeling. *Water Resources Research*, *52*, 8811-8826.

Scott, W. C., Haddad, S. P., Saari, G. N., Chambliss, C. K., Conkle, J. L., Matson, C. W., & Brooks, B. W. (2019). Influence of salinity and pH on bioconcentration of ionizable pharmaceuticals by the gulf killifish, Fundulus grandis. *Chemosphere*, *229*, 434-442.

Seilheimer, T. S., Wei, A., Chow-Fraser, P., & Eyles, N. (2007). Impact of urbanization on the water quality, fish habitat, and fish community of a Lake Ontario marsh, Frenchman's Bay. *Urban Ecosystems*, *10*, 299-319.

Şen, Z. (2017). Hydrological trend analysis with innovative and over-whitening procedures. *Hydrological Sciences Journal*, *62*, 294-305.

Şen, Z. (2014). Trend Identification Simulation and Application. *Journal of Hydrologic Engineering*, *19*, 635-642.

Shambaugh, A. (2008). Environmental Implications of Increasing Chloride Levels in Lake Champlain and Other Basin Waters. *Prepared for the Lake Champlain Basin Program*, *1*, 5-24.

Sharma, A. K., Vezzaro, L., Birch, H., Arnbjerg-Nielsen, K., & Mikkelsen, P. S. (2016). Effect of climate change on stormwater runoff characteristics and treatment efficiencies of stormwater retention ponds: a case study from Denmark using TSS and Cu as indicator pollutants. *Springer Plus*, *5*, 1-12.

Sharpley, A. N., Kleinman, P. J. A., Flaten, D. N., & Buda, A. R. (2011). Critical source area management of agricultural phosphorus: experiences, challenges and opportunities. *Water Science and Technology*, *64*, 945-952.

Sharpley, A., Foy, B., & Withers, P. (2000). Practical and innovative measures for the control of agricultural phosphorus losses to water: an overview. *Journal of Environmental Quality*, *29*, 1-9.

Shrestha, S., Fang, X., & Li, J. (2013). Mapping the 95 th Percentile Daily Rainfall in the Contiguous U.S. *World Env. and Water Resources Congress 2013: Showcasting the Future*, *1,* 219-229.

Shuster, W. D., Bonta, J., Thurston, H., Warnemuende, E., & Smith, D. R. (2005). Impacts of impervious surface on watershed hydrology: A review. *Urban Water Journal*, *2*, 263-275.

Sibert, R. J., Koretsky, C. M., & Wyman, D. A. (2015). Cultural meromixis: Effects of road salt on the chemical stratification of an urban kettle lake. *Chemical Geology*, *395*, 126-137.

Silliman, J. E., Meyers, P. A., & Bourbonniere, R. A. (1996). Record of postglacial organic matter delivery and burial in sediments of Lake Ontario. *Organic Geochemistry*, *24*, 463-472.

Singh, A. (2018). Salinization of agricultural lands due to poor drainage: A viewpoint. *Ecological Indicators*, *95*, 127-130.

Slomp, C. P., & Van Cappellen, P. (2007). The global marine phosphorus cycle: sensitivity to oceanic circulation. *Biogeosciences*, *4*, 155-171.

Smith, P. G. R. (2015). Long-term temporal trends in agri-environment and agricultural land use in Ontario, Canada: transformation, transition and significance. *Journal of Geography and Geology*, *7*, 32-55.

Smith, V. H., Tilman, G. D., & Nekola, J. C. (1999). Eutrophication: impacts of excess nutrient inputs on freshwater, marine, and terrestrial ecosystems. *Environmental Pollution*, *100*, 179-196.

Snodgrass, J. W., Casey, R. E., Joseph, D., & Simon, J. A. (2008). Microcosm investigations of stormwater pond sediment toxicity to embryonic and larval amphibians: variation in sensitivity among species. *Environmental Pollution*, *154*, 291-297.

Snodgrass, J. W., Moore, J., Lev, S. M., Casey, R. E., Ownby, D. R., Flora, R. F., & Izzo, G. (2017). Influence of modern stormwater management practices on transport of road salt to surface waters. *Environmental Science & Technology*, *51*, 4165-4172.

Sobek, S., Durisch-Kaiser, E., Zurbrügg, R., Wongfun, N., Wessels, M., Pasche, N., & Wehrli, B. (2009). Organic carbon burial efficiency in lake sediments controlled by oxygen exposure time and sediment source. *Limnology and Oceanography*, *54*, 2243-2254.

Søndergaard, M., Jensen, J. P., & Jeppesen, E. (2003). Role of sediment and internal loading of phosphorus in shallow lakes. *Hydrobiologia*, *506*, 135-145.

Song, K., Winters, C., Xenopoulos, M. A., Marsalek, J., & Frost, P. C. (2017). Phosphorus cycling in urban aquatic ecosystems: connecting biological processes and water chemistry to sediment P fractions in urban stormwater management ponds. *Biogeochemistry*, *132*, 203-212.

Song, K., Xenopoulos, M. A., Marsalek, J., & Frost, P. C. (2015). The fingerprints of urban nutrients: dynamics of phosphorus speciation in water flowing through developed landscapes. *Biogeochemistry, 125*, 1-10.

Sonzogni, W. C., Richardson, W., Rodgers, P., & Monteith, T. J. (1983). Chloride pollution of the Great Lakes. *Water Pollution Control Federation, 1, 513*-521.

Soranno, P. A., Carpenter, S. R., & Lathrop, R. C. (1997). Internal phosphorus loading in Lake Mendota: response to external loads and weather. *Canadian Journal of Fisheries and Aquatic Sciences*, *54*, 1883-1893.

Soranno, P. A., Hubler, S. L., Carpenter, S. R., & Lathrop, R. C. (1996). Phosphorus loads to surface waters: a simple model to account for spatial pattern of land use. *Ecological Applications*, *6*, 865-878.

Sorichetti, R. J., Raby, M., Holeton, C., Benoit, N., Carson, L., DeSellas, A., … Kaltenecker, G. (2022). Chloride trends in Ontario's surface and groundwaters. *Journal of Great Lakes Research*, *48*, 512-525.

Sparacino, H., Stepenuck, K. F., Gould, R. K., & Hurley, S. E. (2022). Review of reduced salt, snow, and ice management practices for commercial businesses. *Transportation Research Record*, *2676*, 507-520.

Spigel, R. H., & Imberger, J. (1980). The classification of mixed-layer dynamics of lakes of small to medium size. *Journal of Physical Oceanography*, *10*, 1104-1121.

Stammler, K. L., Taylor, W. D., & Mohamed, M. N. (2017). Long-term decline in stream total phosphorus concentrations: A pervasive pattern in all watershed types in Ontario. *Journal of Great Lakes Research*, *43*, 930-937.

Stocker, T. (2014). Climate change 2013: the physical science basis: Working Group I contribution to the Fifth assessment report of the Intergovernmental Panel on Climate Change. *Cambridge University Press*.

Stone, M., & Marsalek, J. (2011). Adoption of best practices for the environmental management of road salt in Ontario. *Water Quality Research Journal of Canada*, *46*, 174-182.

Straile, D., Jöhnk, K., & Henno, R. (2003). Complex effects of winter warming on the physicochemical characteristics of a deep lake. *Limnology and Oceanography*, *48*, 1432-1438.

Sun, H., Huffine, M., Husch, J., & Sinpatanasakul, L. (2012). Na/Cl molar ratio changes during a salting cycle and its application to the estimation of sodium retention in salted watersheds. *Journal of Contaminant Hydrology*, *136*, 96–105.

Sutherland, J. W., Norton, S. A., Short, J. W., & Navitsky, C. (2018). Modeling salinization and recovery of road salt-impacted lakes in temperate regions based on long-term monitoring of Lake George, New York (USA) and its drainage basin. *Science of the Total Environment, 637*, 282-294.

Syers, J. K., Harris, R. F., & Armstrong, D. E. (1973). Phosphate chemistry in lake sediments. *Journal of Environmental Quality*, *2*, 1-14.

Szymczak-Żyła, M., Kowalewska, G., & Louda, J. W. (2011). Chlorophyll-a and derivatives in recent sediments as indicators of productivity and depositional conditions. *Marine Chemistry*, *125*, 39-48.

Tabrizi, S. E., Xiao, K., Thé, J. V. G., Saad, M., Farghaly, H., Yang, S. X., & Gharabaghi, B. (2021). Hourly road pavement surface temperature forecasting using deep learning models. *Journal of Hydrology*, *603*, 126877.

Taguchi, V. J., Olsen, T. A., Natarajan, P., Janke, B. D., Gulliver, J. S., Finlay, J. C., & Stefan, H. G. (2020). Internal loading in stormwater ponds as a phosphorus source to downstream waters. *Limnology and Oceanography Letters*, *5*, 322-330.

Tahvonen, O. (2018). Adapting bioretention construction details to local practices in Finland. *Sustainability*, *10*, 276.

Tao, Y., Yuan, Z., Fengchang, W., & Wei, M. (2013). Six-decade change in water chemistry of large freshwater Lake Taihu, China. *Environmental Science & Technology*, *47*, 9093-9101.

Taranu, Z. E., & Gregory-Eaves, I. (2008). Quantifying relationships among phosphorus, agriculture, and lake depth at an inter-regional scale. *Ecosystems*, *11*, 715-725.

Team, R. C. (2016). R: A language and environment for statistical computing. R Foundation for Statistical Computing, Vienna, Austria.

Tebaldi, C., Hayhoe, K., Arblaster, J. M., & Meehl, G. A. (2006). Going to the extremes: An intercomparison of model-simulated historical and future changes in extreme events. *Climatic Change*, *79*, 185-211.

Telford, J. V, Kay, M. L., Vander Heide, H., Wiklund, J. A., Owca, T. J., Faber, J. A., Hall, R. I. (2021). Building upon open-barrel corer and sectioning systems to foster the continuing legacy of John Glew. *Journal of Paleolimnology*, *65*, 271-277.

Thompson, R., Clark, R. M., & Boulton, G. S. (2012). Core correlation. *Tracking Environmental Change Using Lake Sediments: Data Handling and Numerical Techniques*, *5*, 415-430.

Thorslund, J., & van Vliet, M. T. H. (2020). A global dataset of surface water and groundwater salinity measurements from 1980–2019. *Scientific Data*, *7*, 1-11.

Tiquia, S. M., Davis, D., Hadid, H., Kasparian, S., Ismail, M., Sahly, R., Murray, K. S. (2007). Halophilic and halotolerant bacteria from river waters and shallow groundwater along the rouge river of Southeastern Michigan. *Environmental Technology*, *28*, 297-307.

Tomer, M. D., & Schilling, K. E. (2009). A simple approach to distinguish land-use and climate-change effects on watershed hydrology. *Journal of Hydrology*, *376*, 24-33.

Tong, Y., Wang, M., Peñuelas, J., Liu, X., Paerl, H. W., Elser, J. J., Hu, H. (2020). Improvement in municipal wastewater treatment alters lake nitrogen to phosphorus

ratios in populated regions. *Proceedings of the National Academy of Sciences*, *117*, 11566-11572.

Toronto and Region Conservation Authority (TRCA). (2008). *Humber River watershed plan: pathway to a healthy Humber*.

TRCA. (2018). *Humber River Watershed: Scenario Modelling and Analysis Report*.

Trenouth, W. R., Gharabaghi, B., & Perera, N. (2015). Road salt application planning tool for winter de-icing operations. *Journal of Hydrology*, *524*, 401-410.

Tromboni, F., & Dodds, W. K. (2017). Relationships Between Land Use and Stream Nutrient Concentrations in a Highly Urbanized Tropical Region of Brazil: Thresholds and Riparian Zones. *Environmental Management*, *60*, 30-40.

Tu, L., Jarosch, K. A., Schneider, T., & Grosjean, M. (2019). Phosphorus fractions in sediments and their relevance for historical lake eutrophication in the Ponte Tresa basin (Lake Lugano, Switzerland) since 1959. *Science of the Total Environment*, *685*, 806-817.

Ummenhofer, C. C., & Meehl, G. A. (2017, June 19). Extreme weather and climate events with ecological relevance: A review. *Philosophical Transactions of the Royal Society B: Biological Sciences, 372,* 20160135.

USEPA. (2009). *Technical Guidance on Implementing the Stormwater Runoff Requirements for Federal Projects under Section 438 of the Energy Independence and Security Act*. Washington, D.C.

Utz, R., Bidlack, S., Fisher, B., & Kaushal, S. (2022). Urbanization drives geographically heterogeneous freshwater salinization in the northeastern United States. *Journal of Environmental quality, 51*, 952-965.

Van Cappellen, P., & Berner, R. A. (1988). A mathematical model for the early diagenesis of phosphorus and fluorine in marine sediments; apatite precipitation. *American Journal of Science*, *288*, 289-333.

Van Cappellen, P., & Gaillard, J. F. (2018). Biogeochemical dynamics in aquatic sediments. In *Reactive transport in porous media*, *34*, 335-376.

Van der Molen, D. T., & Boers, P. C. M. (1994). Influence of internal loading on phosphorus concentration in shallow lakes before and after reduction of the external loading. *Nutrient Dynamics and Biological Structure in Shallow Freshwater and Brackish Lakes*, *275*, 379-389.

Van Meter, K. J., McLeod, M. M., Liu, J., Tenkouano, G. T., Hall, R. I., Van Cappellen, P., & Basu, N. B. (2021). Beyond the mass balance: watershed phosphorus legacies

and the evolution of the current water quality policy challenge. *Water Resources Research*, *57*, e2020WR029316.

Van Staden, T. L., Van Meter, K. J., Basu, N. B., Parsons, C. T., Akbarzadeh, Z., & Van Cappellen, P. (2022). Agricultural phosphorus surplus trajectories for Ontario, Canada (1961–2016), and erosional export risk. *Science of The Total Environment*, *818*, 151717.

Verburg, P., Hecky, R. E., & Kling, H. (2003). Ecological consequences of a century of warming in Lake Tanganyika. *Science*, *301*, 505-507.

Verstraeten, G., & Poesen, J. (2000). Estimating trap efficiency of small reservoirs and ponds: methods and implications for the assessment of sediment yield. *Progress in Physical Geography*, *24*, 219-251.

Vincent, L. A., Zhang, X., Mekis, Wan, H., & Bush, E. J. (2018). Changes in Canada's Climate: Trends in Indices Based on Daily Temperature and Precipitation Data. *Atmosphere - Ocean*, *56*, 332-349.

Vollenweider, R. A. (1968). Scientific fundamentals of the eutrophication of lakes and flowing waters, with particular reference to nitrogen and phosphorus as factors in eutrophication. *Paris (France)*, *192*, 14.

Wallace, A. M., & Biastoch, R. G. (2016). Detecting changes in the benthic invertebrate community in response to increasing chloride in streams in Toronto, Canada. *Freshwater Science*, *35*, 353-363.

Walling, D. E., & Webb, B. W. (1985). Estimating the discharge of contaminants to coastal waters by rivers: some cautionary comments. *Marine Pollution Bulletin*, *16*, 488-492.

Walsh, C. J., Fletcher, T. D., & Burns, M. J. (2012). Urban Stormwater Runoff: A New Class of Environmental Flow Problem. *PLoS One*, *7*, e45814.

Walsh, C. J., Roy, A. H., Feminella, J. W., Cottingham, P. D., Groffman, P. M., & Morgan, R. P. (2005). The urban stream syndrome: Current knowledge and the search for a cure. In *Journal of the North American Benthological Society, 24,* 706-723.

Wang, C., Bai, L., & Pei, Y. (2013). Assessing the stability of phosphorus in lake sediments amended with water treatment residuals. *Journal of Environmental Management*, *122*, 31-36.

Wang, H., Appan, A., & Gulliver, J. S. (2003). Modeling of phosphorus dynamics in aquatic sediments: I—model development. *Water Research*, *37*, 3928-3938.

Wang, R., Zhang, Y., Xia, W., Qu, X., Xin, W., Guo, C., Chen, Y. (2018). Effects of aquaculture on lakes in the Central Yangtze River Basin, China, I. water quality. *North American Journal of Aquaculture*, *80*, 322-333.

Wang, Y. S., Lou, Z. P., Sun, C. C., & Sun, S. (2008). Ecological environment changes in Daya Bay, China, from 1982 to 2004. *Marine Pollution Bulletin*, *56*, 1871-1879.

Weisberg, S. (2005). *Applied linear regression* (Vol. 528). New Jersey: John Wiley & Sons.

Wentzel-Viljoen, E., Steyn, K., Lombard, C., De Villiers, A., Charlton, K., Frielinghaus, S., Mungal-Singh, V. (2017). Evaluation of a mass-media campaign to increase the awareness of the need to reduce discretionary salt use in the South African population. *Nutrients*, *9*, 1238.

Whan, K., & Zwiers, F. (2016). Evaluation of extreme rainfall and temperature over North America in CanRCM4 and CRCM5. *Climate Dynamics*, *46*, 3821-3843.

Whan, K., Zwiers, F., & Sillmann, J. (2016). The influence of atmospheric blocking on extreme winter minimum temperatures in North America. *Journal of Climate*, *29*, 4361-4381.

Wilkin, R. T., Barnes, H. L., & Brantley, S. L. (1996). The size distribution of framboidal pyrite in modern sediments: an indicator of redox conditions. *Geochimica et Cosmochimica Acta*, *60*, 3897-3912.

Williams, W. D., & Sherwood, J. E. (1994). Definition and measurement of salinity in salt lakes. *International Journal of Salt Lake Research*, *3*, 53-63.

Wold, S., Esbensen, K., & Geladi, P. (1987). Principal Component Analysis. *Chemometrics and Intelligent Laboratory Systems*, *2*, 37-52.

Wollheim, W. M., Pellerin, B. A., Vörösmarty, C. J., & Hopkinson, C. S. (2005). N retention in urbanizing headwater catchments. *Ecosystems*, *8*, 871-884.

Wong, G. K. L., & Jim, C. Y. (2012). Quantitative hydrologic performance of extensive green roof under humid-tropical rainfall regime. *Ecological Engineering*, *70*, 366-378.

Woolway, R. I., Denfeld, B., Tan, Z., Jansen, J., Weyhenmeyer, G. A., & La Fuente, S. (2022). Winter inverse lake stratification under historic and future climate change. *Limnology and Oceanography Letters*, *7*, 302-311.

Woolway, R. I., & Merchant, C. J. (2019). Worldwide alteration of lake mixing regimes in response to climate change. *Nature Geoscience*, *12*, 271-276.

Worsfold, P., McKelvie, I., & Monbet, P. (2016). Determination of phosphorus in natural waters: a historical review. *Analytica Chimica Acta*, *918*, 8-20.

Wyman, D. A., & Koretsky, C. M. (2018). Effects of road salt deicers on an urban groundwater-fed kettle lake. *Applied Geochemistry*, *89*, 265-272.

Xu, H., Paerl, H. W., Qin, B., Zhu, G., & Gaoa, G. (2010). Nitrogen and phosphorus inputs control phytoplankton growth in eutrophic Lake Taihu, China. *Limnology and Oceanography*, *55*, 420-432.

Yang, K., Luo, Y., Chen, K., Yang, Y., Shang, C., Yu, Z., Zhao, Y. (2020). Spatial–temporal variations in urbanization in Kunming and their impact on urban lake water quality. *Land Degradation and Development*, *31,* 1392-1407.

Yang, X. E., Wu, X., Hao, H. L., & He, Z. L. (2008). Mechanisms and assessment of water eutrophication. *Journal of Zhejiang University: Science B*, *9*, 197-209.

Yang, Y. R., & Chang, C. H. (2007). An urban regeneration regime in China: A case study of urban redevelopment in Shanghai's Taipingqiao Area. *Urban Studies*, *44*, 1809-1826.

Yang, Y. Y., & Toor, G. S. (2018). Stormwater runoff driven phosphorus transport in an urban residential catchment: Implications for protecting water quality in urban watersheds. *Scientific Reports*, *8*, 11681.

Yang, Y. Y., & Toor, G. S. (2017). Sources and mechanisms of nitrate and orthophosphate transport in urban stormwater runoff from residential catchments. *Water Research*, *112*, 176-184.

Yang, Y.-Y., Asal, S., & Toor, G. S. (2021). Residential catchments to coastal waters: Forms, fluxes, and mechanisms of phosphorus transport. *Science of The Total Environment*, *765*, 142767.

Yang, Y.-Y., & Lusk, M. G. (2018). Nutrients in urban stormwater runoff: Current state of the science and potential mitigation options. *Current Pollution Reports*, *4*, 112-127.

Yin, H., Kong, M., & Fan, C. (2013). Batch investigations on P immobilization from wastewaters and sediment using natural calcium rich sepiolite as a reactive material. *Water Research*, *47*, 4247-4258.

Zadereev, Y. S., & Tolomeyev, A. P. (2007). The vertical distribution of zooplankton in brackish meromictic lake with deep-water chlorophyll maximum. In *Hydrobiologia*, *576,* 69-82.

Zahmatkesh, Z., Burian, S. J., Karamouz, M., Tavakol-Davani, H., & Goharian, E. (2015). Low-Impact Development Practices to Mitigate Climate Change Effects on Urban

Stormwater Runoff: Case Study of New York City. *Journal of Irrigation and Drainage Engineering*, *141*, 04014043.

Zehetner, F., Rosenfellner, U., Mentler, A., & Gerzabek, M. H. (2009). Distribution of road salt residues, heavy metals and polycyclic aromatic hydrocarbons across a highway-forest interface. *Water, Air, and Soil Pollution*, *198*, 125-132.

Zhang, Q., Xu, C. Y., Zhang, Z., Ren, G., & Chen, Y. D. (2008). Climate change or variability? The case of Yellow river as indicated by extreme maximum and minimum air temperature during 1960-2004. *Theoretical and Applied Climatology*, *93*, 35-43.

Zhang, X., Zwiers, F. W., Yue, S., & Wang, C. (2004). Comment *on Applicability of prewhitening to eliminate the influence of serial correlation on the Mann-Kendall test by Sheng Yue and Chun Yuan Wang. Water Resources Research, 40,* W03806.

Zhang, Y. F., Li, Y. P., Sun, J., & Huang, G. H. (2020). Optimizing water resources allocation and soil salinity control for supporting agricultural and environmental sustainable development in Central Asia. *Science of the Total Environment*, *704*, 135281.

Zhao, S., Da, L., Tang, Z., Fang, H., Song, K., & Fang, J. (2006). Ecological consequences of rapid urbanexpansion: Shanghai, China. *Frontiers in Ecology and the Environment, 4,* 341-346.

Zhou, B., Shafii, M., Parsons, C. T., Passeport, E., Rezanezhad, F., Lisogorsky, A., & Van Cappellen, P. (2023). Modeling multi-year phosphorus dynamics in a bioretention cell: Phosphorus partitioning, accumulation, and export. *Science of The Total Environment*, *876*, 162749.

Zhu, H., Yu, M., Zhu, J., Lu, H., & Cao, R. (2019). Simulation study on effect of permeable pavement on reducing flood risk of urban runoff. *International Journal of Transportation Science and Technology*, *8*, 373-382.

Zhu, Y., Wu, F., Feng, W., Liu, S., & Giesy, J. P. (2016). Interaction of alkaline phosphatase with minerals and sediments: activities, kinetics and hydrolysis of organic phosphorus. *Colloids and Surfaces A: Physicochemical and Engineering Aspects*, *495*, 46-53.

Zou, H., & Xue, L. (2018). A selective overview of sparse principal component analysis. *Proceedings of the IEEE*, *106*, 1311-1320.

Appendix A
Supplementary material: Chapter 2

Data availability

The sediment core depth profile data obtained in this study are openly available on the Federated Research Data Repository (FRDR) website at the following link: https://doi.org/10.20383/ /103.0634.

Summary of geological and pedological characteristics of the area

The bedrock of the LW watershed is comprised of Blue Mountain Formation Shale overlain with primarily glaciofluvial surficial deposits. The LW area is within the Oak Ridges Moraine formation, which is comprised of a ridge of sand and gravel and Halton till that is composed from glaciolacustrine-derived silty to clayey till (TRCA, 2008). The soils in the LW watershed are predominantly sandy loams with some pockets of clay loam, loam, and muck (Government of Canada, 2013) with mainly imperfect drainage.

Text S1

Summary of geological and pedological characteristics of the study site

The bedrock of the Lake Wilcox (LW) watershed is comprised of Blue Mountain Formation Shale overlain primarily by glaciofluvial surficial deposits. The LW area is within the Oak Ridges Moraine formation, which is comprised of a ridge of sand and gravel and Halton till that is composed from glaciolacustrine-derived silty to clayey till (TRCA, 2008). The soils in the LW watershed are predominantly sandy loams with some pockets of clay loam, loam, and muck (Government of Canada, 2013) with mainly imperfect drainage.

Text S2: Supplementary text for Methods section

Calculation of sediment mass accumulation rates

Mass accumulation rates are calculated as described in Appleby et al. (2001) and Aba et al. (2014). The age (t_z) of the sediment layer at depth (z) is calculated as:

$$t_z = \frac{1}{\lambda} \cdot \ln\left(\frac{A_{tot}}{A_z}\right) \quad \text{(A1)}$$

where, A_{tot} is the total cumulative inventory of unsupported ^{210}Pb in the sediment column (Bq m^{-2}), A_z is the inventory of unsupported ^{210}Pb in the sediment column below depth z

(Bq m^{-2}), and λ is the decay constant of ^{210}Pb. Note that here, $t_0 = 0$ corresponds to 2019 when the sediment cores were collected in the lake.

The mass accumulation rate (R_z) (g cm^{-2} y^{-1}) as a function of depth *z* in the dated core is calculated as:

$$R_z = \frac{m_z}{(\pi \cdot r^2) \cdot \Delta t_z} \quad \text{(A2)}$$

where, m_z is the mass of sediment of the core slice centered on depth z (g), *r* is the inner radius of the core tube (cm) and Δt_z is the duration of deposition of the depth interval of the core slice (y). Linear sedimentation rates (cm y^{-1}) as a function of depth are calculated by dividing R_z by the sediment dry bulk density (g cm^{-3}).

X-ray diffraction (XRD)

Powder X-ray diffraction (XRD) analyses were conducted on freeze-dried and ground (<63 µm particle size) sediments using a PANalytical Empyrean XRD II with a Co-X-ray tube (operated at 40 kV and 45 mA) and a PIXcel3D detector. The XRD sample holder was back-loaded with the sample and the XRD pattern of each sample was collected from 10 to 70° 2θ with a step size of 0.026° 2θ. The X-ray beam path was defined using a fixed 1/2° divergent slit, a 1° anti-scatter receiving slit and 15 mm mask on the incident side, and a large beta-filter (iron) and a 7.5 mm anti-scatter slit on the diffraction side. Soller slits (0.04 rad) were fitted to both the incident and diffracted beams. Scans were accumulated for 5 hours to generate a spectrum. The crystalline phases in the solid samples were identified using HighScore Plus software and a combination of the free Crystallography Open Database and the PAN-ICSD Database. Next, the relative abundance of each crystalline phase was estimated with the Rietveld refinement routine built into the HighScore Plus software.

Scanning Electron Microscopy and Energy Dispersive X-Ray Spectroscopy (SEM-EDS)

The surface morphology of the sediment samples was captured with a scanning electron microscope (SEM) (TM3000, Hitachi) with 15 kV accelerating voltage. The freeze-dried and sieved (< 125 µm particle size) samples were mounted on a carbon tape attached to an aluminum SEM stub and images for each sample were collected using the SEM. The

relative elemental composition on the sediment surfaces was quantified using a Bruker Energy Dispersive X-Ray Spectroscopy (EDS) and the QUANTAX 70 software.

Land use/land cover (LULC) classification

The LULC scheme comprised three classes – forested, agricultural, and urban – based on the widely used classification system developed by Anderson et al. (1976) for the interpretation of remote sensing data at different scales and resolutions (for an example, see: Yuan et al., 2005). In the classification system used, “residential, commercial services, industrial, transportation, communications, industrial and commercial, mixed urban or built-up land, other urban or built-up lands” are all folded into the urban LULC class; forested land includes “deciduous forest land, evergreen forest land, mixed forest land, orchards, groves, vineyards, and nurseries”; while “crop fields, pasture, and bare fields” form the agricultural LULC class.

The LULC values for Phases 4 and 3 are those of Radosavljevic et al. (2022) (listed in the references), based on the reports provided by the City of Richmond Hill (Table A1). For Phase 2, we extracted LULC from historical reports (Robinson & Clark, 2000a,b,c). Manually estimated LULC values for Phase 2 from aerial images (Map and Data Library, 2019) agreed with the values obtained from the reports. For Phase 1, we relied on a detailed historical account of the development of early farming around the lake (Stamp, 1991).

Text S3: Supplementary text for Results section

Delineation of the four LULC phases using breakpoint analysis

To delineate the four watershed development phases, we applied a breakpoint analysis to the sediment mass accumulation rate time series using the Davies Test (DT) in the Segmented Package in R (Muggeo, 2008). The Davies test analyzes variations in slope at k equidistant time points in the data series (Davies, 1987). At each time point, the null hypothesis of no change in slope (i.e., no breakpoint) was tested at a significance level of 5%. In cases with no evidence of a slope breakpoint (i.e., failure to disprove the null hypothesis), a linear regression was performed on the log-transformed data. Further, if

there were less than 5 points on either side of a breakpoint, then the breakpoint was removed, and ordinary least squares regression was used.

The dates where breakpoint occurred in the sediment accumulation rate, as determined by the DT, are given in the table below. The column on the right summarizes our final selection of the dates separating the four watershed development phases after considering the ensemble of historical data and information available. The results of the DT breakpoint analysis methods is also shown in Figure A4.

DT-determined breakpoint years	Selected phase breakpoint years
1944	1945
1975	1975
1997	1997
2014	2014

Supplementary figures

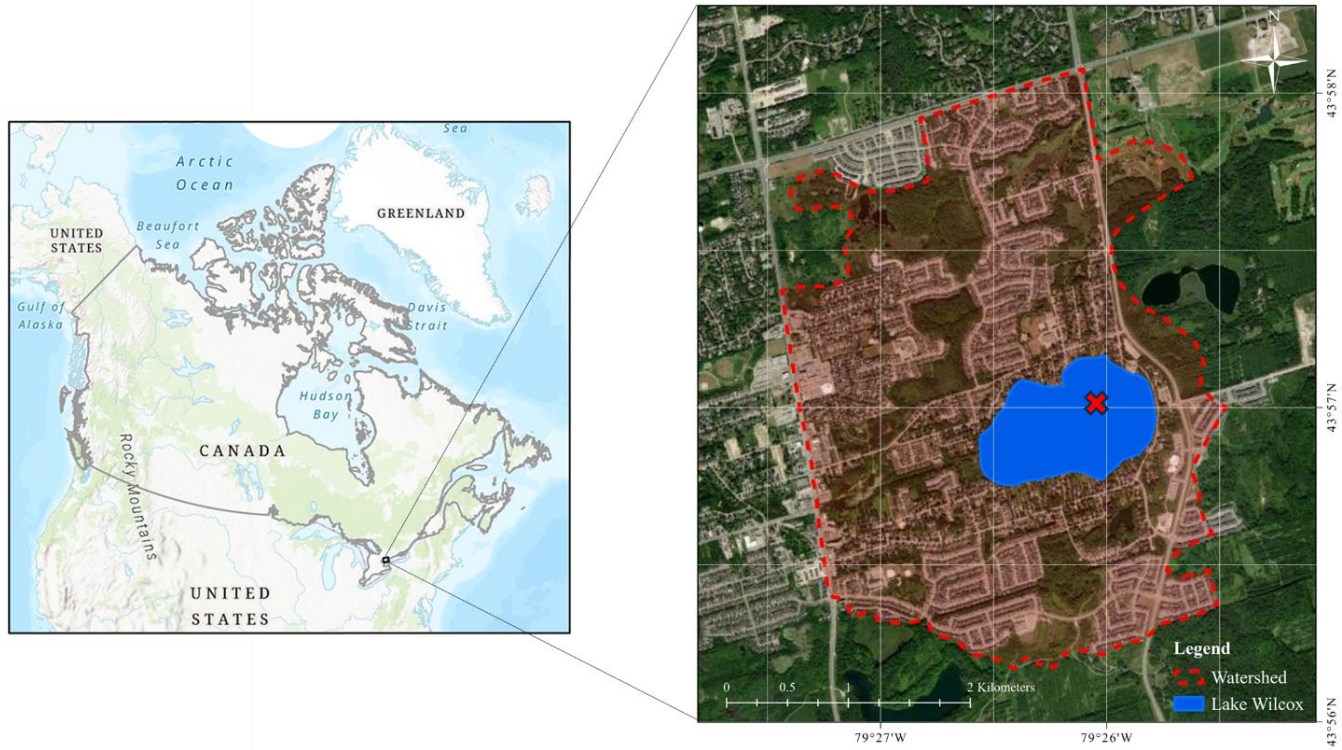

Figure A1. Location of Lake Wilcox in southern Ontario, Canada and the current delineation of the lake's watershed (red dashed line in panel on the right). On the righthand panel, the red "X" symbol indicates the sediment core sampling location.

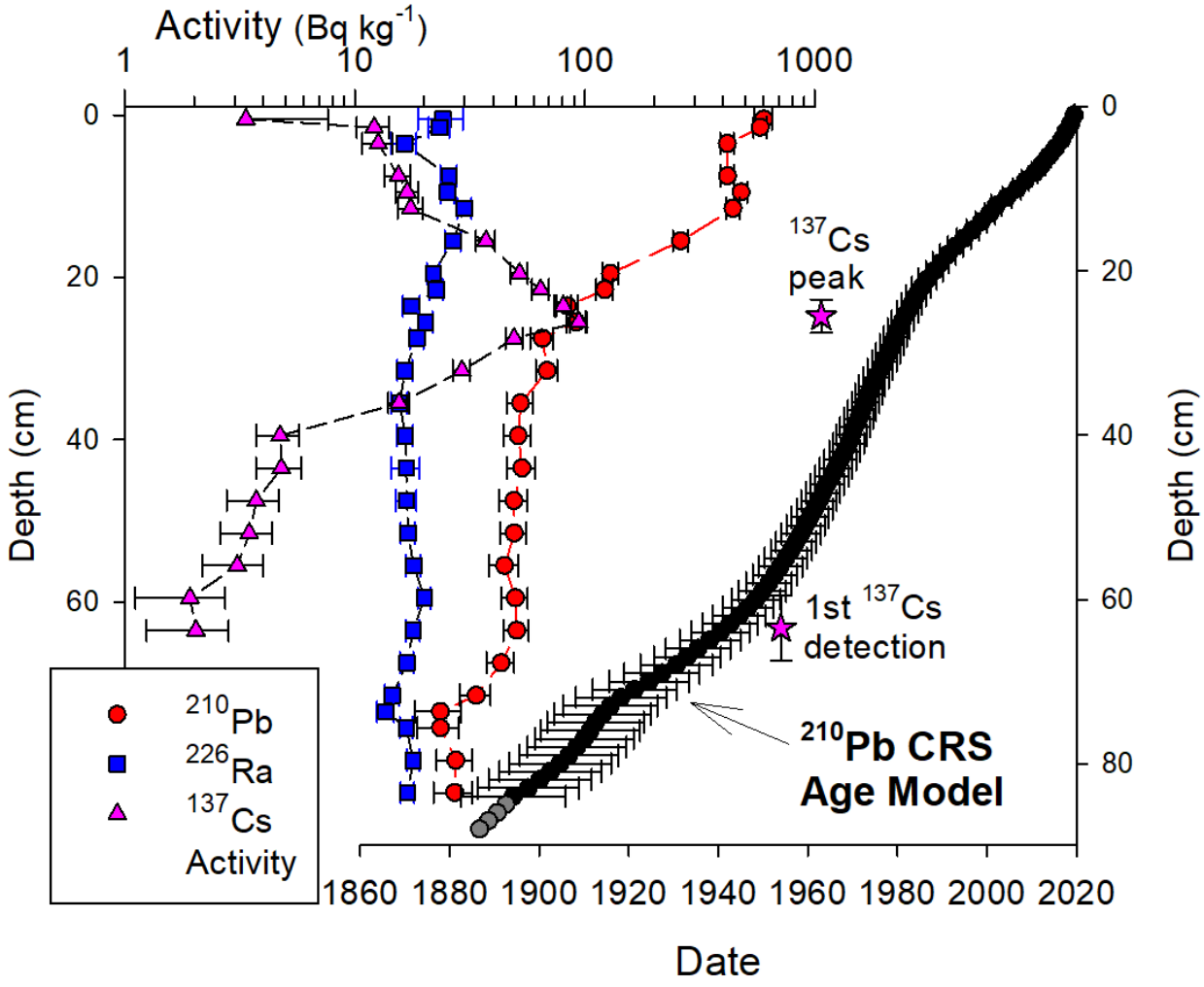

Figure A2. Activities of the radioisotopes ^{210}Pb, ^{226}Ra, and ^{137}Cs (top x-axis), and ^{210}Pb constant rate of supply (CRS) age model-estimated sediment deposition date (bottom x-axis) as a function of depth in sediment core 2.

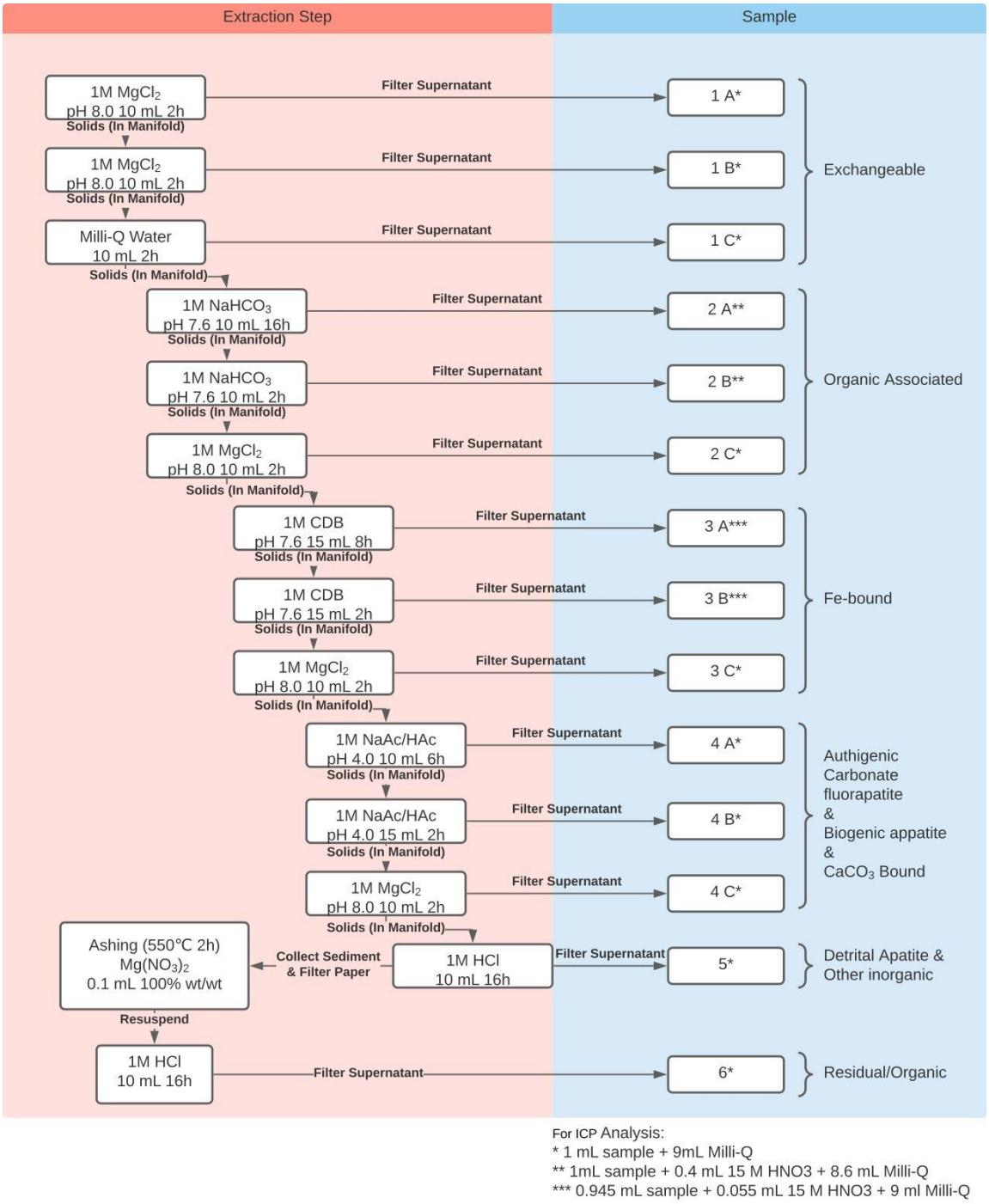

Figure A3. Diagram showing the workflow of the sequential P extraction procedure (SEDEX). (Figure provided by Ariel Lisogorsky.)

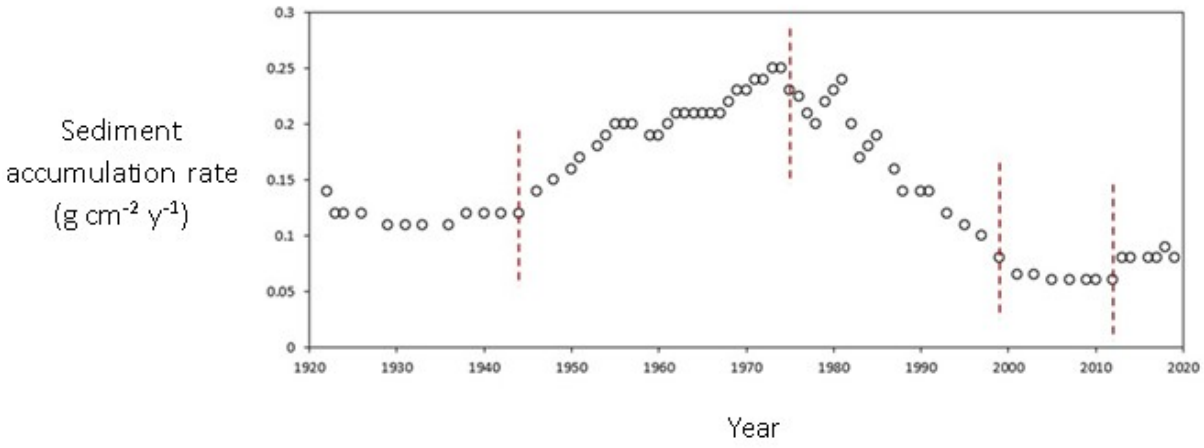

Figure A4. Results of the Davies test (DT) breakpoint analysis of the sediment accumulation rate time series. Vertical red dashed lines represent DT-identified breakpoints in sediment accumulation rate time series.

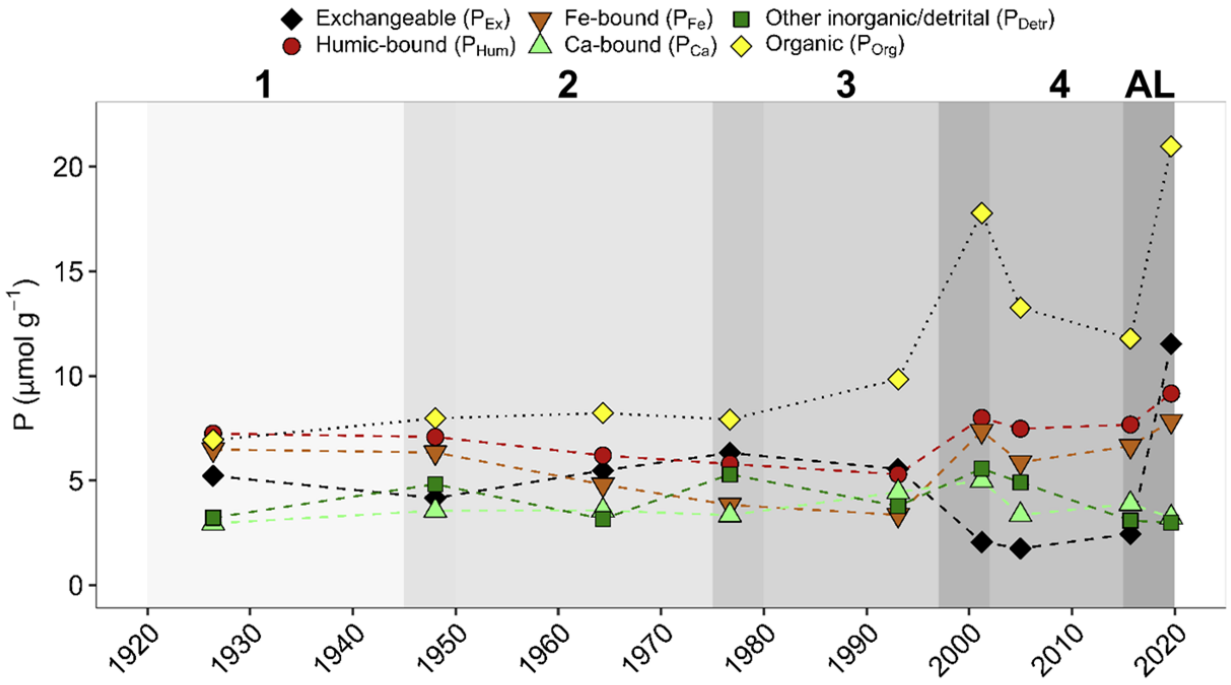

Figure A5. Absolute concentrations of the different sediment P pools determined by sequential chemical extractions versus year of deposition. Numerals 1 to 4 at the top and the corresponding color shadings indicate the four catchment development phases separated by five-year buffer periods between phases; AL stands for the active (or early diagenetic) surface sediment layer.

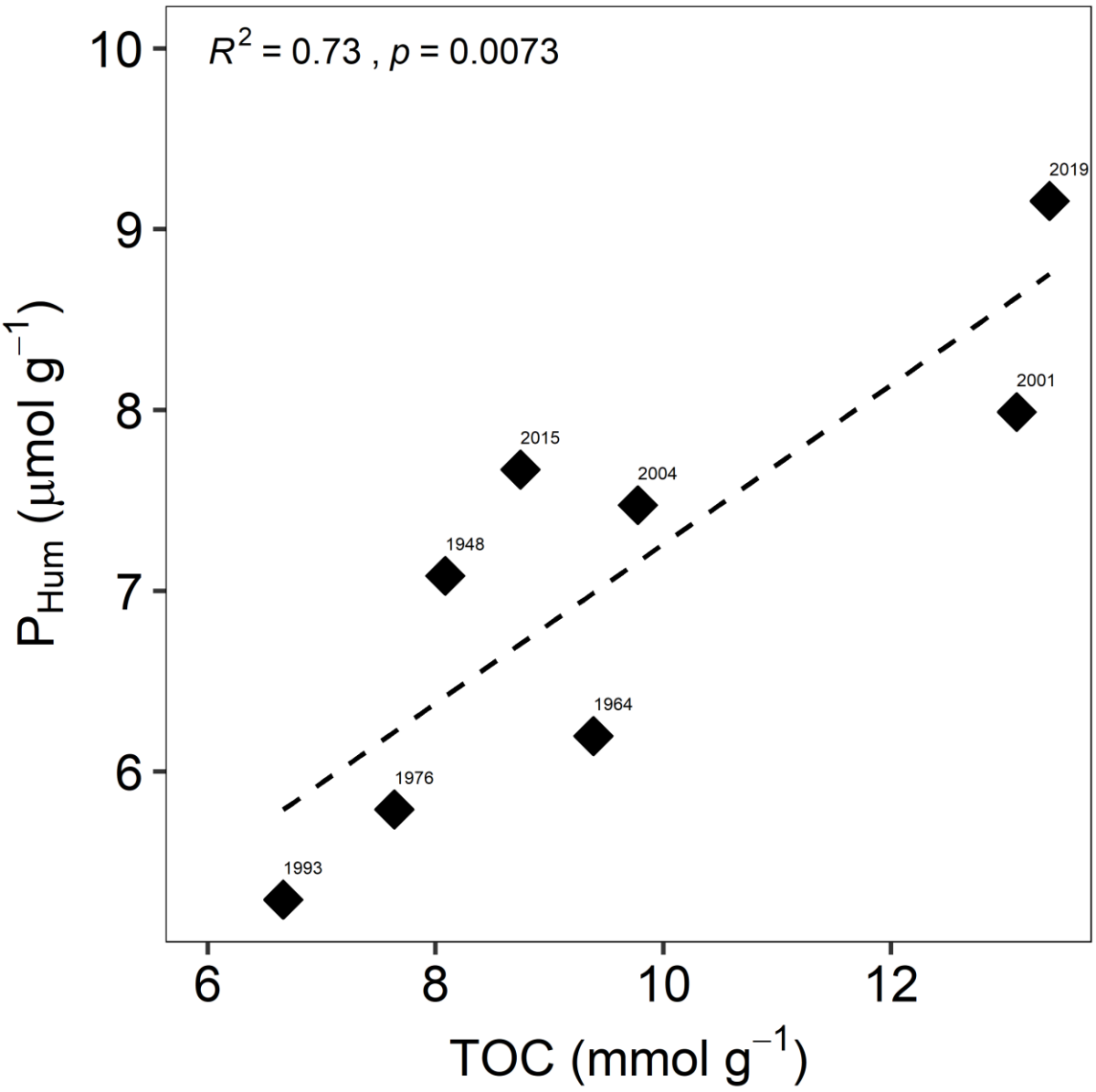

Figure A6. Humic-bound P pool (P_{Hum}) concentration versus TOC concentration. Points are labelled with the year the sediment was deposited (rounded to the closest year).

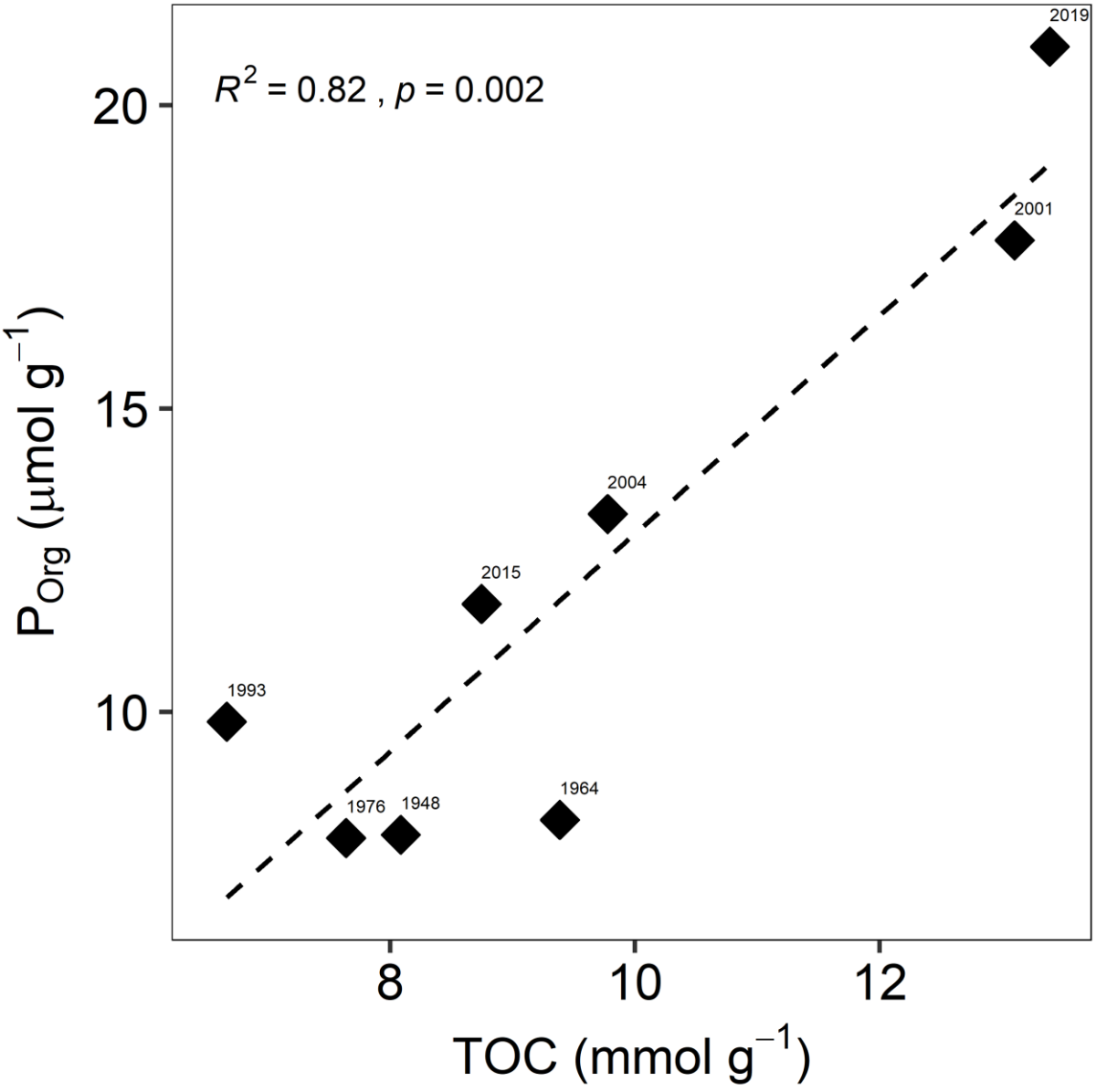

Figure A7. Organic P pool (P_{Org}) concentration versus TOC concentration. Points are labelled with the year the sediment was deposited (rounded to the closest year).

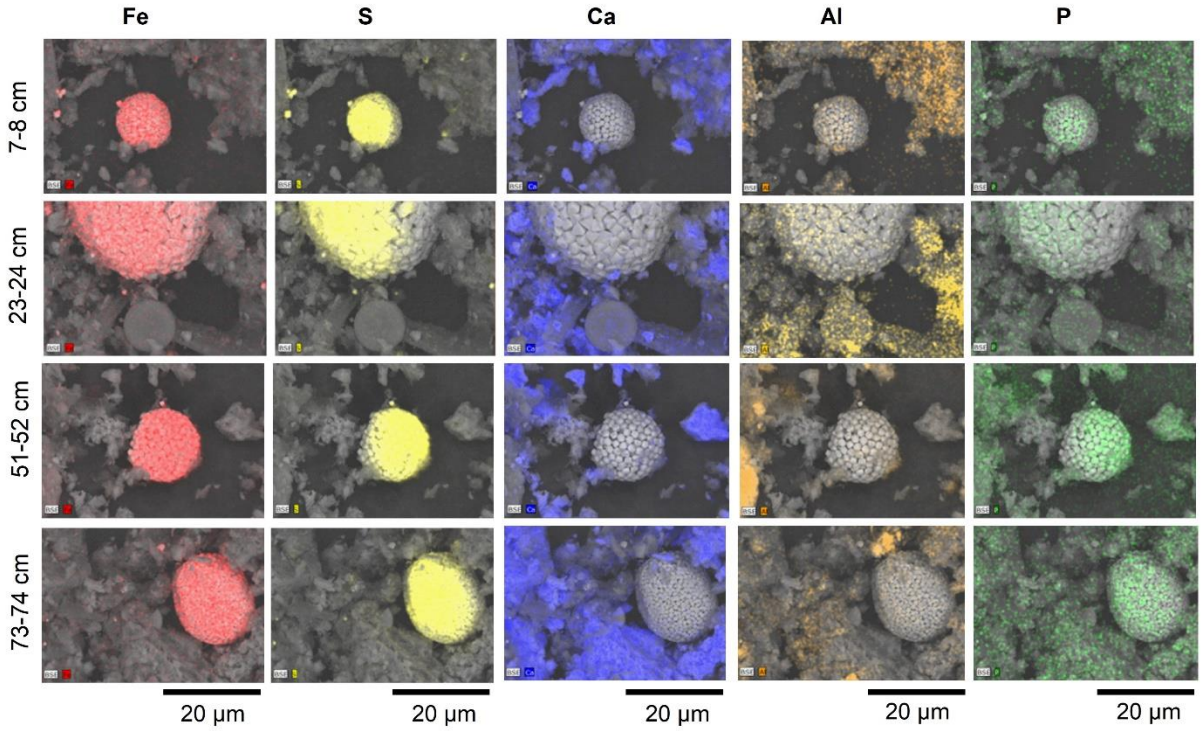

Figure A8. Elemental maps (left to right: Fe, S, Ca, Al, and P) overlain on scanning electron micrographs collected for the sediment core sections corresponding to the depth intervals 7-8 cm, 23-24 cm, 51-52 cm and 73-74 cm (ordered from shallow to deep moving from core top to bottom). The morphology and elemental composition of the large spherical shaped particles are consistent with framboidal pyrite or greigite. These particles were observed in all core sections.

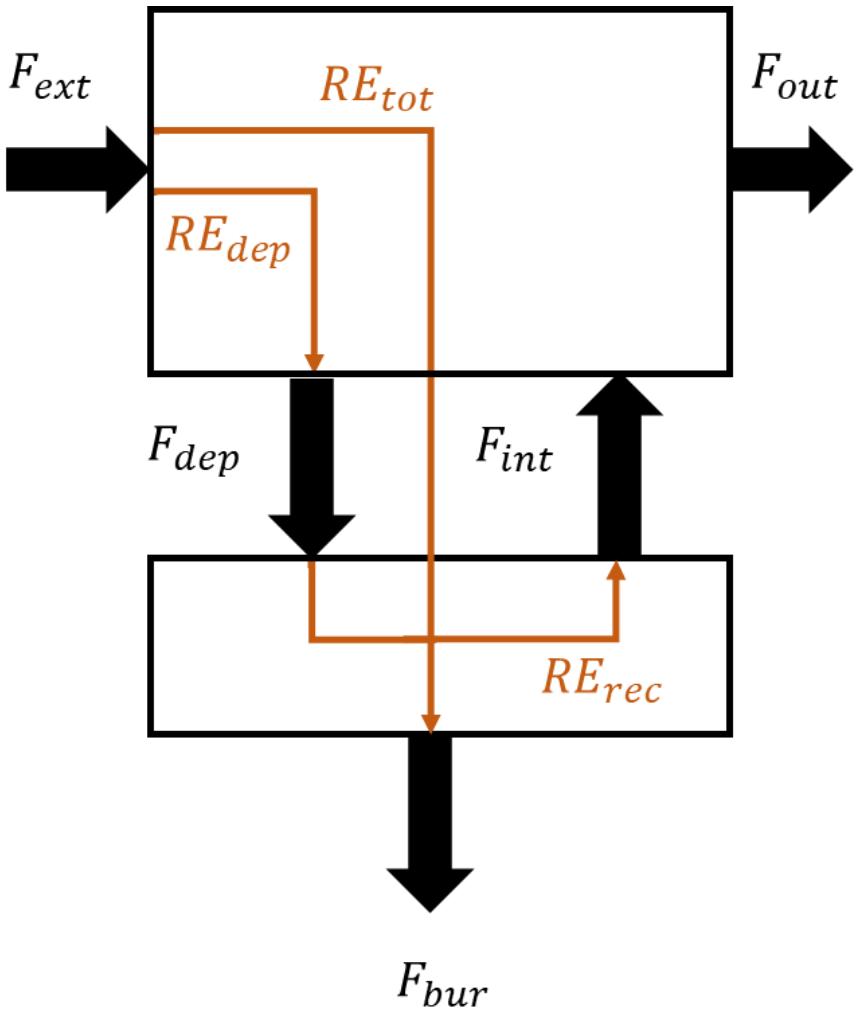

Figure A9. Box model diagram showing the fluxes included in the lake TP budget calculations. Also shown in the lighter color are the efficiency metrics described in the main text (in section 4: Phosphorus budget calculations) and their relationships to the fluxes. F_{ext} is the external loading flux, F_{dep} is the deposition flux, F_{bur} is the burial flux, F_{int} is the internal loading flux, F_{out} is the outflux at the lake outlet, RE_{tot} is the whole-lake TP retention efficiency, RE_{dep} is the efficiency of TP removal from the water column to the sediments (i.e., the deposition efficiency), and RE_{rec} is the sediment TP recycling efficiency.

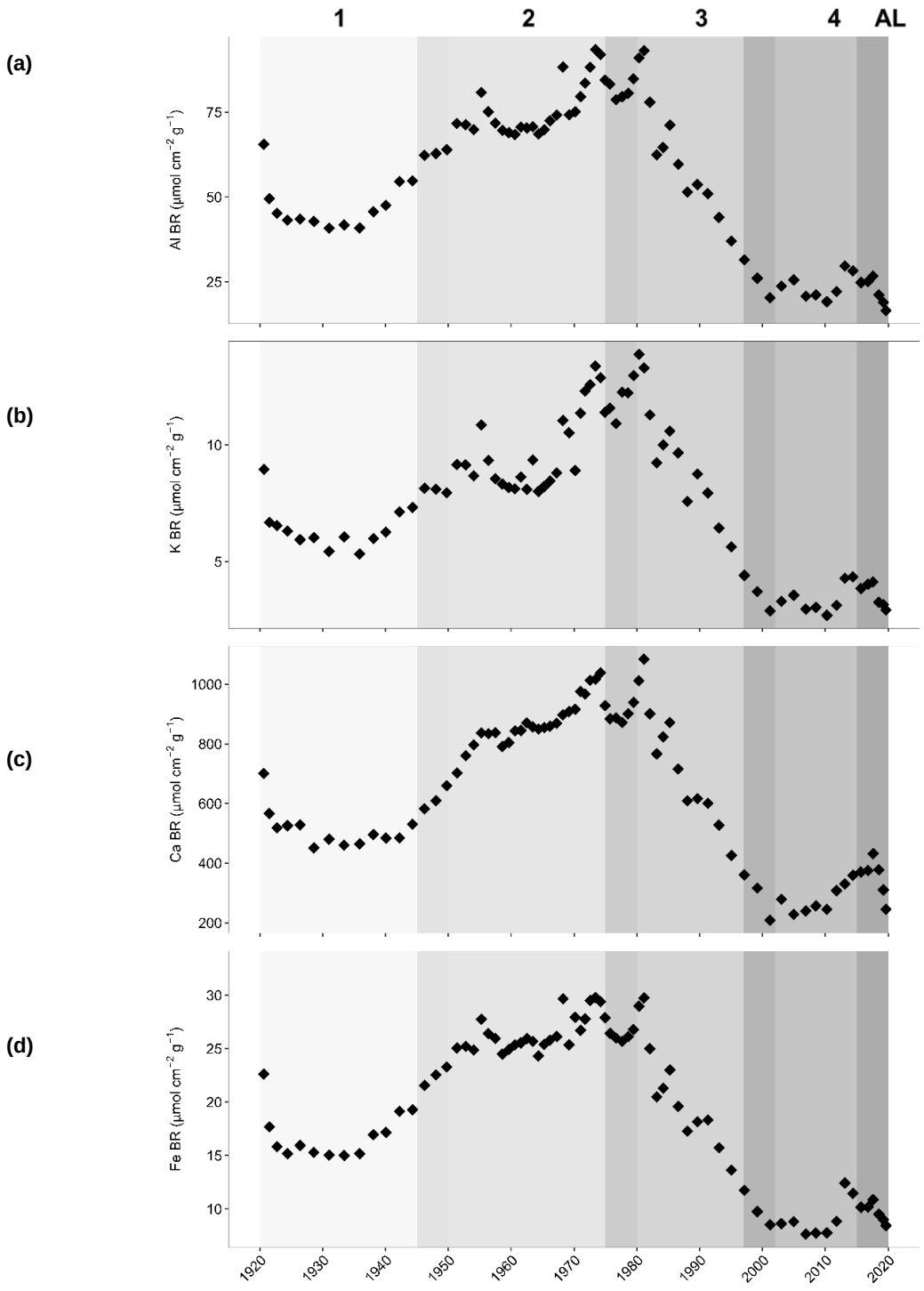

Figure A10. Burial rates (BR) of geogenic elements versus year of deposition: (a) Al, (b) K, (c) Ca, (d) Fe. Numerals 1 to 4 at the top and the corresponding color shadings indicate the four catchment development phases separated by five-year buffer periods between phases; AL stands for the active (or early diagenetic) surface sediment layer.

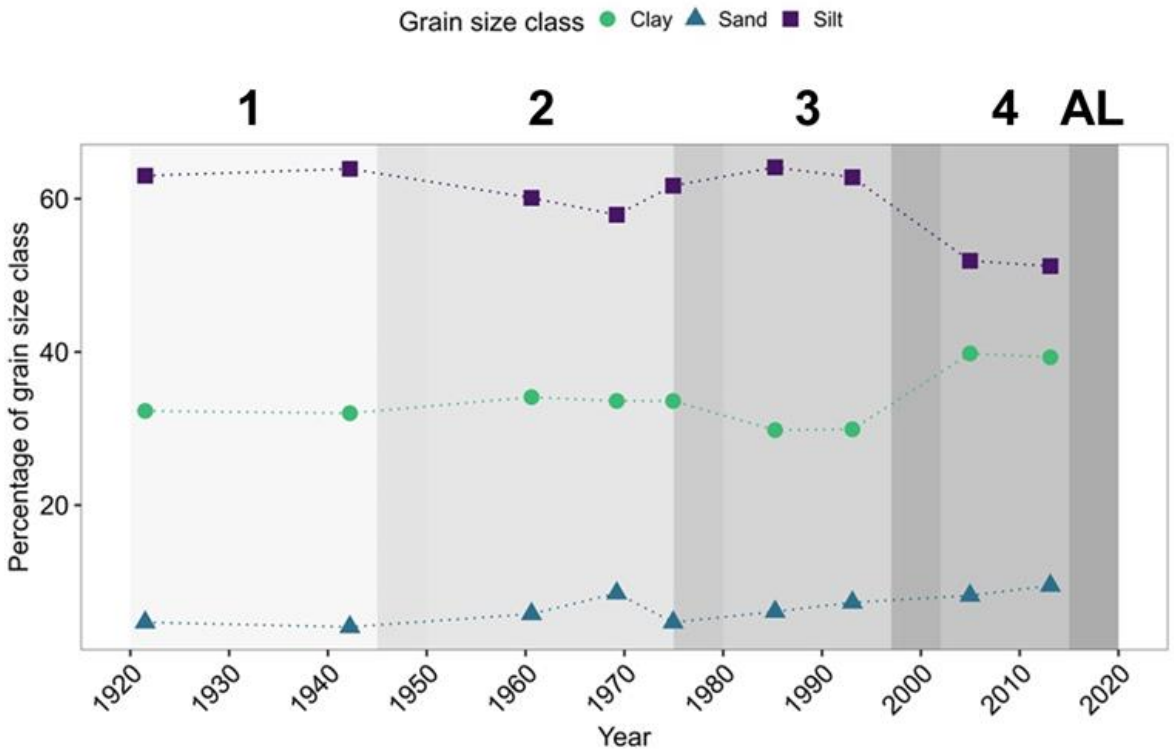

Figure A11. Percentages of clay, silt and sand versus year of deposition. Numerals 1 to 4 at the top and the corresponding color shadings indicate the four catchment development phases separated by five-year buffer periods between phases; AL stands for the active (or early diagenetic) surface sediment layer.

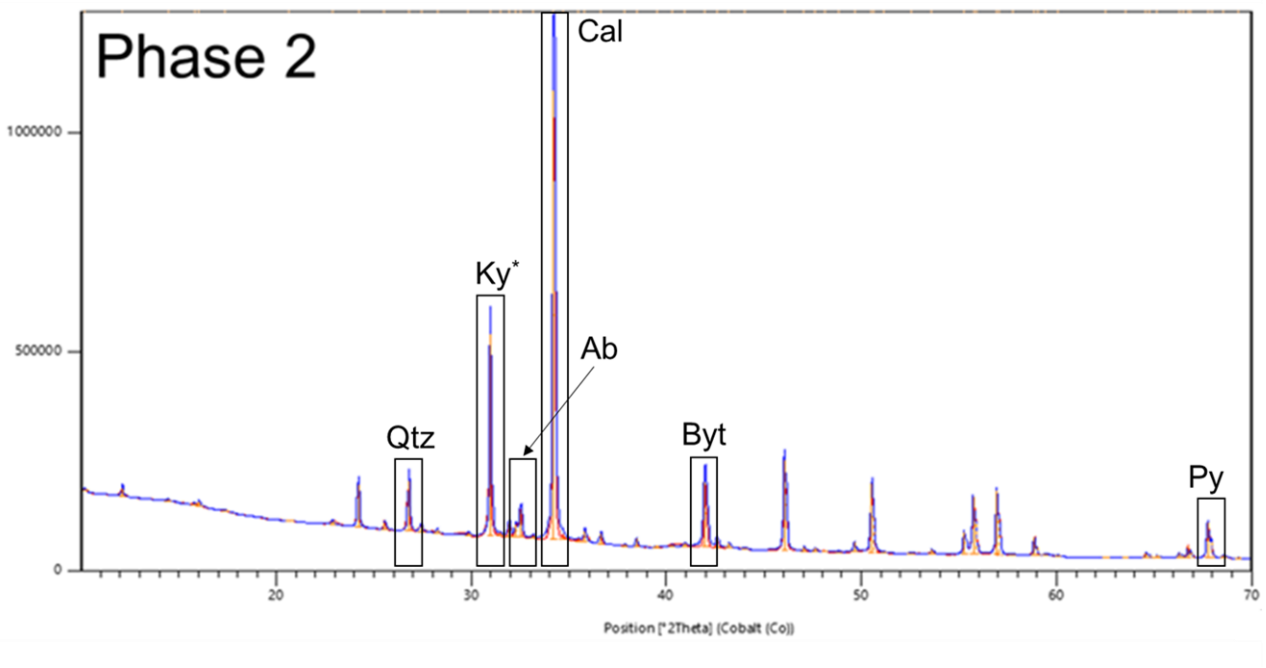

Figure A12. Example of an XRD spectrum for a sediment sample from Phase 2. Main peaks of different minerals were identified. (Qtz – quartz; Ky* - kyanite (* - kyanite XRD pattern, but more likely a plagioclase feldspar mineral); Ab – albite; Cal – calcite; Byt – bytownite; Py – pyrite.

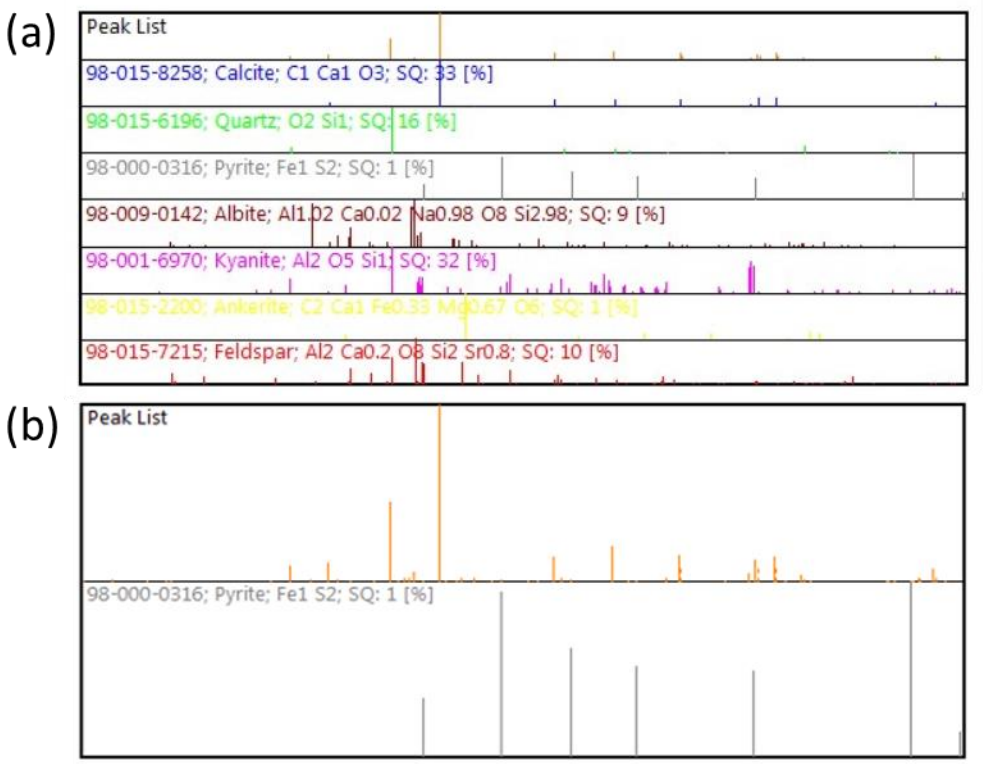

Figure A13. (a) Peak identification for different minerals in Phase 2, and (b) peak identification (upper panel) with reference (bottom panel) for pyrite. Note: score for pyrite identification was 30.

Table A1. Summary list of reports on Lake Wilcox water quality provided by the city of Richmond Hill and referred to in the main text by their corresponding numbers. The reports are available from the authors upon request.

Number of Report & Author(s):	Title:	Year:	Type:
(1) Gore & Storrie	Master drainage/service plan for the Lake Wilcox – Oak Ridge's District	1989	Plan/Report
(2) Gore & Storrie	OPA71 Phase II Environmental Studies.	1993	Technical Appendices
(3) Gore & Storrie	North Lake Road Sanitary Sewer	1994	Report
(4) Lee G. & Freshwater Research	Lake Wilcox Remediation Strategy	1996	Report
(5) Nürnberg G., LaZerte B. & Freshwater Research	Water Quality and Remediation Options for Lake Wilcox	2012	Report
(6) AECOM Canada Ltd.	Richmond Hill Lake Wilcox Management Plan Update	2019	Report

Table A2. Bathymetry of Lake Wilcox (from Report 5 in Table A1).

Water depth (m)	Area (ha)	Volume (10^3 m^3)
0	55.6	941.4
2	38.5	689.9
4	30.5	537.3
6	23.3	397.1
8	16.4	272.2
10	10.8	170.9
12	6.3	92.9
14	3.0	40.5
16	1.1	10.6
17.4	0.03	0

Table A3. Total concentrations of the elements Al, Fe, S, Mn, K, Na and Ca extracted from the sediment core samples using the method of Aspila et al. (1976), as described in section 2.4 of the main text, given along with the year of deposition (rounded). Concentration units are μmol g^{-1}, except for Ca which is in units of mmol g^{-1}.

Year of deposition	Al	Fe	S	Mn	K	Na	Ca
2020	276	141	269	11.6	49	129.8	4.1
2019	271	129	279	12.8	45	57.7	4.4
2019	264	119	267	13.9	41	44.6	4.7
2018	297	121	239	13.2	46	30.7	4.8
2017	314	127	268	13.5	50	34.6	4.7
2016	310	127	290	13.3	48	34.9	4.6
2014	353	143	316	12.6	54	30.1	4.5
2013	371	155	377	13.4	54	32.5	4.1
2012	317	127	318	13.7	45	29.8	4.4
2010	320	129	345	13.1	45	31.0	4.1
2009	353	129	347	13.7	51	30.3	4.3
2007	346	128	394	13.3	50	31.3	4.0
2005	426	147	442	13.0	59	32.0	3.8
2003	339	123	369	15.4	47	31.7	4.0
2001	291	122	492	30.6	41	42.7	3.0
1999	326	122	465	13.5	47	27.7	4.0
1997	350	131	462	12.0	49	25.2	4.0
1995	370	136	438	12.0	56	22.4	4.3
1993	367	131	414	11.8	54	21.5	4.4
1991	364	131	417	11.3	57	20.9	4.3
1990	383	130	408	11.4	63	19.1	4.4
1988	367	123	395	11.1	54	20.1	4.4
1987	373	123	362	11.0	60	19.3	4.5
1985	375	121	343	11.0	56	20.8	4.6
1984	359	118	332	10.7	56	21.9	4.6
1983	368	121	330	10.6	54	17.6	4.5
1982	390	125	351	9.7	56	19.7	4.5
1981	388	124	346	9.4	55	17.8	4.5
1980	396	126	329	9.0	60	17.5	4.4
1979	386	122	322	8.7	59	16.9	4.3
1979	384	124	318	8.6	58	19.4	4.3
1978	398	128	300	8.5	61	16.9	4.4
1977	375	124	304	8.7	52	12.7	4.2
1976	378	120	303	7.9	53	14.9	4.0
1975	367	121	310	8.1	50	14.9	4.0
1974	368	118	291	7.9	52	15.1	4.2
1973	374	119	282	7.6	54	13.5	4.1
1973	353	118	295	7.5	50	12.5	4.1

1972	348	116	303	7.4	51	13.5	4.0
1971	332	111	313	7.1	47	11.4	4.1
1970	326	122	292	8.4	39	8.7	4.0
1969	323	110	299	7.1	46	9.7	4.0
1968	401	135	254	8.6	50	9.7	4.1
1967	353	125	256	8.4	42	7.2	4.1
1966	345	123	277	8.2	40	5.9	4.1
1965	332	121	270	8.0	39	4.9	4.1
1964	326	116	276	8.1	38	6.9	4.0
1963	337	122	264	7.8	45	7.2	4.1
1962	335	124	255	7.8	39	4.9	4.1
1962	353	128	248	7.8	43	4.6	4.2
1961	342	127	248	7.9	41	5.3	4.2
1960	363	131	258	8.0	43	7.0	4.2
1959	366	129	239	7.8	44	3.2	4.2
1957	359	130	244	8.0	43	4.9	4.2
1956	376	132	238	7.8	47	4.9	4.2
1955	404	139	235	7.8	54	4.2	4.2
1954	368	131	240	7.7	46	3.4	4.2
1953	396	140	240	7.7	51	4.5	4.2
1951	422	147	237	7.5	54	4.7	4.1
1950	400	146	241	7.4	50	3.1	4.1
1948	419	150	244	7.4	54	5.5	4.1
1946	445	154	232	7.4	58	5.8	4.2
1944	421	148	223	7.3	56	7.8	4.1
1942	455	160	227	7.4	60	4.5	4.0
1940	396	143	232	7.1	52	3.5	4.0
1938	381	141	232	7.0	50	1.1	4.1
1936	372	138	224	6.9	48	1.9	4.2
1933	380	136	221	6.8	55	3.7	4.2
1931	371	137	229	6.9	49	0.6	4.4
1929	389	139	209	6.5	55	4.8	4.1
1926	363	133	214	6.8	50	26.7	4.4
1924	360	126	191	6.4	53	3.1	4.4
1923	377	132	185	6.5	55	2.4	4.3
1922	354	126	185	6.2	48	2.4	4.1
1921	364	126	180	6.0	50	2.0	3.9
1920	343	126	200	5.8	47	0.1	3.8

Table A4. Relative mineral composition from X-ray diffraction (XRD) data and Rietveld refinement, for selected sediment core sections across the four watershed development. Phases (WDP). BDL stands for below the detection limit; Year indicates the year of sediment deposition (rounded). Note that the analyses only include the well-crystallized mineral phases, not all the mineral phases. Mineral abundances are given as percentages.

Sediment depth interval (cm)	Year of sediment deposition	Watershed development phase	Pyrite %	Calcite %	Quartz %	Andesine * %	Bytownite %	Albite %	Ankerite %
7 to 8	2013	4	1.0	33.0	12.0	25.0	23.0	5.0	1.0
23 to 24	1985	3	BDL	31.3	14.1	27.3	20.2	6.1	1.0
34 to 35	1975	2	1.0	28.7	13.9	24.8	21.8	8.9	1.0
41 to 42	1969	2	1.0	30.0	16.0	27.0	20.0	6.0	BDL
50 to 51	1961	2	1.0	29.7	13.9	28.7	18.8	7.9	BDL
63 to 64	1942	1	BDL	29.0	15.0	27.0	23.0	5.0	1.0
73 to 74	1922	1	BDL	32.3	13.1	25.3	22.2	6.1	1.0

*The software identified the XRD peak with that of the mineral kyanite; however, in our judgment, the peak position is within the general range of more common plagioclase feldspars, such as andesine.

Table A5. Ranges of TP export coefficients reported in the literature for the different watershed LULC types, and the corresponding loading fluxes. The values were used for estimating TP external loading to Lake Wilcox in watershed development Phases 1 and 2.

LULC	TP export coefficients in mg m^{-2} y^{-1}	TP export loads in kmol y^{-1}	Reference(s)
Natural/ Forested	10-80	0.7-5.9	Gore & Storrie (1989)
Agricultural	50-480	3.7-35.6	Xin et al. (2019); Jedrych et al. (2006); Lin et al. (2004)
Urban	10-300	0.7-22.3	Lin et al. (2004); Nürnberg et al. (2012); Donelly et al. (2020)

Table A6. External TP loading fluxes to Lake Wilcox (F_{ext}) calculated by summing TP runoff fluxes from the watershed (F_{run}) and TP atmospheric deposition fluxes (F_{atm}). Ranges of F_{run} are based on the watershed export coefficients reported in Table A5 and the relative LULC distributions for the four watershed development phases. Values of F_{atm} are based on estimates of the areal atmospheric TP deposition rates (r_{atm}) for southern Ontario through time (references given in the table). In addition to the F_{ext} ranges, the F_{ext} values used in the TP budgets shown in the main text Figure 6 are also provided. Units of F_{ext}, F_{run}, and F_{atm} are in kmol y^{-1}, those of r_{atm} in mg m^{-2} y^{-1}.

Watershed development phase	F_{run} range	F_{run} TP budget	r_{atm}	Reference(s)	F_{atm}	F_{ext}
1	1.6 - 15.7	3.8	13	MOE, 2010; Gore & Storrie, 1989	0.24	3.9
2	2.4 - 23.9	6.7	31	MOE, 2010; Gore & Storrie, 1989; Lee, 1996	0.56	7.5
3	1.8 - 20.4	5.2	26	Nürnberg et al., 2012; AECOM, 2019	0.47	5.7
4	1.3 - 19.2	3.7	26	Nürnberg et al., 2012; AECOM, 2019	0.47	4.2

Supplementary References List to Chapter 2:

1. AECOM Canada Ltd. (2019) Richmond Hill Lake Wilcox management plan update, Report.
2. Alvarez-Cobelas, M., Sánchez-Carrillo, S., Angeler, D. G., & Sánchez-Andrés, R. (2009). Phosphorus export from catchments: a global view. *Journal of the North American Benthological Society, 28*, 805-820.
3. Anderson, J. R. (1976). A land use and land cover classification system for use with remote sensor data. *Geological Survey Professional Paper no. 964*. US Government Printing Office
4. Aspila, K. I., Agemian, H., & Chau, A. S. Y. (1976). A semi-automated method for the determination of inorganic, organic and total phosphate in sediments. *Analyst, 101*, 187-197.
5. Donnelly, D., Helliwell, R. C., May, L., & McCreadie, B. (2020). An assessment of the performance of the PLUS+ Tool in supporting the evaluation of water framework directive compliance in Scottish standing waters. *International journal of environmental research and public health*, *17*(2), 391.
6. Gore, C. and Storrie Ltd. (1989) Master drainage/service plan for the Lake Wilcox – Oak Ridge's district, *Report.*
7. Gore, C. and Storrie Ltd (1993) OPA71 phase II environmental studies, *Technical appendices*.
8. Gore, C. and Storrie Ltd. (1994) North lake road sanitary sewer, *Report.*
9. Jedrych, A. T., Olson, B. M., Nolan, S. C., & Little, J. L. (2006). Calculation of soil phosphorus limits for agricultural land in Alberta. 87 pp. *Alberta Soil Phosphorus Limits Project, 2.*
10. Lin, J. P. (2004). *Review of published export coefficient and event mean concentration (EMC) data.* Engineer research and development center Vicksburg ms.
11. Lin, Z., Radcliffe, D. E., Risse, L. M., Romeis, J. J., & Jackson, C. R. (2009). Modeling phosphorus in the Lake Allatoona watershed using SWAT: II. Effect of land use change. *Journal of environmental quality, 38*, 121-129.
12. Lee G. & Freshwater Research (1996) Lake Wilcox remediation strategy, *Report.*
13. Map and Data Library, *1954 Air Photos of Southern Ontario*. https://mdl.library.utoronto.ca/collections/air-photos/1954-air-photos-southern-ontario/index Accessed on: December 2019.
14. Ministry of Environment. 2010. *Lakeshore Capacity Assessment Handbook: Protecting Water Quality in Inland Lakes on Ontario's Precambrian Shield*, Toronto, Ontario.
15. Nuernberg G., LaZerte B. & Freshwater Research (2012) Water quality and Remediation options for Lake Wilcox, *Report.*
16. Robinson M. B. and Clark J. (2000a). The War Years. Later Days in Richmond Hill - A History of the Community from 1930 to 1999. *Town of Richmond Hill/Richmond Hill Public Library Board.*
17. Robinson M. B. and Clark J. (2000b). The Boom Years. Later Days in Richmond Hill - A History of the Community from 1930 to 1999. *Town of Richmond Hill/Richmond Hill Public Library Board.*

18. Robinson M. B. and Clark J. (2000c). Growing Success. Later Days in Richmond Hill - A History of the Community from 1930 to 1999. *Town of Richmond Hill/Richmond Hill Public Library Board.*
19. Stamp, R. M. (1991). *Early Days in Richmond Hill: a history of the community to 1930*. Richmond Hill Public Library Board. https://edrh.rhpl.richmondhill.on.ca/default.asp Accessed on: March 2021.
20. Toronto Regional Conservation Authority (2008). Humber River Watershed Plan. *Pathways to a Healthy Humber*.
21. Xin, Z., Ye, L., & Zhang, C. (2019). Application of export coefficient model and QUAL2K for water environmental management in a Rural Watershed. *Sustainability, 11*, 6022.

Appendix B
Supplementary material: Chapter 3

Data availability statement

The data that support the findings of this study are openly available from the Federated Research Data Repository (FRDR) website at DOI: 10.20383/103.0577. Additionally, the raw data provided by the City of Richmond Hill and used in this study can be obtained at DIO: 10.20383/102.0540 on the FRDR website.

Methods: Images classification

Our classification scheme, with four classes (forested, agricultural, urban, and other land cover), is based on the land use classification system developed by Anderson et al. (1976) for interpretation of remote sensing data at different scales and resolutions. According to the classification system of Anderson et al. (1976), “residential, commercial services, industrial, transportation, communications, industrial and commercial, mixed urban or built-up land, other urban or built-up land” are all folded into to the urban land use class; forested land includes “deciduous forest land, evergreen forest land, mixed forest land, orchards, groves, vineyards, and nurseries”; while “crop fields, pasture, and bare fields” belong to the agricultural land use class.

The land use coverage values we used are those given in reports made available to us by the City of Richmond Hill, complemented with our own estimates obtained manually from aerial images. The latter confirms the values in the reports. In both cases, the classification system developed by Anderson et al., (1976) was adopted, which has been widely used by others (e.g., Yuan et al., 2005).

Supplementary tables and figures to Chapter 3.

Table B1. List of websites from which data were retrieved.

Organization/Name:	Website:	Accessed on:
Toronto and Region Conservation Authority	https://data.trca.ca/dataset/precipitation	Jun, 2019
Environment and Climate Change Canada	https://climate.weather.gc.ca/historical_data/search_historic_data_e.html	May, 2019
Ontario Ministry of Agriculture, Food and Rural Affairs	http://www.omafra.gov.on.ca/english/landuse/gis/agatlas-help.htm#4	Feb, 2019
Ontario Land Information	https://geohub.lio.gov.on.ca/	Feb, 2019
Esri's Wayback Living Atlas Google Earth Pro	https://livingatlas.arcgis.com/wayback/#active=42403&ext=-79.48126,43.92054,-79.37946,43.96516	Dec, 2019
USGS Land Look	https://landsatlook.usgs.gov/explore	Dec, 2019

Table A2. Mean annual concentrations and standard deviations of chemical parameters.

Year		DIP Epil. ($mg\ L^{-1}$)	TP Epil. ($mg\ L^{-1}$)	NH_4^+ Epil. ($mg\ L^{-1}$)	NO_3^{2-} Epil. ($mg\ L^{-1}$)	DIN Epil. ($mg\ L^{-1}$)	DO Epil. ($mg\ L^{-1}$)	Cl^- Epil. ($mg\ L^{-1}$)	Chl-a ($\mu g\ L^{-1}$)	DIP Hypol. ($mg\ L^{-1}$)	TP Hypol. ($mg\ L^{-1}$)	NH_4^+ Hypol. ($mg\ L^{-1}$)	NO_3^2 Hypol. ($mg\ L^{-1}$)	DIN Hypol. ($mg\ L^{-1}$)	DO Hypol. ($mg\ L^{-1}$)
1996	Mean Concentration	0.007	0.036	0.076	0.245	0.412	9.960	43.354	13.631	0.204	0.341	1.448	0.014	1.484	6.966
	Standard Deviation	0.007	0.011	0.102	0.460	0.560	1.843	1.547	11.051	0.132	0.208	1.047	0.021	1.025	1.269
1997	Mean Concentration	0.008	0.039	0.042	0.012	0.133	10.457	43.200	7.340	0.144	0.262	1.475	0.016	1.487	9.339
	Standard Deviation	0.013	0.029	0.155	0.010	0.158	1.603	0.506	3.605	0.105	0.124	0.624	0.012	0.625	1.222
1998	Mean Concentration	0.005	0.045	0.034	0.006	0.083	17.062	45.385	6.933	0.102	0.190	1.029	NA	1.046	10.207
	Standard Deviation	0.005	0.021	0.104	0.004	0.105	6.808	1.212	5.190	0.051	0.062	0.263	NA	0.264	2.076
1999	Mean Concentration	0.006	0.043	0.102	0.016	0.178	14.803	47.400	15.225	0.092	0.228	1.632	NA	1.648	2.639
	Standard Deviation	0.007	0.021	0.188	0.014	0.194	6.260	0.595	2.494	0.072	0.101	0.954	NA	0.957	4.630
2000	Mean Concentration	0.010	0.039	0.060	0.020	0.174	10.574	45.800	10.660	0.161	0.221	1.332	NA	1.370	3.305
	Standard Deviation	0.017	0.024	0.258	0.030	0.185	1.685	1.161	5.783	0.076	0.080	0.671	NA	0.654	2.966
2001	Mean Concentration	0.009	0.040	0.106	0.030	0.222	9.750	52.300	9.360	0.308	0.457	1.736	0.089	1.839	0.416
	Standard Deviation	0.015	0.020	0.217	0.033	0.243	1.290	1.944	5.443	0.110	0.203	0.494	0.123	0.501	0.357
2002	Mean Concentration	0.006	0.035	0.037	0.005	0.072	9.933	55.975	7.400	0.230	0.294	1.658	0.008	1.670	0.718
	Standard Deviation	0.011	0.016	0.093	0.003	0.095	1.976	1.204	5.358	0.139	0.157	0.953	0.013	0.949	1.951
2003	Mean Concentration	0.006	0.037	0.045	0.011	0.103	9.482	62.717	7.508	0.205	0.270	1.544	0.019	1.449	0.250
	Standard Deviation	0.007	0.013	0.114	0.007	0.120	2.108	1.190	3.673	0.075	0.099	0.755	0.037	0.844	0.233
2004	Mean Concentration	0.005	0.039	0.023	0.053	0.150	9.731	64.600	9.438	0.185	0.278	1.337	0.048	1.389	0.656
	Standard Deviation	0.009	0.013	0.155	0.092	0.183	2.313	0.642	6.475	0.110	0.129	0.789	0.097	0.723	1.711
2005	Mean Concentration	0.006	0.034	0.107	0.015	0.161	9.832	74.014	13.636	0.178	0.264	1.309	0.019	1.341	0.785
	Standard Deviation	0.008	0.017	0.115	0.021	0.136	0.973	2.433	9.845	0.123	0.186	0.787	0.055	0.760	2.489
2006	Mean Concentration	0.004	0.037	0.029	0.149	0.203	11.095	80.782	8.333	0.206	0.291	1.388	0.003	1.394	1.253
	Standard Deviation	0.008	0.016	0.119	0.484	0.447	1.515	1.588	4.140	0.099	0.121	0.661	0.003	0.663	3.134
2007	Mean Concentration	0.002	0.031	0.012	0.038	0.068	9.793	85.008	11.862	0.233	0.277	1.849	0.023	1.871	0.378
	Standard Deviation	0.001	0.016	0.044	0.087	0.106	1.261	3.706	4.199	0.115	0.117	0.824	0.024	0.820	0.864
2008	Mean Concentration	0.002	0.042	0.030	0.003	0.087	11.248	89.838	13.431	0.200	0.356	2.048	0.002	1.895	0.233
	Standard Deviation	0.002	0.020	0.144	0.002	0.145	1.993	1.718	9.640	0.116	0.337	1.179	0.002	1.264	0.823
2009	Mean Concentration	0.008	0.031	0.067	0.029	0.164	11.333	93.842	14.950	0.206	0.273	1.907	0.016	1.927	0.171
	Standard Deviation	0.017	0.018	0.185	0.035	0.189	1.489	1.837	8.762	0.134	0.117	0.811	0.020	0.800	0.108

2010	Mean Concentration	0.004	0.030	0.055	0.071	0.241	10.689	95.208	6.800	0.177	0.180	1.615	0.059	1.672	0.358
	Standard Deviation	0.002	0.011	0.381	0.110	0.381	1.495	3.923	3.397	0.154	0.074	1.792	0.107	1.769	0.552
2011	Mean Concentration	0.005	0.033	0.035	0.036	0.130	9.241	98.586	11.886	0.136	NA	1.383	0.047	1.434	0.535
	Standard Deviation	0.006	0.018	0.141	0.047	0.148	1.600	2.415	6.613	0.097	NA	0.720	0.061	0.713	1.549
2012	Mean Concentration	0.002	0.021	0.040	0.038	0.119	9.632	101.583	5.954	0.100	0.101	1.248	0.037	1.289	0.371
	Standard Deviation	0.003	0.009	0.104	0.041	0.137	2.483	4.231	2.532	0.079	0.059	0.715	0.033	0.726	0.364
2013	Mean Concentration	0.009	0.024	0.041	0.077	0.181	11.011	98.273	6.418	0.201	0.254	1.805	0.042	1.851	1.064
	Standard Deviation	0.011	0.017	0.129	0.107	0.171	1.952	2.008	2.602	0.087	0.095	0.719	0.020	0.705	3.418
2014	Mean Concentration	0.007	0.019	0.050	0.090	0.217	10.143	108.667	8.455	0.306	0.356	2.256	0.093	2.343	0.736
	Standard Deviation	0.009	0.015	0.107	0.021	0.106	1.580	3.519	4.108	0.107	0.110	0.848	0.018	0.858	2.243
2015	Mean Concentration	0.006	0.024	0.025	0.052	0.158	9.319	119.471	12.280	0.138	0.168	1.578	0.055	1.521	0.934
	Standard Deviation	0.003	0.010	0.069	0.016	0.076	1.247	4.446	4.282	0.100	0.098	0.887	0.015	0.948	2.432
2016	Mean Concentration	0.004	0.017	0.021	0.020	0.072	9.642	140.923	9.470	0.131	0.151	1.330	0.030	1.368	0.530
	Standard Deviation	0.003	0.007	0.090	0.001	0.088	1.067	3.730	8.261	0.095	0.080	0.702	0.021	0.694	0.937
2017	Mean Concentration	0.005	0.024	0.069	0.033	0.184	9.396	152.667	4.798	0.181	0.187	1.647	0.024	1.576	0.959
	Standard Deviation	0.005	0.008	0.161	0.023	0.173	1.888	5.246	0.805	0.122	0.106	0.999	0.012	1.049	2.495
2018	Mean Concentration	0.004	0.018	0.065	0.031	0.143	9.801	168.133	8.560	0.142	0.164	1.456	0.038	1.504	1.225
	Standard Deviation	0.004	0.008	0.115	0.030	0.136	1.767	4.121	4.006	0.111	0.104	0.996	0.037	0.978	2.327

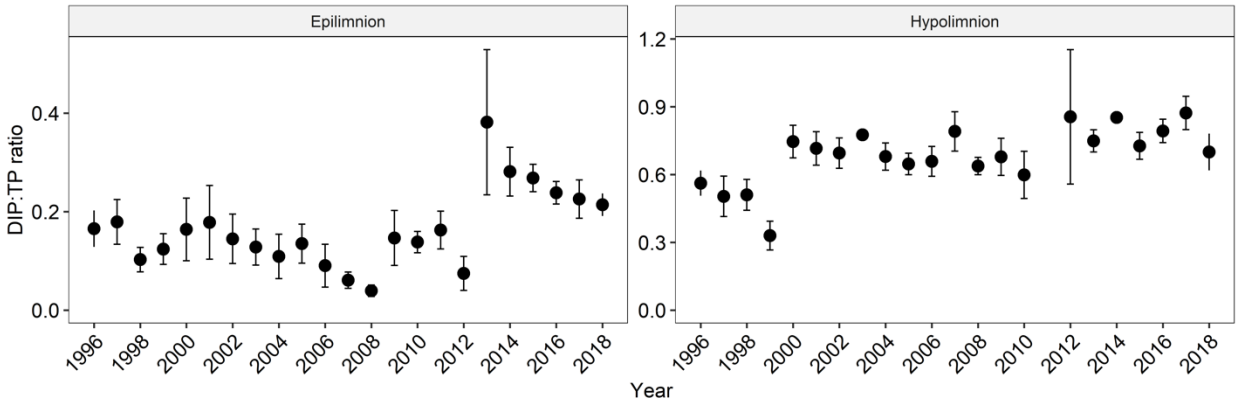

Figure B1. Time series of DIP:TP ratios in epilimnion and hypolimnion for the period 1996 to 2018. The error bars represent standard deviation.

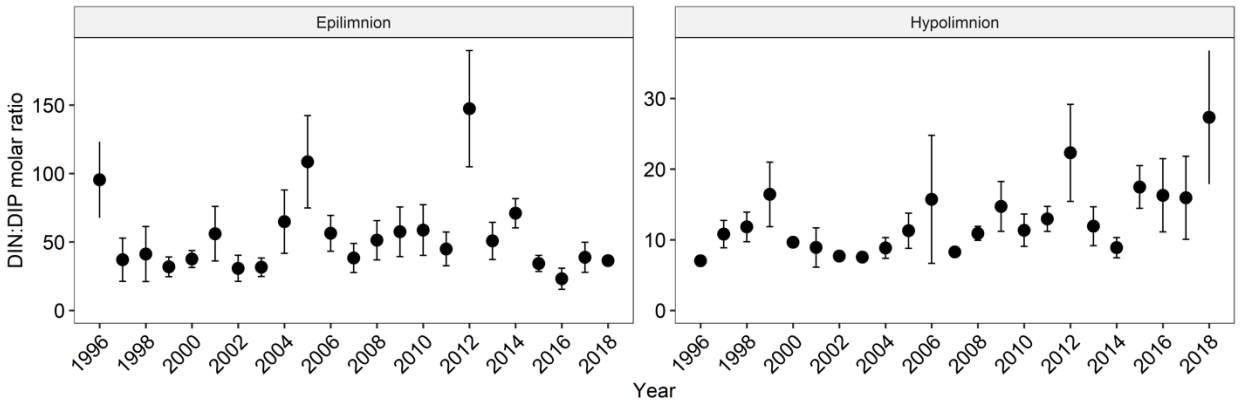

Figure B2. Time series of DIN:DIP molar ratios in epilimnion and hypolimnion for the period 1996 to 2018. The error bars represent standard deviation.

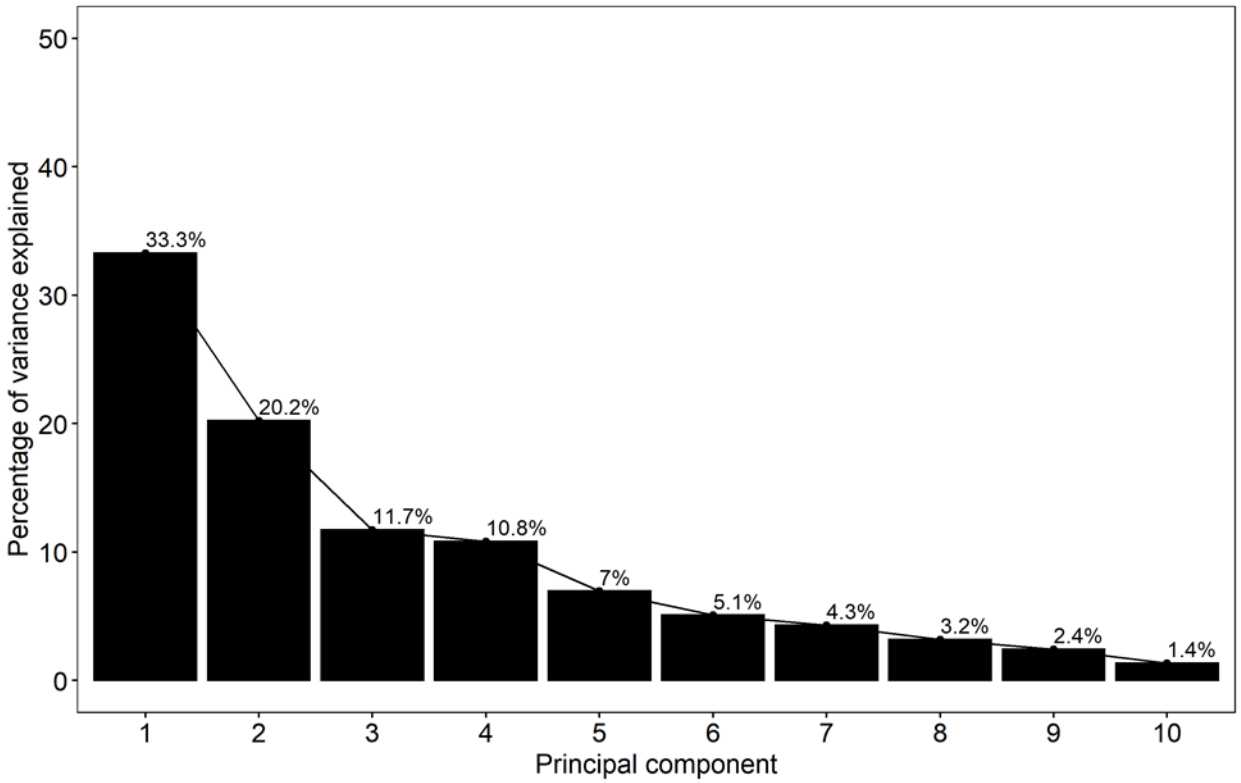

Figure B3. Contributions of principal components in the PCA analysis.

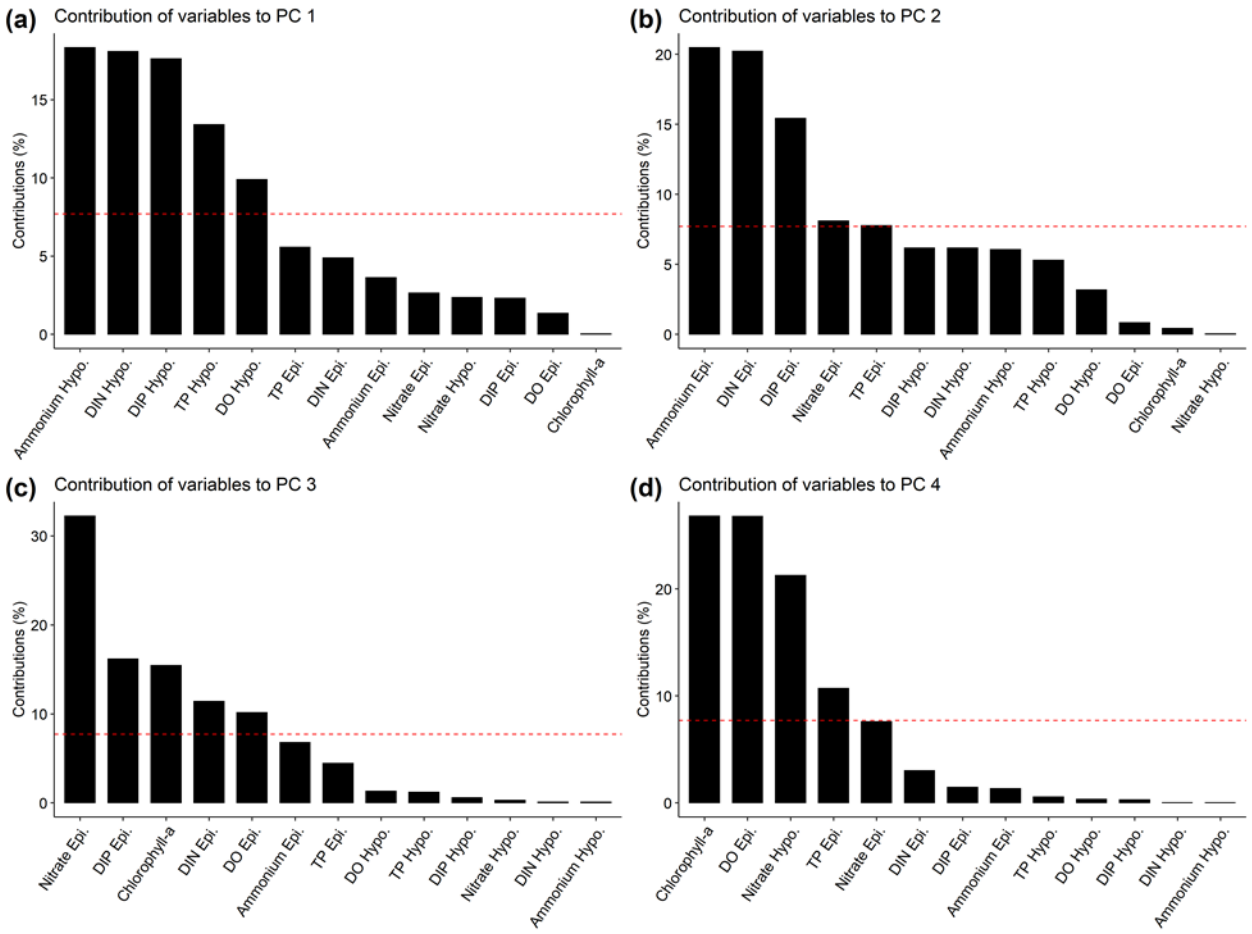

Figure B4. Contributions of explanatory variables for the first four principal components: (a) PC1, (b) PC2, (c) PC3, and (d) PC4.

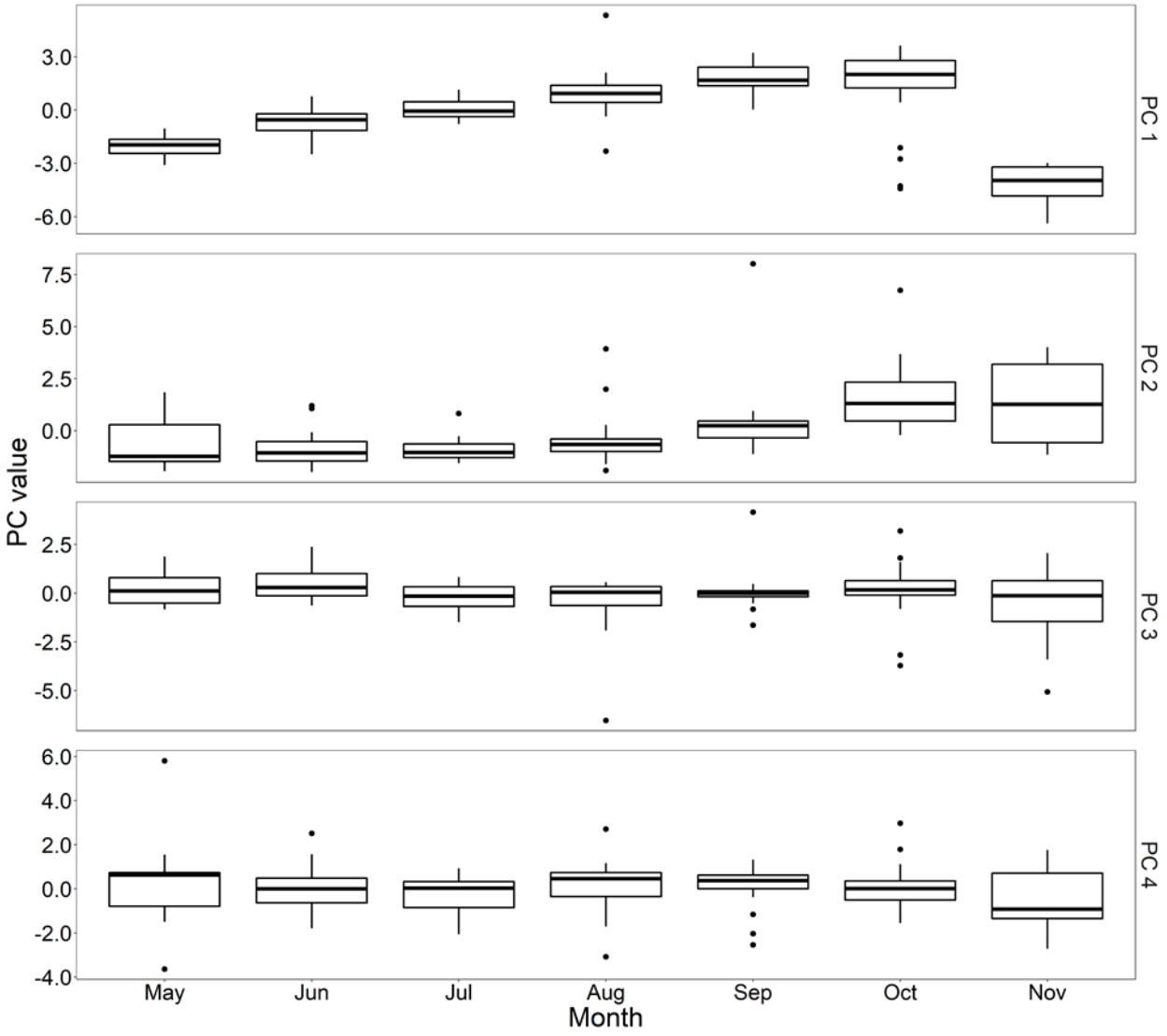

Figure B5. Box and whisker plots of the first four principal component (PC) values grouped by month. For each box, the upper and lower bounds represent the 75th and 25th percentiles, the line in the box represents the median, the whiskers show the minimum and maximum data points, outliers excluded, and the dots indicate outliers.

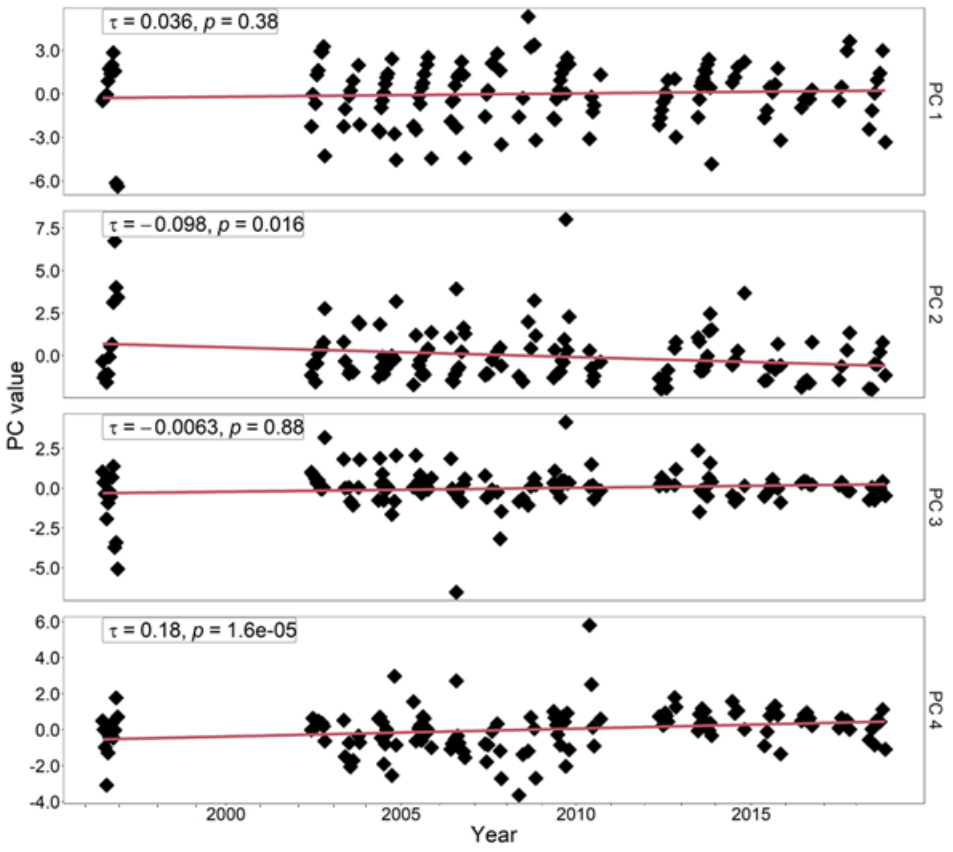

Figure B6. Time series of four PCs. For each of the four PCs, the Kendall's tau correlation coefficient and p value are noted in the top left of the panel. Dark red lines are the linear regression fits to the data. The gap in data between 1997 and 2002 corresponds to the period when the lake was artificially aerated. Data from this period of artificial aeration were excluded from the PCA analysis.

Supplementary References for Chapter 3:

1. Anderson, J. R. (1976). A land use and land cover classification system for use with remote sensor data. Geological Survey Professional Paper no. 964. US Government Printing Office
2. Gore, C. and Storrie Ltd. (1989) Master drainage/service plan for the Lake Wilcox – Oak Ridge's district, *Report.*
3. Gore, C. and Storrie Ltd (1993) OPA71 phase II environmental studies, *Technical appendices*.
4. Gore, C. and Storrie Ltd. (1994) North lake road sanitary sewer, *Report.*
5. Lee G. & Freshwater Research (1996) Lake Wilcox remediation strategy, *Report.*
6. Nuernberg G., LaZerte B. & Freshwater Research (2012) Water quality and Remediation options for Lake Wilcox, *Report.*
7. AECOM Canada Ltd. (2019) Richmond Hill Lake Wilcox management plan update, *Report.*

Appendix C

Supplementary material: Chapter 4

Data availability

The data that support the findings of this study, and provided by City of Richmond Hill are openly available on the Federated Research Data Repository (FRDR) at the following link: http://doi.org/10.20383/103.0592. Additionally, the raw data provided by the City of Richmond Hill and used in this study can be obtained at DOI: http://doi.org/10.20383/102.0540 on the FRDR website.

S1: Details on land use area estimation

In accordance with Anderson et al.'s (1976) classification system, various land use categories such as residential, commercial services, industrial, transportation, communications, industrial and commercial, mixed urban or built-up land, and other urban or built-up land are consolidated into the urban land use class. This classification takes into account the overall percentage of urbanization, which is determined by the degree of imperviousness in a given area. A detailed description of the methodology employed can be found in Radosavljevic et al. (2022) study.

To estimate the impervious cover within the LW watershed, we considered roofs, roads, sidewalks, parking lots, and school property as the components contributing to the total impervious cover. The area of roofs was determined using the approach outlined by Jinghui et al. (2004) and Castango & Atkins (2018). By subtracting the estimated roof area from the total impervious cover, we obtained the area occupied by roads, sidewalks, parking lots, and school property. These areas are deemed to require salting during winter conditions.

For the years 2009 and 2017, we obtained estimates for different imperviousness categories as reported by the CRH (City Regional Hospital), which were then matched with our own estimations with an error margin of approximately 5%. Detailed numerical values for each imperviousness category can be accessed through the link provided in the data availability statement.

S2: Details on Lake Number approach

St also represents the stability of the lake as a whole-basin, and represents the amount of external energy required to mix the whole lake water column (Eq. S1) (Imberger &

Patterson, 1989; Robertson & Imberger, 1994; Lindenschmidt & Chorus, 1998; and Ladwig et al., 2021):

$$St = \frac{g}{Ao}\int_0^z (z - z_{vol.}) \cdot Az \cdot \rho_z dz \quad \text{(S1)}$$

where z is the depth [m] referenced from the water surface; $z_{vol.}$ is the depth of the center of the volume (m); ρ_z is water density [kg m^{-3}], and Az is surface area [m^2] for a given depth.

To quantify the current *St* of LW, we used the lake's total surface area from the lake's bathymetry data (Reports 5 and 6 in Table A1) as the value of Az, and we used the water density that was calculated as a function of temperature and salinity. The density of water was calculated from the corresponding temperature and salinity values with the Javascript calculator developed using equation from Millero & Poisson, by the collaborative Computer Support Group (CSG) Network of University of Michigan and National Oceanic and Atmospheric Administration (NOAA).

The angle between the metalimnion surface and the lake bottom (β) (from Eq. 1) is estimated by dividing the depth of the thermocline (z_t) to the square root of surface area of the lake (Ao) (see Lindenschmidt & Chorus, 1998 and Ladwig et al., 2021 for further details).

The friction velocity (u) is estimated using (Lindenschmidt & Chorus, 1998; and Ladwig et al., 2021):

$$u^2 = \frac{\rho_{air}}{\rho_0} \cdot C \cdot U_{10}^2 \quad \text{(S2)}$$

where, $\frac{\rho air}{\rho o}$ is the dimensionless ratio between the air and surface water densities, C is the dimensionless drag coefficient, and *u* is wind velocity at 10 m above the surface [m s^{-1}]. The values of 0.0012 for $\frac{\rho air}{\rho o}$ and 0.000013 for C were used after Lindenschmidt & Chorus (1998). A wind velocity of 4.8 m s^{-1} was used, which represents the average wind speed for the LW watershed (Government of Canada, 2020).

We quantify the salinity threshold $St*$ that would result in a balance of stabilizing to kinetic forces as:

$$St^* \rightarrow g \cdot \left(St \cdot \frac{Ao}{g}\right) \cdot z_t = \rho_{bottom} \cdot u^2 \cdot A_o^{2/3} \quad \text{(S3a)}$$

This is the critical amount of salt that will – theoretically – result in amixis during fall. Further, St^* was quantified in R using rLakeAnalyzer (Read et al. 2011) to calculate the Lake Number, and the Nelder–Mead optimization routine to derive the state when:

$$St^* \rightarrow LN = 1 = g \cdot \left(St \cdot \frac{Ao}{g}\right) \cdot z_t = \rho_{bottom} \cdot u^2 \cdot A_o^{2/3} \quad \text{(S3b)}$$

In other words, we used the water salinity and temperature data for 2020 to calculate the water density in 2020 and therefore also the 2020 value of St for LW. We then calculated the St, threshold value, St*, which is the theoretical value of St and salinity which would cause meromixis in an initial dimictic lake, by setting *LN* equal to 1 (*i.e.,* when *LN* = 1 (or *LN*>1), $St \rightarrow St$ *). When *LN* is 1, the water column is stable and not prone to mixing (Lindenschmidt & Chorus, 1998).

Code with all summarized inputs parameters can be found on the link under Data Availability section of the paper.

S3: Details on Cl^- (and Na^+) modeling approach

To fit the parameter $\sigma(i)$ for each year being simulated, we fit a polynomial function to the time series Cl^-/Na^+ concentration (*i.e.,* $C(n_i)$) trend using (see Fig. S6 and S9) Eq.S4 for Cl^- and Eq.S5 for Na^+:

$$C(n_i) = 0.057{n_i}^3 - 1.23{n_i}^2 + 11.42n_i + 46.87 \quad \text{(S4)}$$

$$C(n_i) = 0.025{n_i}^3 - 0.55{n_i}^2 + 5.90n_i + 27.83 \quad \text{(S5)}$$

We then took the derivative of Eq. S6 and S7 to describe the dependence of ΔC_{i+1} over time for Cl^- and Na^+, respectively (see Figures S7 and S10):

$$\Delta C_{i+1} = 0.17{n_i}^2 + 2.46n_i + 11.42 \quad \text{(S6)}$$

$$\Delta C_{i+1} = 0.19{n_i}^2 - 3.00n_i + 13.78 \quad \text{(S7)}$$

By setting Eq. 2b (given in the main text) equal to Eq. S6 and S7 and rearranging, we were able to use the polynomial fit parameters for ΔC_{i+1} versus n_i to solve for the value

of σ_{i+1} at each value of *t* (*i.e.,* for each year) using equation S8 and equation S8 for Cl^- and Na^+, respectively:

$$\sigma_i = \frac{0.17{n_i}^2 + 2.46n_i + 11.42 + \gamma \cdot c_i}{n_i} \quad \text{(S9)}$$

$$\sigma_i = \frac{0.19{n_i}^2 - 3.00n_i + 13.78 + \gamma \cdot c_i}{n_i} \quad \text{(S9)}$$

The change in water column Cl^- concentration ($C(i)$) with time is controlled by two factors in this model: the external load to the lake from catchment runoff $(\sigma_{i+1} \cdot n_{i+1})$and the removal from the lake at the outlet by flushing ($\gamma \cdot c_i$). The flushing rate constant (γ) is assumed to be constant because the residence time of water in the lake did not change significantly during the 2001-2020 period. γ is calculated as the reciprocal of the lake's water residence time, which is ~2.03 years (obtained from the data 2001-2018), giving a value for γ of 0.49 y^{-1}. The external load increase rate is variable with time and can be calculated using Eq. 7 to solve for the value of σ for each year. The value of σ_i changed from 2001 to 2010 (from 20.9 to 5.3 mg L^{-1} y^{-2}) but remained relatively constant after 2010 with a rate of 5.3 mg L^{-1} y^{-2}.

S4: Concentrations of chloride vs. salinity

Vengosh, 2003, USGS, 2018, and Walker, 2021 determined that salinity of 1 ppt (1 g kg-1) corresponds to 1000 mg L^{-1} of total dissolved solids (TDS) in freshwater ecosystems highly affected by NaCl. Further, Singh & Kalra, 1975 and Thorslund & van Vliet, 2020 used the electrical conductivity (EC) to estimate TDS ($TDS = f \cdot \mathrm{EC}$, where f is the conversion factor, and for the freshwater with electrical conductivity greater than 800 µS cm^{-1}, the conversion factor is equal to 0.74 (Hem, 1985; Rusydi, 2017).

Figure A11 shows the high relationship between EC and Cl^- concentrations. We used that relationship to predict the concentration of Cl^- that corresponds to salinity of 1.23 g kg^{-1} (using the conversion factor of 0.74, equivalent electrical conductivity is 1662.16 µS cm-1, which corresponds to 385. 24 mg L^{-1} of Cl^-).

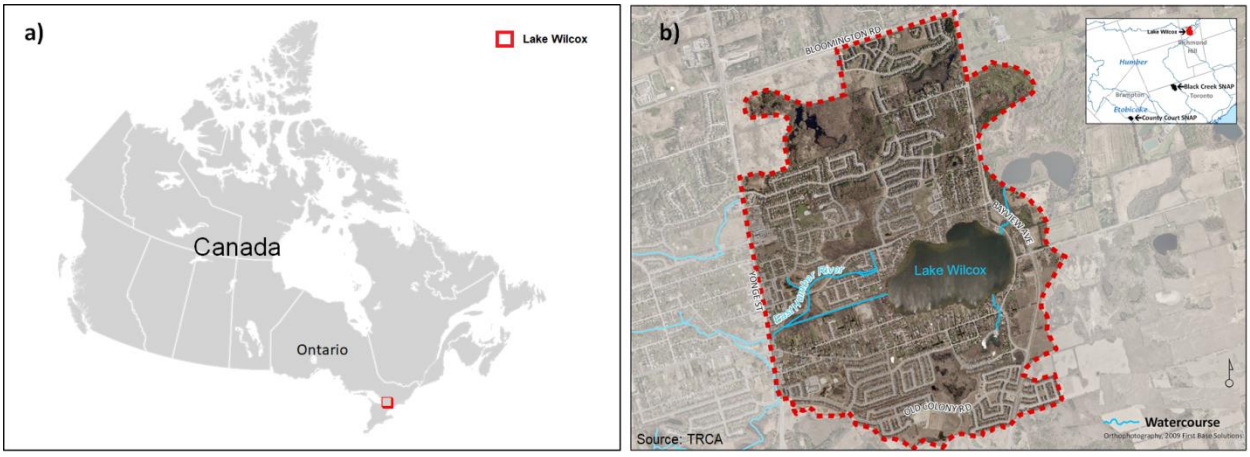

Figure C1. Location of Lake Wilcox (LW) in Ontario, Canada (a), and its watershed (b).

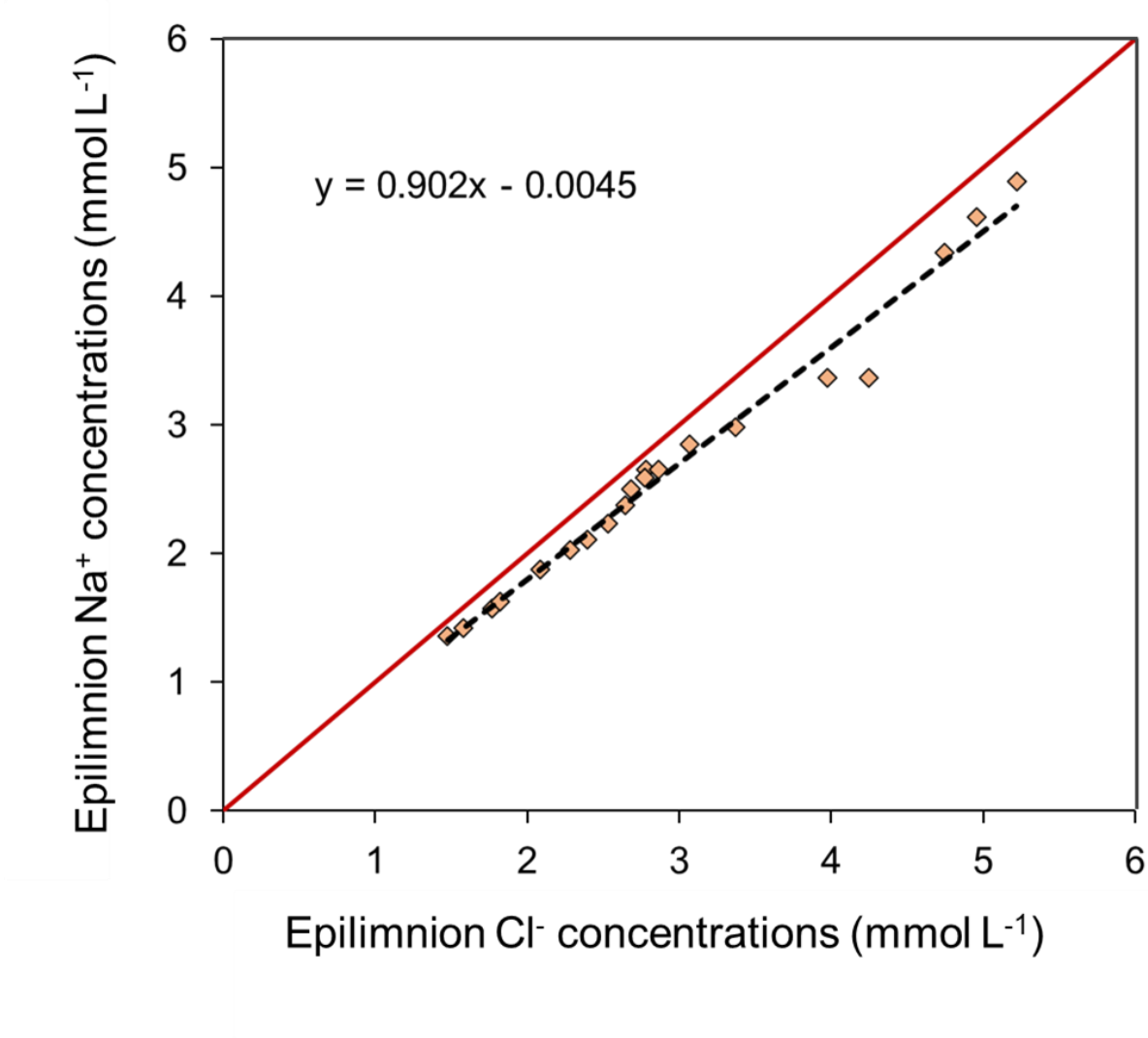

Figure C2. Molar concentrations of Na^+ versus Cl^- in the LW epilimnion. Red line indicates 1:1 parity line, while black dotted line indicates best fit line fitting through data.

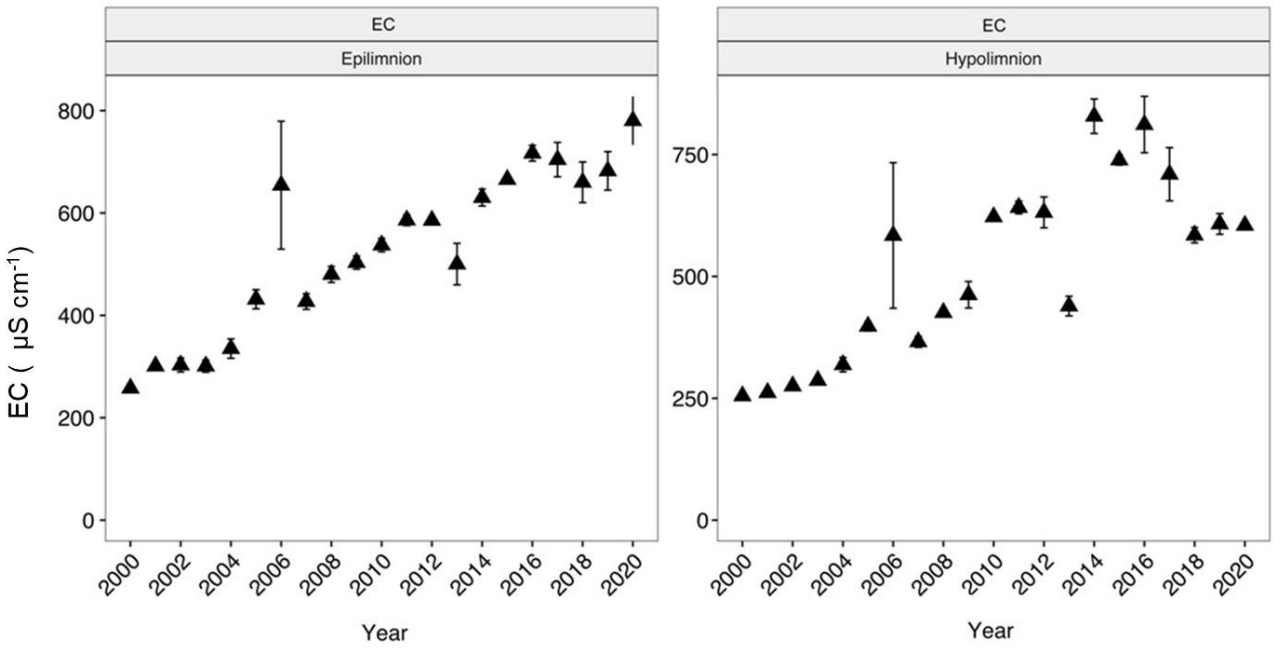

Figure C3. Time series of electric conductivity (EC) measures in epilimnion and hypolimnion for the period 2001 to 2020.

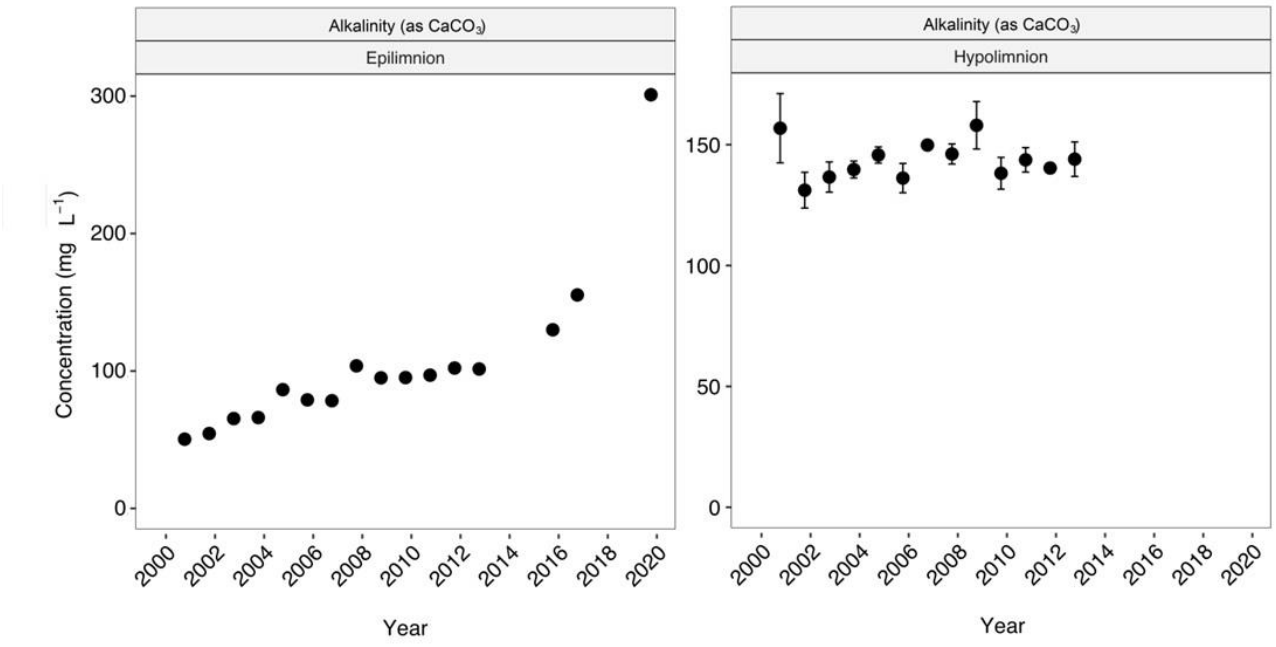

Figure C4. Time series of alkalinity concentrations, measured as $CaCO_3$, in epilimnion and hypolimnion for the period 2001 to 2020.

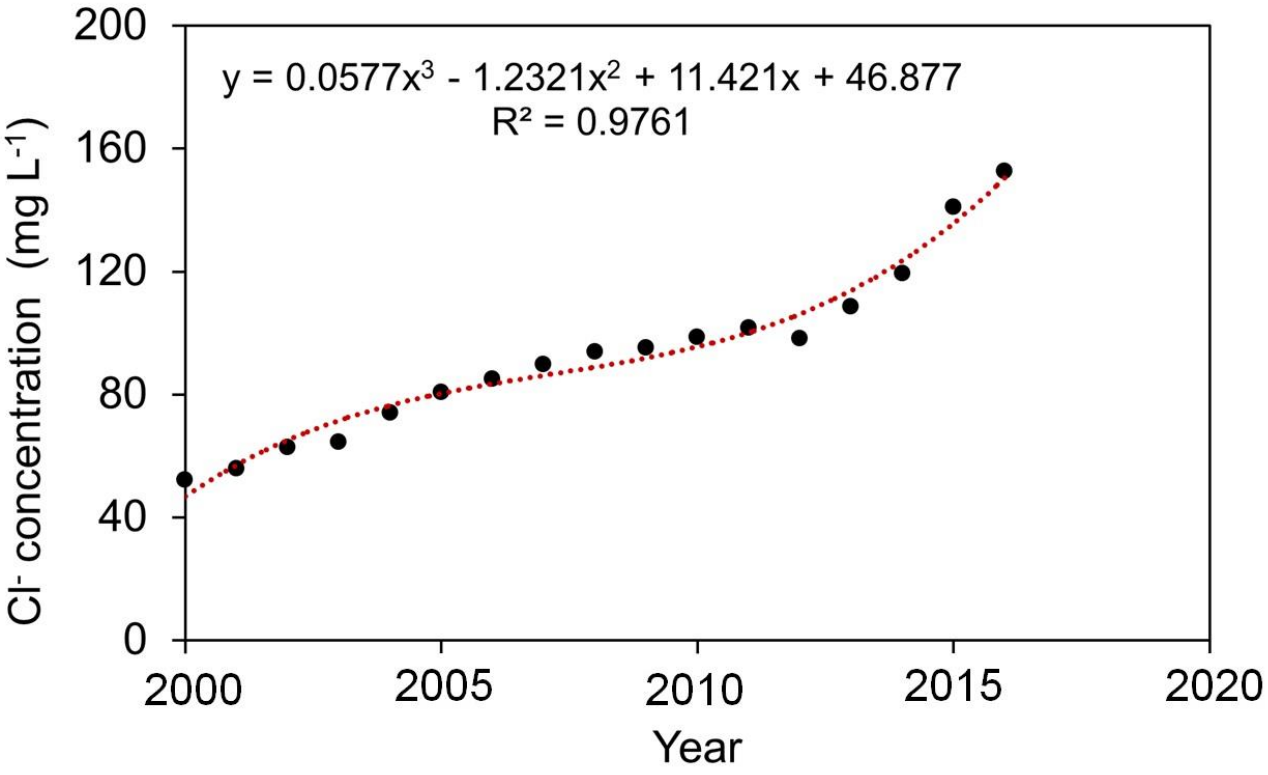

Figure C5. Chloride concentration, *C(i),* versus time with 3rd order polynomial fitting function and R^2 value.

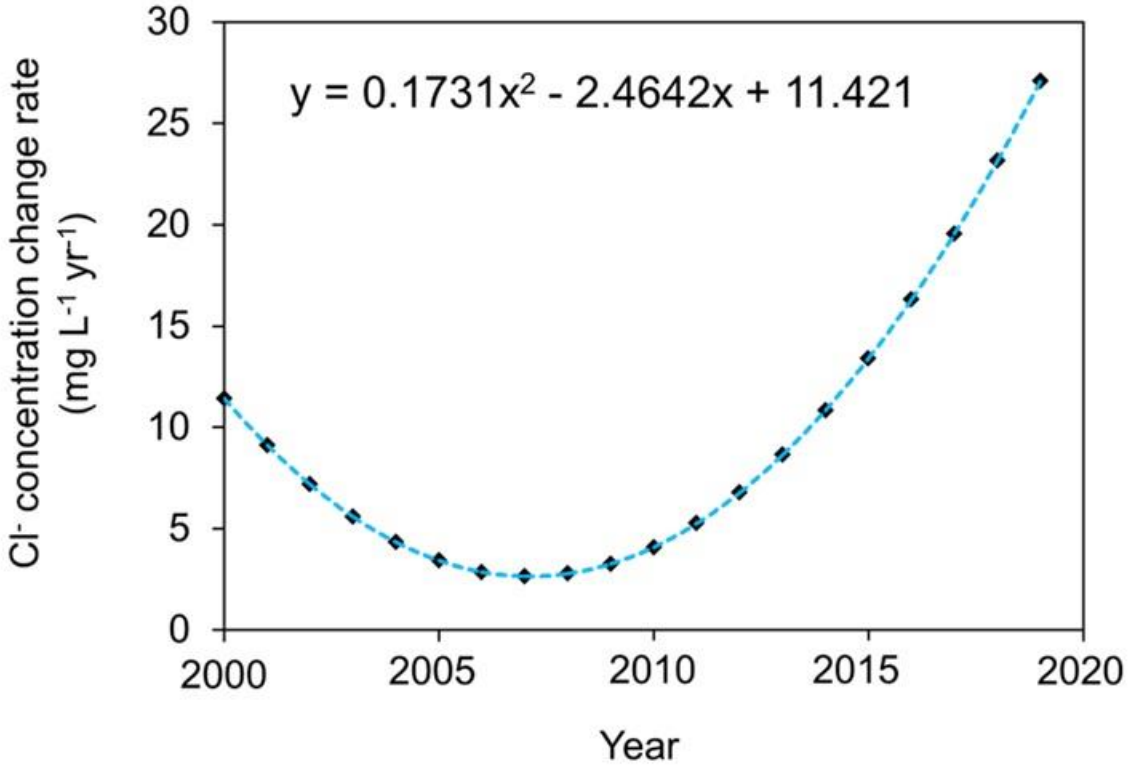

Figure C6. Chloride concentration change rate, versus time with 2nd order polynomial fitting function.

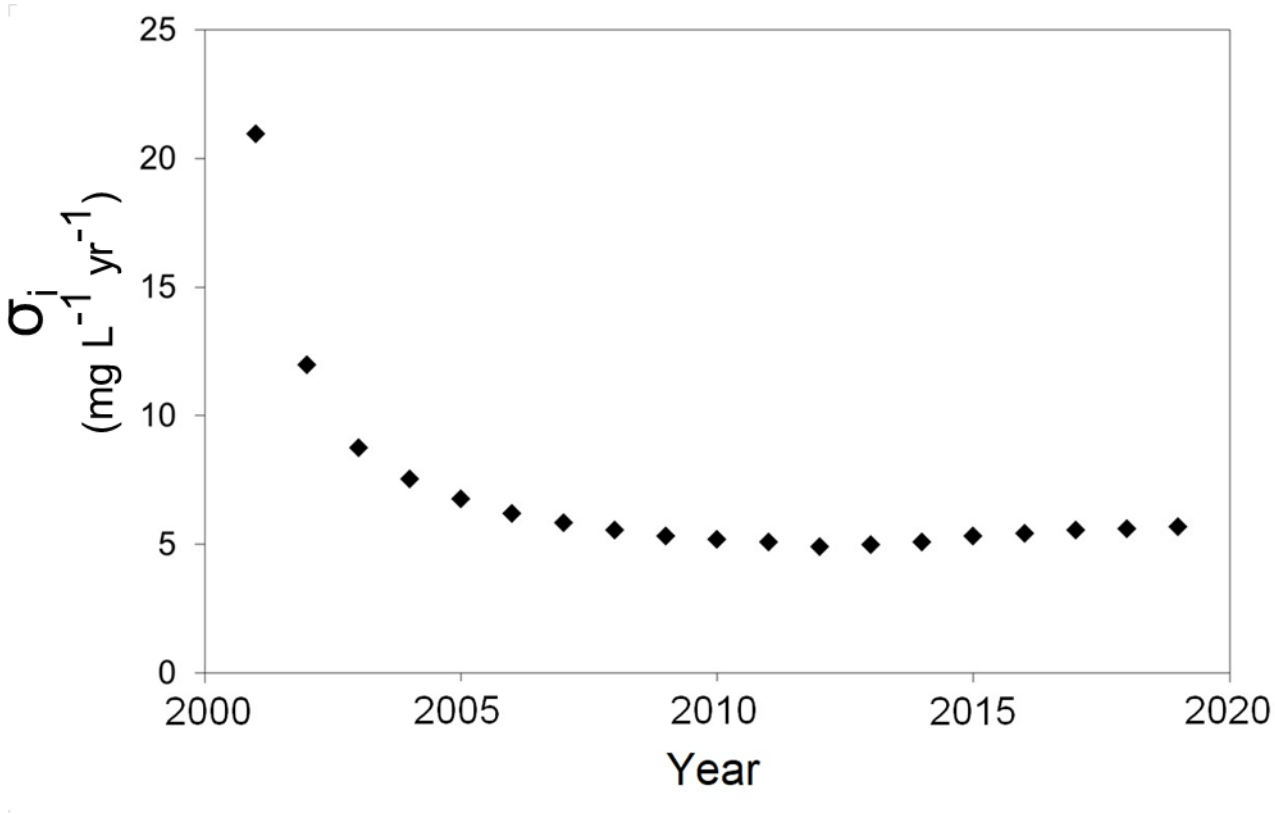

Figure C7. Time series of $\sigma(i)$ values from 2001 to 2020, used for the Cl^- lake model.

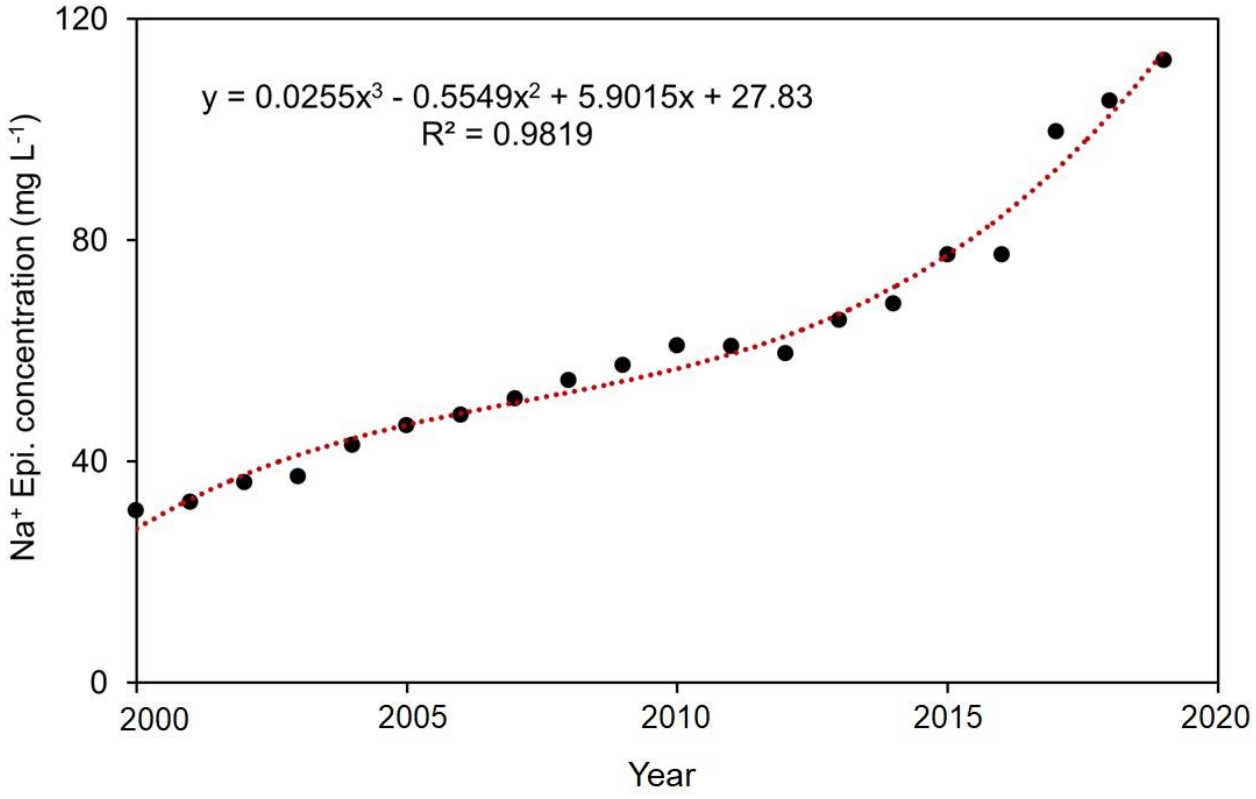

Figure C8. Na^+ concentration, *C(t),* versus time with 3rd order polynomial fitting function and R^2 value.

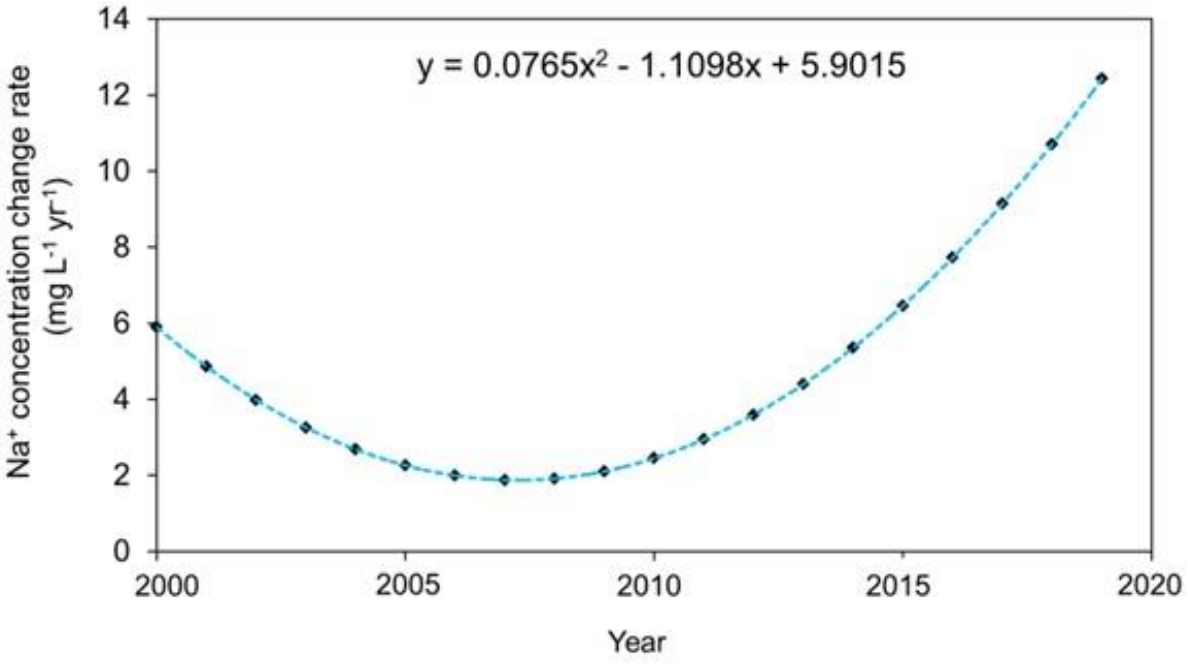

Figure C9. Na^+ concentration change rate, *dC(t)/dt*, versus time with 2nd order polynomial fitting function.

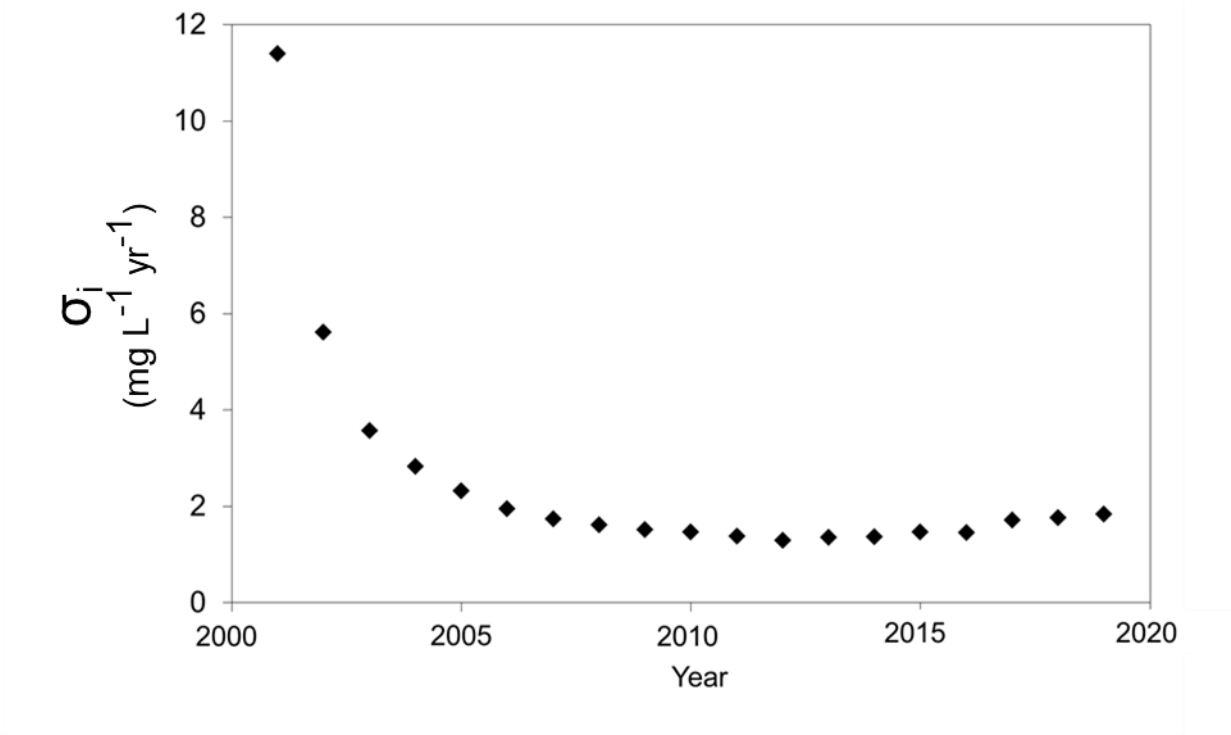

Figure C10. Time series of $\sigma(t)$ values from 2000 to 2020, used for the Na^+ lake model.

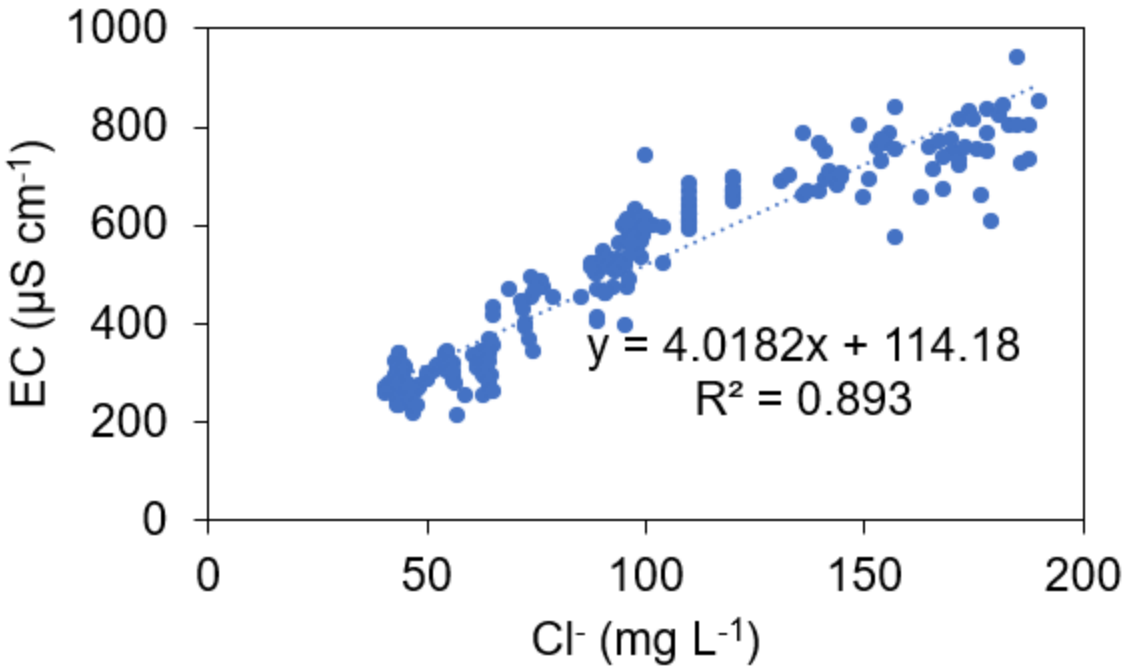

Figure C11. Relationship between chloride and electrical conductivity in Lake Wilcox.

Table C1. Types and components of de-icers used within the Lake Wilcox sub-watershed as part of winter management practice.

Type of salt	NaCl (%)	$MgCl_2$ (%)	$CaCl_2$ (%)	$CaSO_4$ (%)	Other (%)
Clear salt	99.90	-	-	-	0.10
Thawrox™	92.60 - 94.50	0.80 - 1.20	-	0.00 - 3.40	0.00 - 1.85
ClearLine	95.90	1.06 – 1.18	-	-	2.29 - 3.04
Brine	23.30	4.44	14.92	-	57.34

Table C2. Application rates of de-icers used during winter managment practice within Lake Wilcox sub-watershed (note: Ln stands for “lane”).

Material	Surface	Application Rate	Unit
Clear salt	City roads	100 - 130	kg per 2 Ln km
	Regional roads	220 - 400	kg per 2 Ln km
	Commercial	0.08 – 0.11	kg per m^2
	Residential	~ 10% of municipal usage	
Treated salt	City roads	77 - 113	kg per 2 Ln km
Winter mix	City roads	0.04 – 0.08	kg per m^2
	Side walks	0.04	kg per m^2
Brine	Regional roads	80 - 100	L per Ln km
	City roads	100	L per Ln km

Appendix D

Supplementary material: Chapter 5

Data availability statement: All data for the chapter 5 could be found www.doi.org/10.20383/103.0772 (the link will be active upon manuscript submission).

Table D1. List of websites from the data was retrieved (and data are publicly available).

Organization/Name:	Web page:	Data:	Accessed on:
Minnesota pollution control agency	https://www.pca.state.mn.us/	WQ	May, 2022
Minnesota department of natural resources	https://www.dnr.state.mn.us/	WQ	May, 2022
Wisconsin department of natural resources	https://dnr.wi.gov/	WQ	September, 2022
North Temperate Lakes LTER	https://lter.limnology.wisc.edu/	WQ	September, 2022
Dane County Water Quality Plan	https://www.carpcwaterqualityplan.org/	WQ	March, 2023
Lake Simcoe region conservation authority	https://www.lsrca.on.ca/opendata	WQ	January, 2023
University of Minnesota open library	https://conservancy.umn.edu/	WQ	March, 2023
Clean Lake Alliance (water quality monitoring)	https://www.cleanlakesalliance.org/	WQ	March, 2023
USGS, Open-File Report 2016–1050	https://pubs.usgs.gov/	WQ	May, 2022
Environment and Climate Change Canada	https://climate.weather.gc.ca/	CD	July, 2022
National weather services (NOAA)	https://www.weather.gov/mpx/mspclimate	CD	September, 2022
Esri's Wayback Living Atlas Google Earth Pro	https://livingatlas.arcgis.com/wayback	LULC	March, 2023

Table D2. Epilimnion TP concentrations and ratios of DIP and TP in hypolimnion (for the entire period of the available data).

	DIP:TP (hypolimnion)	TP (epilimnion) mg L^{-1}
L1	0.76	0.045
L2	0.6	0.109
L3	0.51	0.043
L4	0.75	0.08
L5	0.4	0.007
L6	0.7	0.025
L7	0.8	0.038
L8	0.9	0.619
L9	0.6	0.186

Table D3. Trend test coefficients for the Brunt-Väisälä frequency calculated without and with salinity (*no statistical significance).

	Kendall's τ: BVF (t) (p>0.1)	**Kendall's τ: BVF (t, S) (p<0.05)**
L1	0.15	0.28
L2	0.08	0.23
L3	0.16	0.21
L4	0.2	0.26
L5	0.12	0.18*
L6	0.15	0.21
L7	0.09	0.15
L8	0.21	0.34
L9	0.16	0.24

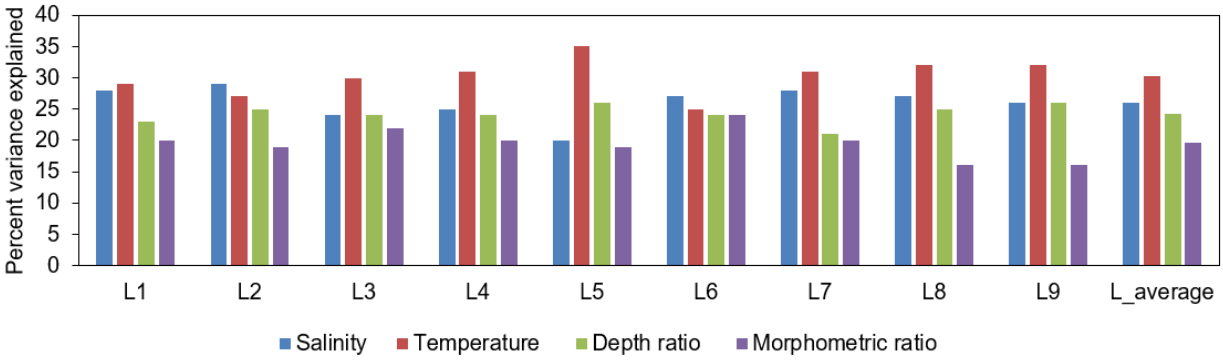

Figure D1. The variance in the first 10-years trends of available data of the BVF explained by four predictor variables as a percentage of variance explained by the full model. L_average represents the average conditions for all lakes.